THE MATERIAL PROPERTIES OF GELATIN GELS

J. Winter, et al

Marvalaud, Incorporated

Prepared for:

Ballistic Research Laboratories

March 1975

Destroy this report when it is no longer needed.
Do not return it to the originator.

Secondary distribution of this report by originating or sponsoring activity is prohibited.

Additional copies of this report may be obtained from the National Technical Information Service, U.S. Department of Commerce, Springfield, Virginia 22151.

The findings in this report are not to be construed as an official Department of the Army position, unless so designated by other authorized documents.

The use of trade names or manufacturers' names in this report does not constitute indorsement of any commercial product.

UNCLASSIFIED

SECURITY CLASSIFICATION OF THIS PAGE (When Data Entered)

REPORT DOCUMENTATION PAGE		READ INSTRUCTIONS BEFORE COMPLETING FORM
1. REPORT NUMBER BRL CONTRACTOR REPORT NO. 217	2. GOVT ACCESSION NO.	3. RECIPIENT'S CATALOG NUMBER AD-A008 396
4. TITLE (and Subtitle) THE MATERIAL PROPERTIES OF GELATIN GELS		5. TYPE OF REPORT & PERIOD COVERED Final Report 6. PERFORMING ORG. REPORT NUMBER
7. AUTHOR(s) J. Winter, D. Shifler		8. CONTRACT OR GRANT NUMBER(s) DAAD-05-73-C-0524
9. PERFORMING ORGANIZATION NAME AND ADDRESS Marvalaud, Incorporated P.O. Box 331 Westminster, MD 21157		10. PROGRAM ELEMENT, PROJECT, TASK AREA & WORK UNIT NUMBERS 1T762708A068
11. CONTROLLING OFFICE NAME AND ADDRESS USA Ballistic Research Laboratories Aberdeen Proving Ground, MD 21005		12. REPORT DATE MARCH 1975 13. NUMBER OF PAGES 170
14. MONITORING AGENCY NAME & ADDRESS (if different from Controlling Office) U.S. Army Materiel Command 5001 Eisenhower Avenue Alexandria, VA 22333		15. SECURITY CLASS. (of this report) UNCLASSIFIED 15a. DECLASSIFICATION/DOWNGRADING SCHEDULE N/A

16. DISTRIBUTION STATEMENT (of this Report)

Approved for public release; distribution unlimited.

17. DISTRIBUTION STATEMENT (of the abstract entered in Block 20, if different from Report)

18. SUPPLEMENTARY NOTES

19. KEY WORDS (Continue on reverse side if necessary and identify by block number)

Material Properties
Mechanics
Behavior

20. ABSTRACT (Continue on reverse side if necessary and identify by block number)

A collection of physical and mechanical properties have been examined for 20% gelatin gels made from Pharmagel A. Among those parameters measured are density, thermal conductivity, specific heat, specific capacitance, ultrasonic wave velocity, and coefficient of rolling friction. The critical field strength above which electrical properties change radically is documented. An equivalent passive circuit model is proposed. Fracture stress and elastic moduli are measured for strain rates from 6×10^{-4} sec^{-1} to 975 sec^{-1}.

DD FORM 1 JAN 73 1473 EDITION OF 1 NOV 65 IS OBSOLETE

UNCLASSIFIED

SECURITY CLASSIFICATION OF THIS PAGE (When Data Entered)

Shear stress at fracture and shear modulii are measured for strain rates from 8×10^{-3} sec^{-1} to 0.4 sec^{-1}. Fracture strains are also documented for many strain rates. The gelatin is examined for piezo-electric effects and electro-optic effects which would modify its stress birefringence by application of an electric field. Surface polarization effects are also examined. The nature of the fracture surface as a function of crack propagation rate is characterized. A visco-elastic transition strain rate is also documented. Finally, changes of density with storage time at fixed temperature and humidity and changes of density with variations in composition are examined.

TABLE OF CONTENTS

TABLE OF CONTENTS (Cont'd)

LIST OF FIGURES

LIST OF TABLES

1.0 Abstract

A collection of physical and mechanical properties have been examined for 20% gelatin gels made from Pharmagel A. Among those parameters measured are density, thermal conductivity, specific heat, specific capacitance, ultrasonic wave velocity, and coefficient of rolling friction. The critical field strength above which electrical properties change radically is documented. An equivalent passive circuit model is proposed. Fracture stress and elastic modulii are measured for strain rates from 6×10^{-4} sec^{-1} to 975 sec^{-1}. Shear stress at fracture and shear modulii are measured for strain rates from 8×10^{-3} sec^{-1} to 0.4 sec^{-1}. Fracture strains are also documented for many strain rates. The gelatin is examined for piezo-electric effects and electro-optic effects which would modify its stress birefringence by application of an electric field. Surface polarization effects are also examined. The nature of the fracture surface as a function of crack propagation rate is characterized. A visco-elastic transition strain rate is also documented. Finally, changes of density with storage time at fixed temperature and humidity and changes of density with variations in composition are examined.

2.0 Introduction

The objective of this work has been to characterize certain physical and mechanical properties of a particular production lot of gelatin. To make meaningful measurements, it is first necessary to create reproducible material for test specimens, and to create a reproducible set of test conditions. Given these conditions, it is then possible to proceed with experiments. The choice of parameters measured has been motivated by two considerations. The first is to provide numbers for use in models of dynamic behavior at high strain rates. The second is to examine properties which might lead to better ways of obtaining documentation of dynamic deformation at high strain rates.

3.0 Chemistry of Gelatin

The term "gelatin" is used to refer to a yellow-white powder, 100% protein, extracted by acid or base hydrolysis from collagen, the main matrix material of hide, bone and connective tissue. The term "gelatin" is also used to refer to a water solution of this powder. Gelatine refers to the material extracted by acid or base hydrolysis before electrolytes have been removed. When the electrolytes are removed (with ion-exchange resins), the purified material is gelatin.

Gelatin (the powder) is an aggregate, that is, there is no single molecular size and formula. Instead, gelatin is a collection of large protein molecules similar in amino acid composition. In a given gelatin sample there may be molecules of 17,000 m.w. and others of 300,000 m.w. Thus only the average molecular weight can be used in characterizing the gelatin.

Collagen is a structural protein in animal tissues. Some authorities believe there is a basic repeating unit in collagen, known as tropocollagen.[1]* The existence of tropocollagen is not generally recognized. There is not conclusive evidence to prove or deny its existence. Collagen's main importance is in gelatin manufacture. Therefore collagen research has not been extensive except as it relates to gelatin.

Gelatin is extracted from hide or other tissue by hydrolysis of the collagen molecule into smaller, water-soluble units in dilute acid or base. Gelatin extracted in acid differs from gelatin extracted in base. In fact, gelatin extracted at one pH differs from that extracted at pH $\pm$ one unit in either direction.[2] It would appear that the bonds broken (hydrolyzed) in acid differ from those hydrolyzed in base. This is consistent with the general properties of long organic molecules. Not only is the extracted material characteristic of and dependent on pH, but it is similarly dependent on electrolyte concentration. Gelatin can be "salted in" or "salted out" of solution.[3] Low concentrations of electrolyte aid in dissolving gelatin, and high concentrations reduce gelatin solubility.

There are ionizable hydrogen ions on the amino acid residues that will come off, depending on pH, to give the molecule a charge. There is a pH where the protein molecule as a whole is neutral, and will not

*Superscript numerals refer to references found on Page 148.

migrate in an electric field. This point is the pI, the isoelectric or isoionic point.[4] The pI is one parameter used to characterize gelatin.

Gelatin solutions above ½% (w/w) gelatin (in H_2O) have a sol to gel transition. In the sol form, the solution cannot support its own weight. In the gel form, the solution can support its own weight and can be molded into various shapes. This transition is temperature and concentration dependent. The sol-gel transition temperature is actually a range of temperatures. If you heat a gel to make the sol form, the transition temperature will be higher than if you coll the sol to form the gel. The transition range is about 5°. (Our gelatin solutions are 20% and the sol-gel transition range is just above room temperature, 30-35°C.)

The thermal history of gelatin solutions is very important.[5] Heat tends to break down the gelatin molecules and changes the nature of the solution. This process is an acceleration of the process known as ageing, where the inter- and intramolecular bonds break and reform into a least energy configuration. This is a continual process, hastened and sometimes even altered by bacterial action and thermal history. Once a least-energy configuration is reached, it is not necessarily stable. A large protein molecule such as gelatin has a three-dimensional structure and shape where the chain folds over itself and bonds form between different parts of the chain. Because of this structure, there are sometimes stresses along the chain such that when one bond is broken or formed along the chain, other bonds are then affected. There is no single final structure to end this sequence of changes. Eventually, the chain becomes small enough that it is relatively stable, but by that point the chain is so small that it could hardly be called gelatin, as we know it. The thermal history, the temperature changes over time, greatly affects the structure and thus the properties of gelatin. A gel solution cooled down to 25°C from 40° will differ in composition and properties from a gelatin solution warmed to 25° from 10°.

Gelatin is an aggregate, a collection of long chain molecules similar in amino acid composition. As a powder, it can sit for months with no noticeable change in composition.[6] But a gelatin solution undergoes noticeable change (ageing) in several days. There are several important parameters to control in making gelatin solutions. These are listed and dealt with in the section on preparing reproducible samples.

4.0 Preparation of Reproducible Samples

The first step in the program was to make a reproducible gelatin solution. Interested in the quality control in gelatin manufacture, we contacted Kind and Knox, producers of Pharmagel A, ordnance type gelatin.[7] From their information we ascertained that the only conventional quality control between lots is the Bloom jelly strength test. A given batch of gelatin must have a jelly strength within certain limits of a standard, so that all batches of certain type of gelatin have approximately the same jelly strength.

We concluded that the best way to insure a homogeneous gelatin supply

was to purchase all the test gelatin from one lot. Our test gelatin is from lot 14, Kind and Knox ordinance type Pharmagel A. The balance of the lot was purchased by BRL. Thus, the gelatin we are testing is from the same lot as that which BRL will later use in their test program.

The water used in making the sample gelatin is distilled, demineralized water, boiled before use. Distilled water was commercially obtained, and then passed through an ion-exchange resin cartridge before use. The water was boiled before use, not to get rid of CO_2 but to kill bacteria.

Initially, several methods of gelatin solution preparation were attempted. Low speed stirring solves the problem of foam developing on the top of the solution. But clumping of the gelatin is a problem then. High speed stirring reduces the clumping, but then foam is a problem. Of the two, the foam was less of a problem than the clumps. The small clumps of gelatin are caused when the gelatin powder imbibes water. They will eventually dissolve. But if one wishes to immediately cast the gelatin in a mold, the clumps and foam must be drawn off and discarded.

There is a method of gelatin solution preparation that simply calls for the gelatin to be added to water without mixing of any sort. The gelatin forms one large lump, and eventually goes into solution. During this process, the water must be kept at 65-70°C. After 15-20 minutes, the solution is stirred slightly. This method of preparation was unacceptable because the gelatin solution is at elevated temperature for too long. Also in making up large samples, without thorough mixing, the solution cannot be homogeneous. Therefore, it did not suit the purpose.

In making up samples for the Bloom gelometer test (test of jelly strength) the samples are made by a variation of the above technique. Only small samples are made up, and they are meticulously made. 7.50 g of gelatin are weighed into a special Bloom bottle. 105.0 g of distilled water at 25° are added. During this addition, the solution is stirred with a brass stirring rod. The sample is allowed to stand 1-3 hours. The bottle is placed in a 65° C bath for 8-10 minutes and stirred "just enough to effect thorough mixing, "[8] until the temperature is 61°. At this time, if viscosity of the sample is to be determined, part of the sample is removed and its viscosity measured. The sample bottle is then placed in a 45° bath for 30-40 minutes. The bottle is inverted several times to mix in any water condensed above the liquid level, foam is removed, and the sample placed in a 10° bath "undisturbed for not less than 16 nor more than 18 hours."[9] Then the measurement is made. The measurement made is the mass of lead shot poured into a receiver on top of a plunger to depress that plunger a certain distance (4 mm) into the gelatin. If it takes 300 grams of polished lead shot to depress the plunger that distance into the sample, the sample is said to be 300 bloom.

This is the test used by gelatin manufacturers to test individual lots of gelatin. This is the only test mentioned in the literature specifically for quality control. This test controls thermal history, and ageing, by specifying time and temperature. Because of the nature

of the substance gelatin, thermal history and ageing must be specified. But that does not make the Bloom gelometer test a valid test of reproducibility of sample. As of now, there is no accepted test of reproducibility other than this.

4.1 Small Sample Method (500g)

During the first quarter of the program, a 500 gram sample of gelatin solution was made in the following manner: 400 grams of distilled, demineralized water are brought to a boil, then allowed to cool slightly. (A small amount of water is lost due to the boiling.) Enough water is added to the boiled water to make 400.0 grams. If the temperature is not now at 75°C after the addition of the small amount of water, it is allowed to cool to that temperature. 100 grams of gelatin is added to the water, in a slow even stream, while the water is stirred with a 2" high speed stirrer. If the water is stirred at high speed, and the gelatin added slowly, and evenly in a fine stream, there will be a good mix, without clumping. Any small clumps which may develop can be dissolved by high-speed stirring. The gelatin solution should now be at 50-60°C, and can be poured into molds easily. Any bubbles or foam should be removed with a spoon before pouring.

At the end of the first quarter, three revisions were made in this method. First, the temperature of mixing gelatin with water was decreased from 75°C to 70°C. Second, the gelatin was added to the water more quickly. Finally, the gelatin was sealed and allowed to stand at room temperature (approximately 20°C) until 90 minutes lapsed from the time the gelatin was initially added to the water.

Since heat tends to break down the gelatin molecules and change the properties of its solution, we were interested in minimizing temperatures used. It was found that the gelatin can still be dissolved completely to form a 20 per cent solution when the temperature is lowered from 75°C to 70°C. The lower temperature should decrease the rate of gelatin degradation. During all subsequent work, all samples were prepared by mixing the gelatin at 70°C.

During the first quarter the gelatin was added slowly and evenly in a fine stream. In the revised method, the gelatin is added more rapidly into solution, still in an even stream. Any clumps which are formed are dissolved by high speed stirring. Less foam was produced by this technique. For example, 2-15g of foam is produced in a 500g batch of gelatin.

The time needed to dissolve any clumps varies from sample to sample. Air bubbles and foam may still be interspersed throughout the gelatin solution 15-20 minutes after stirring. Therefore, each sample was sealed with aluminum foil after stirring, and allowed to stand until 90 minutes had lapsed from the time the gelatin powder was first introduced to the water, before casting. This was to insure that all the foam has risen to the surface. The temperature of the gelatin decreased from the initial 70°C to 40-45°C each time before casting.

As a preservative, 0.02ml of cinnamon oil is added to each 500g gelatin batch during mixing.

4.2 Large Sample Method (8750g)

About one hundred blocks of 20 per cent gelatin were needed for the density experiment. To guarantee that the initial densities of all the blocks were identical, the blocks were all cast at one time from one large batch. Several adaptations of the method developed in the first quarter for 500g samples were attempted. First, a portable household mixer was tried. It completely dissolved the 3500g of gelatin, but 600g of foam was produced. The gelatin density was then measured and found to be 1.052 $\pm$ 0.003g/ml. The density of 20 per cent gelatin from small sample preparation is 1.059, $\pm$ .001g/ml. Apparently, the foam is not the same composition as the solution. Therefore the amount of foam produced affects the gelatin density.

In order to minimize the amount of foam produced, a second adaptation was to go back to the stirrer used in the small sample preparation and use it for a large gelatin batch. Complete solution occurred and only 300 grams of foam was produced. The density of the gelatin was 1.054 $\pm$ 0.002g/ml. This arrangement was rejected because the small stirrer did not appear to mix the entire batch homogeneously.

By using a larger stirrer (4" x 5" oval steel), a high speed mixer, a temperature of 68-72°C during mixing, a 10 liter container, and a 2 hr. mixing time, gelatin with a density essentially equal to small sample gelatin density was produced (1.063 $\pm$ 0.005 g /ml). Holding the temperature at 68-72°C helps put the gelatin into solution. The larger stirrer at high speed mixes the gel solution more uniformly. (For diagram of the large sample apparatus see Figure 1). Mixing for shorter times (eg $\frac{1}{2}$ hr.) gave rise to large deviations in density, apparently due to inhomogeneities.

The large gelatin batch was prepared by first heating 7.000kg of demineralized distilled water to boiling and then allow it to cool to about 75°C. Enough demineralized distilled water was added to make up for the water boiled off and then the water was cooled to 70°C. At 70°C, the gelatin was added slowly in five 350g portions over a two hour period to form the 20 per cent solution. The temperature was kept at 68-72°C to ease mixing and high speed stirring was used to dissolve any clumps formed. Cinnamon oil (0.35ml) was added as a preservative during mixing. After mixing, the gelatin solution set for 20 minutes to allow the foam to rise toward the surface. The foam was removed and the gelatin was siphoned into polystyrene cups. The cups were sealed with aluminum foil and placed overnight in the refrigerator. The next day (13-14 hours later) the gelatin blocks were placed in constant humidity chambers. Appendix A lists density measurements for some selected typical examples of both the small and large sample preparation methods.

5.0 Thermal Conductivity

Thermal conductivity is an experimentally measured quantity. By designing apparatus such that heat flow is one-dimensional, experimental design and interpretation is simplified. Our experimental design approximated one-dimensional heat flow by casting polyurethane insulation tightly around the heat source and gelatin specimen. Figure 2 shows the

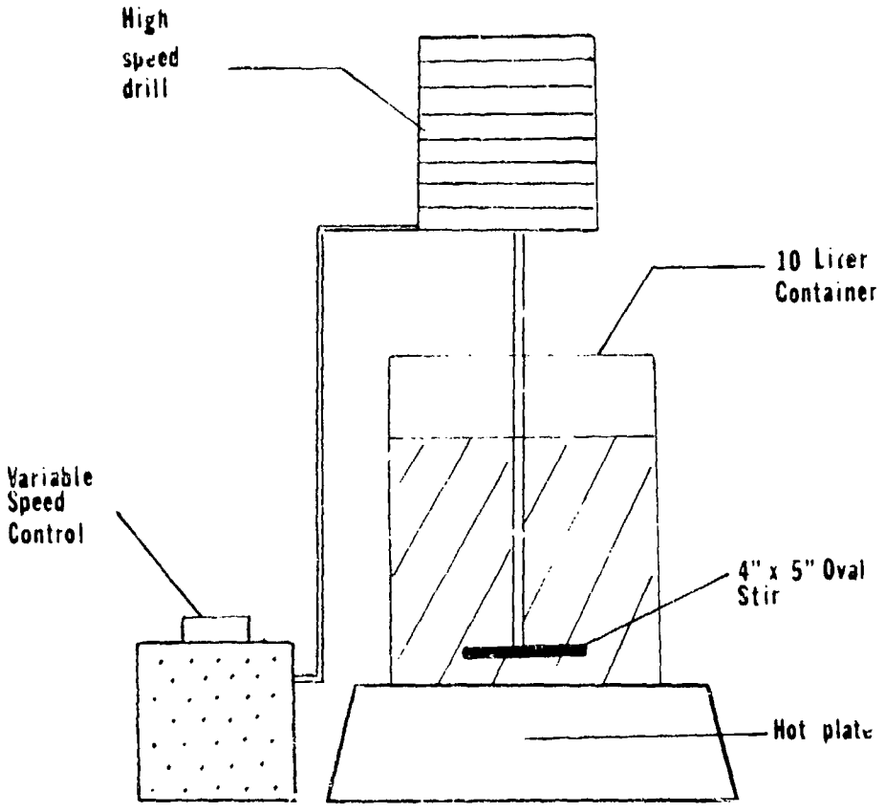

Figure 1

Large Sample Apparatus

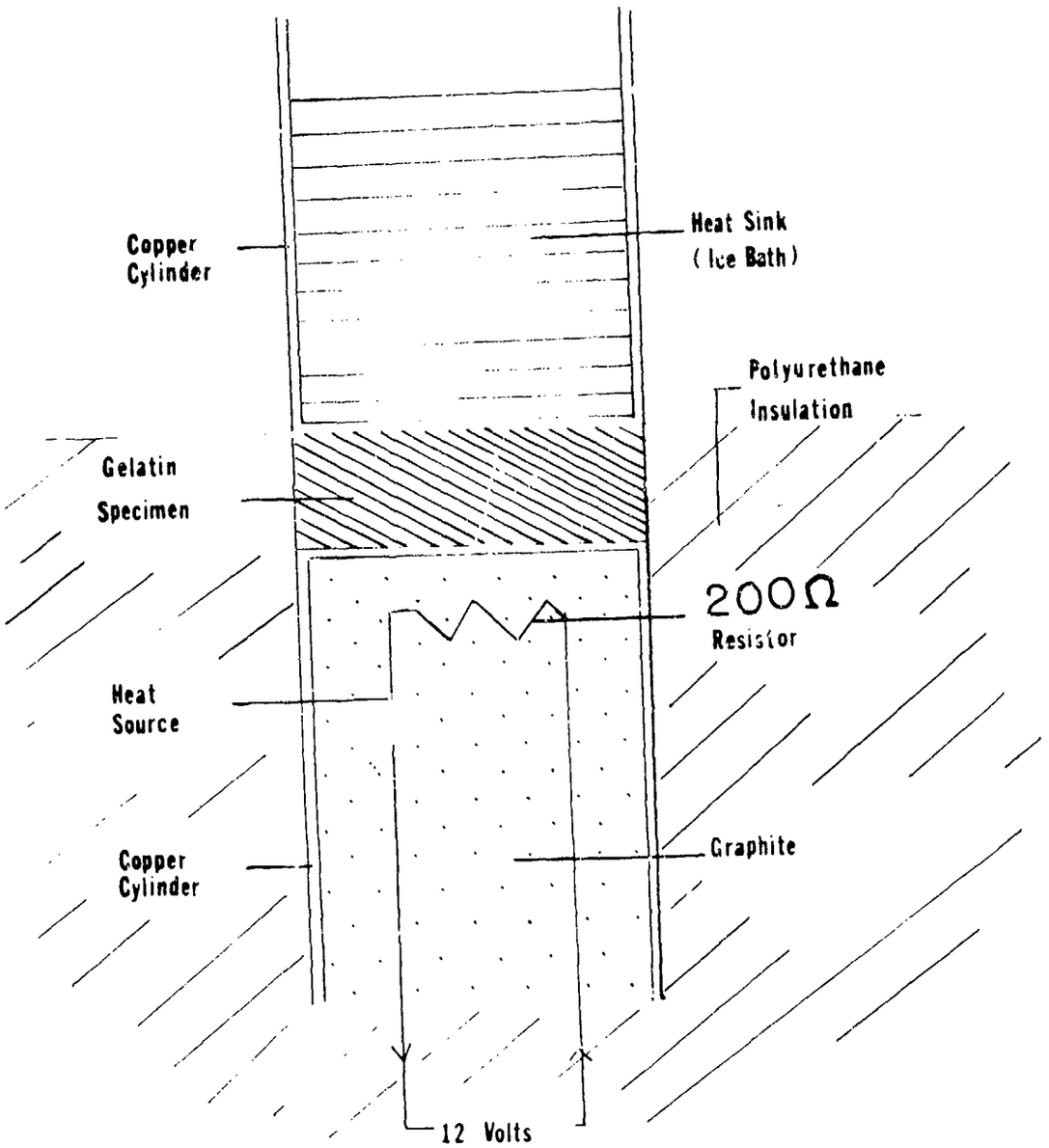

Figure 2

Thermal Conductivity Design

apparatus design. Temparatures on either side of the specimen are measured by iron constantan thermocouples. The heat sink is a copper crucible, filled with melting ice. By keeping the copper crucible filled with ice, its temperature can be kept constant without gradients inside the crucible. This is particularly important once the steady state is reached. Joule heating is used to accurately put a known quantity of heat per unit time into the source. The source is a copper crucible with a resistor imbedded in carbon inside. The crucible is sealed and inverted. The carbon serves to spread out the heat uniformly and the copper provides good thermal contact with the gelatin specimen. Gelatin was prepared by the small sample method.

The data for thermal conductivity runs is given in Appendix B. For the first run, a 300 ohm resistor was imbedded in the copper crucible. The temperature difference between top and bottom of the gelatin specimen was 8.8°. A 12 V potential was placed across the resistor, giving 0.480 watts of power. A value of 0.00089 cal/(sec cm^2) (°C/cm) was calculated.

This first run was done to experiment with the proposed technique, more than to measure thermal conductivity accurately. Improvements were made in the insulation and the heating unit. For the next run, a 200 ohm resistor was imbedded in the copper crucible heat source. A 12 V potential is again placed across the resistor. The temperature differential of 20.6° was measured. The thermal conductivity calculated from this run is 0.00085 cal/ (sec cm^2) (°C/cm).

The third run was done with exactly the same equipment and conditions. The temperature differential was 19.8°C. The calculated thermal conductivity here was 0.00081 cal/ (sec cm^2) (°C/cm).

The average thermal conductivity as measured is 0.00085 cal/ (sec cm^2) (°C/cm). The value for water is 0.0014 cal/ (sec cm^2)(°C/cm).[10]

6.0 Specific Heat

The procedure for measuring the specific heat of 20% gelatin gel has undergone major modifications. The initial procedure was to have a gelatin sample at one temperature and a bath at a higher temperature. The gelatin warms up as the bath cools down. The heat lost by the bath should equal the heat gained by the gelatin sample. See Appendix C for method of calculation.

For the first run, ninety grams of gelatin prepared by the small sample method was cast into a 100 ml beaker. The gelatin and beaker were allowed to equilibrate at 6° C in the refrigerator, overnight. 300 g of water (distilled) was placed in a large Dewar flask. The beaker with the gelatin in it is placed in the bath suspended by a thin wire hanger so that the level of the bath is only 1/2 inch below the lip of the beaker. Temperature of the bath and of the gelatin is monitored by thermocouples. The Dewar is sealed with a styrofoam lid which fits down inside it. The bath water is initially at room temperature, 26.5°C, and the gelatin block at 6.5°. When equilibrium is established, both the bath and the gel are at 25° C. Assuming the specific heat of gelatin

to be constant over the range involved, the specific heat of water could be used to calculate the specific heat of gelatin. The experiment was repeated using water at 6.5° in a beaker instead of gelatin in the beaker. This technique showed gelatin to have a specific heat of 0.344 cal/g/°C. The second run, done in the exact same manner gave a value of 1.06 cal/g/°C, followed by values of 0.843, 1.57, etc. See Figure 3, class 1.

The first modification in technique was the use of hexane in the bath instead of water. This allowed us to immerse the gelatin blocks directly in the bath without the glass beaker. (See paragraph 7.0 for the justification of this method). This allowed for faster equilibration. In this same modification, the Dewar was assumed to have no heat loss under the temperature gradient of the experiment and in the time necessary for equilibrium, about 20 minutes. The validity of assuming no heat loss through the Dewar rests in an experiment where 200 g of hexane were placed in the Dewar at 4-5° above ambient temperature. Temperature of the solution was monitored over time, and no noticeable temperature difference was recorded in a 45 minute period. Also the idea of preconditioning the Dewar to the hexane temperature prior to the run was initiated here. This was to insure that the Dewar is not taking heat from the bath.

This method gave values like 1.65, 1.60, 1.18, 1.09, 1.13, .68, etc. and offered little improvement over earlier work as far as reproducibility and consistency of specific heat values. See Figure 3, class 2. During this time three runs on samples from the same batch of gelatin gave a value of 1.13±0.03. This is the greatest precision found between different samples from the same batch. While its precision is high, the accuracy of this number was in doubt. More runs were undertaken to prove or disprove this value.

These runs gave values like 0.483, 0.340, 1.63, 0.668, etc. See Figure 3, class 3. New modifications were discussed in the attempt to get consistent data.

Preconditioning the Dewar was abandoned because it was thought to be ineffective. A significant modification was to move the entire apparatus into an underground tunnel at Marvalaud. A chamber in the tunnel, sealed from the surface is at relatively constant temperature and humidity. The experiment was moved to this underground chamber to minimize effects of change in room conditions from day to day. The hexane was stored in the tunnel at the tunnel room temperature. With these modifications, values for specific heat in calories/g/°C were 1.04, 0.70, 0.81, etc. See Figure 3, class 4. The range of values had begun to lessen. At this point, the gelatin sample temperature was changing 10-12° but the bath temperature was changing only 1-2°. The gel samples weighed 30 g; the mass of the bath was 300 grams.

In order to increase the temperature change of the bath, two, and then three samples at a time were immersed in the bath, and the mass of the bath was decreased to 200 g. Bath temperature changes of 5.7° for two samples (with 130 g of hexane in the bath) and 6.8° for three samples (with 200 g of hexane in the bath.) Values of specific heat of 0.62 cal/g/°C for two thirty gram blocks immersed at the same time, and

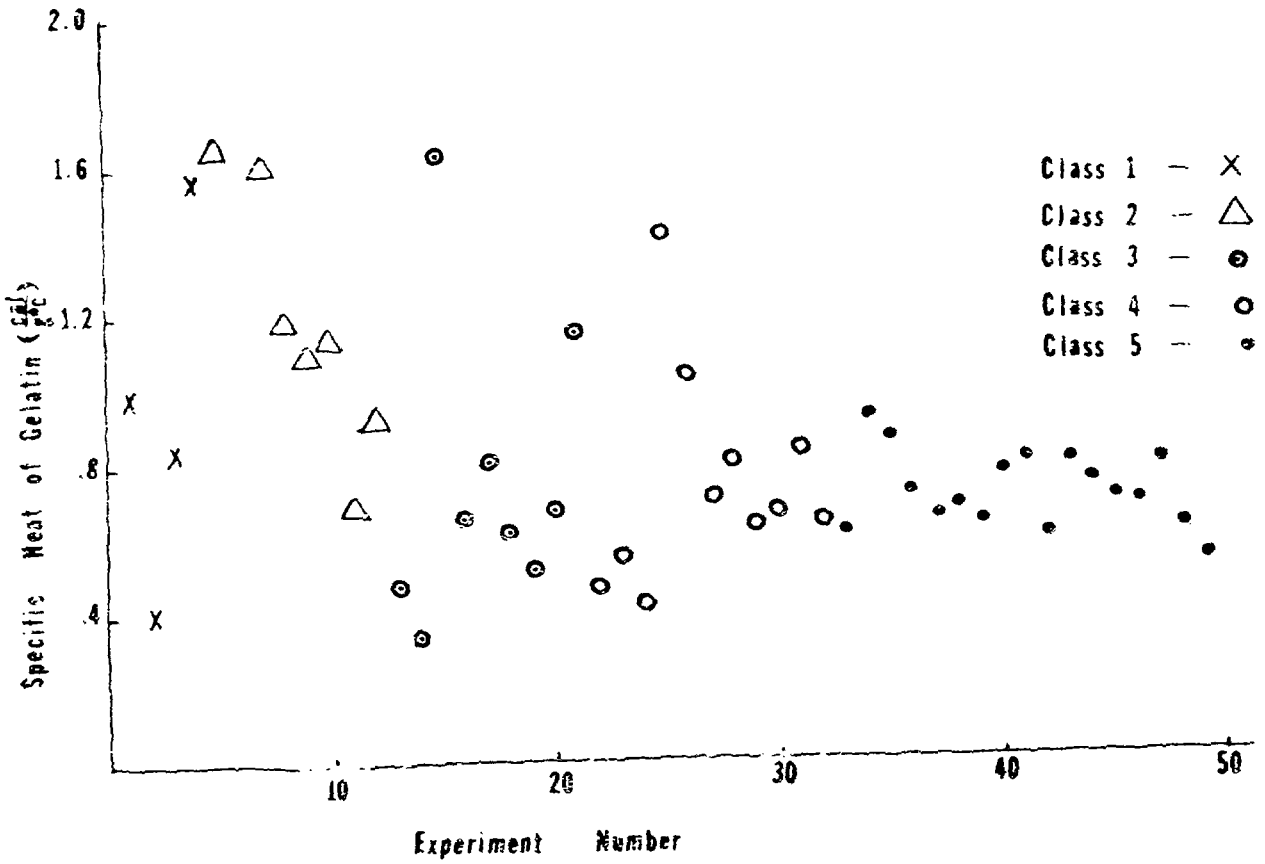

Figure 3: Specific Heats of Gelatin by Technique Used

0.92 cal/g/°C for three blocks immersed at one time. Later values using three blocks at a time were 0.86, 0.72, 0.66, 0.68, 0.64, 0.77, etc. See Figure 3, Class 5. For these later values, the hexane used in the bath was equilibrated at 31° in a constant temperature water bath prior to use. The temperature change in the hexane during the run increased to a 9° change, and the change in gel temperature was about 13°. The gel blocks were alway completely immersed in the hexane which required about 150 g of hexane.

On the basis of the last series of runs, those done in the tunnel chamber using three blocks of gelatin per run, an average value of 0.72 cal/g/°C (for 17 runs averaged) was calculated, with a standard deviation of 0.08.

To determine whether the revisions in the small sample preparation technique significantly altered anything, the specific heat of gelatin was measured again. Using the same technique (class 5 of specific heat measurement), the values obtained were 0.69, 0.66, 0.77, 0.53, 0.32, 0.75, 0.72, and 0.69 cal $gm^{-1}\ ^{o}C^{-1}$. The average value of these eight points is 0.64. It is felt the difference is not significant.

7.0 Density Measurement

Archimedean displacement measurement is the simplest method of volume determination in density measurement, useful especially for irregular geometry not readily measurable. However, a block of 20% gelatin- 80% water can not be immersed in water without affecting the gel block. Actually, two processes occur, both osmotic in nature. The gelatin dissolves in the water, and water is taken up by the gelatin block. It is clear that either of these two processes will change the density of the gelatin block. Since the gelatin gel is soluble in water, a search was conducted to find a liquid that would be totally inert to the gel, and that had a density less than the gel. There is an organic chemistry rule of thumb that polar solvents dissolve polar materials. A corollary of that is non-polar solvents will not dissolve polar materials. A gelatin gel is 80% water, a polar substance. Although the large gelatin molecules are overall neutrally charged or nearly so, they contain polar groups throughout. Thus it was reasoned, a non-polar solvent should be totally inert to the gelatin block. This was found experimentally to be true for hexane, an alkane commonly used in chromatographic work when a non-polar solvent is required. Using hexane, we could use the Archimedean displacement method for density determination. Later, we found a report in the literature in which benzene was used for the same purpose.[11]

The hexane used for the Archimedean displacement method of density measurement was a mixture of hexanes, mostly n-hexane, obtained as a reagent grade chemical. Mass in air and mass immersed in hexane were recorded. The difference in these masses equals the mass of hexane displaced. By knowing the density of the hexane, the volume of hexane displaced (which equals volume of gel block) could be calculated. The density of the hexane was determined by measuring the mass of 25.00 ml of hexane in a volumetric flask. This measurement was done immediately after the gelatin measurements. Significant changes in hexane density

can occur if its temperature changes very much.

Mass measurement was done with an analytical balance, yet the masses are only recorded to hundredths of a gram. There is an important reason for this. The samples measured were stored prior to measurement over $ZnSO_4 \cdot 7H_2O$ saturated solution at 6° C, giving a 94.5% relative humidity environment.[12] (Hygroscopic salt solutions are used to control humidity so that it is constant and reproducible.) When these gelatin samples were removed from their low temperature, high humidity environment, they began to gain in apparent mass at the rate of 5-6 mg/minute, up to a maximum point and then they lose apparent mass. Our technique was to measure to the nearest hundredth of a gram in less than two minutes, before the change in mass became significant.

Early in the program of density measurements, two other problems were discovered. First, the density or the hexane used slowly increased during a 3-4 week period. Second, the hexane density changed during the measurement because it was slowly changing temperature. Therefore, changes were made in the density measurement procedure.

With respect to the first problem, the density of the hexane used in the initial gelatin density determination increased from 0.6630 g/ml to 0.6680 g/ml during a period of one month. Hexane has a small but finite solubility in water, (0.0138 g hexane / 100 g H_2O at 15°C).[13] To determine whether the change in hexane density was because of its exposure to gelatin during the Archimedean density measurement, the densities of several gelatin samples and some hexane were measured and the gelatin was then stored in the hexane for two weeks. The gelatin was weighed in air and in the hexane in which it was stored. Density of this same hexane was also measured. Both the gelatin density and hexane density were unchanged during the two weeks. Therefore, the hexane density should not change during the brief time gelatin is weighed in hexane. However, just to be sure, thereafter fresh reagent grade hexane was used each time.

The second problem arises because the gelatin is stored at 5-7°C, while the density measurement is made at room temperature. If the hexane is also stored at 5-7°C, then it slowly warms toward room temperature as the density measurement is made. If the hexane is stored at a higher temperature, it is slowly cooled by the gelatin as the density measurement is made. To solve this problem, the density of fresh reagent grade hexane was measured at several different temperatures and a hexane density-temperature graph plotted. (Figure 4) The temperature of hexane was then measured just as each gelatin block was weighed in the hexane. The hexane density corresponding to that temperature was then used for calculating the gelatin density.

7.1 Change of Density with Composition

Information on how the density changes with composition is useful in two areas. First, it provides insight on how well the reproducibility of specimen preparation can be checked by density measurements. Second, it serves to enable estimates of water loss in the experiments which measure change of density with time of storage at constant humidity and temperature.

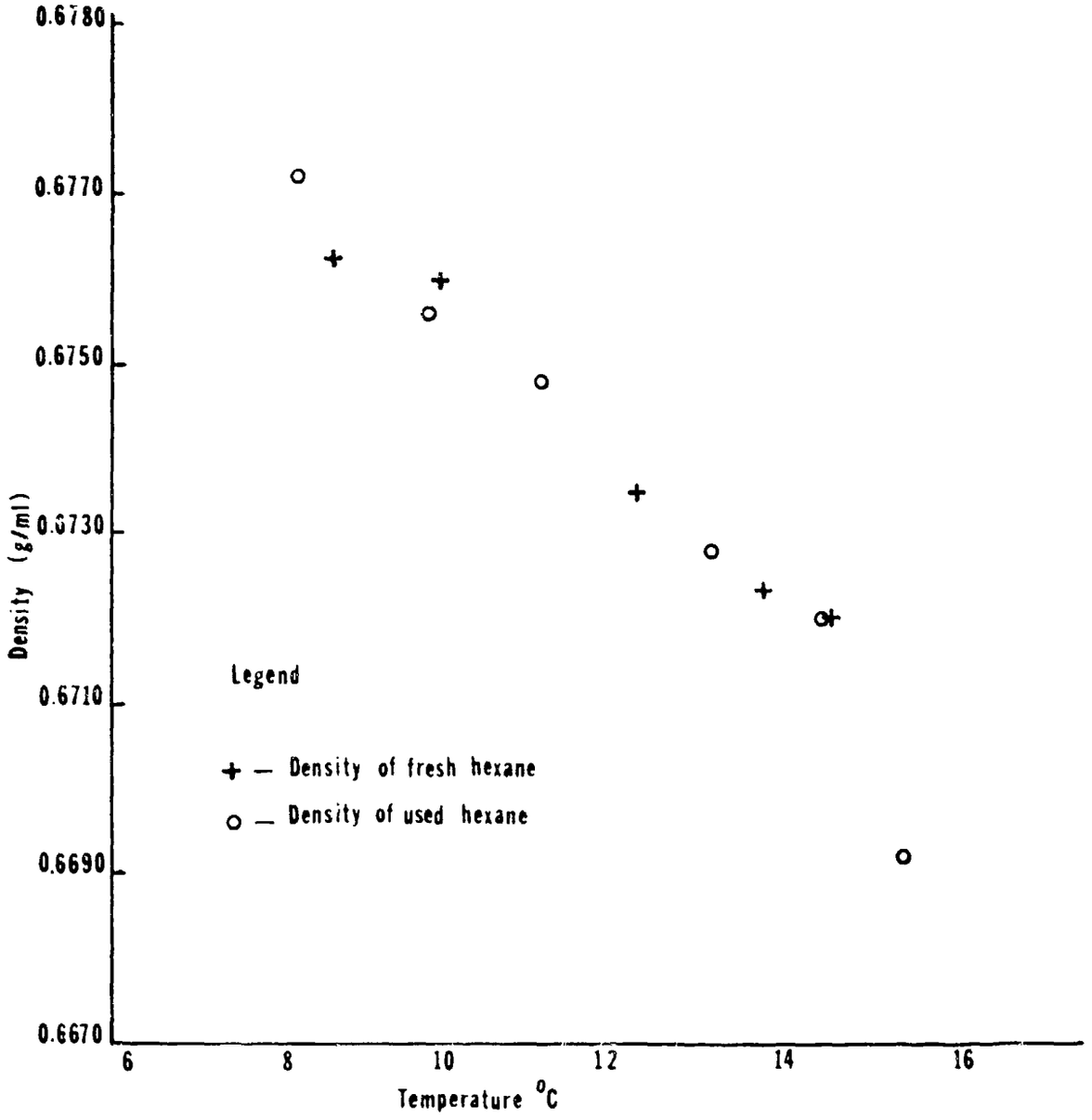

Figure 4

Hexane Density vs. Temperature

To establish a plot of density versus weight percent gelatin, we chose to measure the density of 5.0, 10.0, 12.5, 15.0, 17.5, 20.0, 22.5, 25.0, 27.5, and 30.0 weight percent gelatin solutions. For each, 400-500g gelatin solutions were prepared. About ten samples were taken at each concentration. The densities were measured, averaged, and the average density of each batch is plotted in Figure 5 as a function of its composition. Appendix D gives the details of the data.

Errors in Figure 5 may be assessed as follows. The apparent density of gelatin can be affected by the temperature dependence of the hexane density. Furthermore, the actual density of the gelatin can be affected by the amount of foam removed from a gelatin batch. For example, in the 30.0% gelatin preparation, 43g of foam was recovered out of a total of 400g of water and gelatin powder. If one assumes (as a worst case) that the foam contains 5% gelatin, the weight percentage of gelatin in the remaining defoamed solution would be 33%. Similarly, for a 20% gelatin preparation a maximum of 10g of foam is recovered. Again using the assumption that the foam contains 5% gelatin, the remaining solution would be 20.3% gelatin. The hexane density changes 0.0008 - 0.0010 g ml^{-1} deg^{-1}. A 2 C° temperature uncertainty implies an uncertainty in the density of both gelatin solutions of 0.002 g/ml. The errors introduced by foam and the temperature dependence of hexane density can be represented by the error bars in Figure 5.

7.2 Change of Density with Storage Time

The next and final step in the density work was to monitor changes in density with time, under constant temperature and constant humidity.

The experiment was designed to keep the humidity constant by using a saturated aqueous calcium chloride solution in a sealed container. When water is saturated with anhydrous calcium chloride, the hexahydrate of calcium chloride ($CaCl_2 \cdot 6H_2O$) is formed. At a constant temperature, the hexahydrate, the saturated water solution, and water vapor will exist at an equilibrium pressure. The humidity in the container will remain constant as long as the three phases exist in the system, and the temperature remains constant.[14] The three phase system was prepared by adding 64.0g of anhydrous $CaCl_2$ to every 100g demineralized distilled water.[15] Some solution was then placed in each container; the containers were sealed, and placed in the refrigerator. The refrigerator temperature is near 7°C. At this temperature, the relative humidity within the containers was 37-38%. (See Figure 6).

Gelatin was prepared by the large batch preparation method, cast into blocks, and placed in storage in the refrigerator inside the sealed constant-humidity containers.

Ten gel blocks were initially randomly picked from the large batch. The average initial density of these samples was 1.063 g/ml. The average deviation was $\pm$ .005 g/ml.

The density of gelatin was measured during the next seventy days. Two to four samples were measured at a time to evaluate reproducibility. The specimens show an increase in density, which undoubtedly stems from

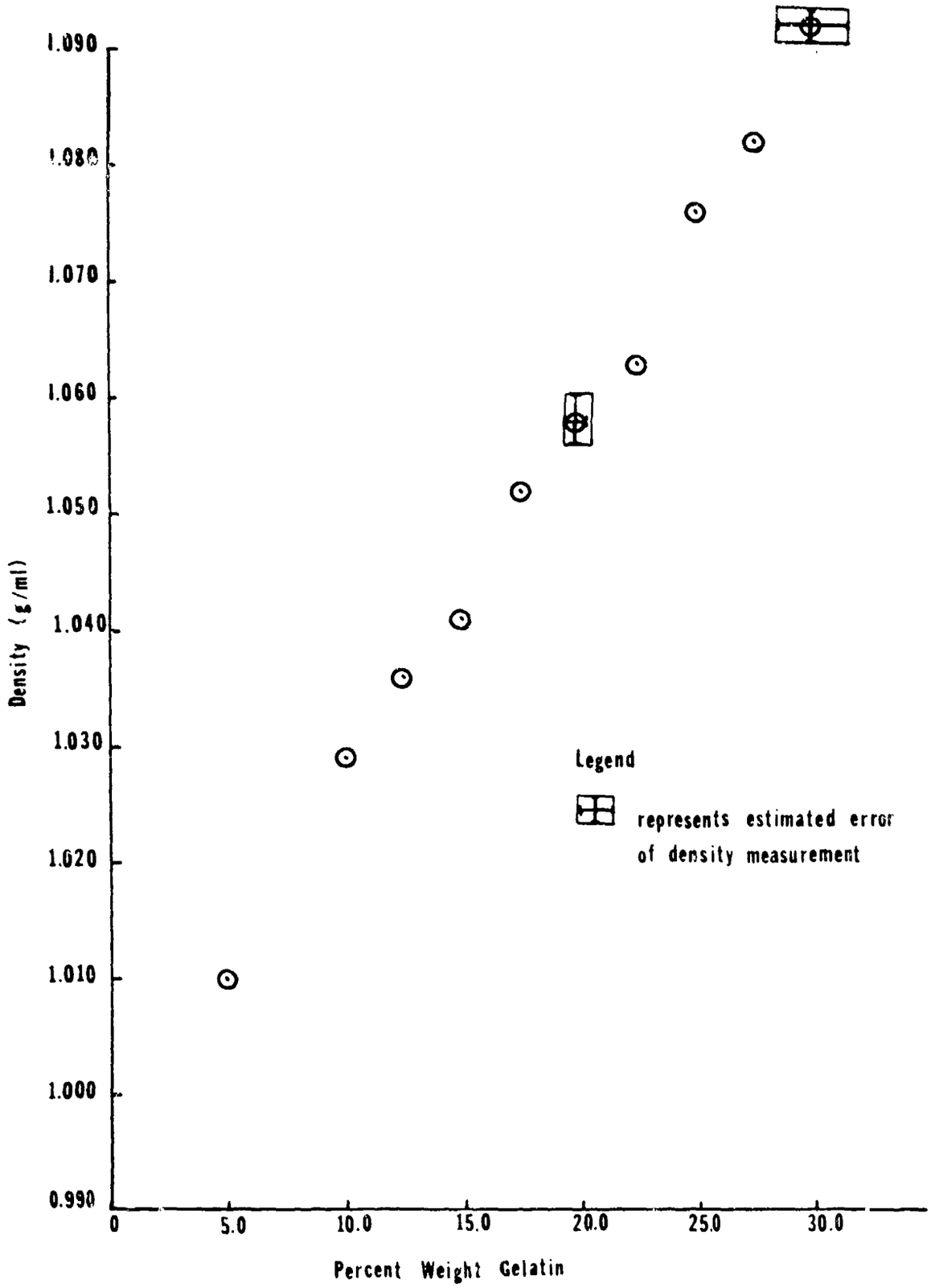

Figure 5: Weight Percent Gelatin vs. Density of Gelatin

From CRC Handbook of Chemistry and Physics 36th ed. p. 2310

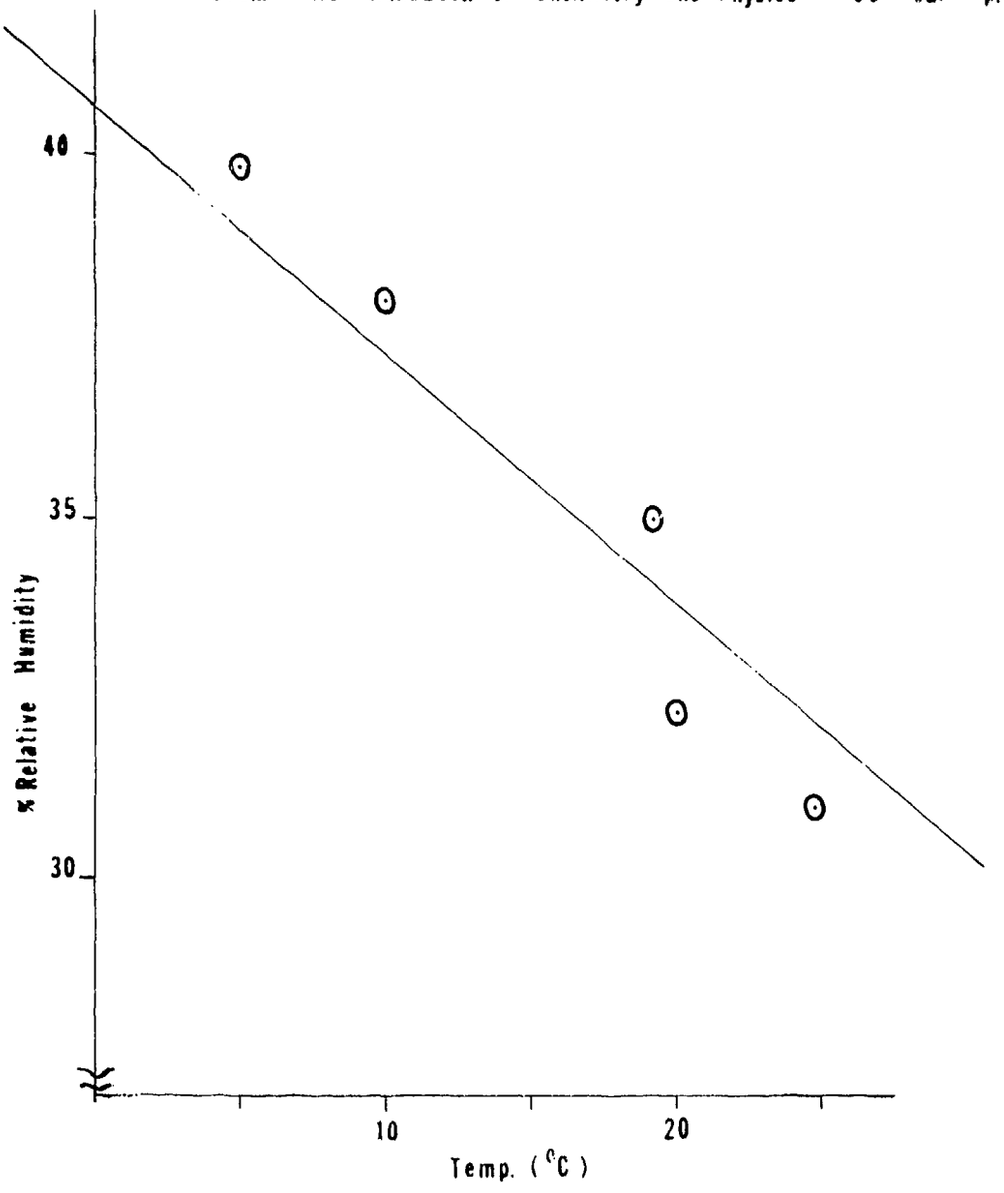

Figure 6

Relative Humidity above saturated $CaCl_2$ solution

the water lost from the gelatin surface. However, the experiment revealed the presence of a humidity gradient inside the humidity chambers. There was a difference in gelatin density depending on where the sample was placed in the humidity chamber. Each chamber had two layers. Above the top layer, water had condensed on the bottom of the lid for the container, effectively placing the upper layer near 100% humidity. The gelatin must have effectively masked the top of the container from the hydroscopic effect of the salt solution system below. One particular container had its lower level completely filled with gelatin blocks. The gelatin blocks on its upper level were not noticably deformed, indeed, some samples appeared totally unchanged after 75 days in the container. Another particular container had only two samples on the lower level with the upper level completely filled. The samples on the upper level were deformed and had acquired a hard skin on its surface. Their density had increased.

The results were separated into two groups, one for the upper layer and one for the lower layer. See Figure 7, and Appendix E. The samples on the lower layer became deformed after only 4 days and this deformity gradually increased with time. The lower layer gelatin first developed a hard outer skin and then gradually shrank in size and changed from its initial pale yellow color to a dark amber color. The density of gelatin on the lower level on day 67 was 1.222 $\pm$ 0.010 g/ml for four samples. This corresponds to a composition of between 80-90 weight percent gelatin. This means 18-21 grams of water was lost from a 20% gelatin sample with an initial weight of 30 grams.

The density of the top layer gelatin increased slowly after the 28th day (it remained unchanged for the first 28 days). The average density for four samples on day 35 was 1.070 $\pm$ 0.004 g/ml. The density on day 67 was 1.087 $\pm$ 0.022 g/ml. The gelatin by day 67 had obtained a plastic outer shell and the color had changed from a pale yellow to only a more intense yellow. The amount of water loss for a 30g gelatin sample on the upper level was about 2-3 grams during the 67 day period.

A second experiment was conducted with some revisions to eliminate the problems described for the first experiment. In the first experiment, a fine wire screen was used to shelve the gelatin blocks in each container. For the second, revised, experiment, one-half inch holes were punched in the screen so that the ventilation would be improved in each container. Each container also had only one layer of gelatin for the second experiment. In the second experiment, the calcium chloride solution was prepared as before, but an additional 15g anhydrous $CaCl_2$ was added for every 164g of solution, to insure that the three phrases were present. Once gelatin was placed in the chambers, the solid hexahydrate slowly went into solution. Therefore, anhydrous calcium chloride was added each week to maintain the hexahydrate phase.

In the second experiment, the density of gelatin was measured during fifty-eight days by our Archimedean displacement method.

The gelatin in the first set (Series A) was prepared by the large batch preparation method. Ten samples were measured to determine the initial density of the first run. The initial density of all the blocks

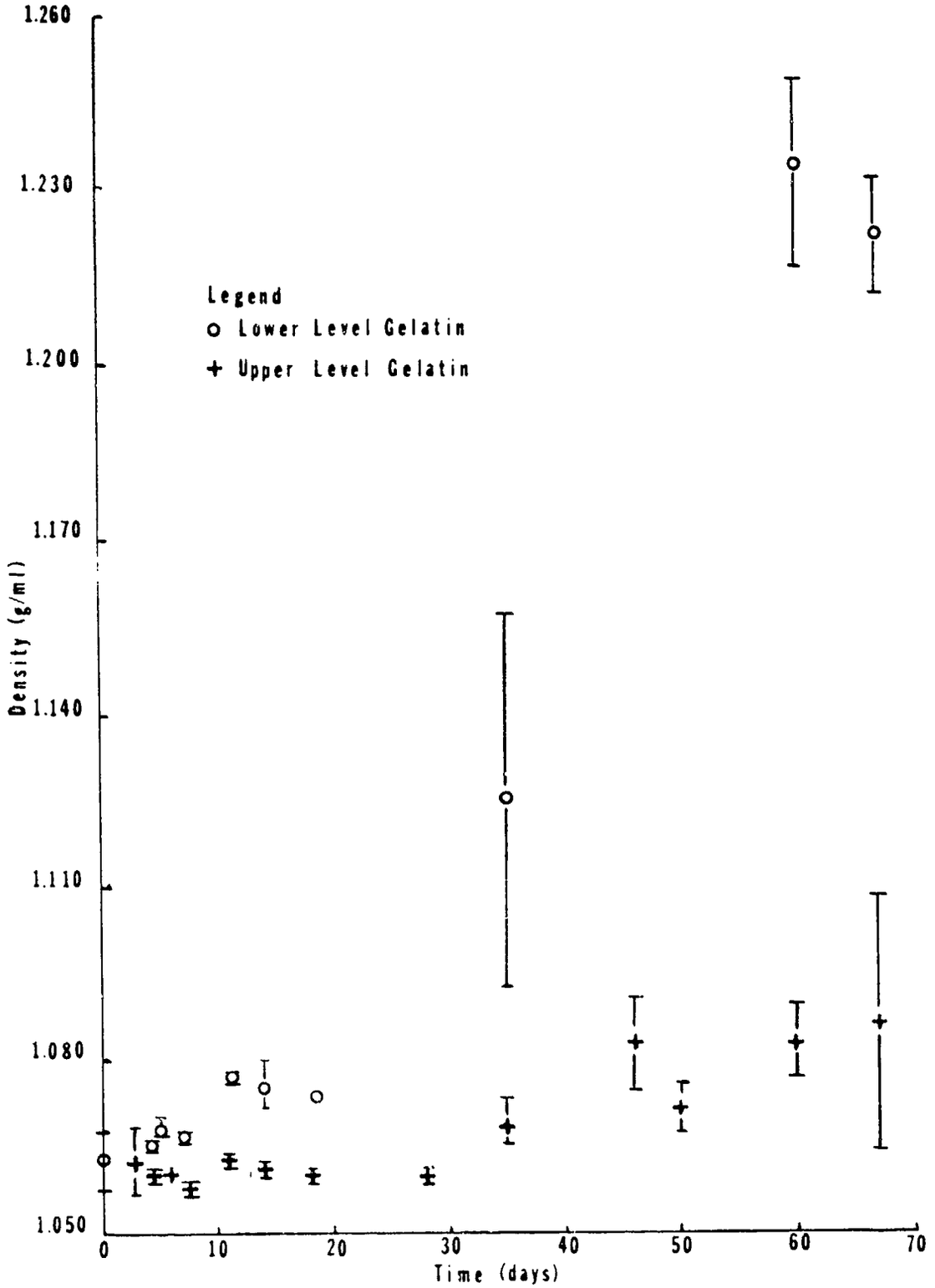

Figure 7 Density of Gelatin vs. Storage Time

was assumed to be identical, 1.062±0.001g/ml. One to three samples were measured each day. After measurement the sample was numbered and put back into the container for occasional later measurements. In recording, the gel sample has two numbers. For example, 35-48 would mean that sample 35 was measured during the 48th day the sample had been at 37-38% relative humidity.

To check the first set, a second set, (Series B) was prepared. The gelatin in this series was made by our small sample preparation method. The average initial density of three samples was 1.058±0.002g/ml.

The density changes for runs A and B are similar. The results are summarized in Figures 8 and 9, and Appendices F and G. The density increase does not seem to be constant but has a spread of values. In both the A and B series the density increased slowly to about 1.08g/ml after five days. Gelatin density then remained between 1.080-1.090g/ml for 7-20 days. After this period the density increased more rapidly, about 0.008-0.010g/ml per day in both runs. In series A, the density eventually seemed to reach a limiting maximum density of between 1.310-1.320g/ml after 40 days. In series B, gelatin density did not seem to have reached a limiting density. The density of 2-41B was 1.287g/ml. However, voids developed inside all of the gelatin blocks in series B after 30 days. This would have little effect on the gelatin weight, but would increase the apparent volume and decrease the apparent density of gelatin. This is noted in Figures 8 and 9.

The gelatin in both runs began to develop a hard outer skin after 3 days and gradually shrank in size. A gel block lost about 19-21 grams of water after 35 days, but only 1-2 grams between 35-58 days. This corresponds to an 80-90 percent gelatin concentration by weight.

8.0 Electrical Resistivity

An interesting phenomenon of 20% gelatin gel is its change in electrical resistivity with time under the influence of an applied field. This phenomenon is qualitatively understandable when one considers the mobile ions and readily-removable groups in gelatin. Amino, hydroxyl, and thiol groups are present as well as a multitude of hydrogen ions. As well, small chain fragments (m.w. up to several thousand) can readily migrate through the gel under the influence of just a small field. At first, resistance measurements were made with a field-effect-transistor volt-ohm-meter (FET-VOM), and the observation was made that resistance, measured that way, changed with time. Soon thereafter, it was recognized that during the "resistance" measurements, the gelatin was becoming charged. More descriptively, one could stop the "resistance" measurement and then measure significant voltages across the gelatin. Not only that, but if one were to short out the electrodes across the gelatin (to "discharge" it) for a few minutes, and then make a voltage measurement, there would still be a significant voltage present. This voltage would, however, slowly decay with time.

The gelatin was apparently becoming polarized (as well as storing surface charge) so that it behaved like a low grade electret. A little consideration of what a FET-VOM "resistance" measurement really means

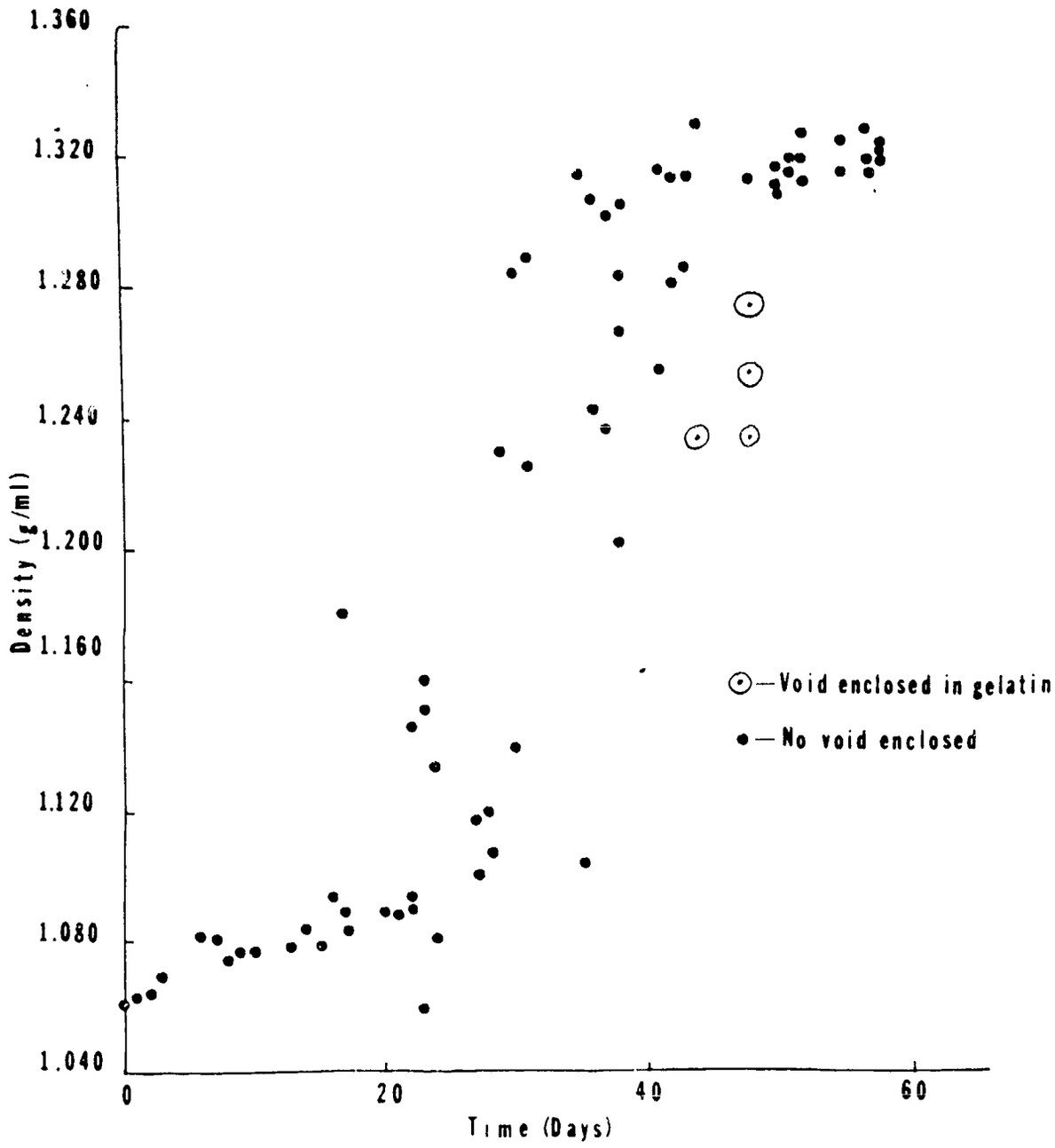

Figure 8: Gelatin Density vs. Storage Time Series A

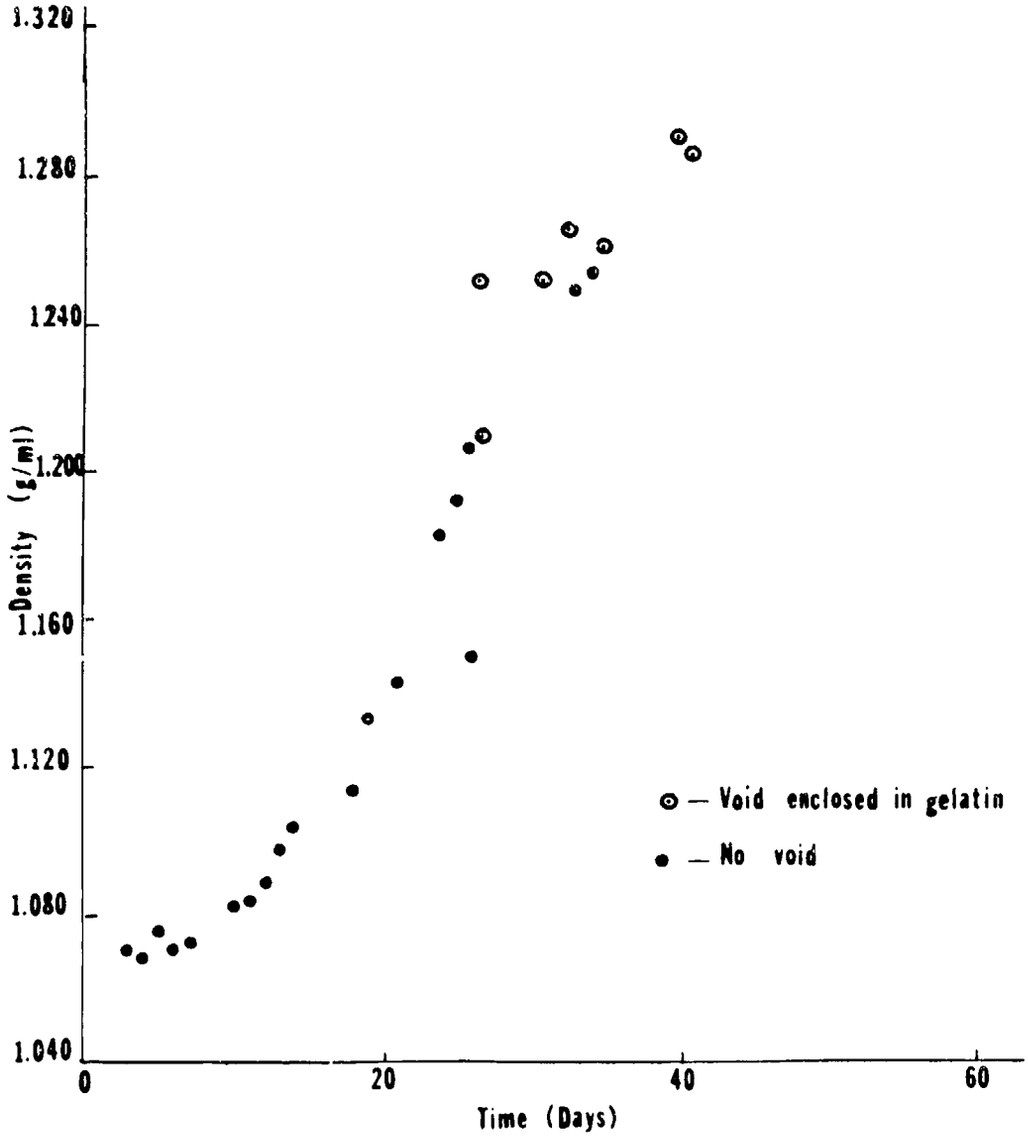

Figure 9: Gelatin Density vs. Storage Time Series B

under these circumstances convinces one that such a measurement is meaningless. The resistance measurement (meaning the instrument response) is based on the assumption that the unknown is a passive resistive network, not an active network with a battery which increases in voltage output as the measurement progresses in time.

8.1 Design of the Experiment

As a result of these observations, the electrical properties experiment was redesigned. It was decided to apply a range of fixed known voltages to the gelatin and to monitor the current it would draw during this "charging" stage as a function of time. That would establish an effective resistance as a function of time for a given applied voltage. Then the next step would be to monitor the open circuit voltage decay characteristic for the electret which was created by charging with this particular applied voltage.

The experiment required a voltage source which could provide varying amounts of current to a load at constant voltage. This was constructed in the classic manner using a lead-acid battery and a voltage divider. See Figure 10. The battery voltage (V_B) could be either 2 or 6 volts. In order for the charging voltage (V_C) to be independent of the charging current (I_L), one must meet the requirement that:

$$I_L \ll I_2$$

This is accomplished by selection of a suitably small value for (R_1+R_2) as compared to R_L. And, of course, a particular V_C is obtained by suitable selection of R_1/R_2.

The voltage drop introduced by the presence of the ammeter was measured using a substitution method in separate experiments. In these experiments for each charging voltage, the gelatin was replaced with a variable resistor which could be adjusted to get the same I_L that is measured during charging. These resistance values (R_0) were then measured. The actual voltage drop across the gelatin is then simply calculated, $(I_L R_0)$. The voltage drop across the ammeter is then $V_C - I_L R_0$. This was found to be small for all the current ranges used. The ammeter was a laboratory grade FET-VOM (Heath IM -104).

Measurement of the open circuit voltage decay characteristic was made directly using the same meter which has an input impedence of 10^7 ohms for voltage measurements. Since the R_0's which are measured as described above never exceeded 10^5 ohms (indeed under most conditions they are much less), it is fair to assert that the presence of the meter did not significantly alter the decay characteristic.

8.2 Experimental Procedure

It was noted that when measurements extended over a significant time (an hour) one could observe a greenish tinge in the gelatin in the vicinity of the copper electrodes. To eliminate the reaction between the gelatin and the electrode, we switched to using electrodes which are polished chromium-plated steel. There has been no sign of any interaction between these electrodes and the gelatin.

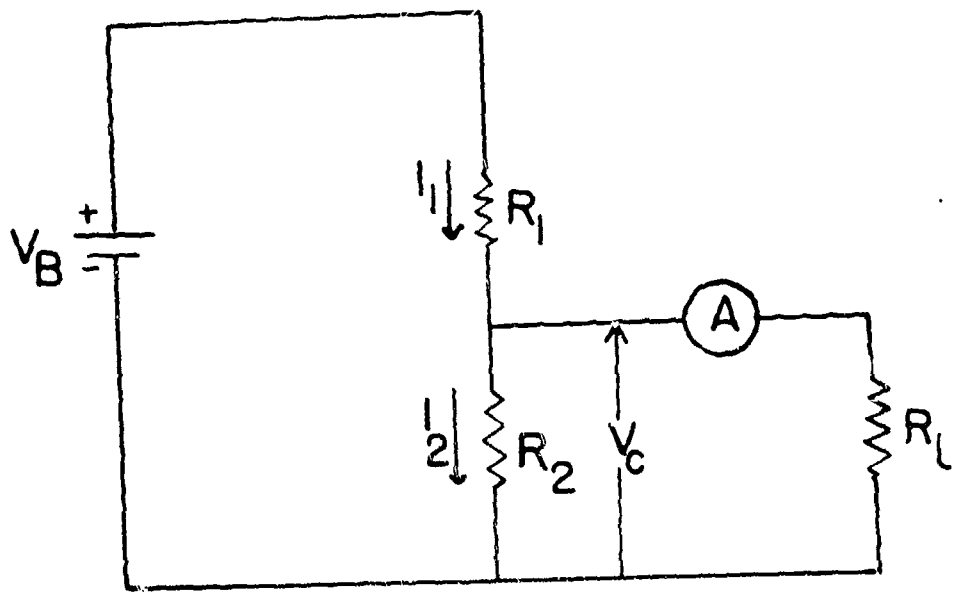

Figure 10

"Charging" Circuit

The gelatin is cast in a cylindrical geometry and allowed to gel and equilibrate for at least 4 hours in the refrigerator at about 60-80% relative humidity. The gel cylinder is then removed from its mold and the thickness and diameter measured. The electrodes are cleaned before each run with trichloroethylene, then by demineralized distilled water and dried. The electrodes are placed above and below the gelatin. A paper towel is placed upon the upper electrode and a weight is placed on the plate and towel to keep the gelatin firmly in contact with the electrodes.

Measurements are conducted with the sample in the refrigerator, after about half an hour has been allowed for equilibration. If a re-run is conducted on a sample, the sample will have been kept undisturbed (with its electrodes still in place) in the refrigerator between runs.

8.3 Results and Discussion

Samples are identified alphabetically, and if a measurement is re-run on a particular sample, it is indicated numerically. For example, a plot for K-2 would be a second run on sample K. Table I lists all the samples, their dimensions, and their age for various runs, as well as notes on other details. Some selected plots of the measured data for a range of charging voltages (from 0.096 to 6.20 volts) are shown in Figures 11 through 16. For the complete set of plots which go with the samples listed in Table I, the reader is referred to Figures 6 thru 36 in the Second Quarterly Report for this contract.

Table II lists the individual runs, the measured charging voltage (V_C), the measured charging current (I_L), the calculated R_L, the measured R_O, the calculated $I_L R_O$ and a voltage called V_O. V_O is the apparent initial voltage at the beginning of the voltage decay characteristic. It is obtained by extrapolating the voltage decay curve back to the time at which charging was discontinued. V_C was often measured before and after a run, and was not found to vary. The current I_2 (in Figure 10) was always greater than 500 ma, satisfying the condition that I_L be much less than I_2, as can be seen from the values of I_L in Table II. The value of R_L listed in the table is the apparent load resistance of both the meter and gelatin in series (Figure 10 again) just before charging is terminated. The values of R_O are either measured directly (about ten values for each charging voltage) or interpolated from the measured curves of R_O versus I_L. The calculated $I_L R_O$ should represent the actual voltage across the gelatin, and must be less than V_C. The fact that it isn't in all cases has to reflect the size of cumulative errors in measurements of V_C, I_L, and R_O for each run. In some runs this appears trivial, but in some, such as E-2 and G-1, it appears large.

Several observations can be made with respect to the data. First, the R_L of the specimens stays consistently high until V_C approaches 1 to 2 volts. Above this voltage, R_L is low. Figure 17 shows this in more proper form, where the R_L has been converted to resistivity for each specimen and V_C has been converted to electric field. Field strength around 0.7 to 1.0 volts/cm apparently begins to break bonds in the gelatin.

TABLE I

Geometry and Age of Electrical Test Samples

Sample	d (cm)	A/d $(\frac{cm^2}{cm})$	Date of sample preparation	Age at Time of Run (hrs)	Temperature (°C) of Sample	Comments
A	1.560	8.1	10/25	32	7.0	
B	1.290	9.8	10/25	96	6.0	
C-1	1.600	8.1	10/29	24	2.0	
C-2	1.600	8.1	10/29	27	4.0	
D	1.655	7.7	10/30	22	3.4	Meter removed from circuit for 10 minutes during voltage decay
E-1	1.640	7.8	10/31	4.5	4.1	
E-2	1.640	7.8	10/31	6	4.0	Voltage increased from 2 to 6 volts between E-1 and E-2
F-1	1.730	7.5	11/01	22	3.8	
F-2	1.730	7.5	11/01	24	3.7	Possible poor contact. Added pressure to electrodes during voltage decay
G-1	1.650	7.7	11/05	46	3.5	
G-2	1.650	7.7	11/05	53	3.5	Alternate Voltage and Current measurement in open circuit during voltage mode
J	1.610	8.0	11/14	5	5.0	
K-1	1.390	9.5	11/14	25	6.0	
K-2	1.390	9.5	11/14	30	5.0	
K-3	1.390	9.5	11/14	45	2.8	
L	1.620	7.9	11/15	19	3	
M-1	1.290	9.8	11/15	24	2.5	
M-2	1.290	9.8	11/15	26	3.8	
MA	1.620	7.9	11/19	24	3.2	
N-1	1.500	8.8	11/19	27	2.0	
N-2	1.500	8.8	11/19	30	2.0	
O-1	1.550	8.4	11/19	48	4.1	Voltage clgs from DC (+) to DC (-) during voltage decay for O-1, O-2
O-2	1.550	8.4	11/19	49	4.7	

Sample	d (cm)	A/d $\left(\frac{cm^2}{cm}\right)$	Date of sample preparation	Age at Time of Run (hrs)	Temperature (°C) of Sample	Comments
P	1.870	6.9	11/21	6.5	5.0	
Q	1.510	8.6	11/21	7.5	5.3	
R	1.660	7.8	11/26	5	3.0	
S	1.390	9.2	11/26	7	4	
T	1.400	9.6	11/26	8	6.5	
U	1.840	7.2	11/26	23	4	
V	1.630	7.9	11/27	28	5.0	
W	1.670	7.6	11/29	24	--	Voltage from DC (+) to DC (-)
X	1.050	12.0	11/29	96	5.0	Some shrinkage of gelatin cylinder

Samples are cylindrical; "d" is their height, and A is their cross-sectonal area.

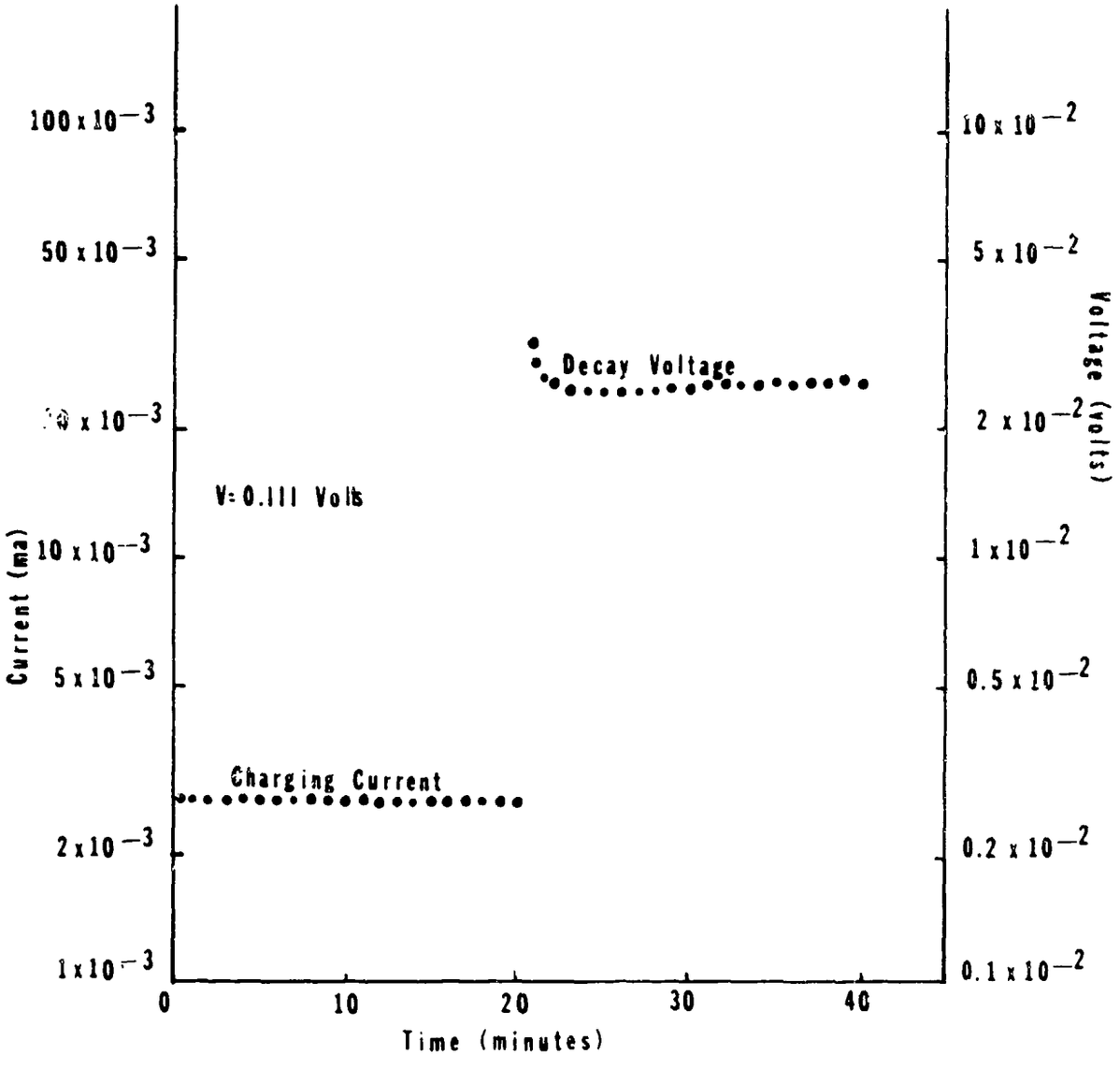

Figure 11

Charging Current and Decay Voltage Characteristics of Sample K-2

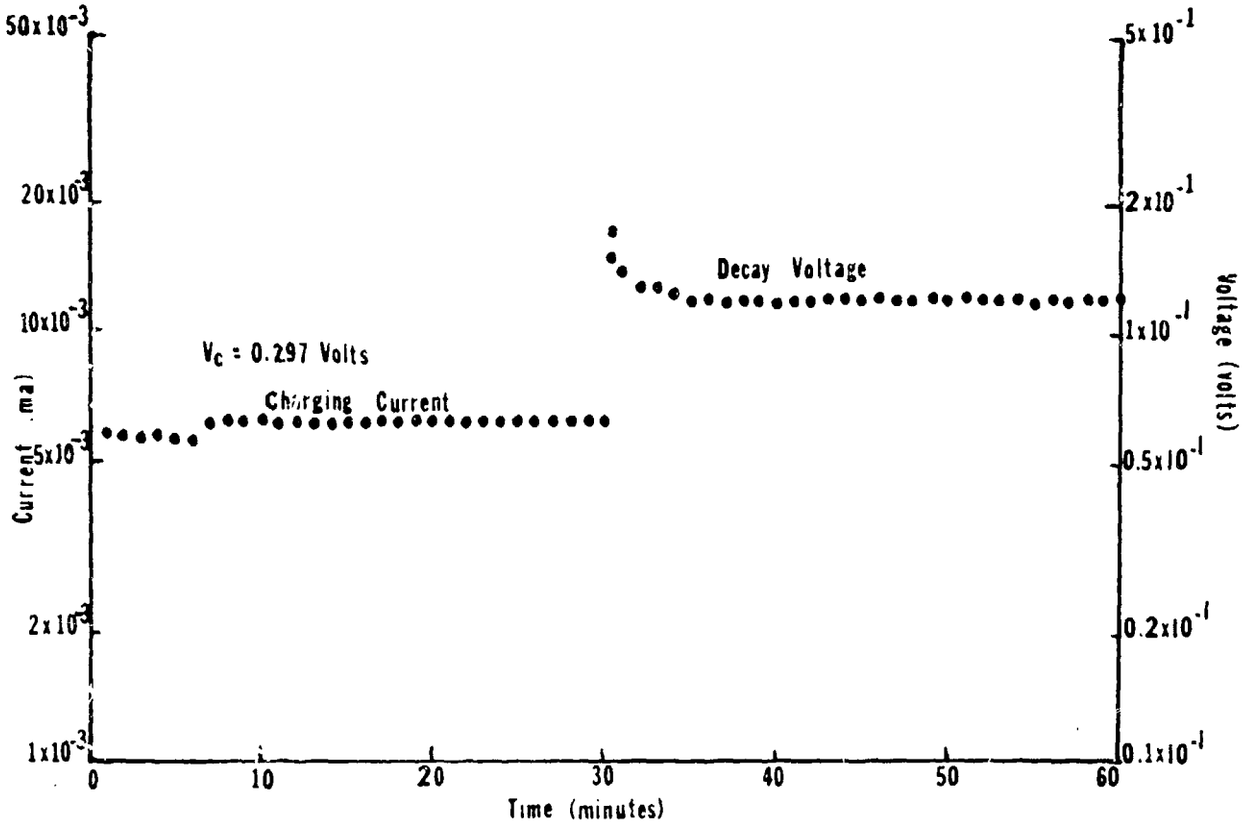

Figure 12

Charging Current and Voltage Decay
Characteristics of Sample N-2

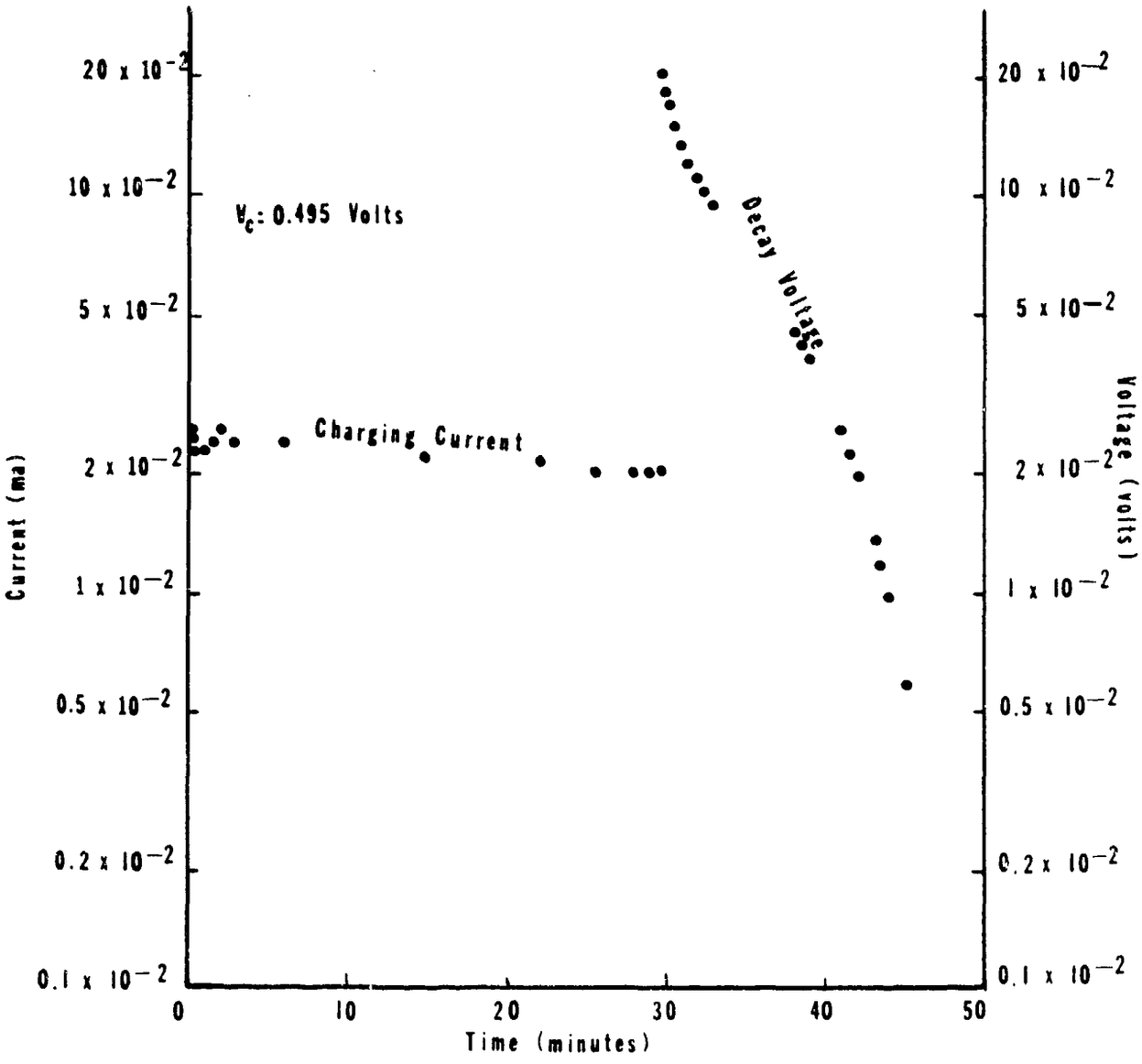

Figure 13

Charging Current and Voltage Decay Characteristics of Sample X

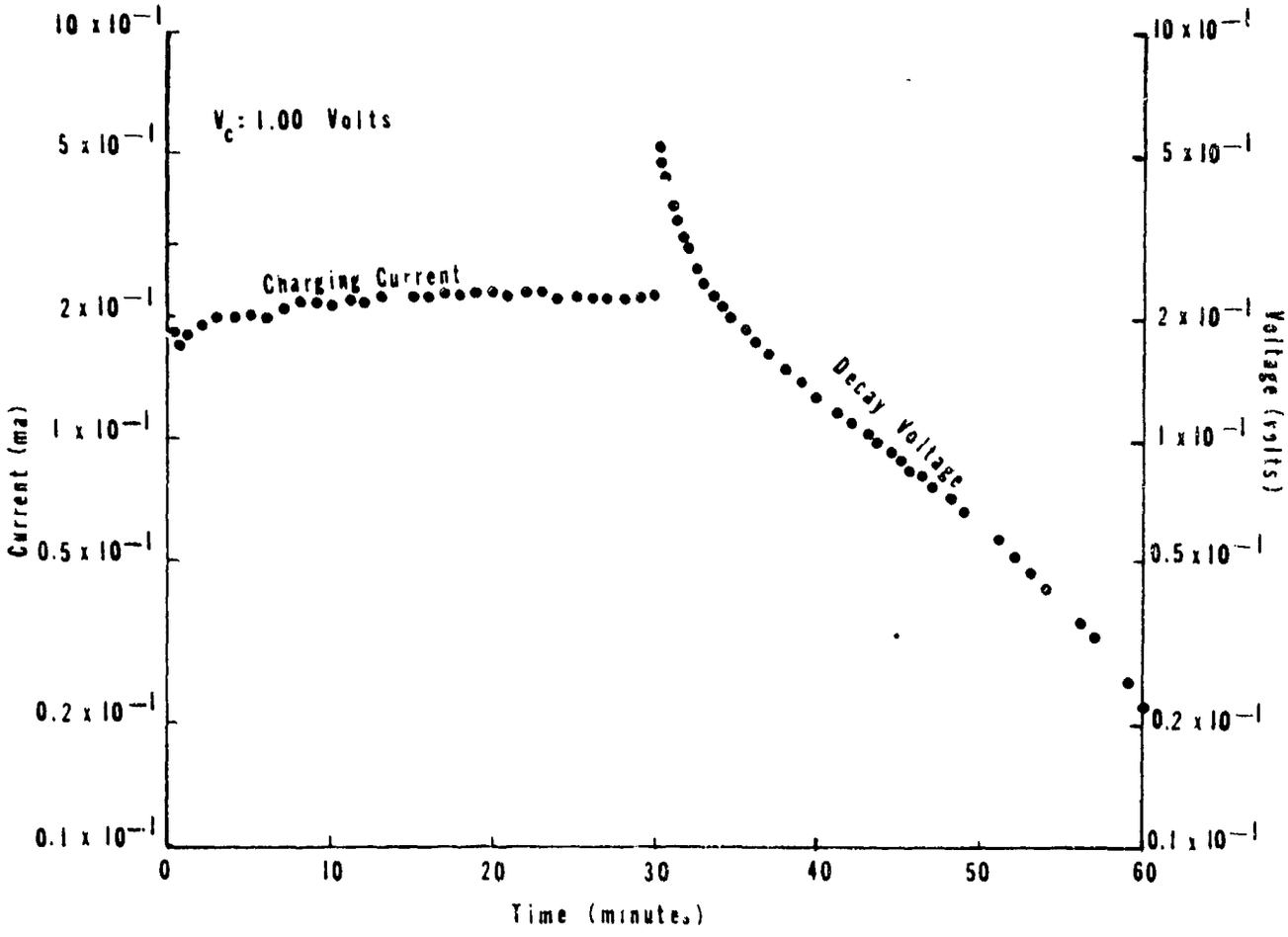

Figure 14

Charging Current and Voltage Decay
Characteristics of Sample R

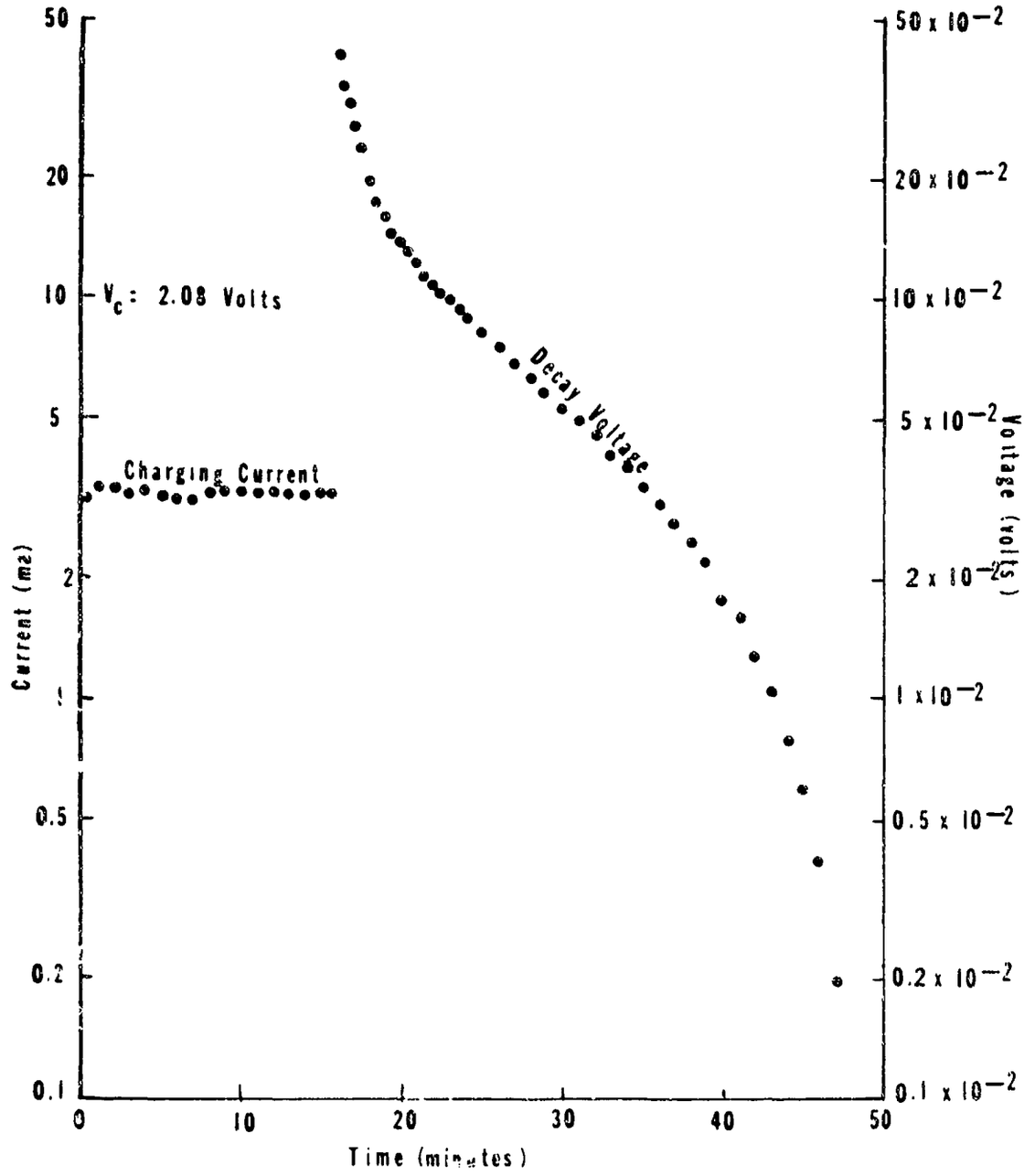

Figure 15

Charging Current and Voltage Decay Characteristics of Sample A

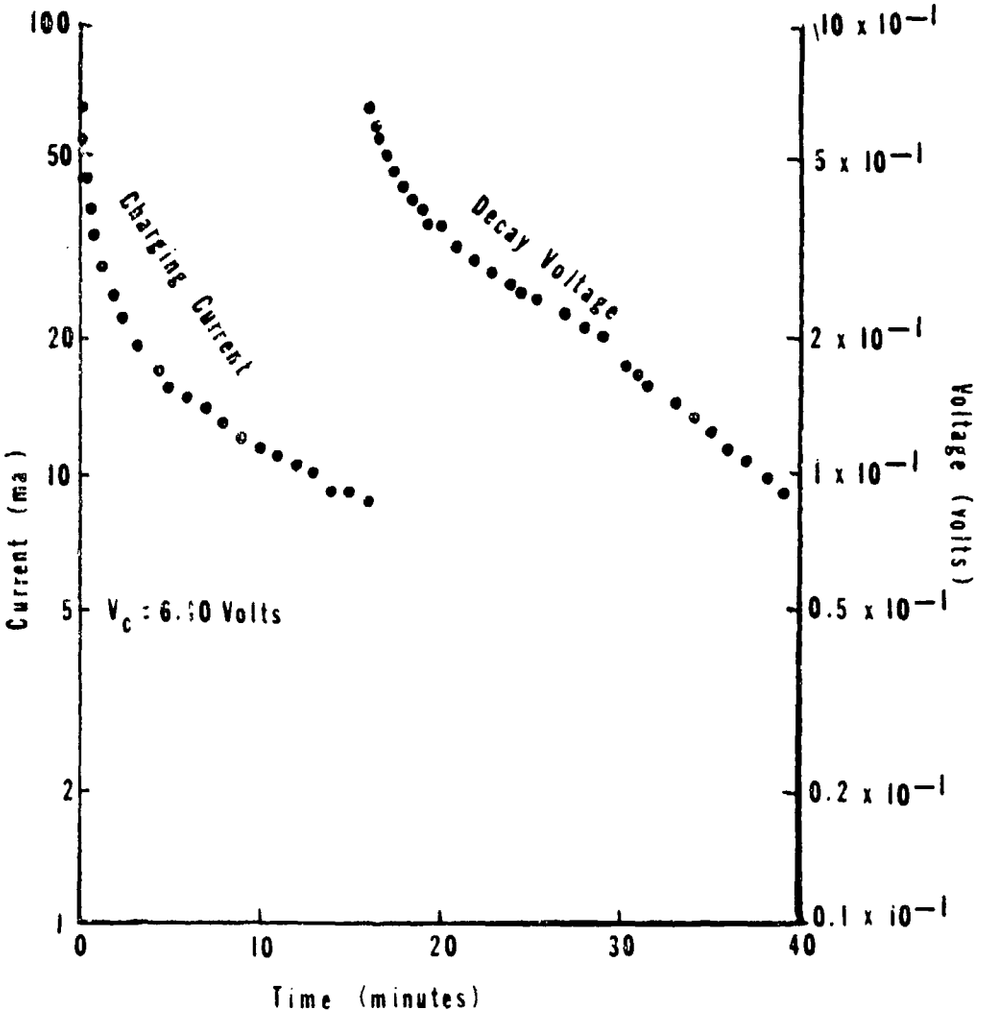

Figure 16
Charging Current and Voltage Decay Characteristics of Sample T

TABLE II

Summary of Selected Electrical Data and Calculations

Sample	Measured V_C	Measured I_L	$R_L = \frac{V_C}{I_L}$	Measured R_O	Calculated $I_L R_O$	Measured V_O
A	2.06 volts	3.30 ma	625 ohms	620 ohms	2.04 volts	0.46 volts
B	2.05 "	3.55 "	568 "	588 "	2.09 "	0.52 "
C-1	2.05 "	4.00 "	514 "	510 "	2.04 "	0.47 "
C-2	2.05 "	3.95 "	519 "	516 "	2.03 "	0.50 "
D	2.05 "	6.10 "	337 "	332 "	2.03 "	0.55 "
E-1	2.05 "	3.90 "	527 "	523 "	2.04 "	0.73 "
E-2	6.20 "	7.80 "	795 "	829 "	6.48 "	0.72 "
F-1	2.04 "	3.80 "	538 "	536 "	2.03 "	0.55 "
F-2	2.04 "	3.30 "	619 "	620 "	2.04 "	0.56 "
G-1	6.20 "	4.20 "	1475 "	1550 "	6.50 "	0.41 "
J	1.02 "	215 μa	4730 "	4700 "	1.01 "	0.41 "
K-1	0.100 "	4.6 "	21750 "	13100 "	0.060 "	0.046 "
K-2	0.111 "	2.7 "	41200 "	28300 "	0.077 "	0.040 "
K-3	0.105 "	2.0 "	52500 "	40000 "	0.080 "	0.045 "
L	0.115 "	5.2 "	22100 "	8500 "	0.044 "	0.028 "
M-1	0.510 "	24.5 "	20800 "	18800 "	0.46 "	0.24 "
M-2	0.285 "	8.5 "	33600 "	27300 "	0.23 "	0.11 "
MA	0.298 "	8.4 "	35500 "	27800 "	0.23 "	0.14 "
N-1	0.297 "	6.35 "	46800 "	40200 "	0.25 "	0.18 "
N-2	0.297 "	16.0 "	18500 "	19700 "	0.32 "	0.19 "
O-1	0.291 "	15.0 "	19400 "	20800 "	0.31 "	0.22 "
O-2	0.291 "	14.0 "	20800 "	22000 "	0.31 "	0.27 "
P	0.297 "	7.0 "	41800 "	35700 "	0.25 "	0.096 "
Q	0.297 "	7.9 "	37600 "	30200 "	0.24 "	0.060 "
R	1.00 "	225 "	4450 "	4500 "	1.01 "	0.52 "
S	1.88 "	5.50 ma	342 "	332 "	1.83 "	0.70 "
T	6.10 "	8.8 "	693 "	700 "	6.16 "	0.83 "
U	0.096 "	1.1 μa	87400 "	74400 "	0.082 "	0.080 "
V	0.099 "	1.05 "	94200 "	85300 "	0.090 "	0.07 "
W	0.098 "	3.7 "	25500 "	16800 "	0.062 "	0.06 "
X	0.495 "	20.5 "	24100 "	24200 "	0.498 "	0.23 "

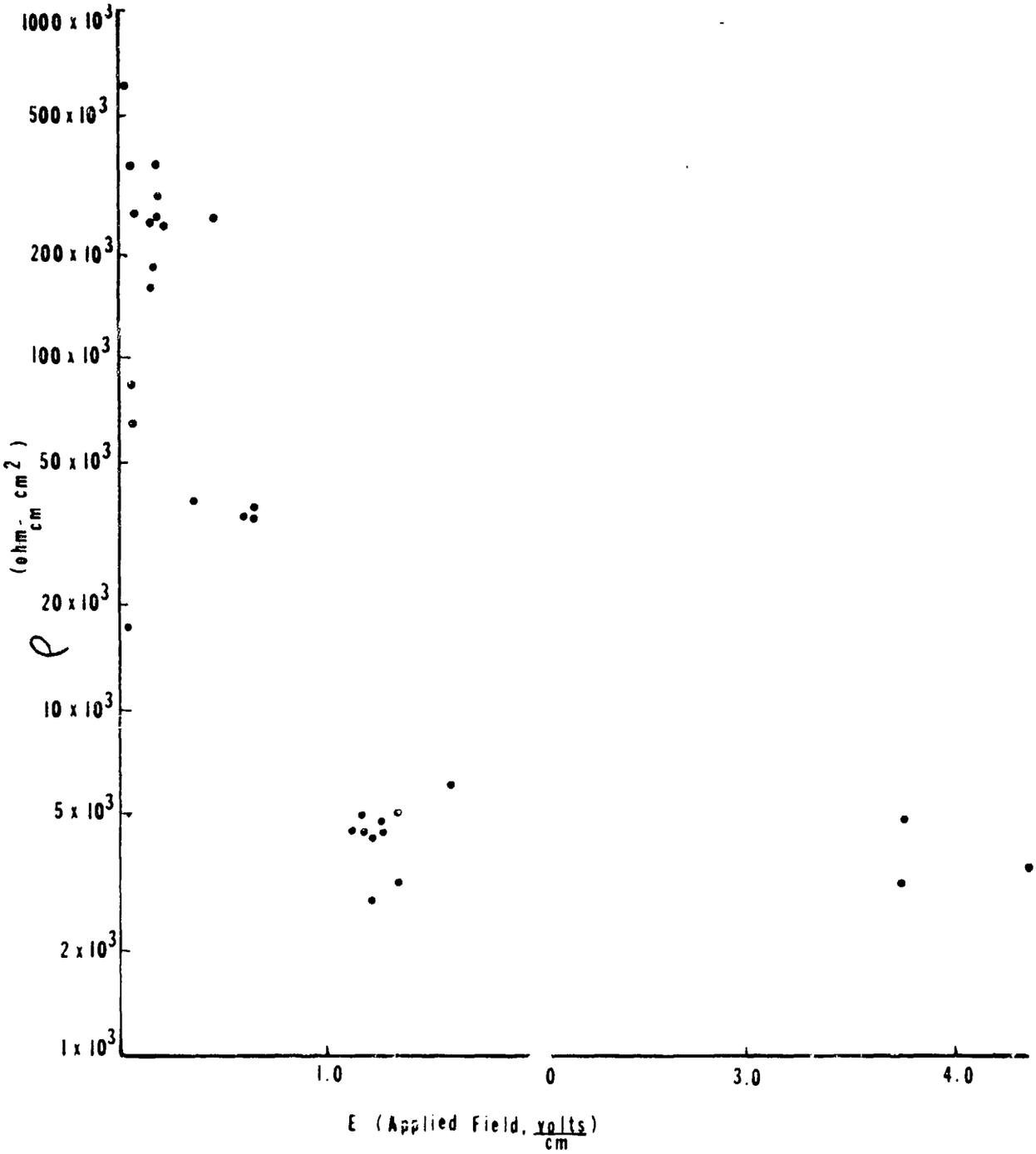

Figure 17

Resistivity vs. Applied Field

Secondly, the voltage decay characteristic seems to fall into two groups. At fields below 0.2 volts/cm, the time constant is generally very large (50,000 sec.), with a few exceptions. At larger fields, the time constant is generally between 200 and 2000 seconds, again with some exceptions. Table III shows τ for each run and Figure 18 is a plot of these data. The slopes assigned to each run which were used to compute τ were based on the bulk of the data points and tended to ignore the initial effects.

Another consistent observation is that V_0 (the voltage across the gelatin at the beginning of the voltage decay after charging is stopped) is always less than V_C. One might expect V_0 to be equal to V_C. The fact that it is not implies that the gelatin must be equivalent to a circuit that looks like Figure 19. One can then conclude the measured R_0 listed in Table II must be $R_3 + R_4$. Also, one must conclude that

$$\frac{V_o}{V_c} = \frac{R_4}{R_3+R_4} = \frac{R_4}{R_0}$$

Therefore one can compute an R_3 and an R_4 for each run in Table II. These are shown in Table IV.

Since the external circuit impedence is so high during the voltage decay measurements, the voltage decay has to occur by discharge of C through R_4.

Therefore, the time constant "τ" discussed previously should be given by:

$$\tau = CR_4$$

This in turn, implies a C for each τ and R_4.

Table V lists the result of this calculation both as a capacitance "C", and a normalized capacitance "c", where

$$C = \tau/R_4 \quad \text{farads}$$

$$c = \frac{\tau d}{R_4 A} \quad \frac{\text{farads -cm}}{\text{cm}^2}$$

where τ is taken from Table III
R_4 is taken from Table IV
A/d is taken from Table I

Defining a normalized capacitance this way means it is analogous to resistivity. It is a measure of a material property, not dependent on experimental geometry. Figure 20 is a plot of "c" versus applied field, and Figure 21 is a blown up plot of the lower left portion of Figure 20. Figure 20 shows that at a field strength of about 0.6 volts/cm, the normalized capacitance begins to increase. For field over 10 volt/cm, the material exhibits large (and erratic) normalized capacitances.

TABLE III

Voltage Decay Characteristics for Various Applied Fields

Sample	E (volt/cm)	τ (sec)
A	1.33	600
B	1.59	630
C-1	1.28	750
C-2	1.28	1380
D	1.24	480
E-1	1.25	360
E-2	3.77	1290
F-1	1.18	1830
F-2	1.18	1170
G-1	3.75	5090
J	0.62	700
K-1	0.071	585
K-2	0.080	"
K-3	0.071	"
L	0.074	795
M-1	0.387	105
M-2	0.224	66
MA	0.183	
N-1	0.197	"
N-2	0.197	"
O-1	0.187	1840
O-2	0.187	1300
P	0.162	"
Q	0.196	78
R	0.604	2090
S	1.34	2340
T	4.35	1310
U	0.052	"
V	0.061	"
W	0.059	330
X	0.470	2020

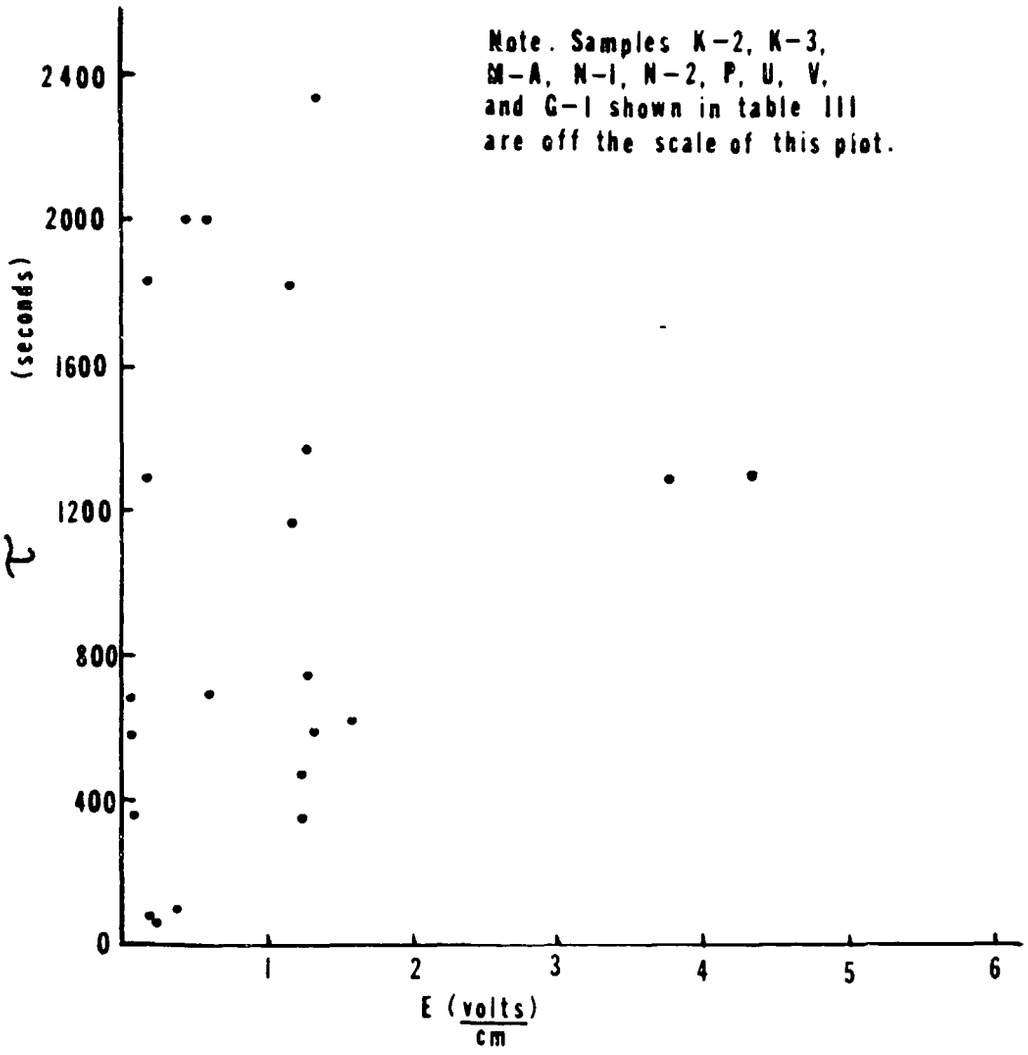

Figure 18

Decay Time Constant vs. Applied Field

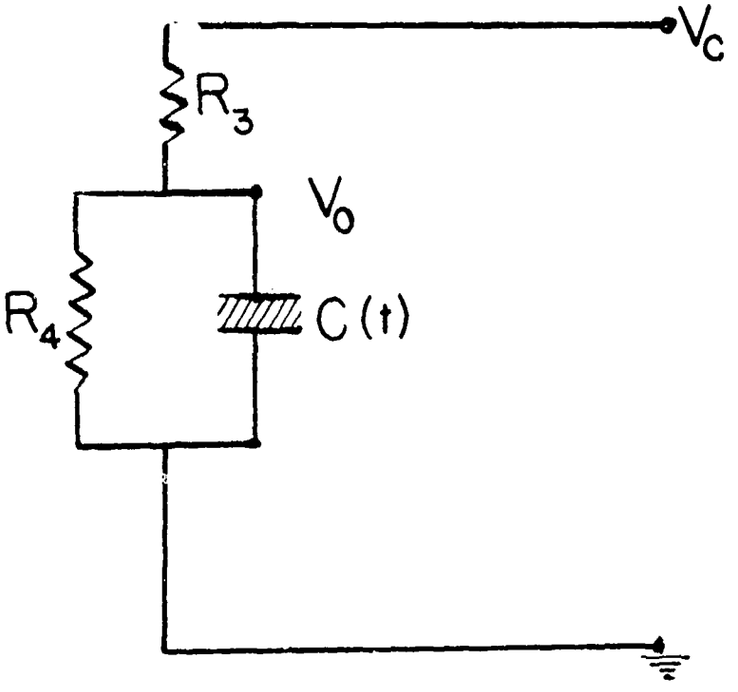

Figure 19

Equivalent Circuit for Gelatin

TABLE IV

Equivalent Circuit Resistances

Sample	R_3 (ohms)	R_4 (ohms)	R_3/R_4	$R_3 + R_4$ (ohms)	$\frac{V_o}{V_c} = R_4/(R_3+R_4)$
A	483	137	3.5	620	0.221
B	440	148	3.0	588	0.252
C-1	393	117	3.4	510	0.229
C-2	390	126	3.1	516	0.244
D	243	89	2.7	332	0.268
E-1	337	186	1.8	523	0.356
E-2	733	96	7.7	829	0.116
F-1	388	144	2.7	536	0.269
F-2	450	170	2.6	620	0.274
G-1	1448	102	14.2	1550	0.066
J	2780	1920	1.4	4700	0.410
K-1	7000	6100	1.1	13100	0.465
K-2	18100	10200	1.8	28300	0.360
K-3	21850	18200	1.2	40050	0.455
L	6500	2000	3.2	8500	0.234
M-1	9800	9000	1.1	18800	0.480
M-2	17000	10300	1.6	27300	0.376
MA	10000	17800	0.56	27800	0.641
N-1	21300	18900	1.1	40200	0.470
N-2	8100	11600	0.70	19700	0.590
O-1	5100	15700	0.32	20800	0.755
O-2	1600	20400	0.078	22000	0.93
P	24200	11500	2.1	35700	0.323
Q	24100	6100	4.0	30200	0.202
R	2160	2340	0.92	4500	0.520
S	208	124	1.7	332	0.374
T	605	95	6.4	700	0.136
U	12400	62000	0.20	74400	0.834
V	27600	57700	0.48	85300	0.676
W	11650	5150	2.3	16800	0.306
X	13000	11200	1.2	24200	0.465

TABLE V

Capacitance and Normalized Capacitance for Various Applied Fields

Sample	E ($\frac{\text{volt}}{\text{cm}}$)	Capacitance (farads)	Normalized Capacitance $\frac{\text{farad - cm}}{\text{cm}^2}$
A	1.33	4.4	0.54
B	1.59	4.3	0.44
C-1	1.28	6.4	0.79
C-2	1.28	11.0	1.4
D	1.24	5.4	0.70
E-1	1.25	1.9	0.25
E-2	3.77	13.4	1.7
F-1	1.18	12.7	1.7
F-2	1.18	6.9	0.92
G-1	3.75	50	6.5
J	0.62	0.36	0.046
K-1	0.071	0.096	0.010
K-2	0.080	[illegible]	[illegible]
K-3	0.071	[illegible]	[illegible]
L	0.074	0.40	0.050
M-1	0.387	0.012	0.0012
M-2	0.224	0.006	0.0007
MA	0.183	[illegible]	[illegible]
N-1	0.197	[illegible]	[illegible]
N-2	0.197	[illegible]	[illegible]
O-1	0.187	0.12	0.014
O-2	0.187	0.064	0.0076
P	0.162	[illegible]	[illegible]
Q	0.196	0.013	0.0015
R	0.604	0.89	0.11
S	1.34	18.9	2.1
T	4.35	13.8	1.4
U	0.052	[illegible]	[illegible]
V	0.061	[illegible]	[illegible]
W	0.059	0.064	0.0084
X	0.470	0.18	0.015

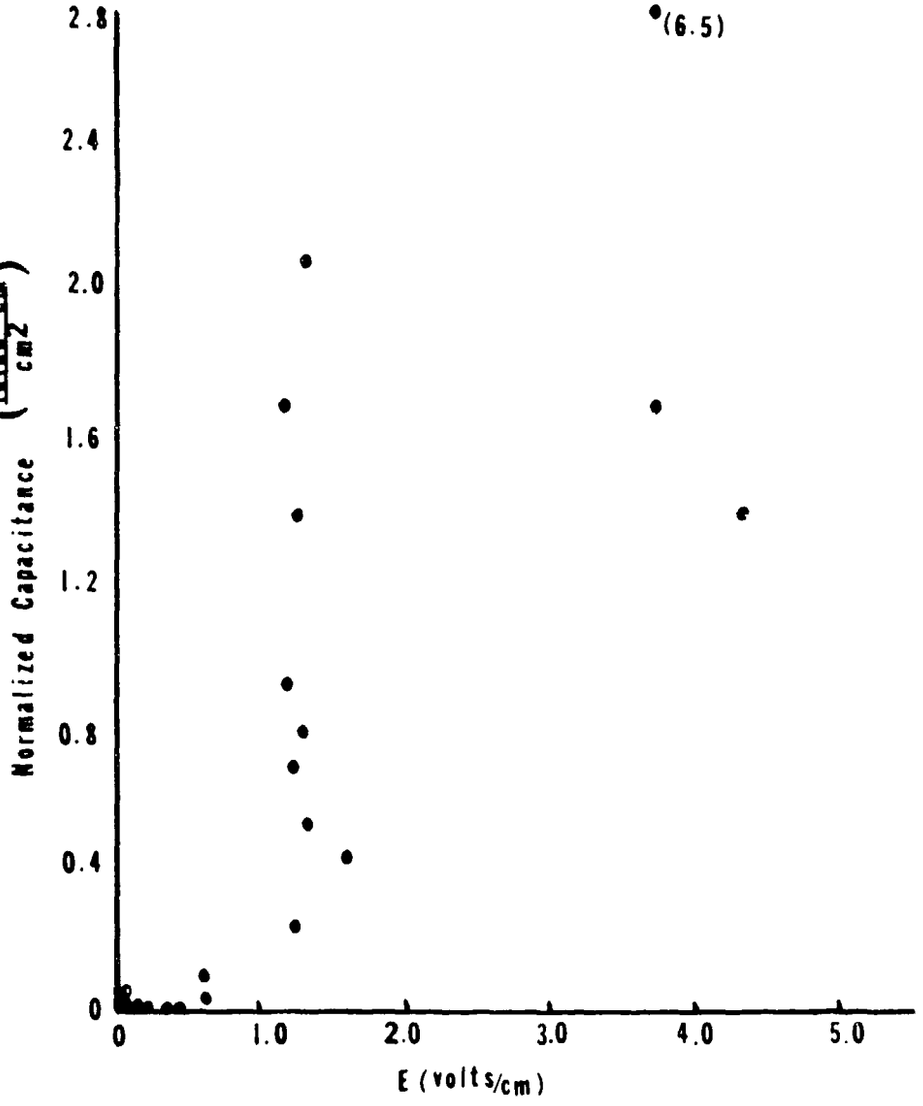

Figure 20

Normalized Capacitance vs. Applied Field

The increase must be associated with the breaking of bonds by the applied field. This could, in turn, create smaller arrays more easily oriented in the electric field, with a corresponding increase in the polarizability of the material. The electrical properties of the material which has been "damaged" by the high field are not particularly reproducible.

In contrast, Figure 21 shows that a magnified view of the portion of Figure 20 which is below 0.6 volts/an reveals consistent behavior. With the exception of one point (sample L) the normalized capacitance groups around 0.01 farads - cm x cm^{-2}. This would imply the normalized capacitance is independent of applied field until the field is large enough to break bonds. It should be noted that the runs which show very large (∞) time constants in Table III do not appear on the plots of capacitance versus applied field. In these runs, the material behavior is not understood. It would seem most reasonable, however, that those particular time constants are large because R_4 is much larger than computed rather than C being larger than computed.

As mentioned previously, shorting out the electrodes on the gelatin will not quickly "discharge" the capacitor formed by the polarized gelatin. Figure 22 shows a run (G-2) which was the same as those described previously, except that during the decay mode, an ammeter was directly applied to the electrodes and current through the ammeter was recorded. This was essentially the short-circuit current. Between each current measurement, the open circuit voltage was monitored, as shown in the plot.

9.0 Other Properties

9.1 Piezoelectric Effects

Another interest centered on whether a piezoelectric effect exists in gelatin. Two pairs of electrodes were placed on orthagonal faces of a rectangular block of gelatin. One pair was stainless steel, the other pair was chromium plated steel. Glass plates were used to electrically insulate the apparatus from its surroundings. Gelatin was prepared by the small sample technique and cast in lucite molds.

The piezoelectric voltage (V_p) was measured by a laboratory FET-VOM (10^7 imput impedance). The V_p was measured between the two stainless steel electrodes with and without a force applied normal to the stainless steel electrodes. This process was then repeated when a charging voltage, V_c, was applied through the chromium plated electrodes, creating a field perpendicular to the applied force.

Gelatin showed no apparent piezoelectric effect. Only a small voltage did occur (1-2 millivolts/cm) when a nominal stress of 0.1 lbs. in^{-2} was applied to the gelatin solid and no orthagonal field was present. When a field (V_c=0.56, 1.9 volts/cm) was applied, the voltage did increase when the same nominal stress was added to the solid. Shunting the FET-VOM with a 100K resistor, the voltage change was almost nonexistent (20 microvolts) when a larger stress (0.2 lb. in^{-2}) was applied. V_o was between 0.65 and 0.75 volts for the gelatin solid. V_o is the

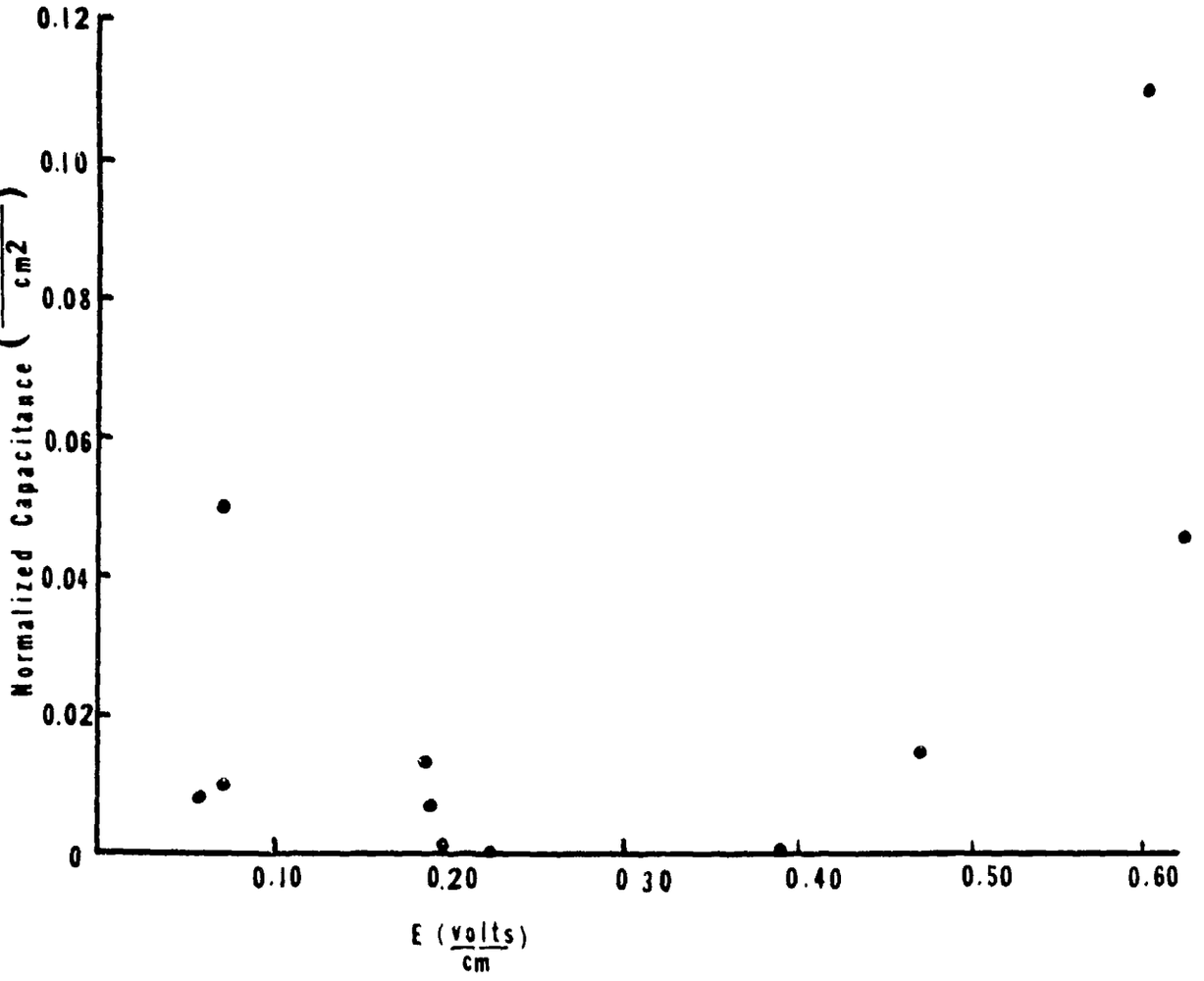

Figure 21

Magnification of Part of Figure 20

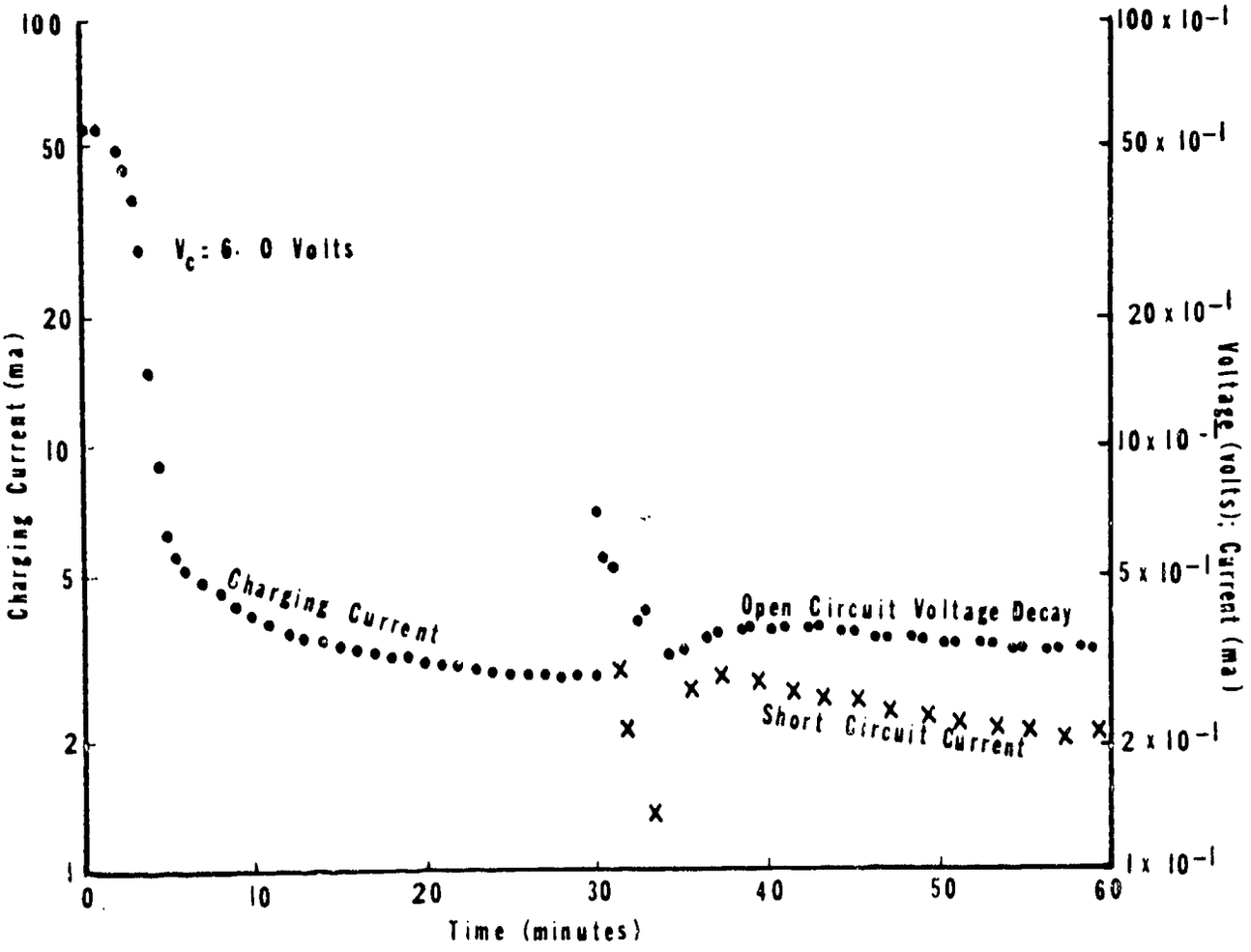

Figure 22

Charging Current, Open Circuit Voltage Decay, and Short Circuit Current Decay of Sample G-2

apparent initial voltage at the beginning of the voltage decay characteristic of a gelatin sample, as described in section 8.3.

9.2 Electro-optic Effects

Gelatin is stress birefringant and this property was quite useful in evaluating grip design for mechanical testing. One additional possibility was that its optical activity was affected by applied electric fields. The birefringence pattern of a gelatin specimen was found to be independent of an applied external electric field. This was true whether the external field was above or below the critical field (around 0.6 volt/cm) which apparently begins to break bonds.

9.3 Static Surface Polarization Effects

It was found that the gelatin was becoming polarized without applying an external field. To observe this behavior, a rectangular block of gelatin was placed between two chromium plated steel electrodes. Voltage was measured with the FET-VOM shunted by a 100K resistor across the terminals. Twenty percent gelatin was prepared and cast into molds made of various materials, stored in the refrigerator and allowed to set for fifteen minutes at room temperature prior to any measurements. The six faces of the gelatin solid were labeled. Voltage was measured across the electrodes when the gelatin solid was positioned in each of its six possible orientations with respect to the electrodes. The electrodes were placed just firmly enough for good contact with the gelatin. Voltages were measured with respect to the upper electrode relative to the lower electrode. No electric fields were applied throughout the experiment.

Samples 1 and 2 were 9 day old gelatin cast in lucite molds. In sample 1-A, the surface was melted away to expose a fresh surface. Sample 3 was a 19 hour old gelatin block cast in glass. Samples 4 and 5 were prepared and cast largely in darkness in cardboard and glass molds respectively.

The gelatin did possess a definite surface charge. See Appendix H. Each face of the gelatin solid generally had the same surface polarity when the gelatin was oriented in each of its six positions with respect to the electrodes. For example, from sample 3 each surface in the six positions in contact with the upper electrode would be positive relative to the opposite surface in contact with the lower electrode. If the electrodes themselves were interchanged, a different behavior was observed. A particular surface exhibited the same charge whether the surface was in contact with either electrode. The opposite gelatin surface exhibited the opposite polarity.

It was decided to test gelatin (sample 5) immersed in hexane. Sample 5 possessed the same characteristics as the other gelatin samples measured in air.

10.0 Mechanical Properties

10.1 Theoretical

As a reference point for further work, it was decided it would be useful to examine the classical models for linear viscoelastic behavior and compare one of them to the experimental behavior of our gelatin in relatively "static" (low strain rate) testing. In so doing, the inadequacy of representing an actual material with a simple model is fully recognized.

Classically, viscoelastic materials are taken to exhibit creep, meaning increasing deformation under sustained load, with the strain rate depending on the stress. Models using springs and dashpots have been found to be descriptive in characterizing linear viscoelastic behavior in uniaxial deformation. The most simple versions of these models are the Maxwell fluid and the Kelvin solid (or Voight solid). The former is a spring and dashpot in series; the latter is a spring and dashpot in parallel. The next level of model sophistication describing a solid is a spring in series with a Kelvin solid. This is known as a "three parameter solid", or the "standard linear material". One can then proceed to a "four parameter solid", which is two Kelvin solids in series.

It was decided that the disadvantage of the increased analytical complexity of the latter more than outweighed its advantages. The "three parameter solid" was selected as a model (Figure 23). The following discussion of the details of this model is based on Flugge's excellent exposition (with minor corrections).[16]

The three parameter solid is characterized by a constitutive equation of the form:

$$\sigma + p_1 \dot{\sigma} = q_0 \epsilon + q_1 \dot{\epsilon} \qquad \text{(equation 1)}$$

where p_1, q_0, and q_1 are the three parameters which describe the material. Note that p_1, has the dimensions of time, q_0 has the dimensions of stress/strain, and q_1 has the dimensions of stress-time/strain. It turns out that they must satisfy the relation:

$$q_1 > p_1 q_0$$

if the constants of the component parts (1, 2, and 3 in Figure 23) of the model are to be real and positive. The behavior of the three parameter solid can be characterized by an imaginary test in which first a constant stress is applied instantaneously and the material is allowed to deform uniaxially, followed by arresting the deformation at a particular strain and allowing the stress to relax. Diagrams of stress versus time and strain versus time for such a test are schematically indicated in Figures 24 and 25. Imagine in the test that a constant stress, σ_o, is imposed at t=0. The series spring "1" (Figure 23) permits an instantaneous elastic strain, ϵ_o, followed by a gradual increase in elastic strain by the assembly of spring "2" and dashpot "3". This responce is termed "delayed elasticity", and is shown by the representation

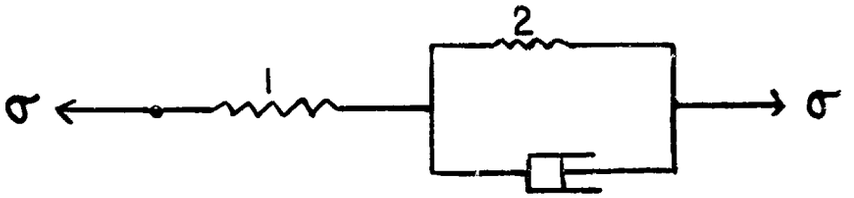

Figure 23: Three Parameter Solid

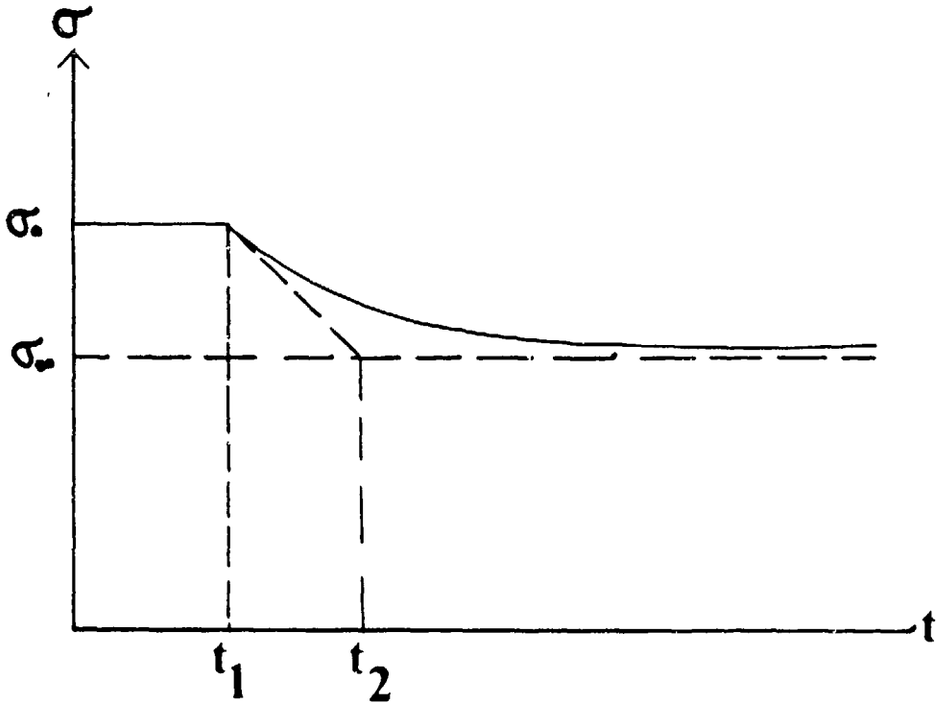

Figure 24

Stress vs. Time for Idealized Test of Three Parameter Solid

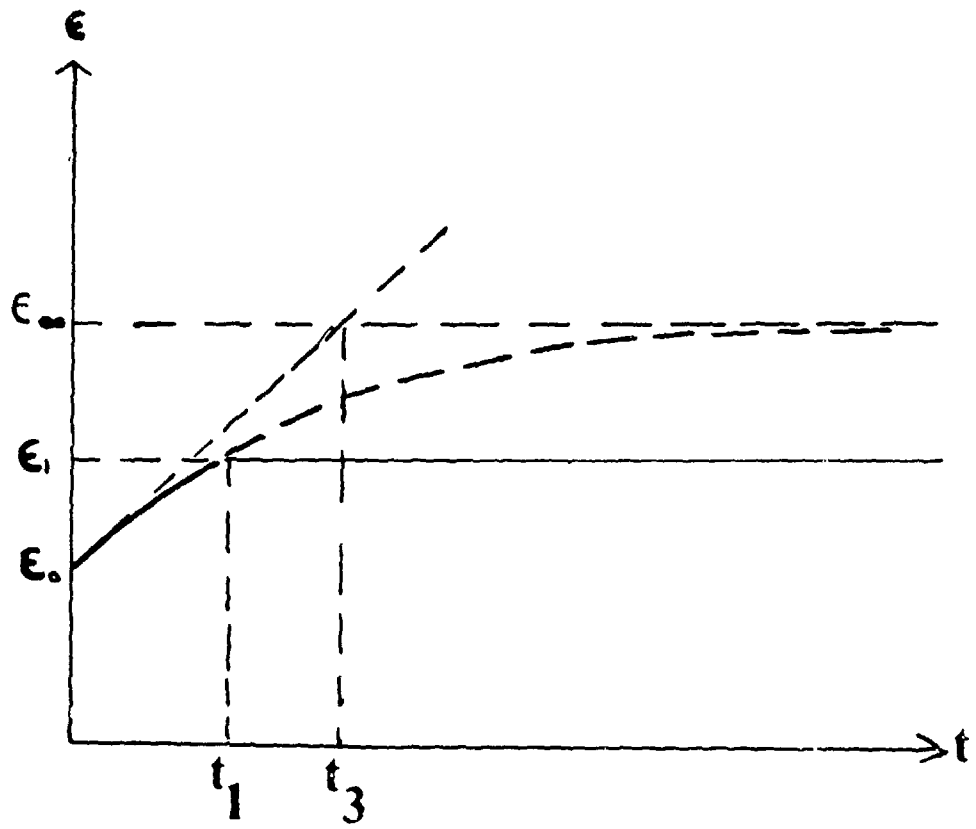

Figure 25

Strain vs. Time for Idealized Test of Three Parameter Solid

of strain between t=0 and $t=t_1$ in Figure 25. At $t=t_1$, the strain is fixed at ϵ_1 from then on, and the stress is monitored as it exhibits relaxation with increasing time, as shown in Figure 24.

The strain for the imaginary test shown in Figures 24 and 25 can be obtained by applying the appropriate initial conditions to the solution to equation (1), and it can be expressed as follows:

$$\epsilon(t) = \frac{\sigma_0}{q_0}\left[1-\left(1-\frac{p_1 q_0}{q_1}\right)\right] e^{-q_0 t/q_1} \qquad \text{(equation 2)}$$

Note that:

$$\text{at } t=0, \quad \epsilon_0 = \sigma_0\left(\frac{p_1}{q_1}\right) \qquad \text{(equation 3)}$$

$$\text{or} \quad \sigma_0 = q_1/p_1 \epsilon_0 \equiv E_0 \epsilon_0$$

So that

$$E_0 \equiv q_1/p_1 \qquad \text{(equation 4)}$$

Equation (4) is by definition an "elastic modulus for instant elasticity".

Similarly,

$$\text{at } t=\infty, \quad \epsilon_\infty = \sigma_0/q_0 \qquad \text{(equation 5)}$$

$$\text{or } \sigma_0 = q_0 \epsilon_\infty \equiv E_\infty \epsilon_\infty$$

$$\text{So that} \quad E_\infty \equiv q_0 \qquad \text{(equation 6)}$$

Equation (6) is by definition an "asymptotic elastic modulus for delayed elasticity".

The stress for the imaginary test shown in Figures 24 and 25 can also be found by applying appropriate boundary conditions to the solution for the constitutive equation (eqn. 1), and it can be expressed as follows:

$$\text{for } 0 \le t \le t_1, \; \sigma = \sigma_0 \qquad \text{(equation 7)}$$

$$\text{for } t_1 \le t \le \infty, \; \sigma = q_0 \epsilon_1 \left(1 - e^{-\frac{(t-t_1)}{p_1}}\right) + \sigma_0 e^{-\frac{(t-t_1)}{p_1}}$$

Note that at $t=\infty$

$$\sigma_\infty = q_0 \epsilon_1 = E_\infty \epsilon_1 \qquad \text{(equation 8)}$$

So that $E_\infty = q_0$ (equation 9)

which is consistant with the definition of E_∞ given in equation (6).

In Figure 24, the time t_2 can be computed by evaluating the time derivative of equation (7). One obtains the relation:

$$\dot{\sigma}(t_1) = \frac{-(\sigma_0 - q_0 \epsilon_1)}{p_1}$$

$$= \frac{-(\sigma_0 - \sigma_\infty)}{p_1} \quad \text{(using equation 8)}$$

Setting this equal to the geometric slope in Figure 24

$$-\frac{(\sigma_0 - \sigma_\infty)}{t_2 - t_1} = -\frac{(\sigma_0 - \sigma_\infty)}{p_1}$$

Solving for t_2:

$$t_2 = t_1 + p_1 \quad \text{(equation 10)}$$

Similarly, in Figure 25, the time t_3 can be computed by evaluating the time derivative of equation (2) at t=0. One obtains the relation:

$$\dot{\epsilon}(0) = \frac{\sigma_0}{q_1}\left(1 - \frac{p_1 q_0}{q_1}\right)$$

Setting this equal to the geometric slope in Figure 25, and using equations (3) and (5):

$$\frac{\sigma_0}{q_1}\left(1 - \frac{p_1 q_0}{q_1}\right) = \frac{\epsilon_\infty - \epsilon_0}{t_3 - 0} = \frac{\sigma_0\left(\frac{1}{q_0} - \frac{p_1}{q_1}\right)}{t_3}$$

Solving for t_3:

$$t_3 = \frac{q_1}{q_0} \quad \text{(equation 11)}$$

Equations 3, 5, 8, 10, and 11 all relate the experimentally measureable quantities σ_0, ϵ_0, ϵ_∞, t_1, t_2, and t_3, with the three material parameters, q_0, q_1, and p_1. Since it is felt that ϵ_∞ (and therefore t_3) cannot be as accurately determined as the other quantities, equations 3, 8, and 11 represent 3 independent equations which would be best to determine q_0, q_1, and p_1.

If one applies a step stress, σ_o, to the material at t=0, then in general one can define a function J(t) such that

$$\epsilon(t) = \sigma_o J(t) \qquad \text{(equation 12)}$$

where J(t) is a monotonically increasing function which by definition is the creep compliance. Similarly, if one has a stress applied to the material such that some strain ϵ_1 has been obtained at a time $t=t_1$, and if at t_1 one fixes the strain at ϵ_1, then in general one can define a function

$$\sigma(t-t_1) = \epsilon_1 Y(t-t_1) \qquad \text{(equation 13)}$$

And the function "Y" is by definition the stress relaxation modulus.

The functions "Y" and "J" are connected through their La Place Transforms by the relation

$$\overline{J}(s)\,\overline{Y}(s) = 1/s^2 \qquad \text{(equation 14)}$$

where

$$\overline{J}(s) = \int_0^\infty J(t)\, e^{-st}\, dt$$

$$\overline{Y}(s) = \int_0^\infty Y(t)\, e^{-st}\, dt$$

For a three parameter solid,

$$J(t) = \frac{p_1}{q_1} e^{-(q_0/q_1)t} + \frac{1}{q_0}\left(1 - e^{-(q_0/q_1)t}\right) \qquad \text{(equation 15)}$$

and $$Y(t) = \frac{q_1}{p_1} e^{-t/p_1} + q_0\left(1 - e^{-t/p_1}\right) \qquad \text{(equation 16)}$$

10.2 Experimental

After some initial false starts on tensile specimen geometry, the geometry shown in Figure 26 was chosen. This specimen has a 4" gauge length and a 1" x 1" cross section in the gauge section of the specimen. An aluminum master specimen was machined with precision. This served as a positive for casting many permanent molds with polystyrene. The polystyrene molds accurately replicated the shape of the master specimen. The two flat faces of the molds were sealed with glass plates, and gelatin was cast into these molds through a hole in one of the grip ends (the top while casting). After the specimen had gelled, the glass plates were removed and the specimen lifted from the mold.

Initial tests used to evaluate preliminary tensile specimen geometries

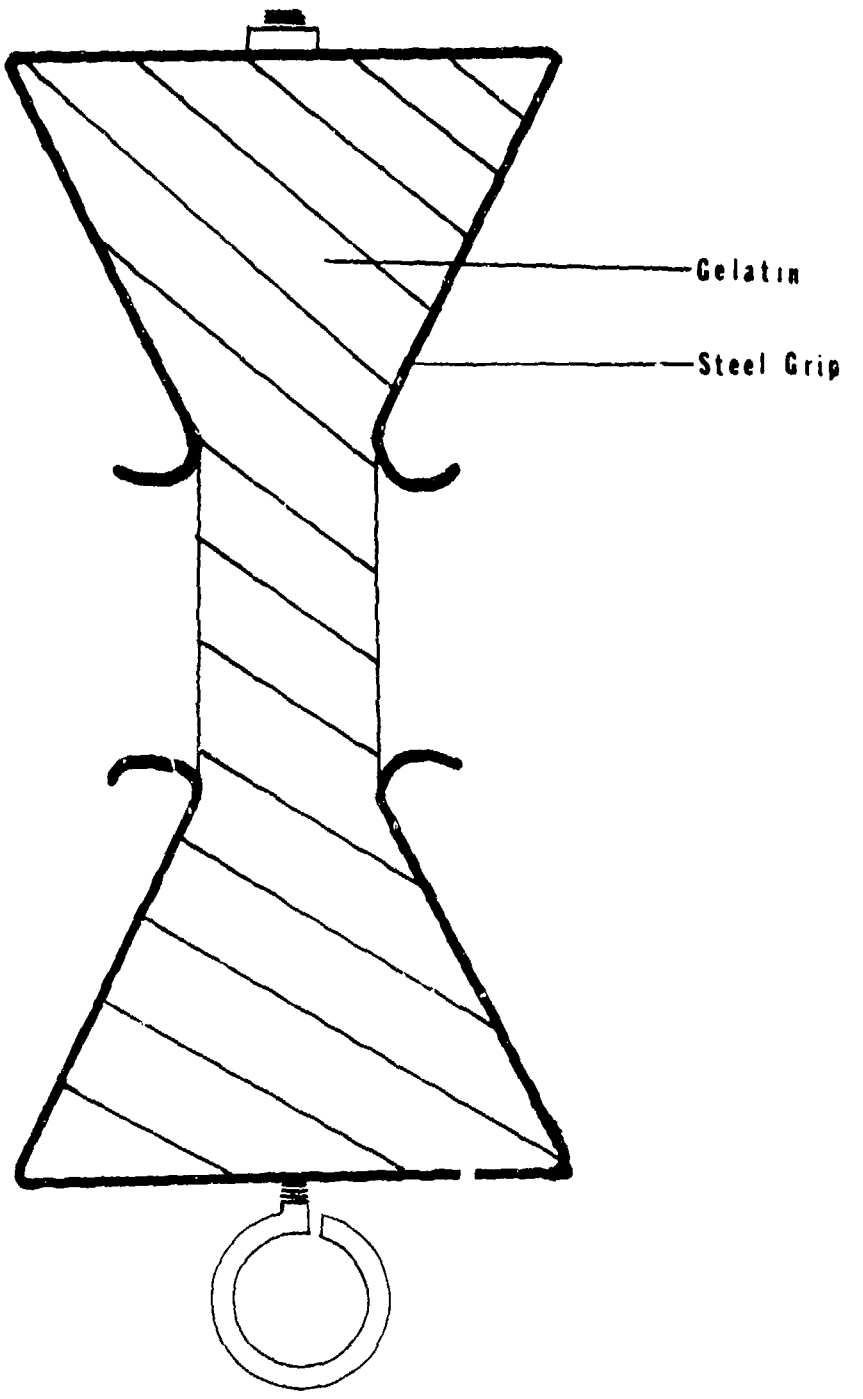

Figure 26

Final Specimen and Grip Design

demonstrated that the gelatin undergoes plastic deformation (creep) at low strain rates. It quickly became apparent that this behavior, (not allowed for in the development of the classical theoretical model discussed in section 10.1), would limit the usefulness of the model described in section 10.1.

10.2.1 Quasi-Static Tests

Several gelatin specimens were hung freely with a grip attached to each end. Small weights of 1-5 lbs. were added to the lower grip. The specimen was allowed to deform over a period of time due to the effect of its own weight and the added weight. The temperature was constant during the test. If the specimen fractured, the weight of the gelatin below the point of fracture, the grip weight, and the added weight were combined to measure the fracture stress. If the combined stresses were smaller than some minimum fracture stress, the specimen would not fracture in tests up to 120 hours. Tests were not run beyond that time.

The quasi-static fracture stress was between 5.7-6.1 lb/in^2 at 10°C. See Table VI. The 6°C tests showed the threshold fracture stress found at 10°C is certainly temperature dependent.

Table VI

Quasi-Static Stress versus Time

Sample	Stress(psi)	Time(hrs.)	Temp.(°C)	Comments
A	9.8	less than 48 hrs.	6.0	fracture
B	8.8	"	6.0	fracture
C	7.7	"	6.0	fracture
D	8.7	"	10	fracture
E	6.3	1.5	10	fracture
F	5.4	96	12.2	No fracture
G	5.7	120	10.0	No fracture
H	6.1	24	10.0	fracture

10.2.2 Oil Cylinder Tests

10.2.2.1 Apparatus

One of our objectives was to observe the properties of gelatin over a wide range of strain rates. Four different apparatus modifications

were used to study this range: an oil cylinder test, an air cylinder test, a drop weight test, and a gas gun test.

A pneumatic-hydraulic double acting cylinder (Flairline F-2½" x 8") was used to deform gelatin specimens in the oil cylinder tensile tests. A framework and manifold system incorporating the cylinder was built. Strain rates of 10^{-4} - 0.1/sec were measured when oil was used in the cylinder. A lever arrangement was later added onto the system increasing the stroke produced by the cylinder from 8 to 12 inches. The tensile specimens were cast in glass and polystryrene molds. Small metal rings (3/4" I.D.) were placed in the grip sections of the specimens to stiffen the gelatin inside the grip sections. Without the rings, a gelatin tensile specimen could not be pulled to fracture without the specimen slipping out of the grips. The responses from the load cell and clip gauge were recorded on Foxboro Dynalog recorders.

Both the clip gauge and the load cell for the experiments were custom built. The load cell consisted of two equivalent rectangular phosphor-bronze strips. The strips were given similar curvatures and were soldered rigidly into end plates. A strain gauge was glued firmly to the interior surface of one strip and one to the outer surface of the other strip. The strain gauges vary their resistance when the strips are compressed or extended under load - one resistance is decreased, the other resistance is increased. This arrangement doubles the response of the recorder as compared to that for a single strain gauge. A clip gauge consisted of only one curved phosphor-bronze strip with one strain gauge glued firmly to each side.

The clip gauge and load cell were calibrated frequently, and the calibrations were found to be generally stable for both.

10,2,2,2 Results

The oil cylinder tests are summarized in Table VII. Each test was plotted with engineering stress on the ordinate and the engineering strain on the abscissa. The engineering stress is the load divided by the original cross-sectional area of the gauge length, which for all the tensile specimens was 1.0 in^2. The engineering strain was calculated by dividing the elongation in inches by the initial gauge length which was 4.0 inches. The engineering strain rate was calculated by dividing crosshead velocity by the initial gauge length of 4.0 inches. The stress and strain discussed in this report will always refer to engineering stress and engineering strain.

In the plots of strain rates of 5 - 8 x 10^{-4}/sec (Figures 27 and 28), the modulus began to decrease at an engineering strain of about 0.17. Creep was probably responsible for this behavior. At the strain rate of 2.2×10^{-3}/sec, the stress-strain curve for Sample R (Figure 29) was linear nearly up to fracture. The visco-elastic transition strain rate was between 8×10^{-4} - $2. \times 10^{-3}$/sec. Sample R had passed beyond this transition strain rate. Creep was not an appreciable part of the total strain for strain rates above the transition strain rate.

Table VII Summary of Oil Cylinder Tests

Sample No.	Temp °C	Elongation at fracture(in)	Strain at fracture($\frac{in}{in}$)	Peak Stress (psi)	Strain Rate (in/in)(sec^{-1})	Elastic Modulus (psi)
A	5.7	3.9	0.98	13.1	2.9×10^{-3}	24.0
B	5.7	4.6	1.15	12.9	4.3×10^{-3}	16.0
D	5.7	4.6	1.15	10.2	1.7×10^{-2}	14.4
G	6.0	4.2	1.05	8.4	1.6×10^{-2}	11.4
C	5.7	4.4	1.10	11.0	2.5×10^{-2}	14.4
E	6.0	4.3	1.08	13.8	2.4×10^{-2}	18.4
F	6.0	4.4	1.10	12.7	2.4×10^{-2}	15.2
L	9.5	2.2	0.55	9.5	5.5×10^{-4}	30.0
Q	9.5	1.3	0.32	5.8	7.8×10^{-4}	28.0
R	10.0	1.4	0.35	6.8	2.2×10^{-3}	22.8
X	10.3	2.0	0.50	9.1	2.5×10^{-3}	27.2
O	9.5	1.6	0.40	7.7	3.0×10^{-3}	28.0
V	10.2	1.6	0.40	10.5	3.0×10^{-3}	29.2
N	9.4	2.4	0.60	9.4	3.2×10^{-3}	19.2
M	9.5	1.5	0.38	6.9	3.5×10^{-3}	25.6
U	10.2	1.9	0.48	10.9	4.0×10^{-3}	37.0
W	10.2	2.2	0.55	14.5	4.0×10^{-3}	47.0
S	9.3	2.4	0.60	7.7	8.5×10^{-3}	19.6
2C	10.2	3.0	0.75	15.4	1.7×10^{-2}	32.0
2D	10.2	2.4	0.60	12.7	1.7×10^{-2}	34.0
2E	10.3	3.3	0.78	15.3	2.0×10^{-2}	25.6

Table VII - Continued

Sample No.	Temp °C	Elongation at fracture(in)	Strain at fracture($\frac{in}{in}$)	Peak Stress (psi)	Strain Rate (in/in)(sec^{-1})	Elastic Modulus (psi)
P	10.0	2.8	0.70	10.0	2.1×10^{-2}	21.2
Y	10.2	3.5	0.88	19.0	2.2×10^{-2}	32.0
2B	10.2	4.4	1.10	18.1	2.5×10^{-2}	33.2
2A	10.2	3.5	0.88	16.5	3.5×10^{-2}	28.8
H	10.2	3.8	0.95	13.7	4.2×10^{-2}	19.6
Z	10.2	4.4	1.10	21.3	4.2×10^{-2}	27.6
2F	10.2	4.6	1.15	20.9	6.0×10^{-2}	28.0
K	10.0	4.1	1.02	8.5	8.5×10^{-2}	15.0
I	10.0	4.3	1.08	14.2	9.2×10^{-2}	16.4

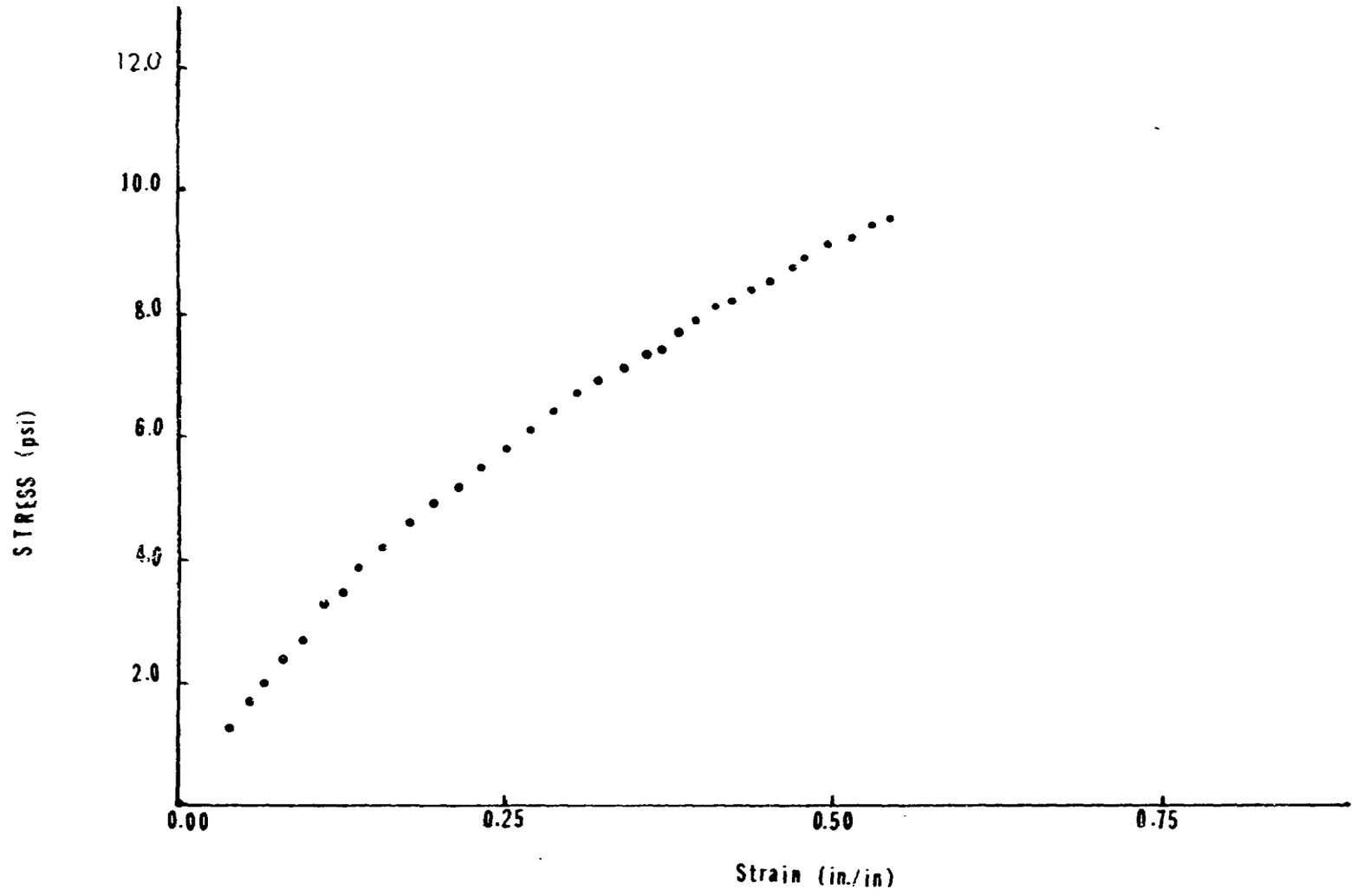

Figure 27: Stress vs. Strain - Sample $\dot{\epsilon} = 5.5 \times 10^{-4}$/sec

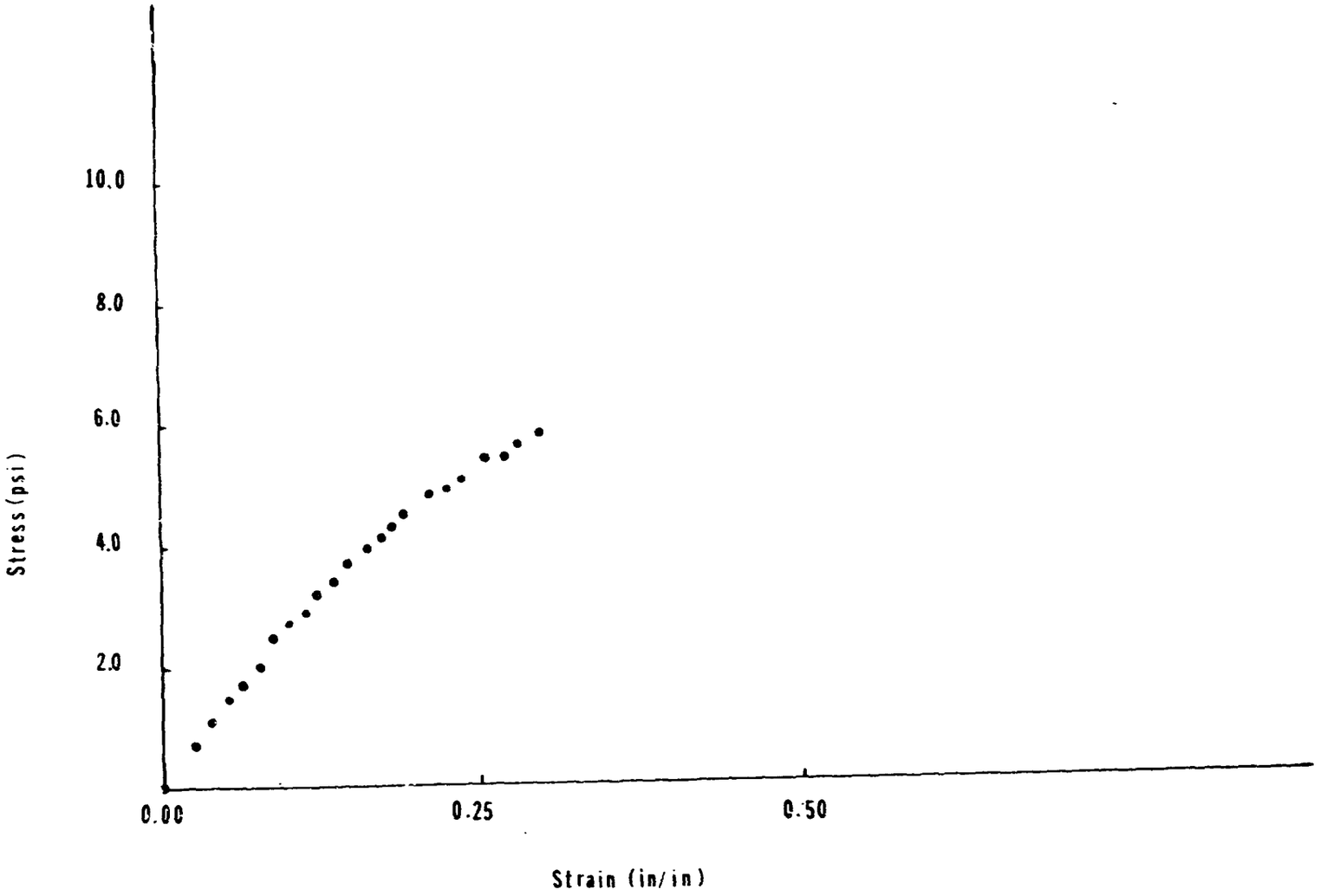

Figure 28: Stress vs. Strain - Sample Q - 7.8×10^{-4} / sec

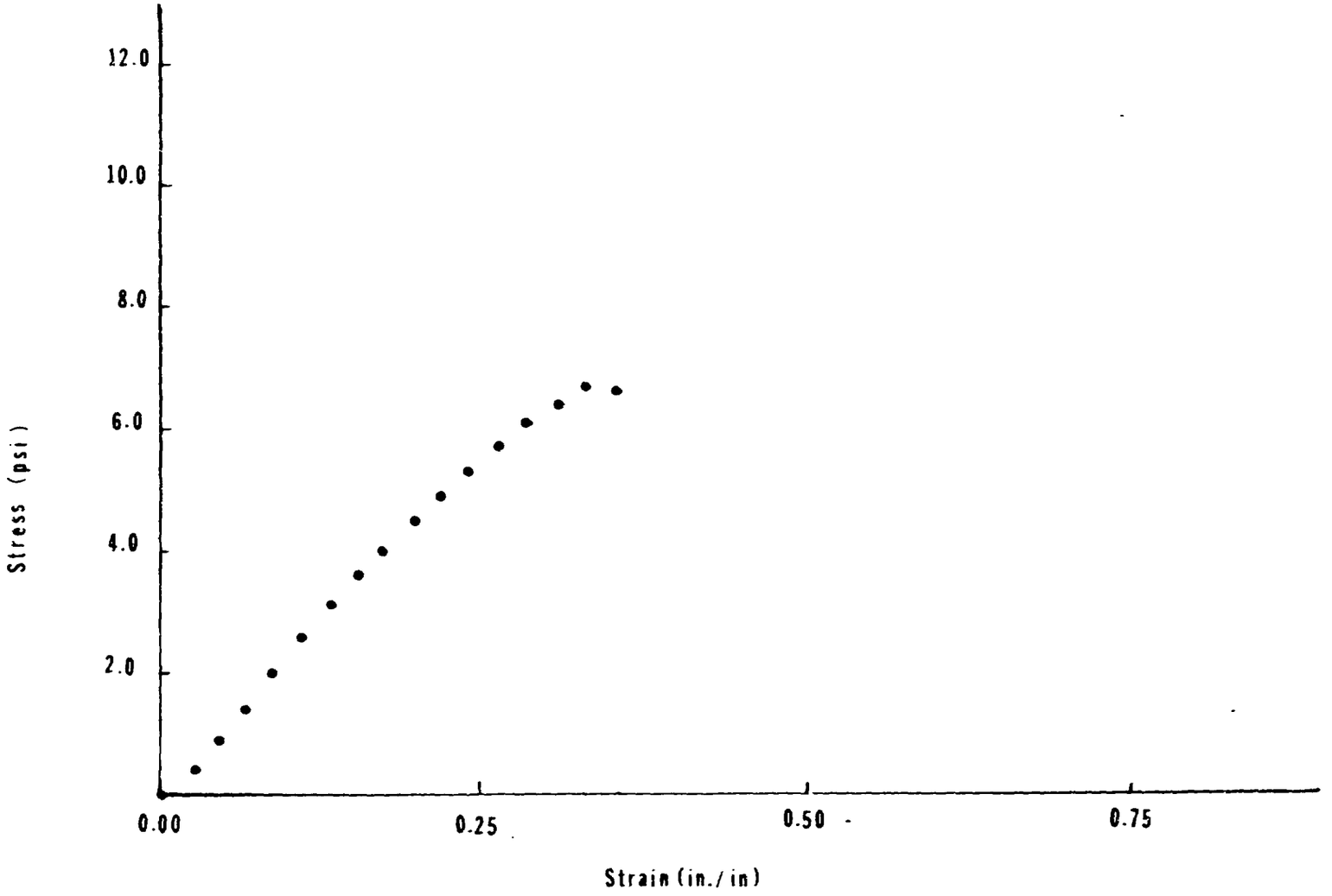

Figure 29: Stress vs Strain - Sample R - 2.2×10^{-3}/sec

As the strain rate increased, the peak stress on the specimens before fracture increased. Figure 30 shows peak stress plotted on the ordinate and strain rate plotted logarithmically on the abscissa. The gelatin specimen fractured within a range of stresses at a particular strain rate.

As the nominal strain rate increased, the strain of the gelatin specimen at fracture generally increased. See Figure 31. Having compared tests at the same strain rate but different temperatures, the lower temperature tests fractured at higher strains. The 6.0°C tests fractured at a nominal strain of 1.0-1.15 at strain rates between $3x10^{-3}$/sec and $2.5x10^{-2}$/sec. Specimens at 10°C fractured at strains of 0.30-1.10 for strain rates between $5x10^{-4}$/sec and $9x10^{-2}$/sec.

The elastic modulus, E, was 29 psi at strain rates between 5 and $8x10^{-4}$/sec. See Figure 32. The elastic modulus for each of the tests was calculated by measuring the initial slope of the stress-strain curve through the point where the specimen was under zero stress. The elastic modulus at 10°C tended to decrease from strain rates of about $4x10^{-3}$/sec to a minimum at a strain rate of about $9x10^{-2}$/sec. Young's modulus for 6°C tests were lower than tests at 10°C.

The stress-strain plots of the remaining oil cylinder tests can be found in Figures 33 through 49. Several tests are grouped together when they have similar strain rates.

10.2.3 Air Cylinder Tests

10.2.3.1 Apparatus

A double-acting air cylinder (WABCO-L3W-1½"x16") was used for the air cylinder tests. The cylinder was mounted on a frame and the specimens were mounted on a crossbeam in line with the cylinder rod. Compressed air (90psi capacity) was used to drive the cylinder. The piston velocity was controlled by altering the input air pressure or adjusting a valve constriction on the input air line. Strain rates of 0.025/sec to 5.1/sec were measured with the air cylinder. At higher strain rates, the limitation of response time on the Foxboro recorders made it necessary to use an oscilloscope (Tektronics 545A with a Type Q plug-in unit) and a timer (Transitor Specialities Model 385-R). The oscilloscope displayed load versus time directly. The oscilloscope was calibrated before each run by hanging a known weight on the load cell. The strain rate was obtained by measuring the time interval for the moving grip to traverse a known distance during the actual test (while under load).

At higher strain rates (0.50/sec) the gelatin specimen would slip completely out of the grips used previously. After trying several approaches, it was decided to incorporate the grips into the gelatin directly. A short piece of ½" rod was cut to fit across the widest part of the grip section. A piece of terry cloth was draped across the rod and a clip was slipped over both the terry cloth and rod. The clips were 5/8" I.D. tubing as long as the rod and with ¼" longitudinal slots cut into them. A second piece of terry cloth was draped over the clip. The four resulting terry cloth strips extended down into the gauge section, and were separated from each other (with small rolls of paper) to maximize the gelatin-cloth adhesion.

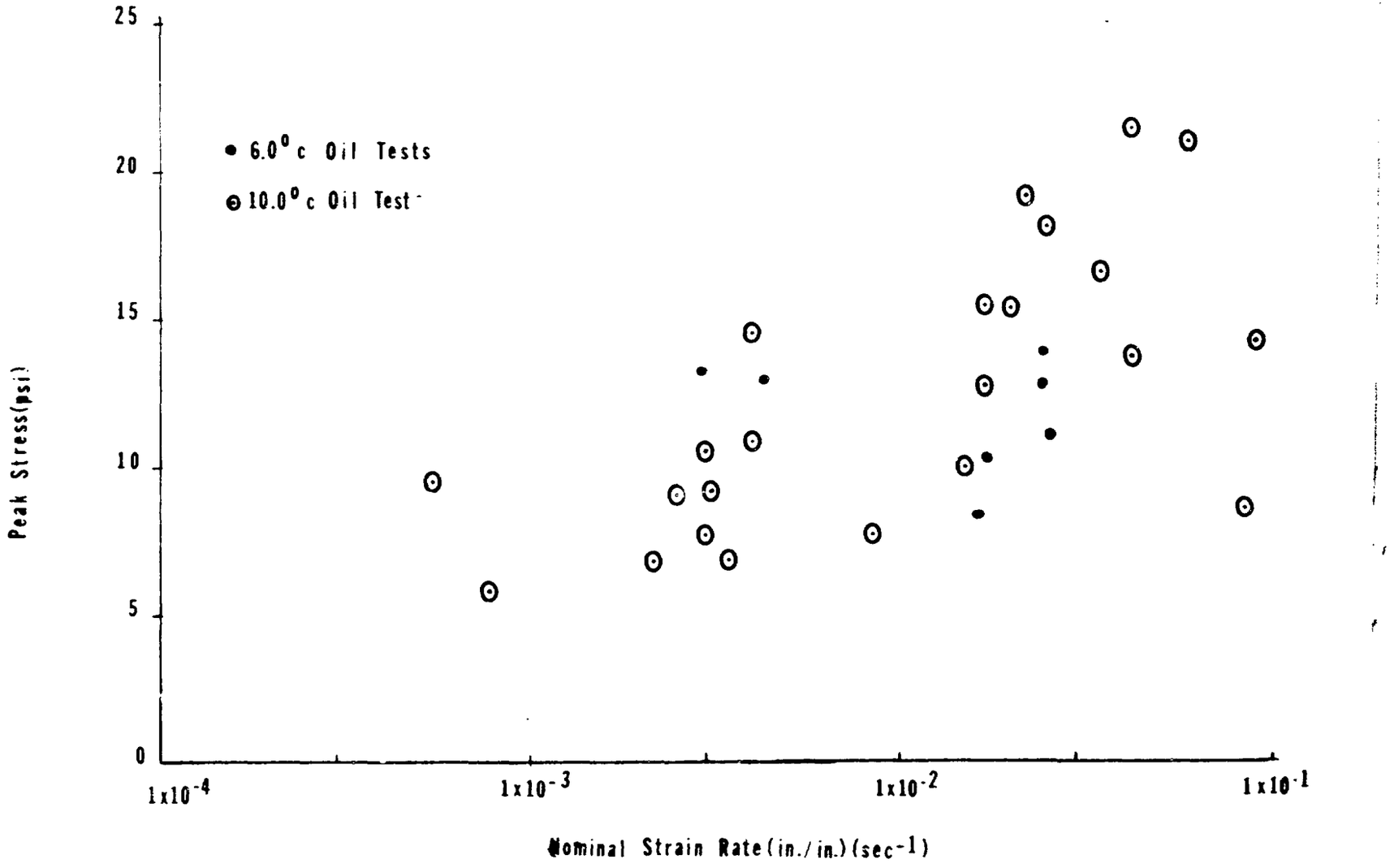

Figure 30: Peak Stress vs. Nominal Strain Rate -Oil Tests

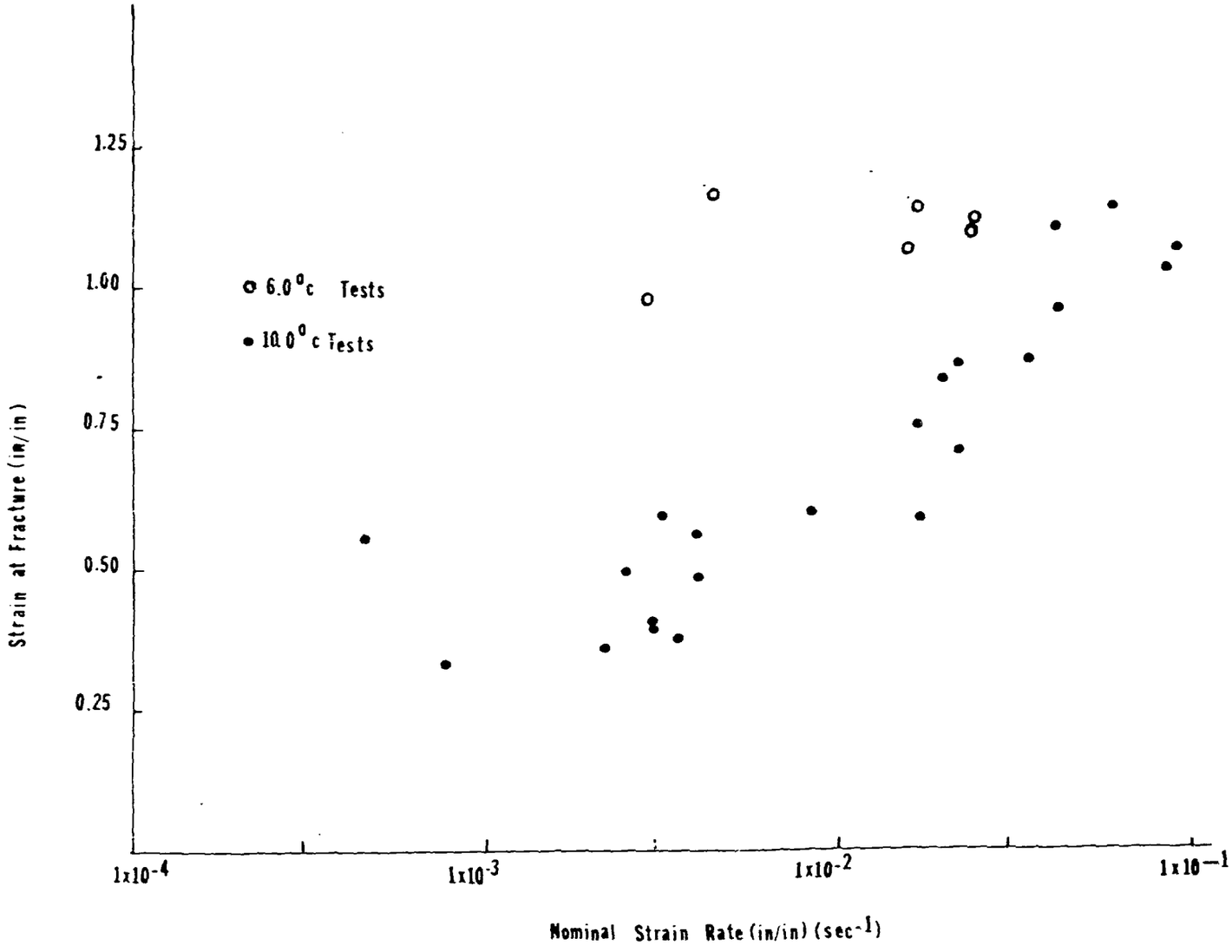

Figure 31: Strain at Fracture vs. Nominal Strain Rate - Oil Tests

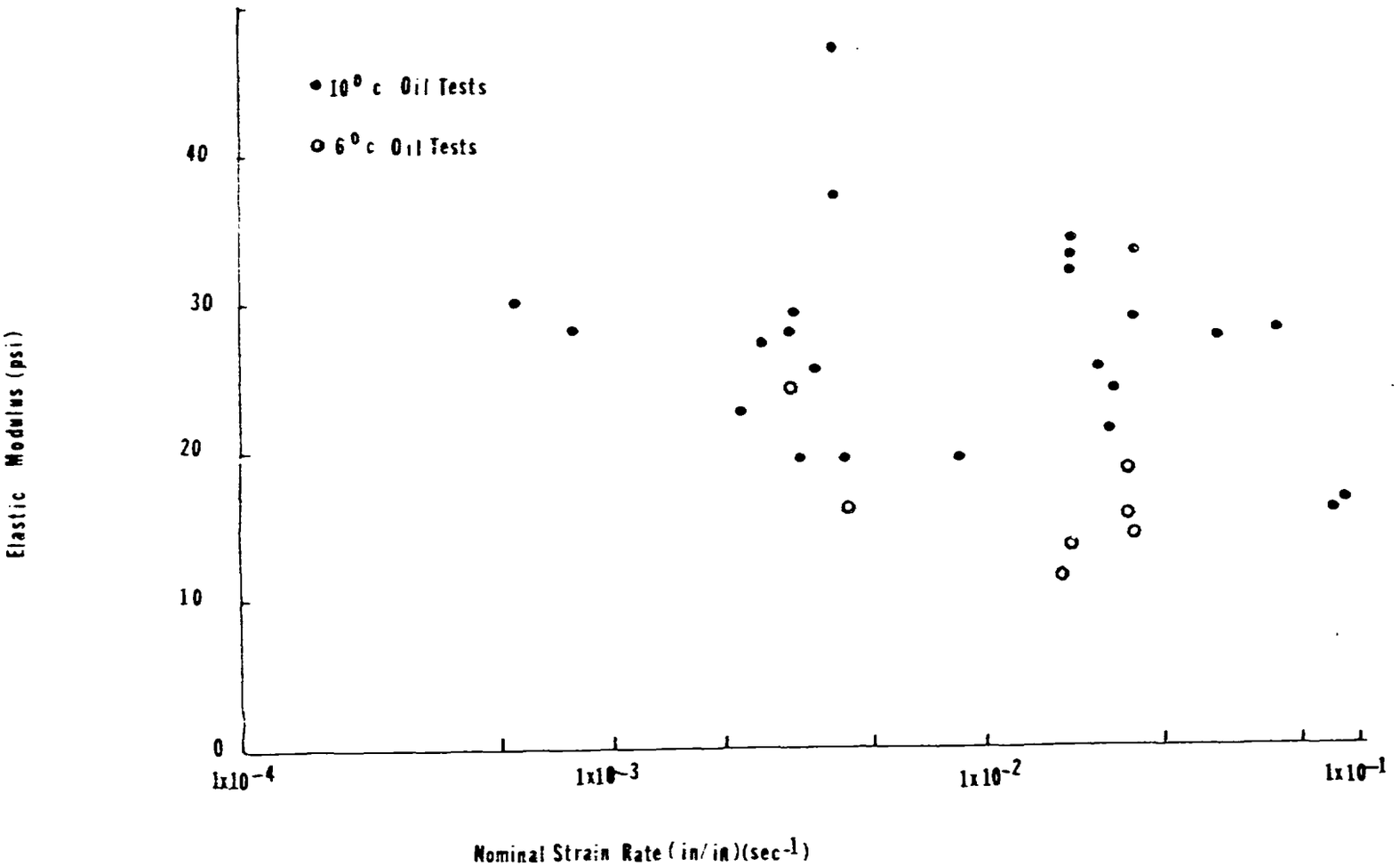

Figure 32: Elastic Modulus vs. Nominal Strain Rate - Oil Tests

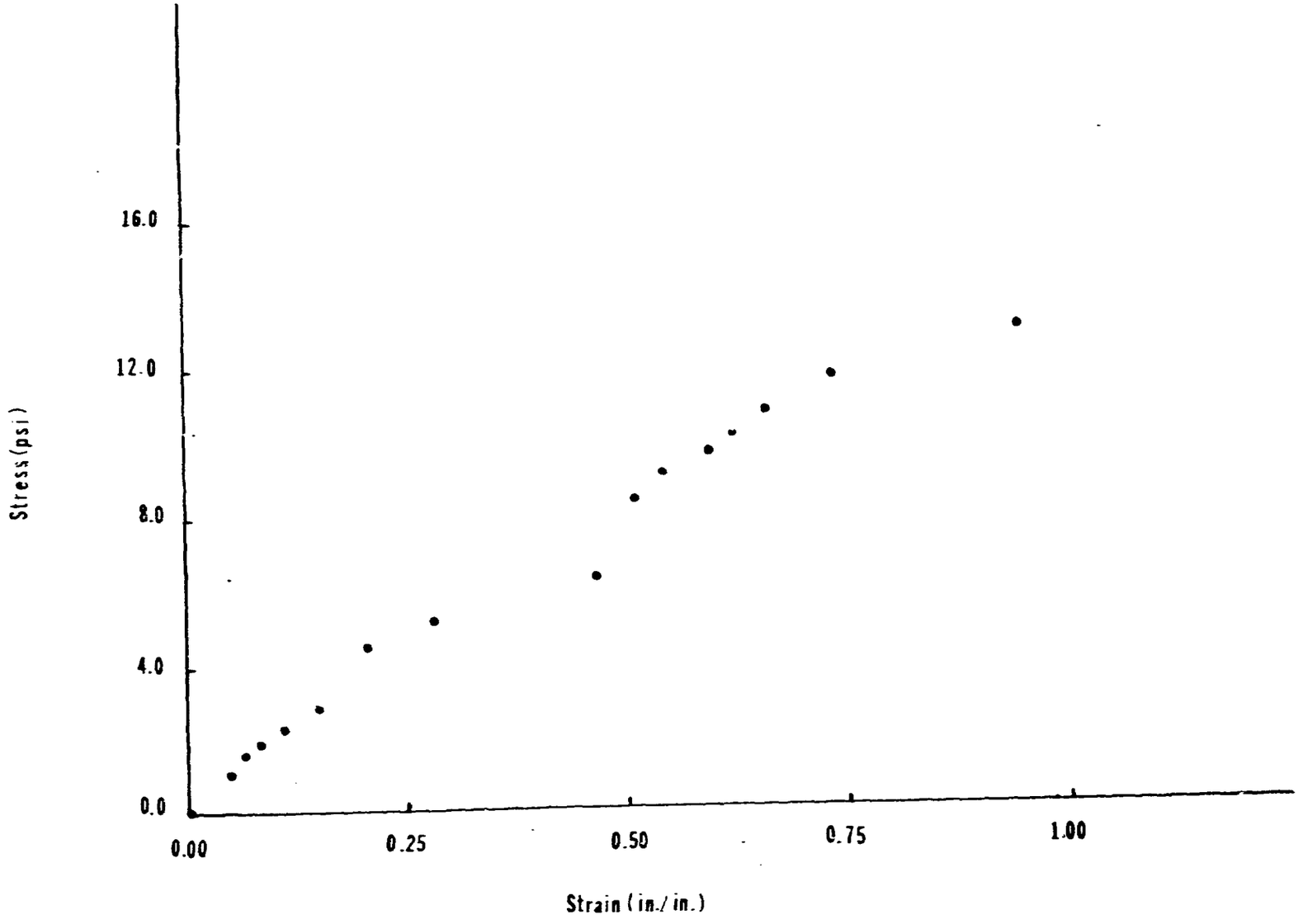

Figure 33: Stress vs. Strain – Sample A – 2.9×10^{-3}/sec.

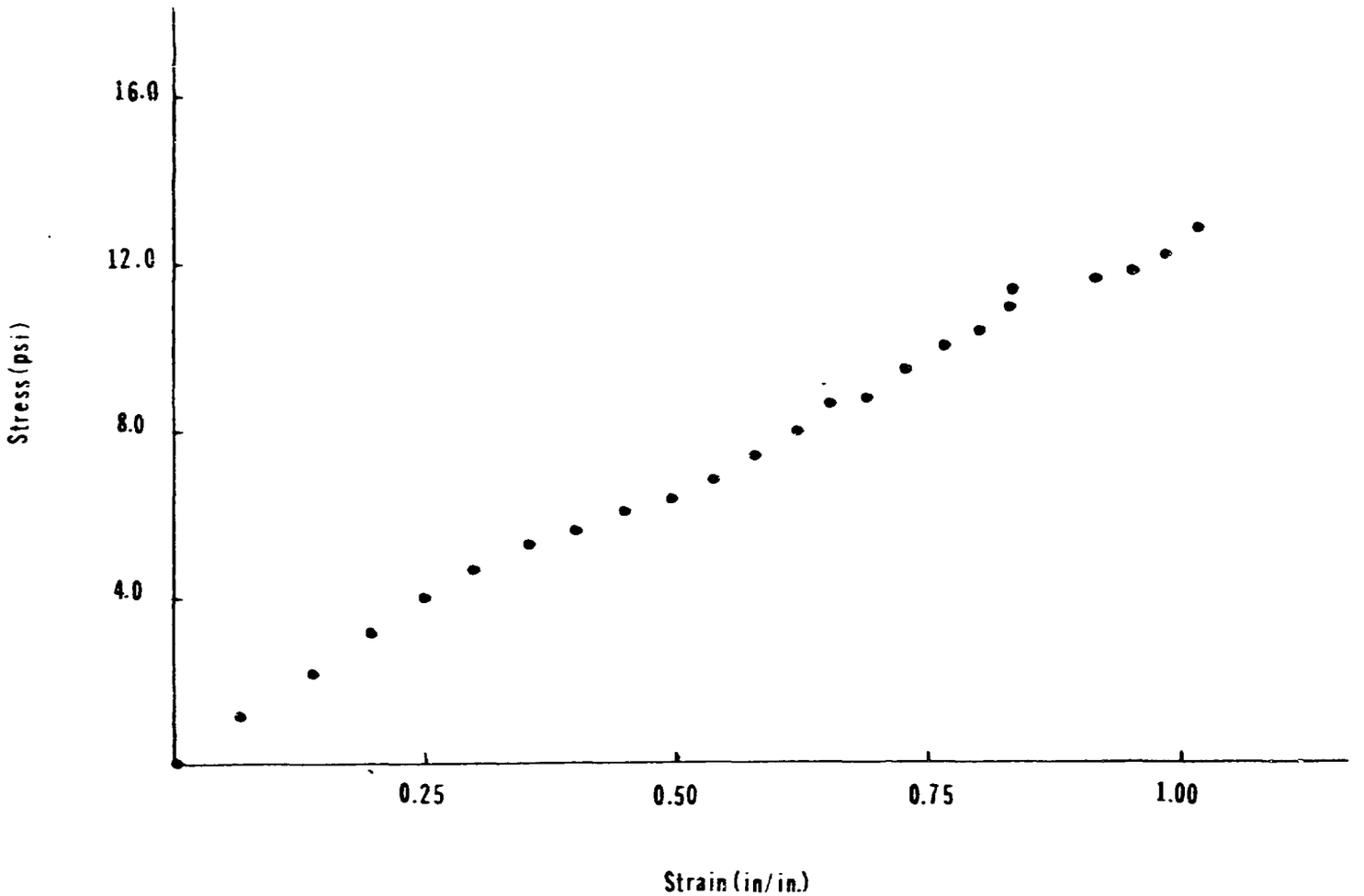

Figur 34: Stress vs. Strain - Sample B - 4.3×10^{-3}/sec.

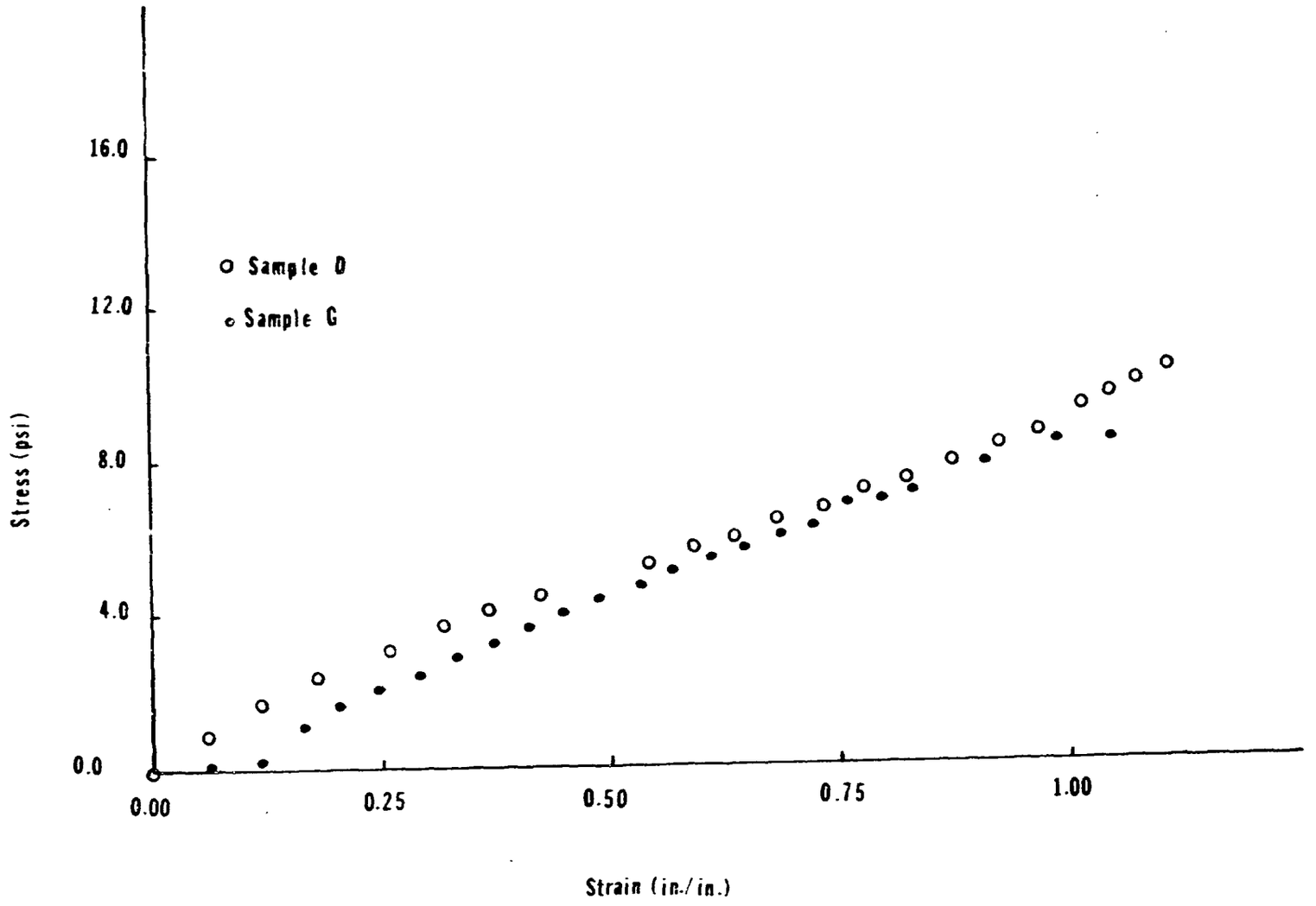

Figure 35: Stress vs. Strain- Samples D and G - 1.7×10^{-2}/sec.

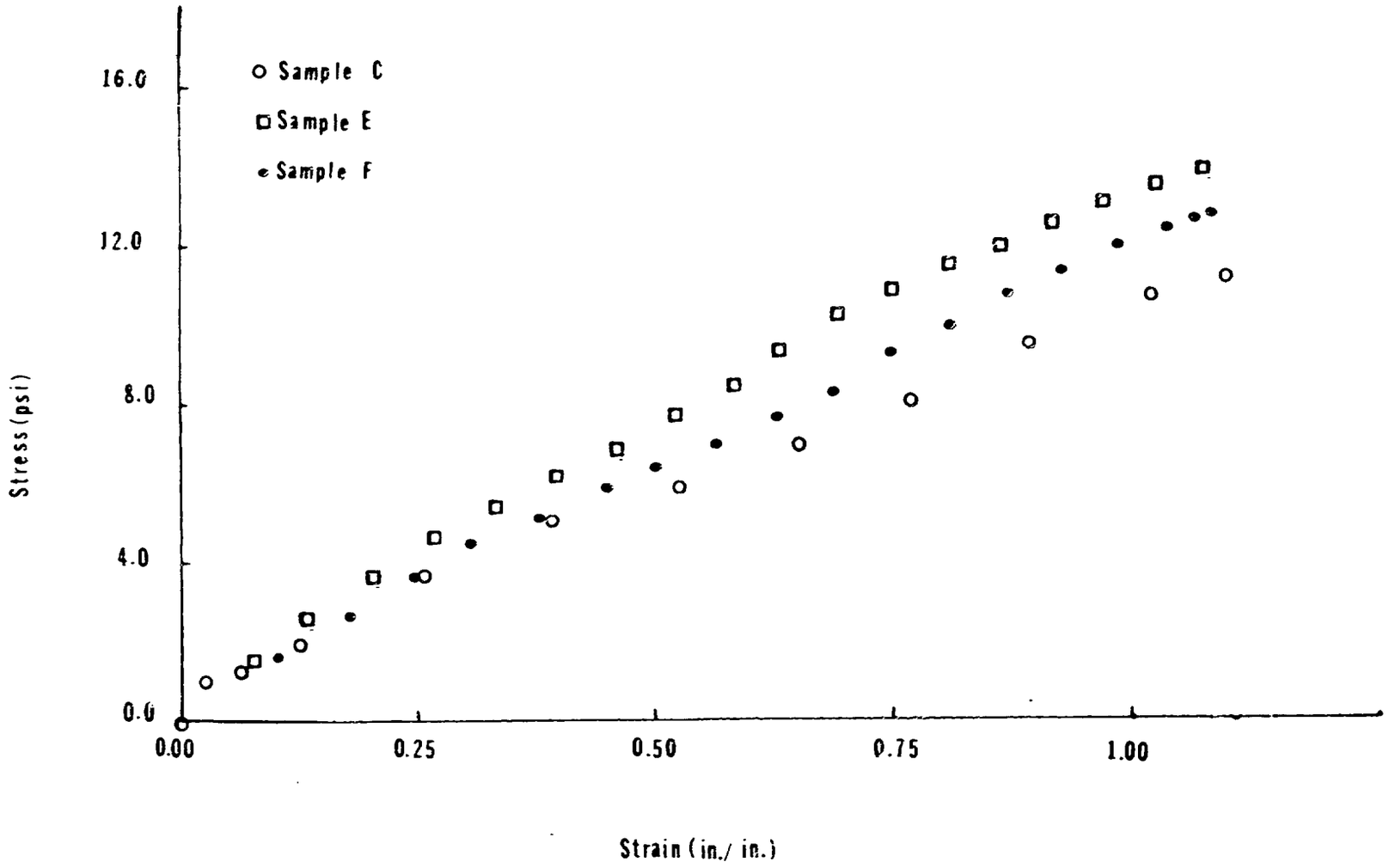

Figure 36: Stress vs. Strain – Samples C, E, and F – 2.5×10^{-2}/sec

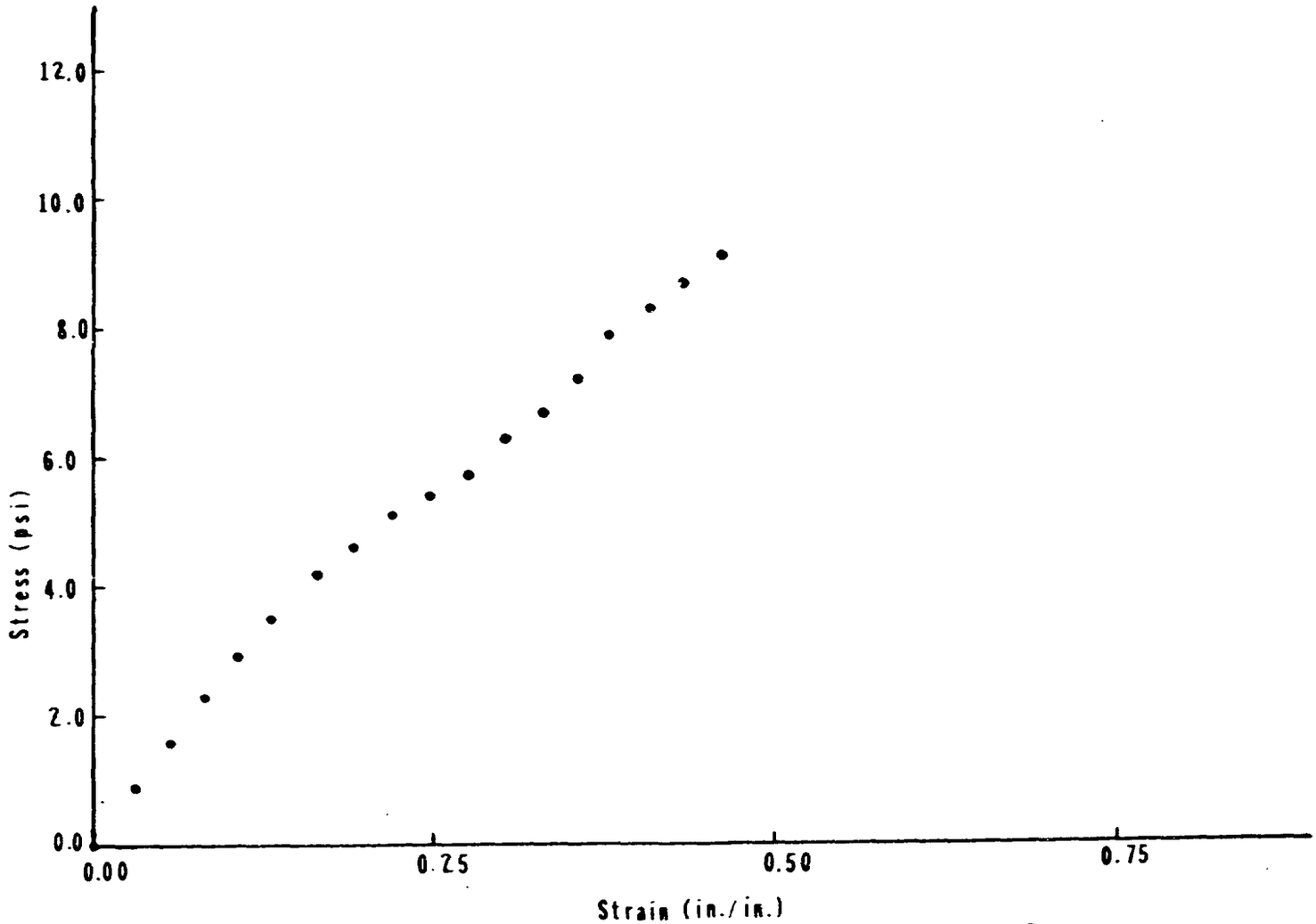

Figure 37: Stress vs. Strain - Sample X - 2.5×10^{-3}/sec

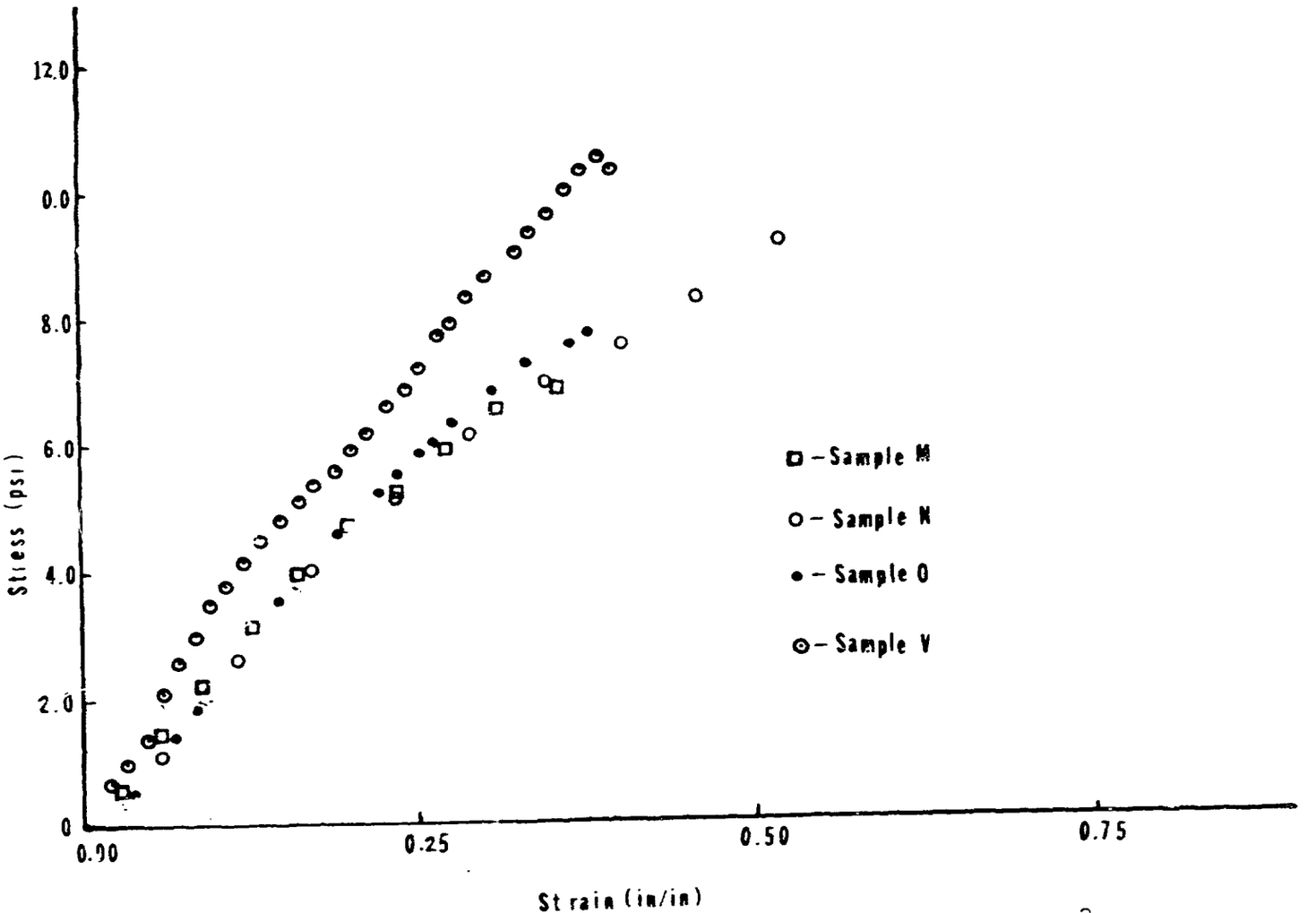

Figure 38: Stress vs. Strain - Samples M, N, O, and V - 3.2×10^{-3}/sec

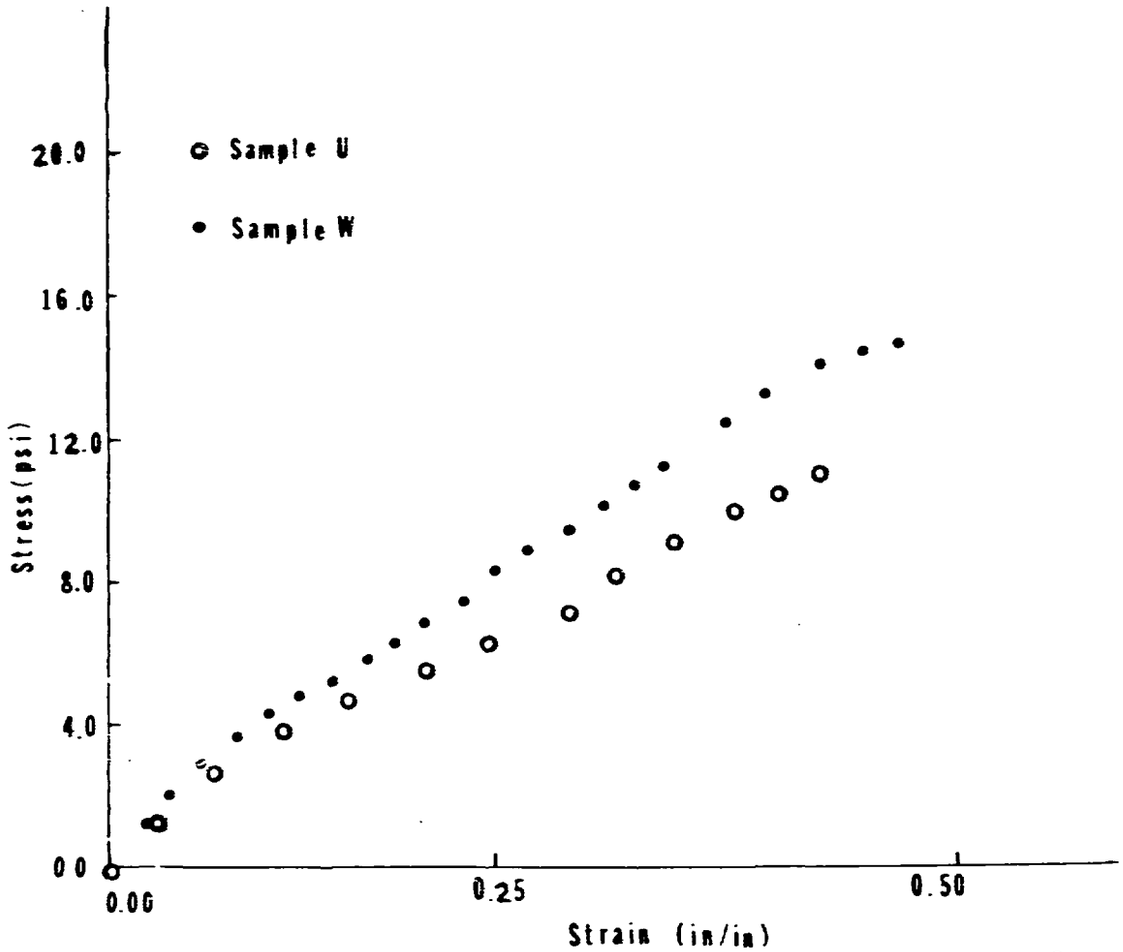

Figure 39: Stress vs. Strain - Samples U and W - 4.0 x 10^{-3}/sec

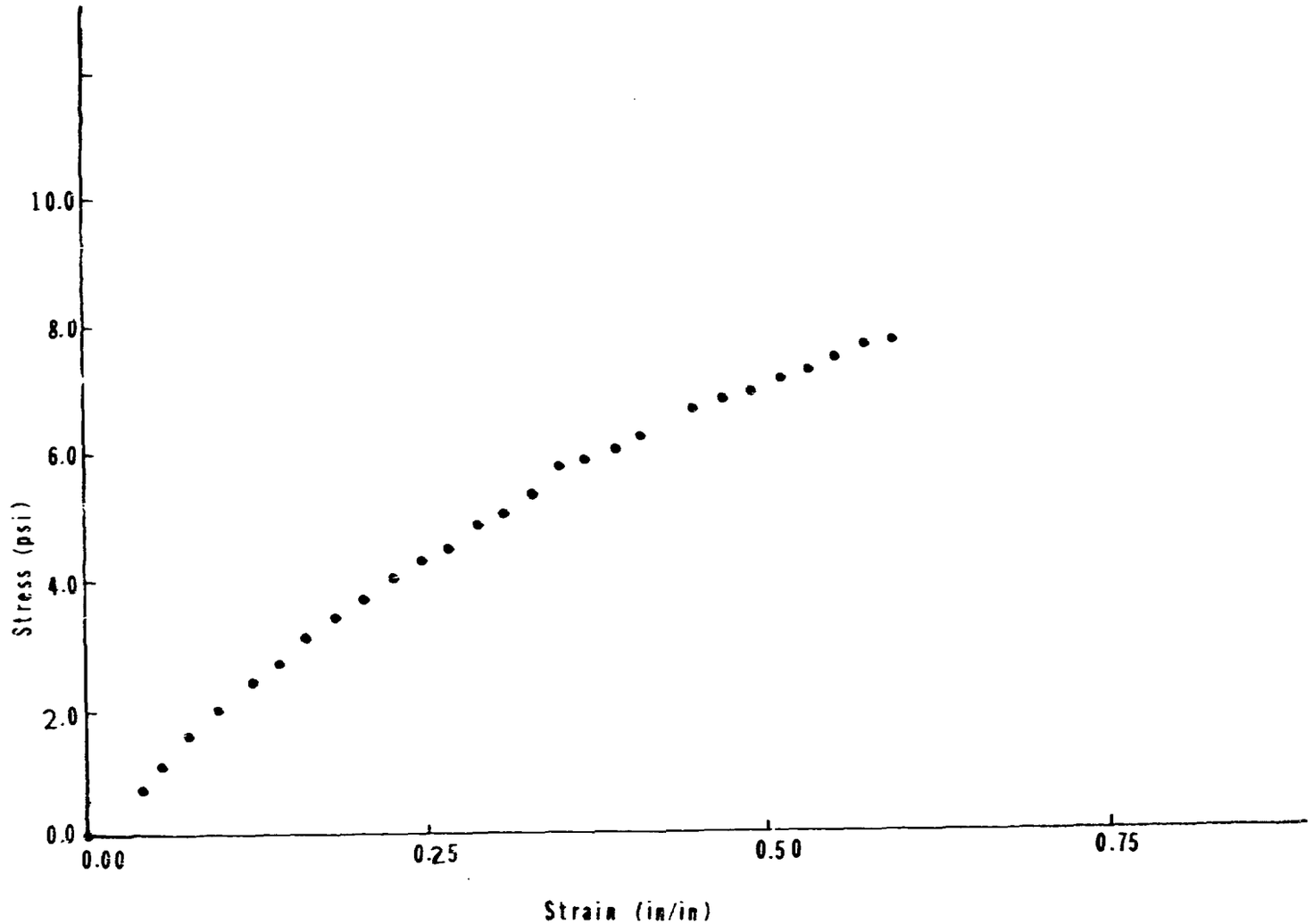

Figure 40: Stress vs. Strain - Sample S - 8.5×10^{-3}/sec

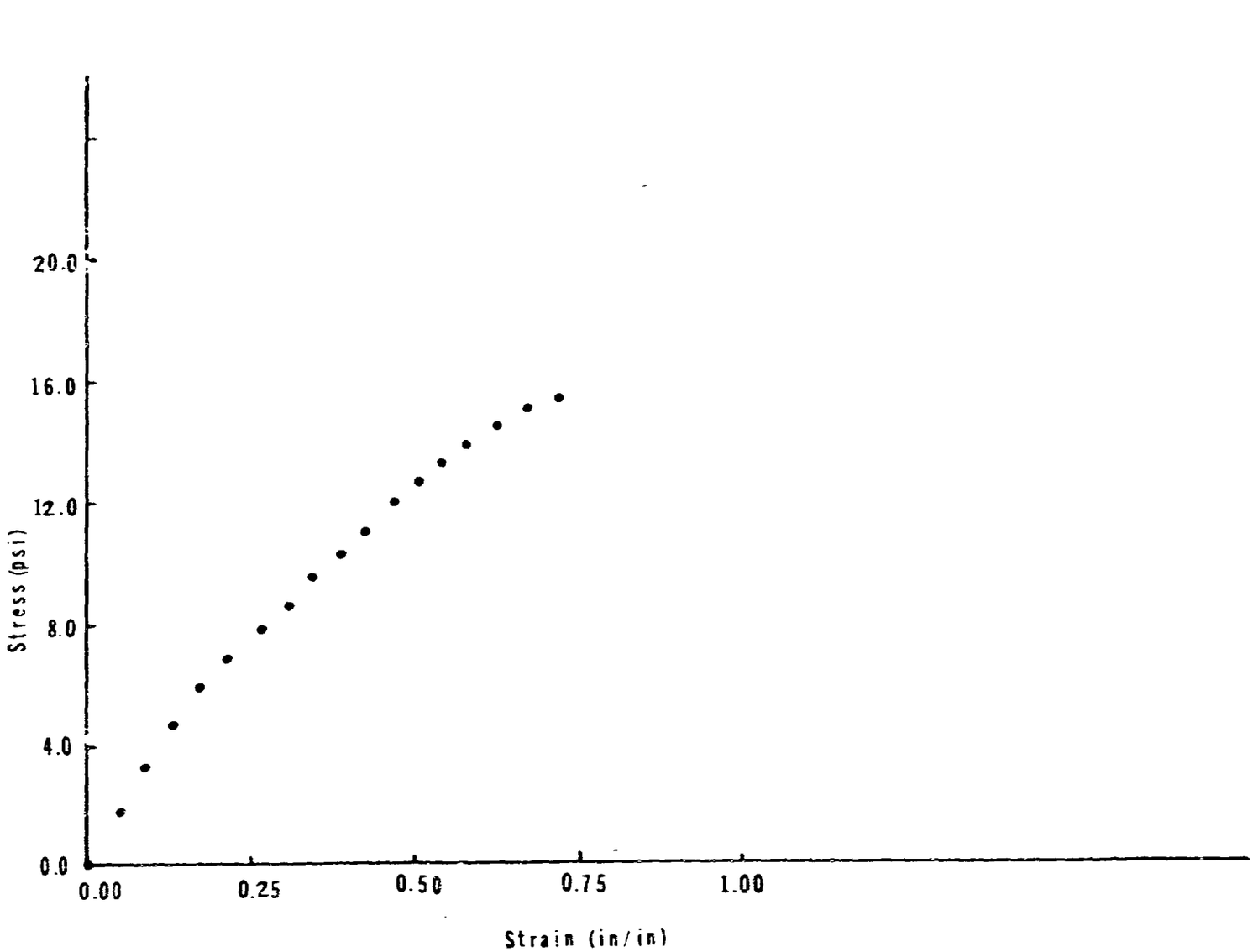

Figure 41: Stress vs. Strain - Sample 20 - 1.7×10^{-2}/sec

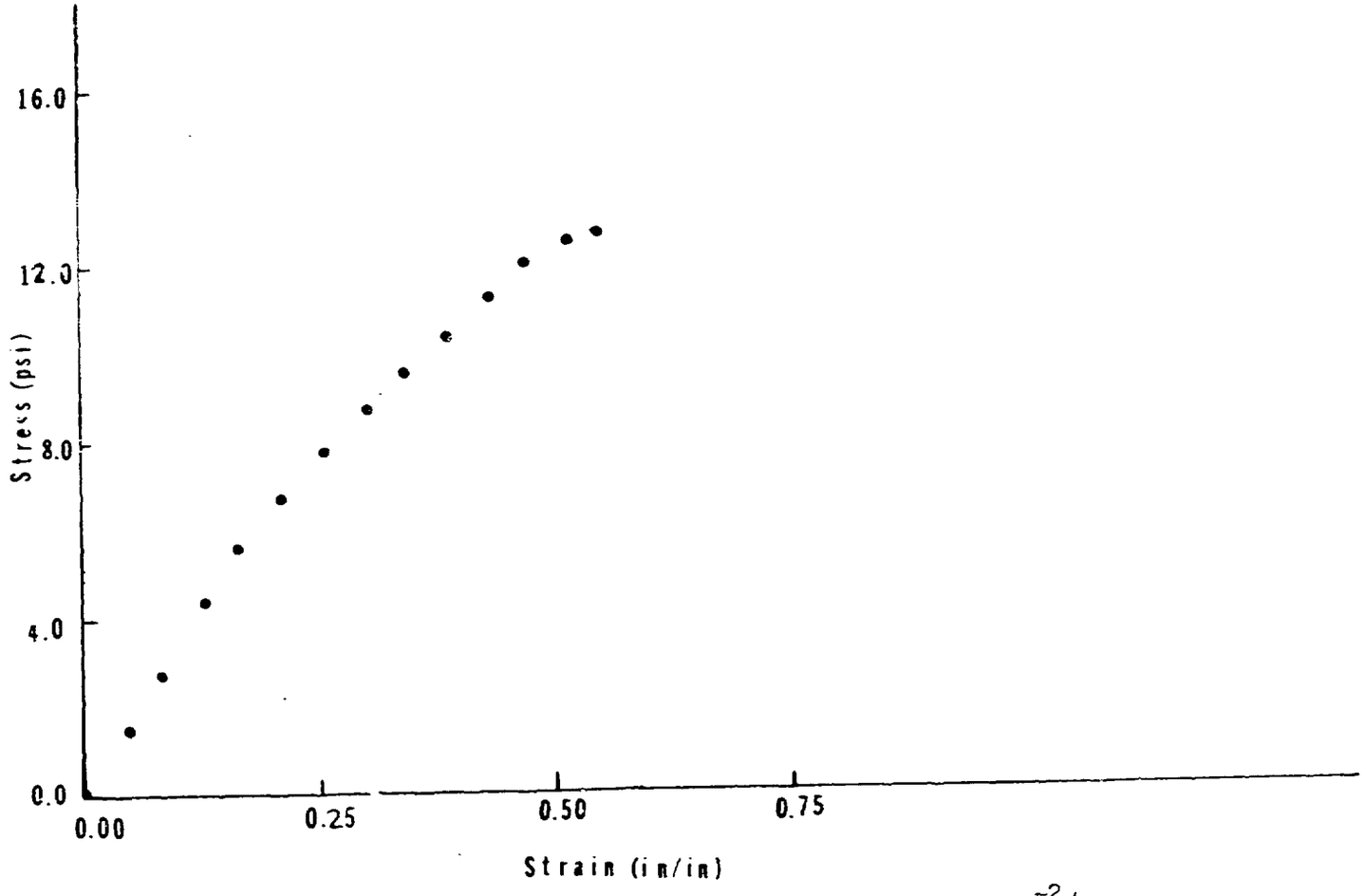

Figure 42: Stress vs. Strain - Sample 2D - 1.7 x 10^{-2}/sec

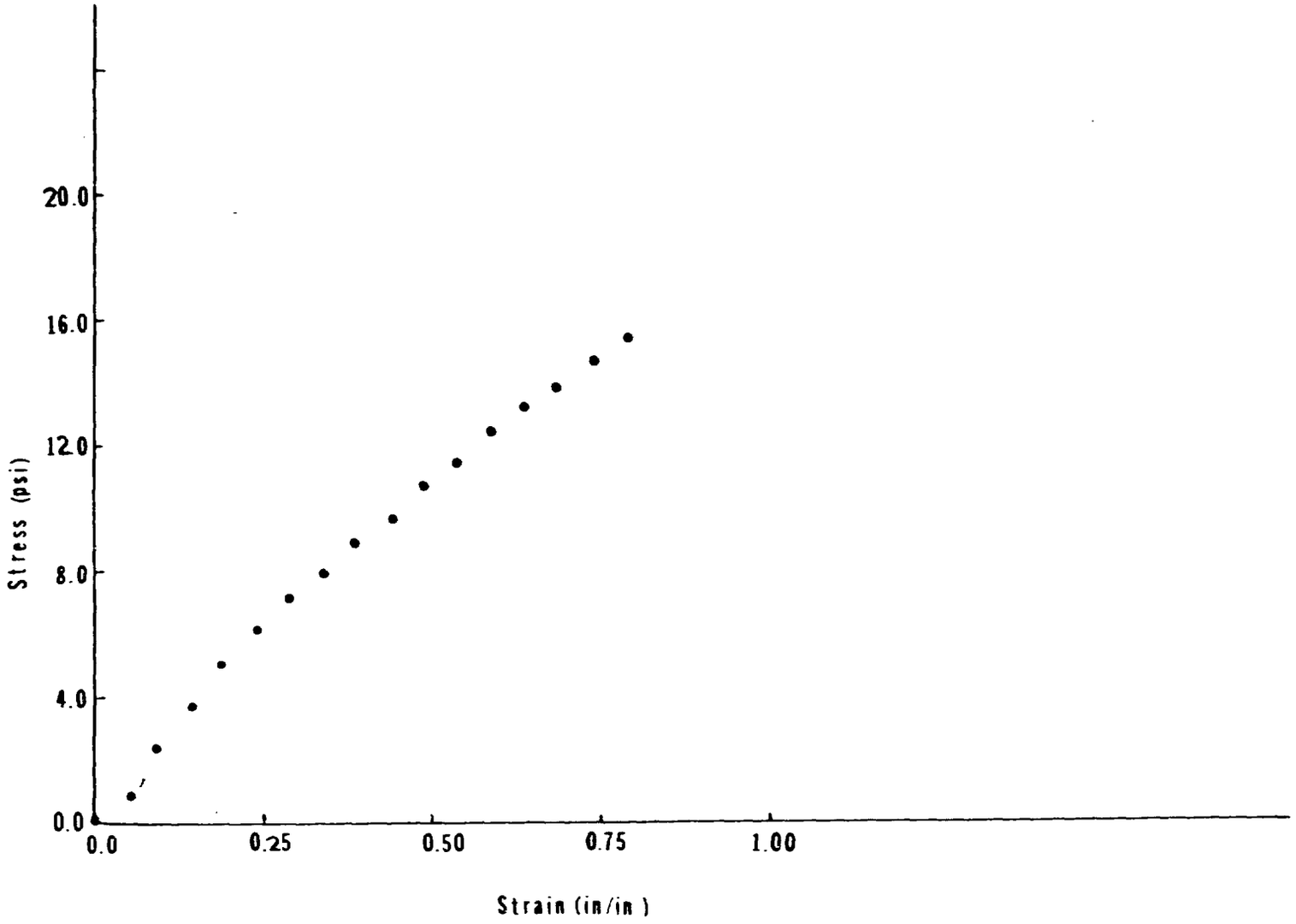

Figure 43: Stress vs. Strain - Sample 2E - 2 x 10^{-2}/sec

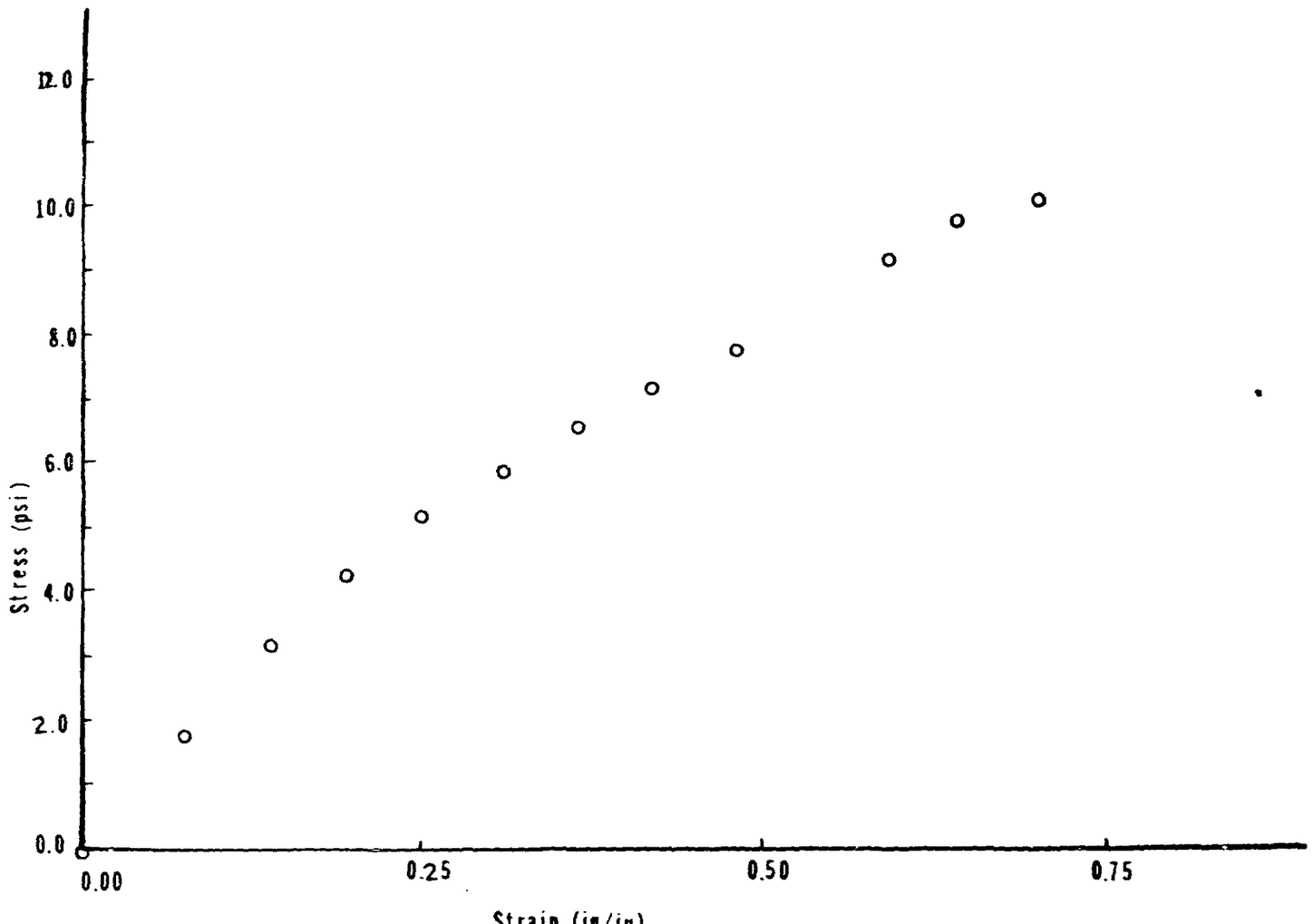

Figure 44: Stress vs. Strain - Sample P - 2.1 x 10^{-2}/sec

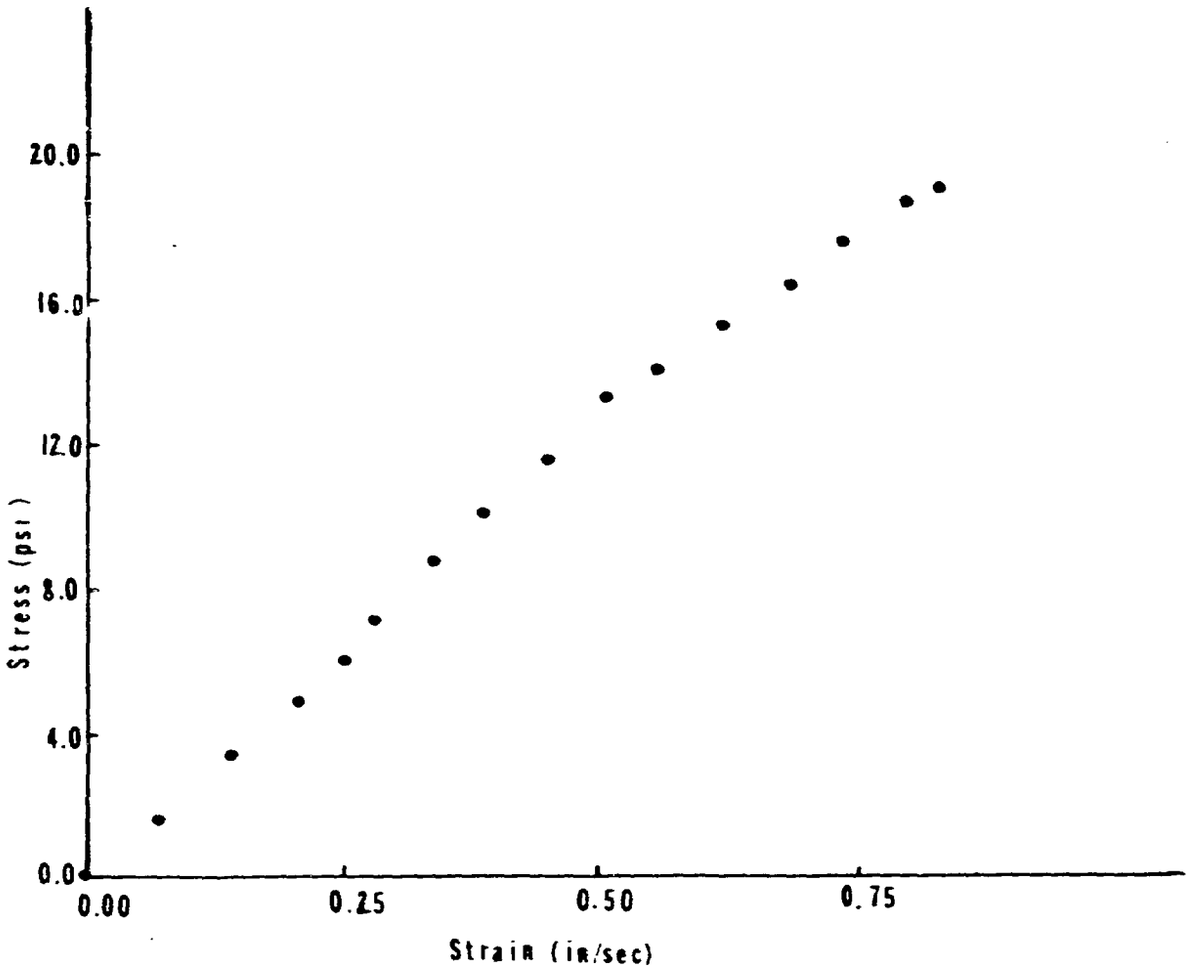

Figure 45: Stress vs. Strain - Sample Y-2.2 x 10^{-2}/sec

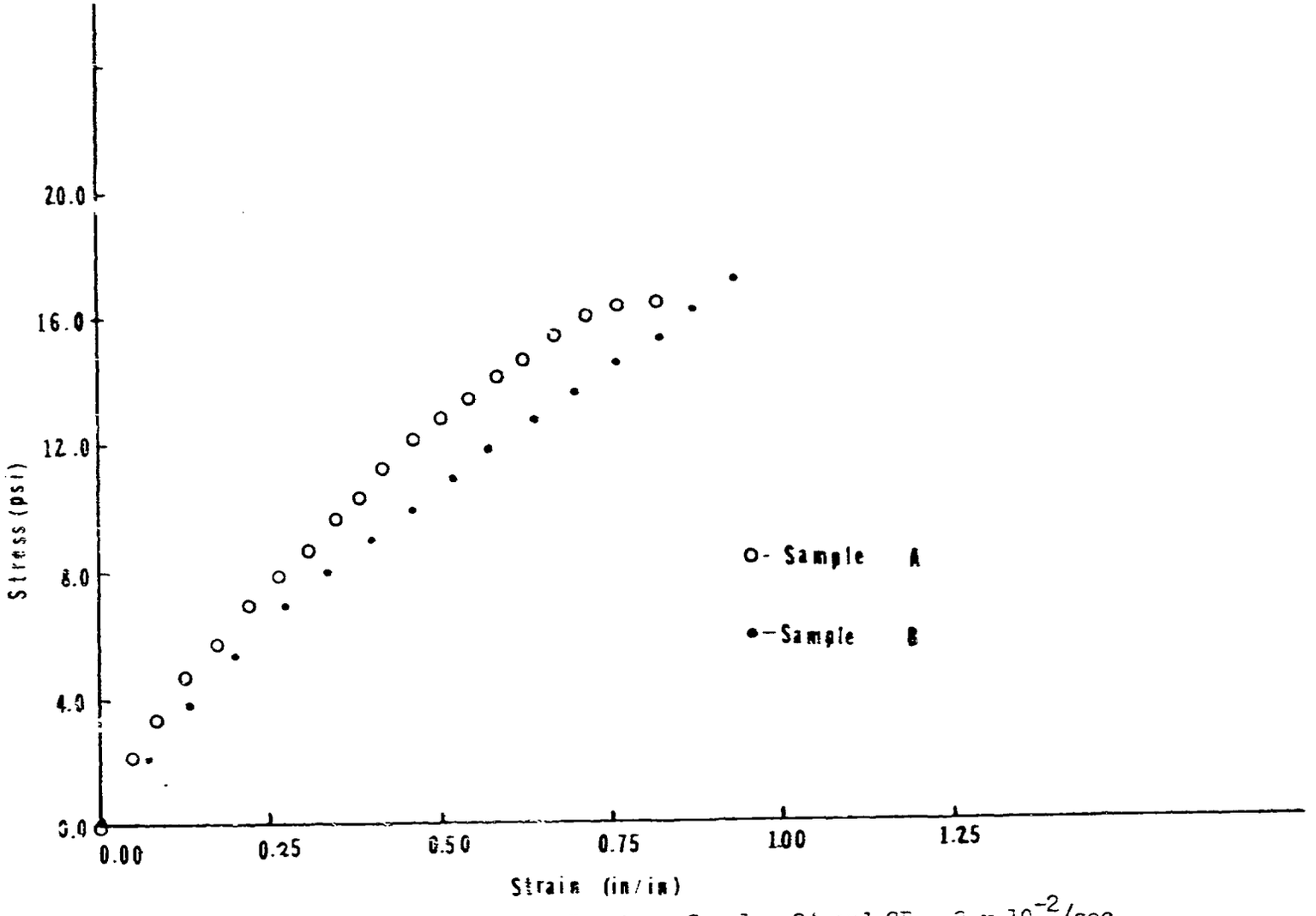

Figure 46: Stress vs. Strain - Samples 2A and 2B - 3×10^{-2}/sec

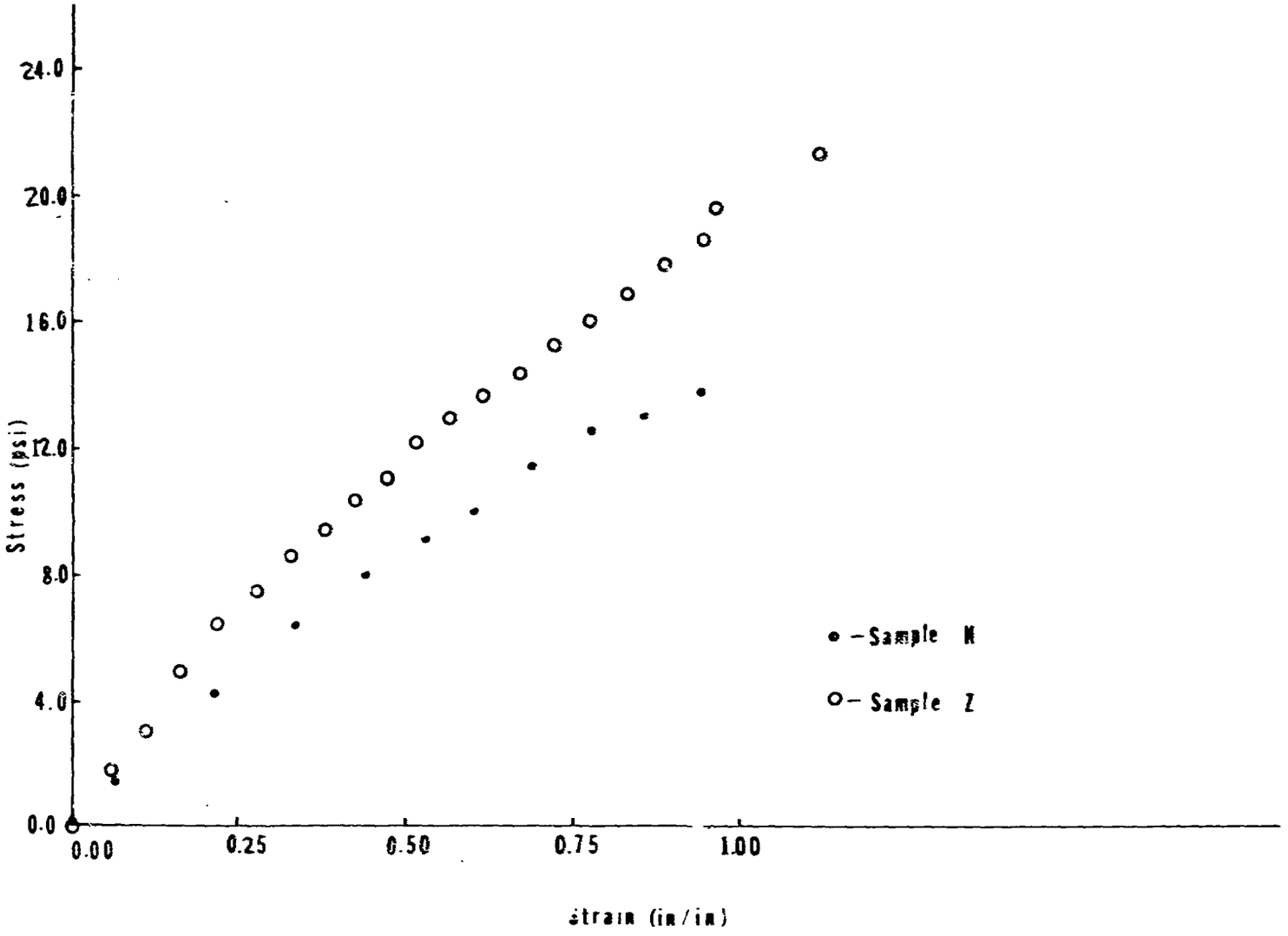

Figure 47: Stress vs. Strain - Samples H and Z - 4.2×10^{-2}/sec

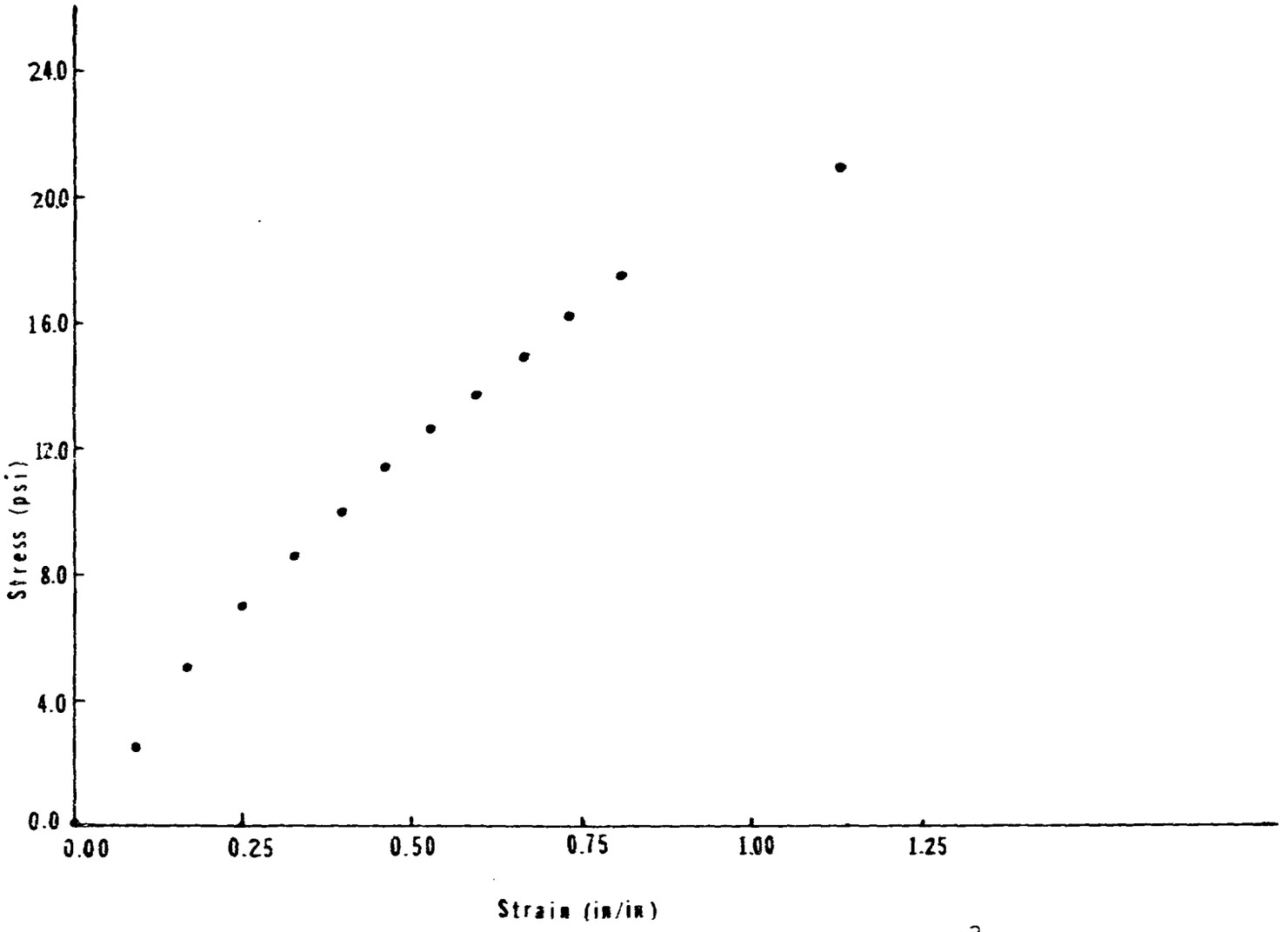

Figure 48: Stress vs. Strain - Sample 2F - 6 x 10^{-2}/sec

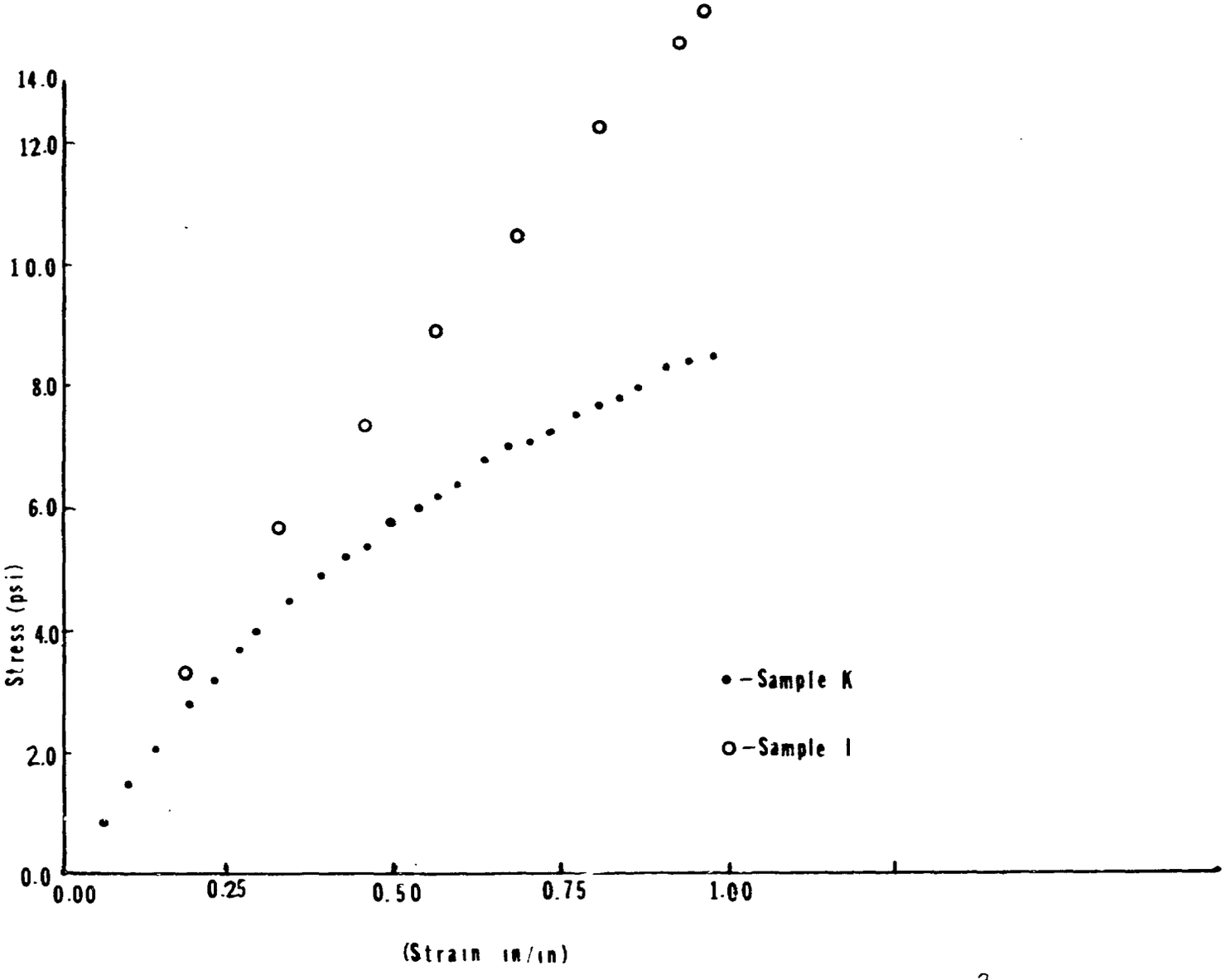

Figure 49: Stress vs. Strain - Samples I and K - 9.2×10^{-2}/sec

After the gelatin was cast and gelled, the short rod was replaced with a longer rod, which provided stub ends for securing the specimen in the various test configurations.

The gelatin specimens were kept at refrigerator temperature for one day prior to testing. Each specimen was then taken out of the refrigerator and the test was run within 2 minutes to prevent the gelatin from warming excessively.

10.2.3.2 Results

The air cylinder test results are summarized in Tables VIII and IX. The air cylinder data was divided into tests recorded by the Foxboro recorders and tests recorded by the oscilloscope and timer.

Peak stress continued to increase with increasing nominal strain rates. The peak stress prior to fracture increased roughly 20 psi as the strain rate increased tenfold. See Figure 50.

The strain at fracture also increased as the strain rate increased. See Table VIII. The strain was 1.1 at a strain rate of 0.025/sec, 1.6 at a strain rate of 0.14/sec, and 2.0 at a strain rate of 0.51/sec.

The modulus of elasticity decreased to the range of 12 to 20 psi at nominal strain rates between 0.1/sec and 1.0/sec. This represented a minimum when compared to the elastic moduli of the oil tests and subsequent air tests. See Figure 51. In these tests the gelatin specimens contained metal rings in the grip sections to improve the rigidity of the grip sections. Stress and strain were plotted simultaneously on two Foxboro Dynalog recorders. The slope of the initial stress-strain curve was measured to calculate the elastic modulus.

Observing the curves for Samples 2-G to 2-N (Figures 52 to 57) the initial elastic modulus appeared to be constant to a strain of about 0.50. From that point the elastic modulus approximately doubled and the modulis appeared to remain constant at its new value.

It must be kept in mind that the air cylinder test was a "soft test machine" test. The air in the cylinder was compressible allowing for a decreasing strain rate as an opposing force, in this case from the gelatin specimen, increased.

The elastic modulus for the air cylinder test within a strain rate of 1.0/sec to 5.0/sec was between 31-50 psi. In all these tests the new grips which we embedded in the gelatin specimen were used. The stress and strain were measured by the oscilloscope and timer. The strain rate acquired from the timing measurement was used as though it was a "hard" test measurement although the air test was actually a "soft" test. To calculate the strain at fracture, the product of the crosshead velocity and rise time was divided by the gauge length (4 in.). Rise time is the time interval between zero stress and peak stress on the stress-time curve. See Figures 58 through 61. Since the strain rate was larger than the viscoelastic transition velocity, the stress-strain curve was assumed to be linear. The elastic modulus for the oscilloscope tests was calculated by dividing the

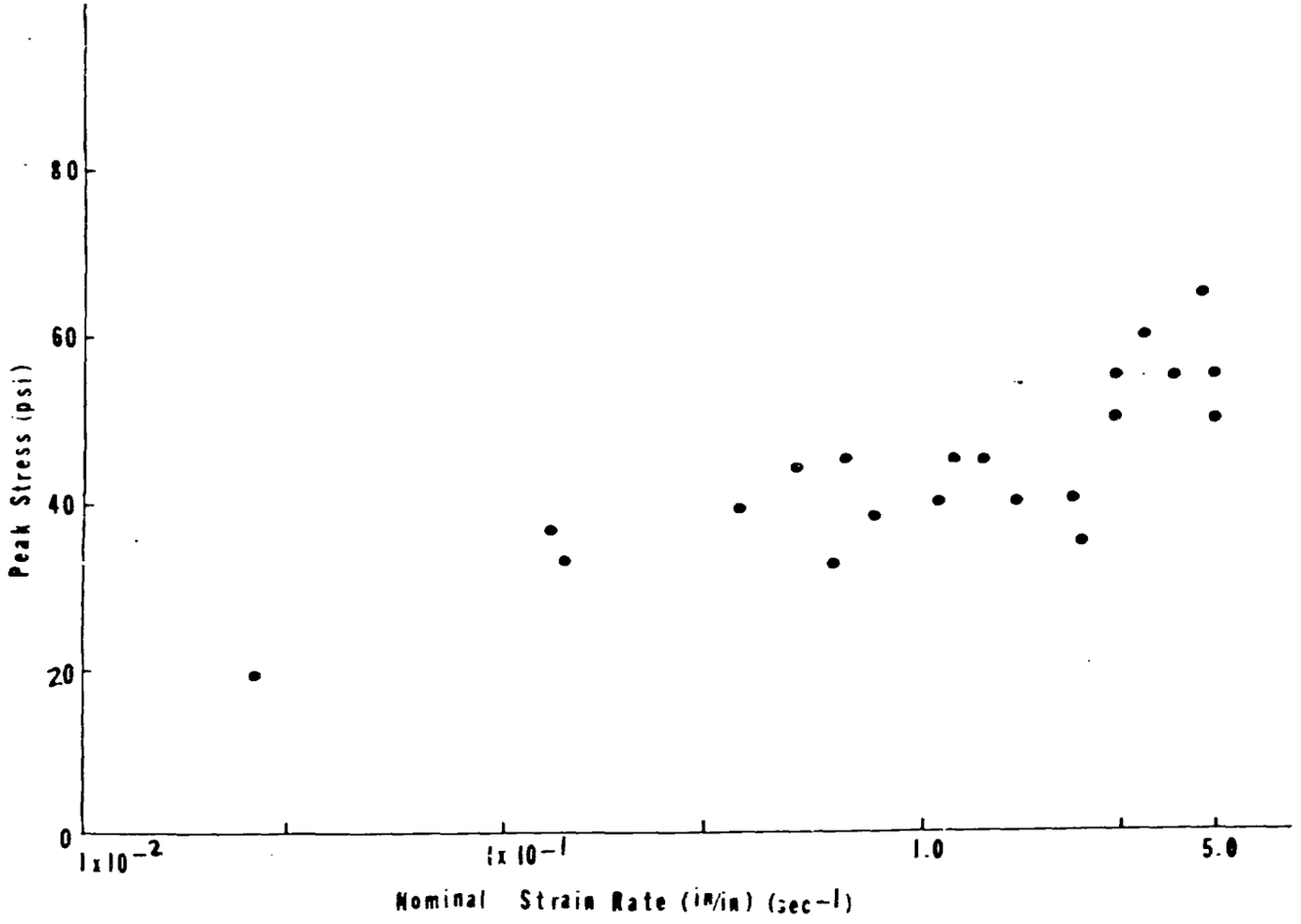

Figure 50: Peak Stress vs. Nominal Strain Rate - Air Tests

Table VIII Summary of Air Cylinder Tests - Foxboro Measurements

Test No.	Temp. (°C)	Tank Pressure (psi)	Strain Rate (in/in)(sec^{-1})	Peak Stress (psi)	Elongation at Fracture (in)	E (psi)
2M	12.3	45	0.025	18.8	4.5	16.0
2K	12.3	45	0.13	36.4	6.9	19.1
2L	12.3	45	0.14	33.2	5.7	20.0
2N	12.2	45	0.37	39.2	7.7	12.8
2H	12.3	45	0.51	44.0	8.1	16.8
2G	12.3	45	0.62	32.4	7.9	12.5
2I	12.3	45	0.65	45.3	8.2	16.8
2J	12.3	45	0.78	38.2	7.6	12.0

Table IX Summary of Air Cylinder Tests - Oscilloscope Measurements

Test No.	Tank Pressure (psi)	Rise Time t_f (ms)	Peak Stress (psi)	Time Elapsed 4.5" distance (ms)	Crosshead Velocity (in/sec)	Strain Rate (sec^{-1})	Elastic Modulus (psi)
31	65	280	55	282	16.0	4.0	49
32	65	240	50	222	20.2	5.0	42
34	40	500	40	486	9.3	2.3	35
35	40	800	45	836	5.4	1.4	40
36	40	880	45	908	5.0	1.2	43
37	55	370	50	393	11.4	2.9	47
38	55	400	55	397	11.3	2.8	49
39	80	260	55	222	20.2	5.0	42
40	80	280	65	241	18.7	4.7	50
41	65	370	60	328	13.7	3.4	48
42	40	480	35	480	9.4	2.4	30
43	30	800	40	992	4.5	1.1	44
44	65	220	50	217	20.5	5.1	44
45	40	620	40	635	7.1	1.8	36

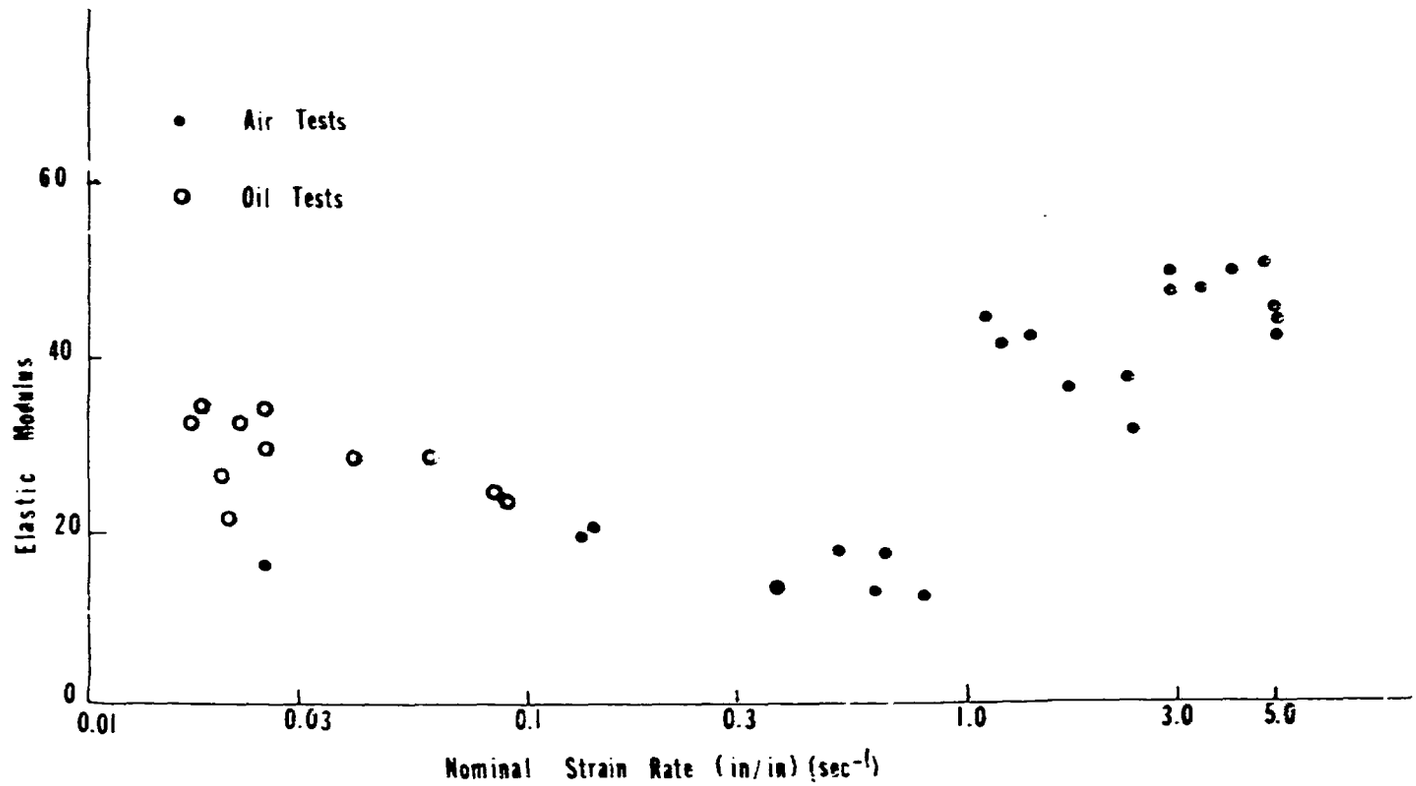

Figure 51: Elastic Modulus vs. Nominal Strain Rate - Air Tests

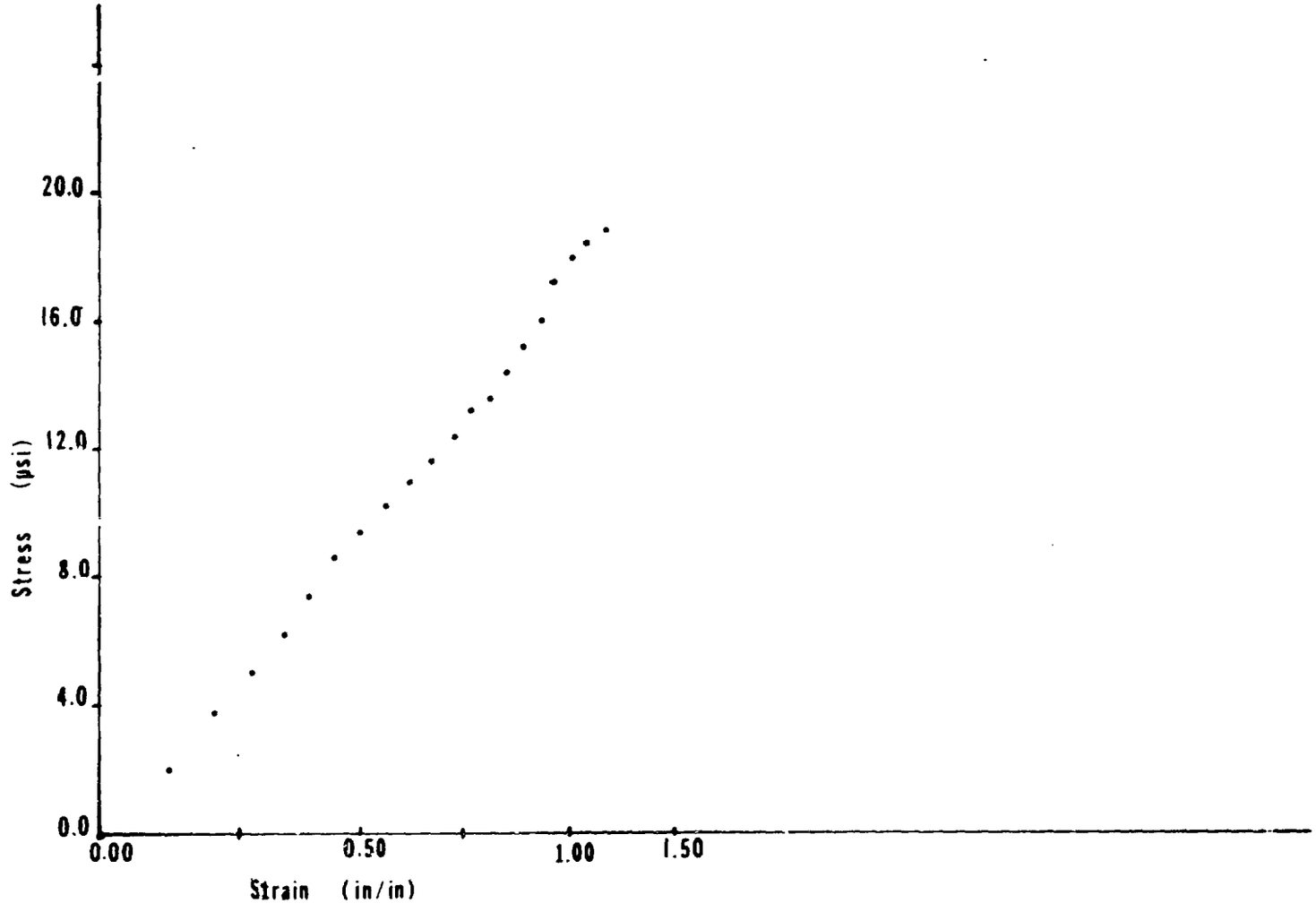

Figure 52: Stress vs. Strain - Sample 2M - 0.025/sec

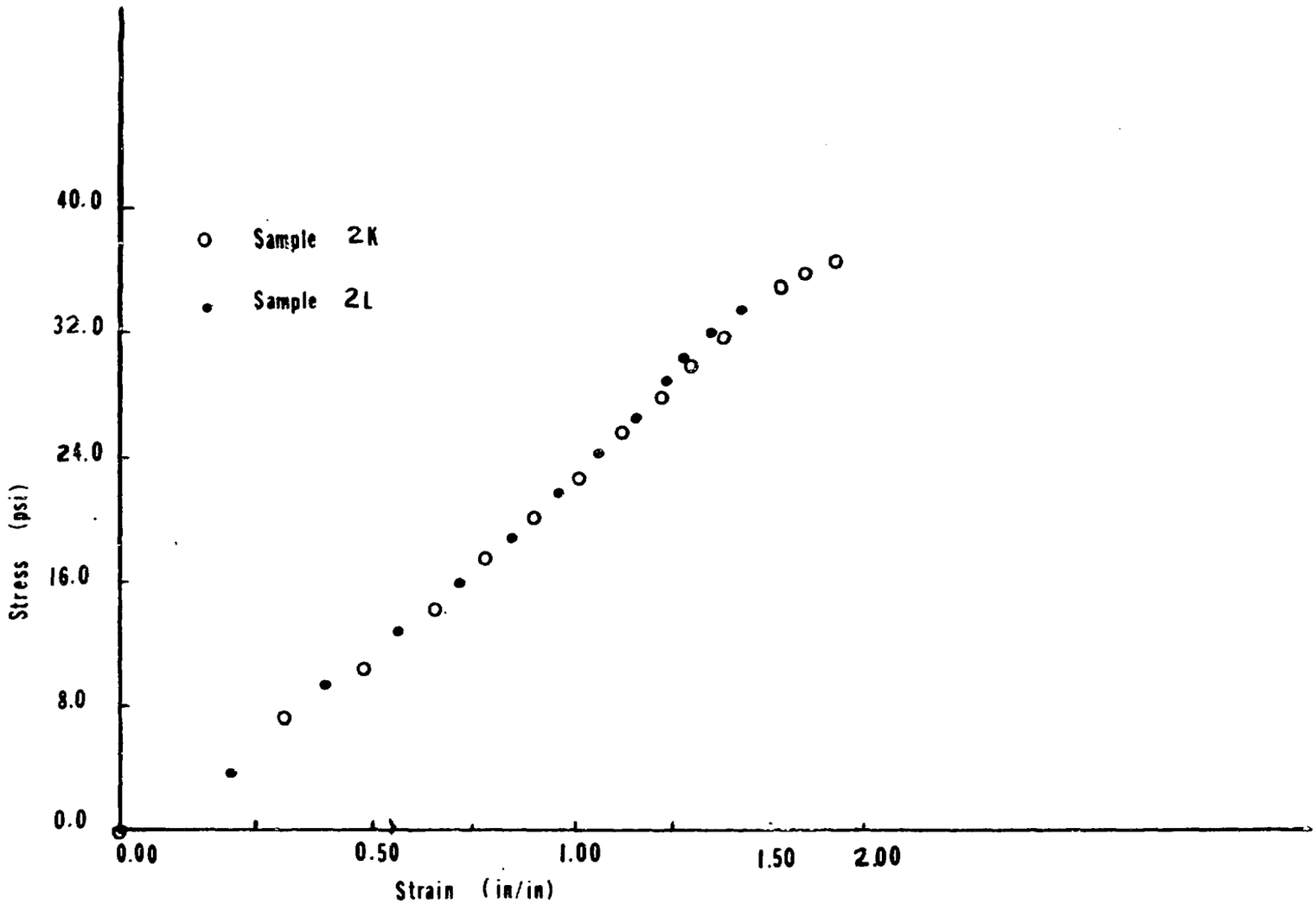

Figure 53: Stress vs. Strain - Samples 2K and 2L - 0.14/sec

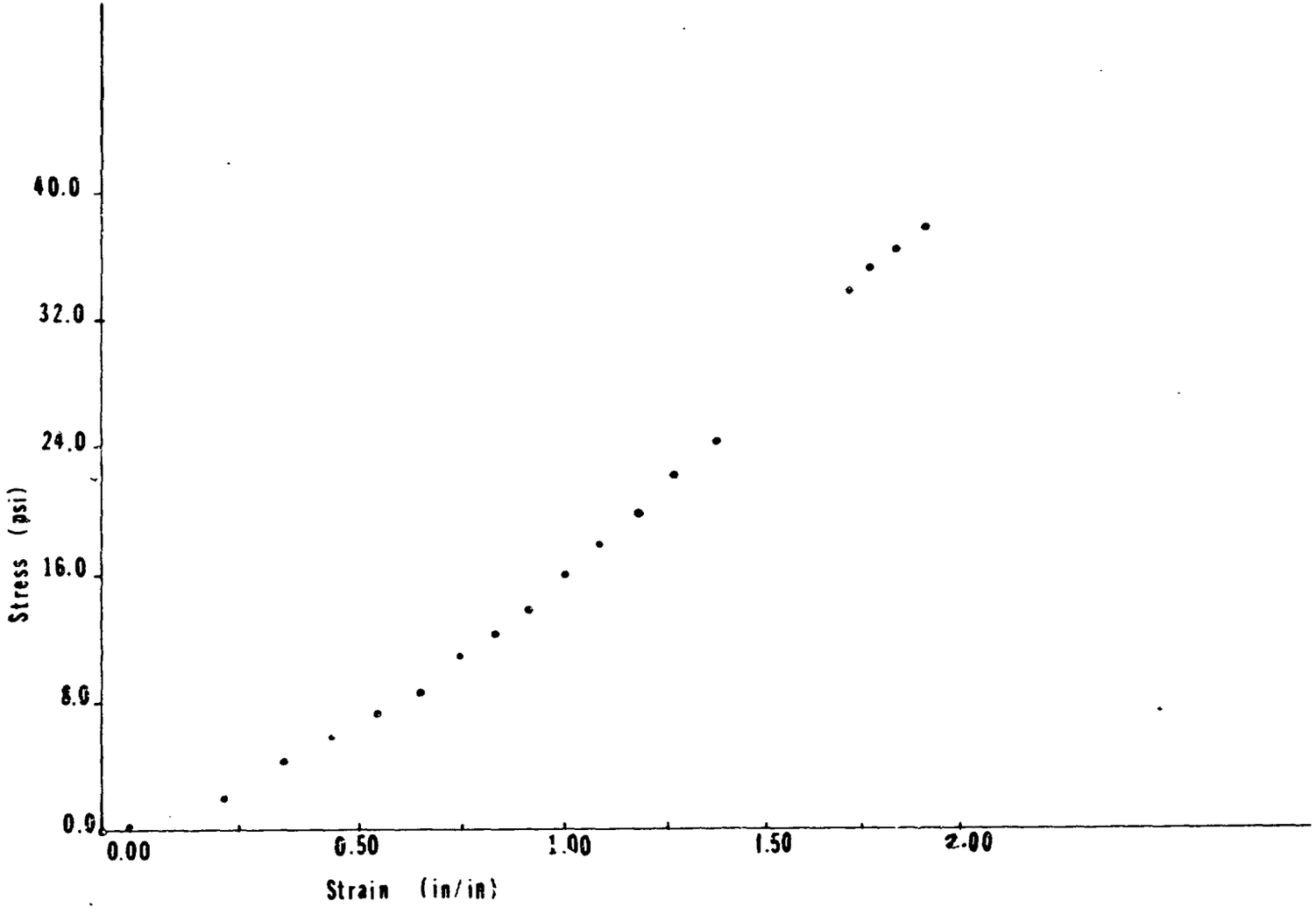

Figure 54: Stress vs. Strain - Sample 2N - 0.37/sec

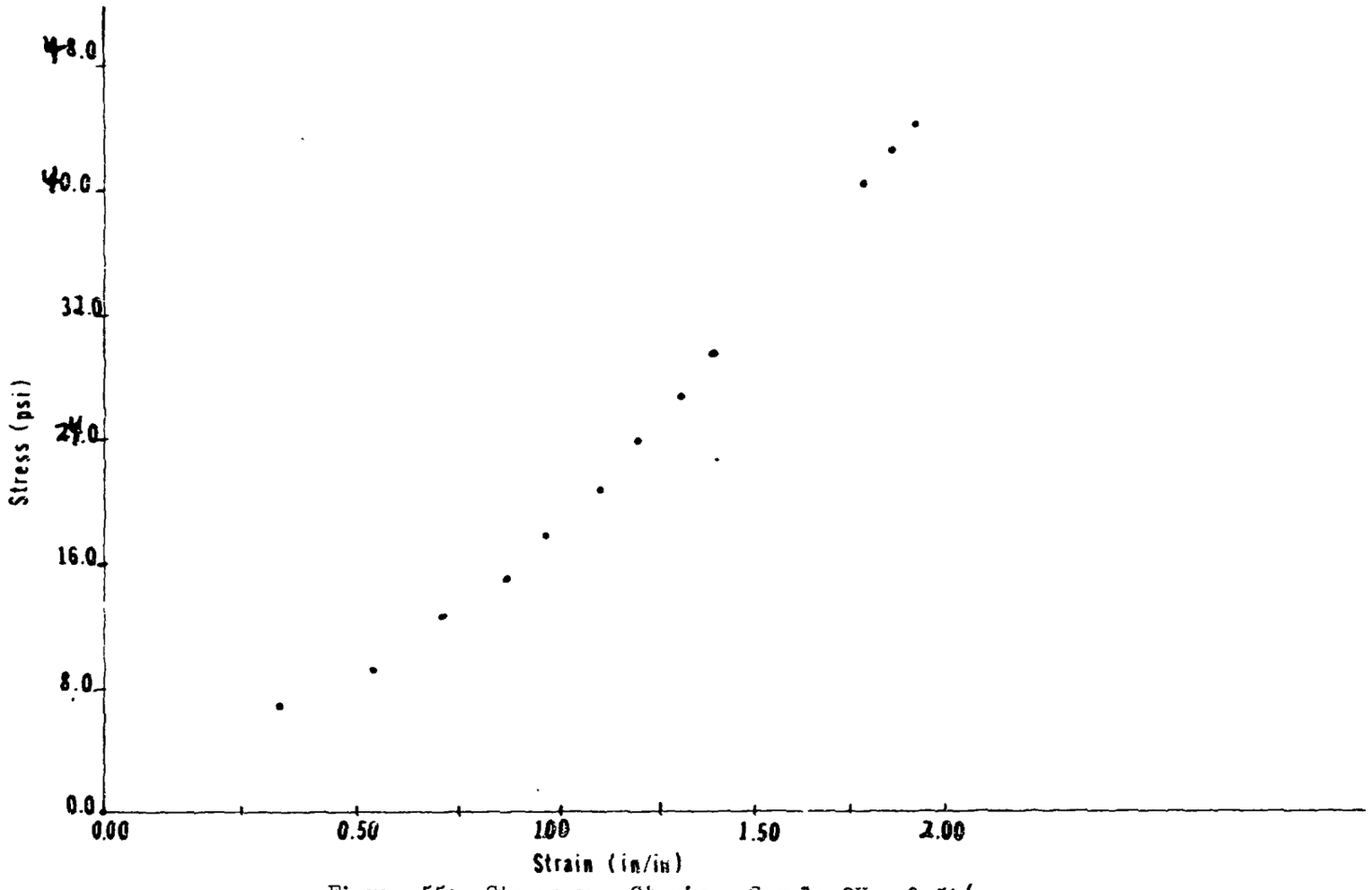

Figure 55: Stress vs. Strain - Sample 2H - 0.51/sec

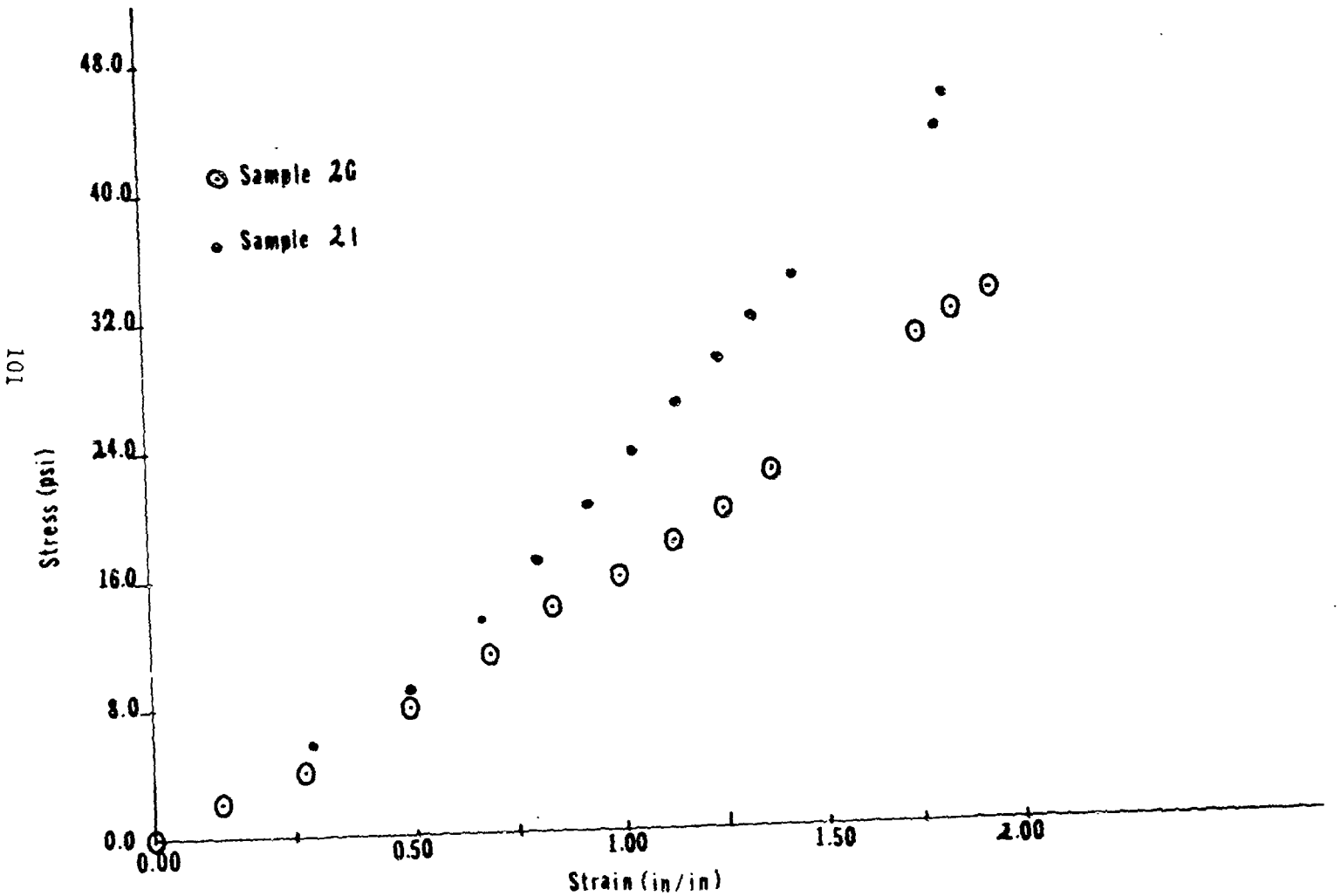

Figure 56: Stress vs. Strain - Samples 2G and 2I - 0.64/sec

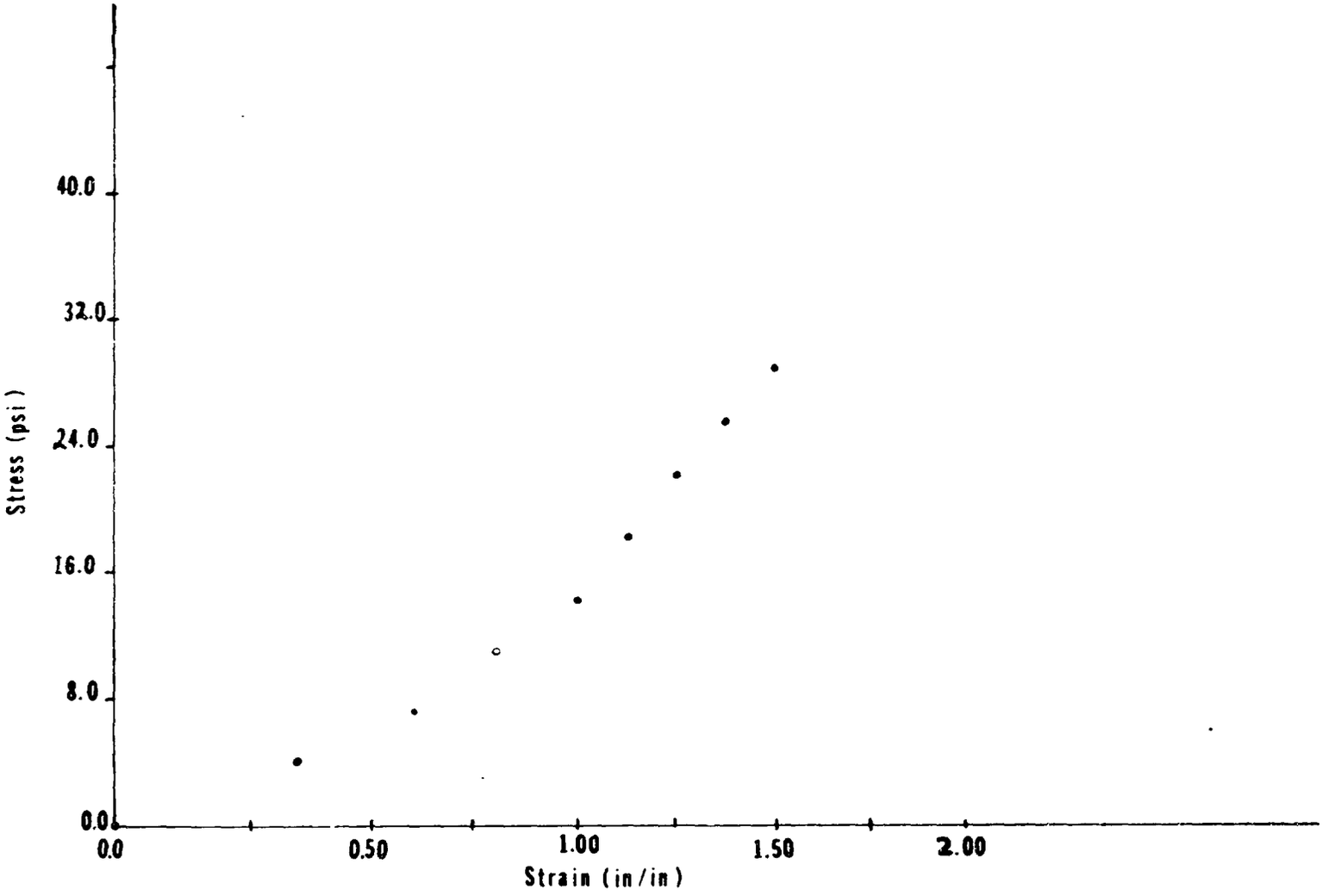

Figure 57: Stress vs. Strain - Sample 2J - 0.78/sec

Test 31
4.0/sec

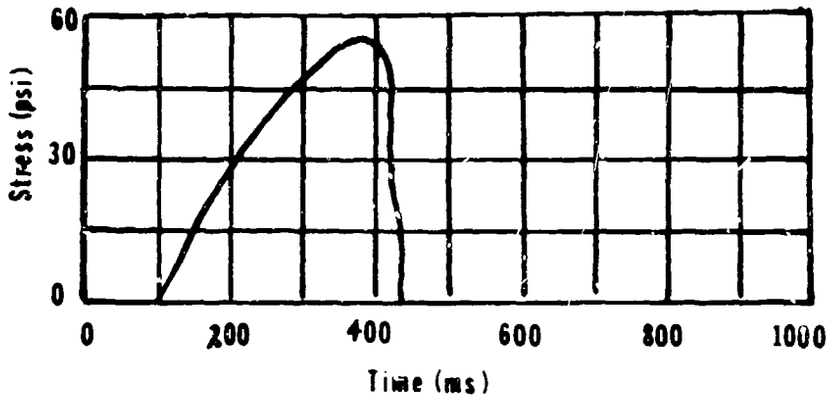

Test 32
5.0/sec

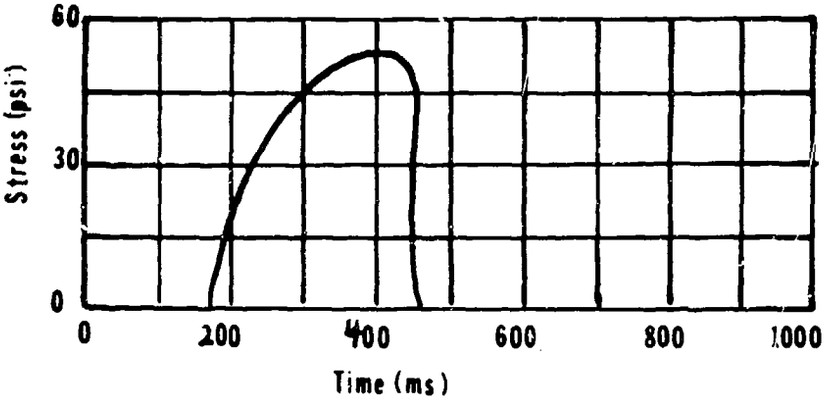

Test 34
2.3/sec

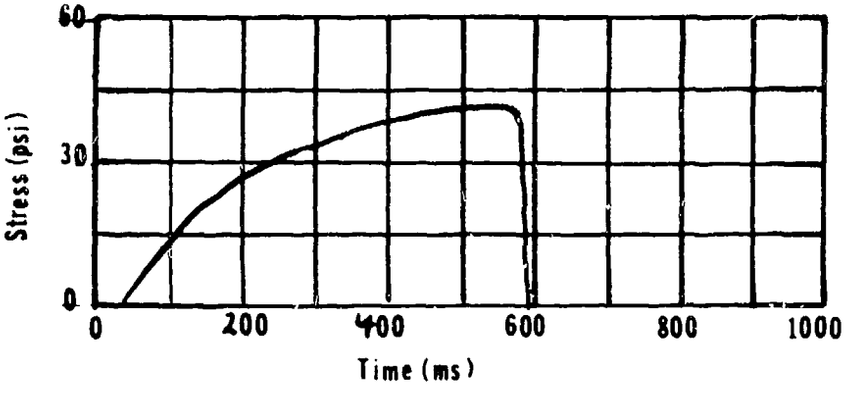

Figure 58: Stress vs. Time - Air Tests 31,32 and 34

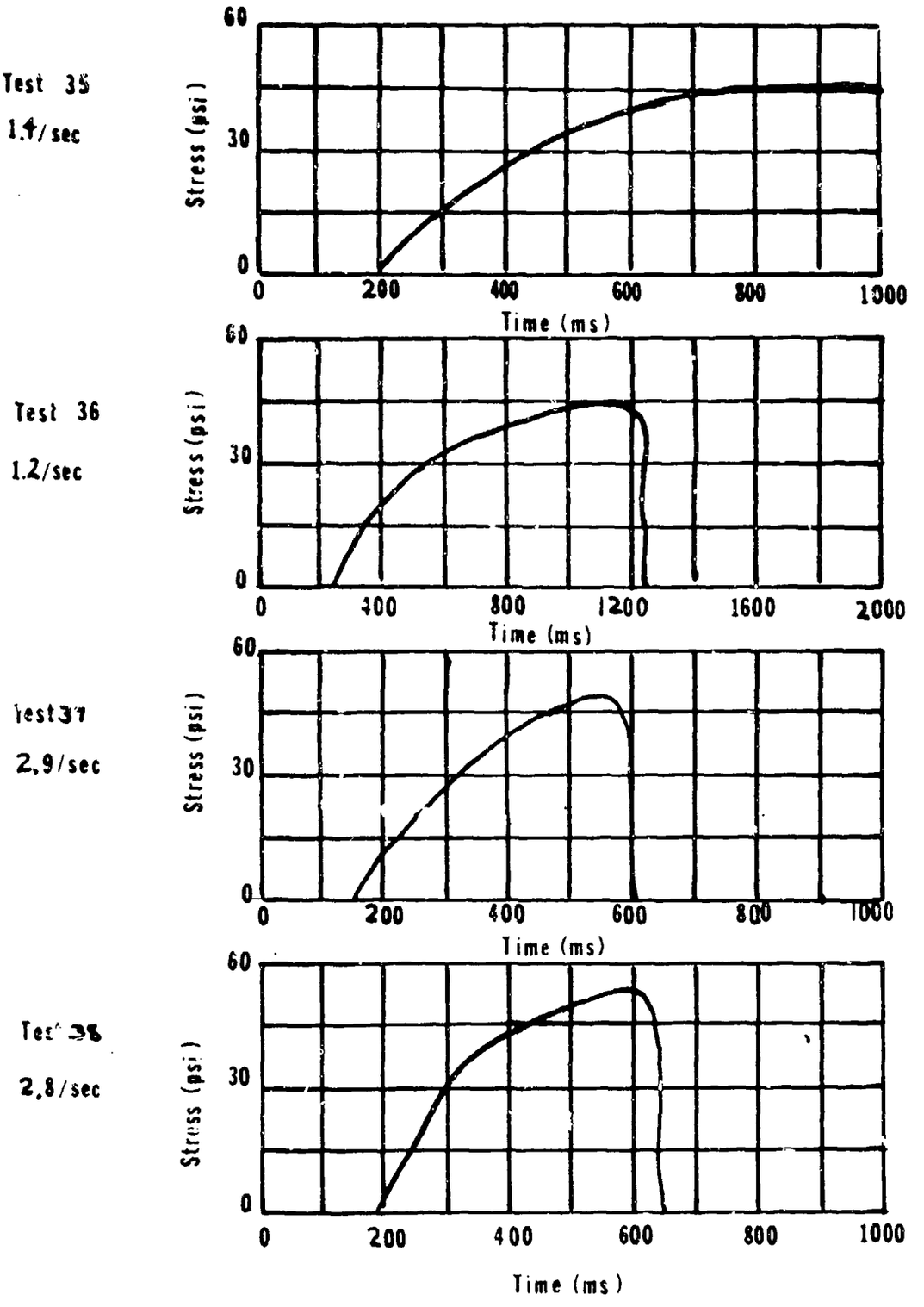

Figure 59: Stress vs. Time - Air Tests 35,36,37 and 38

Test 39
5.0/sec

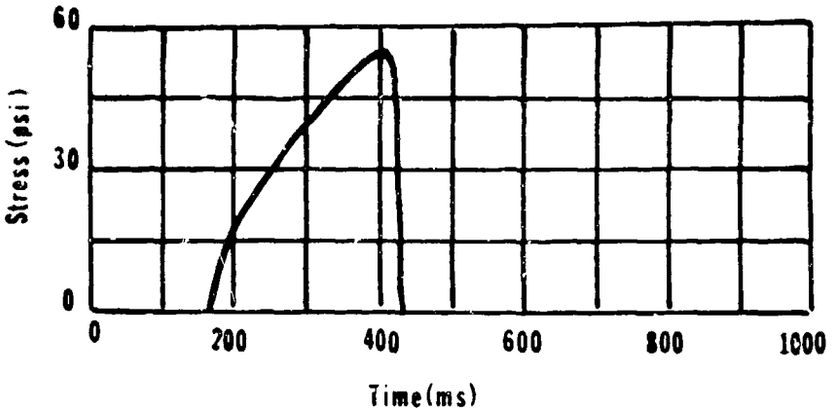

Test 40
4.7/sec

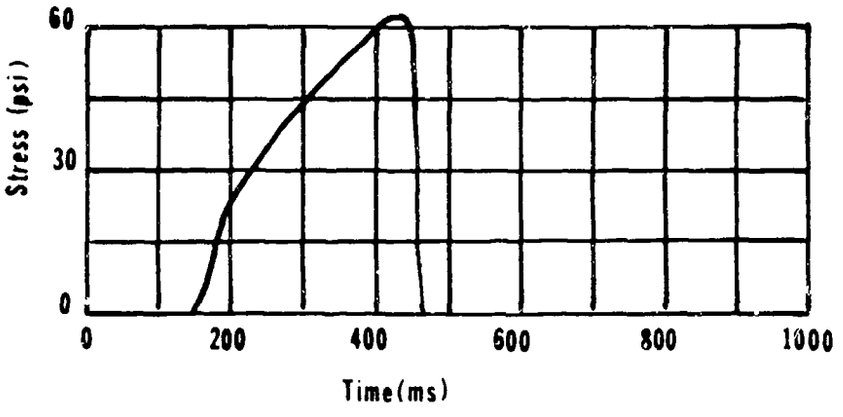

Test 41
3.4/sec

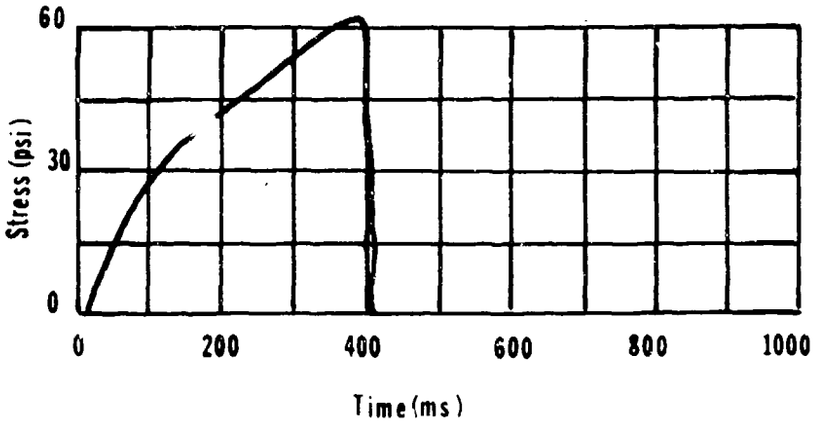

Figure 60: Stress vs. Time - Air Tests 39,40, and 41

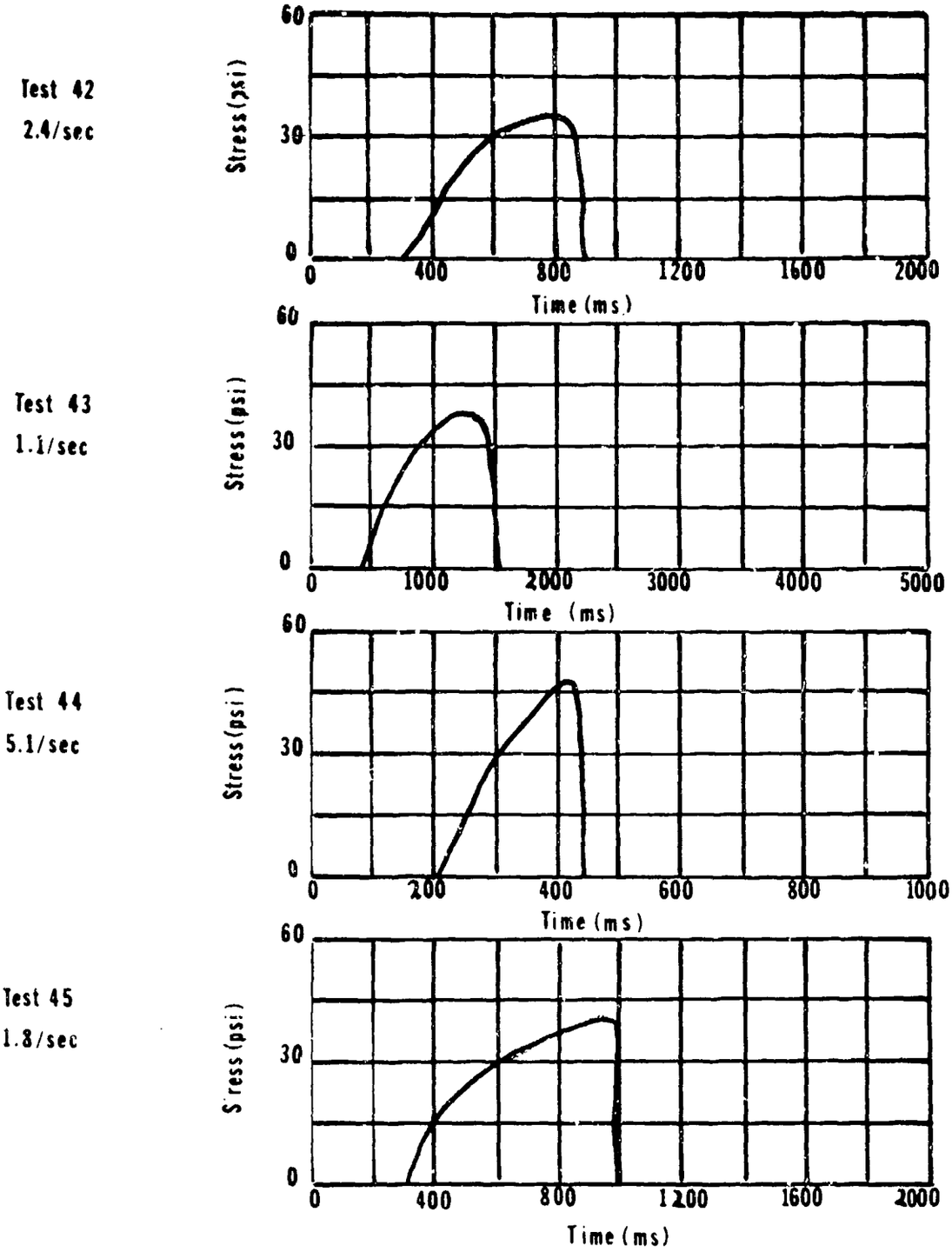

Figure 41: Stress vs. Time - Air Tests 42,43,44, and 45

peak stress by the calculated strain at fracture.

10.2.4 Drop Weight Tests

10.2.4.1 Apparatus

In the drop weight test two gelatin specimens were fractured simultaneously by dropping a large weight from various heights. Since the height varied from 1 to 25 feet, the test was conducted outside the lab on cooler days during the spring. Four concrete pillars were erected to support the experiment. Two gelatin specimens were used for each test; one for the stress-time measurement, and one as a dummy to provide loading symmetry. A gelatin specimen was hung from a crossbeam between each pair of pillars. One of the crossbeams was instrumented with a load cell in the form of a simply supported beam with an array of strain gauges attached. The lower grip of each specimen was attached to a heavy angle iron which was horizontally disposed between the two pairs of pillars such that the dropping weight would impact on it at its center. The weight of this angle iron was carried before impact by hanging it from light strings which broke on impact. The four strain gauge load cell output was appropriately connected to a Tektronics 545B oscilloscope with a Type Q plug-in unit. Calibration was checked before each test by hanging a known weight from the load cell. The 120 lb. drop weight was raised to a measured distance above the angle iron bar, two specimens removed from the refrigerator and affixed in the grips, and the test was run immediately, usually in less than a minute after the specimens came out of the refrigerator. All specimens were used one day after they were cast. The data obtained were in the form of a stress-time curve immediately following impact of the 120 lb. weight. The velocity of the weight at impact was accurately known by calculation, and since its kinetic energy was far in excess of the work required to break the specimen, the experiment could be considered a "constant crosshead velocity" or a "hard test machine" test.

10.2.4.2 Results

The results from the drop weight tests are summarized in Figures 62 through 64 and are shown in Figures 65 through 68 and in Table X. The peak stress continued to increase as the strain rate became larger. See Figure 62. The strain of the gelatin at fracture decreased from 2.4 to 1.0 between the strain rates of 24/sec and 48/sec. See Figure 63. The fracture strain then remained nearly constant between the strain rates of 48/sec and 120/sec. The strain of 2.4 at 24/sec was roughly equal to the measured strain of 1.9-2.1 found in the air cylinder tests at a strain rate of 0.78/sec.

The elastic modulus at 24/sec was nearly equal to the moduli of the air cylinder tests. See Figure 64. The modulus increased from 50 psi to 160 psi when the strain rate increased from 24/sec to 48/sec. The elastic modulus, E, continued to increase as the strain rate became larger, reaching 225 psi at 120/sec.

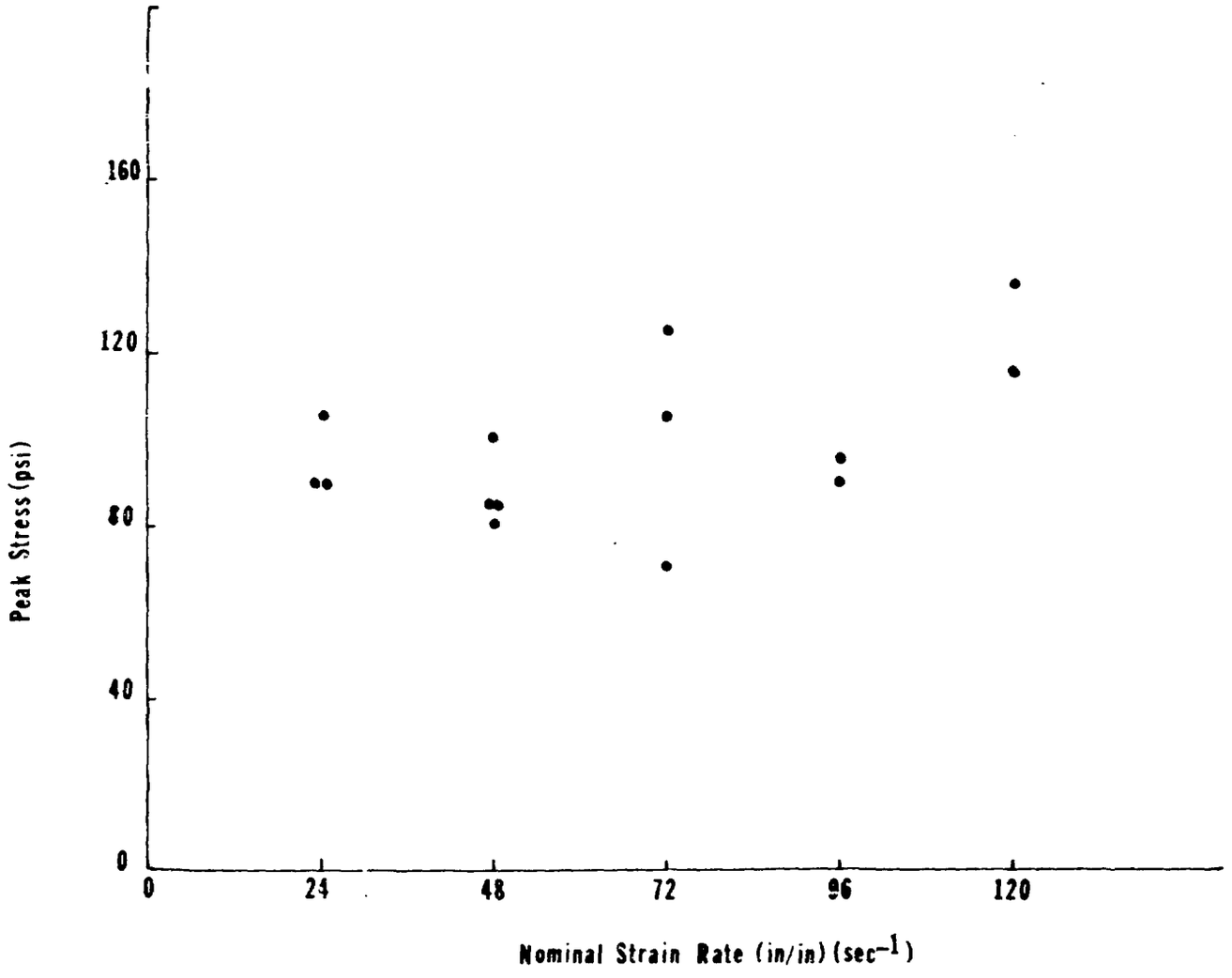

Figure 62: Peak Stress vs. Nominal Strain Rate - Drop Weight Tests

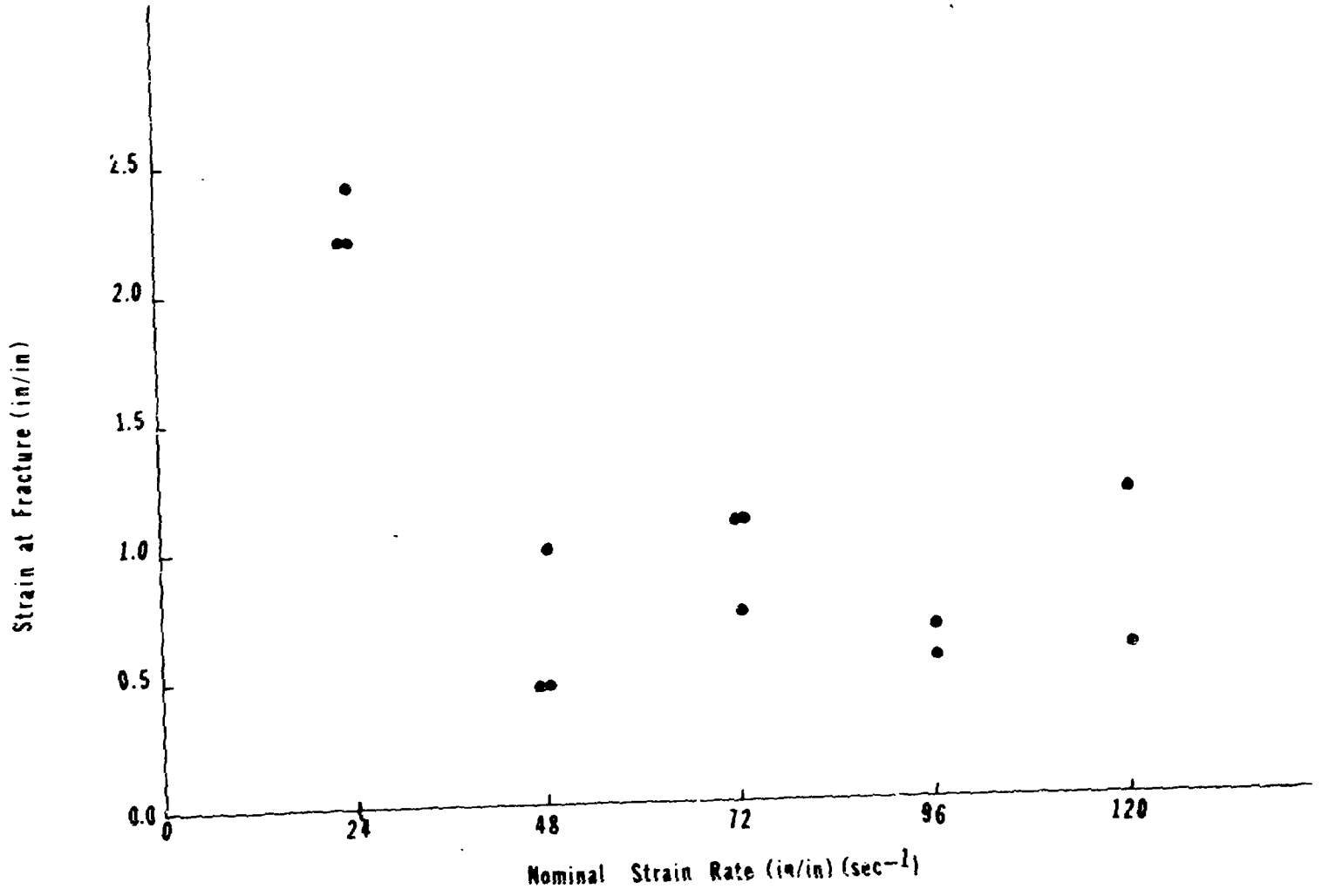

Figure 63: Strain at Fracture vs. Nominal Strain Rate - Drop Weight Tests

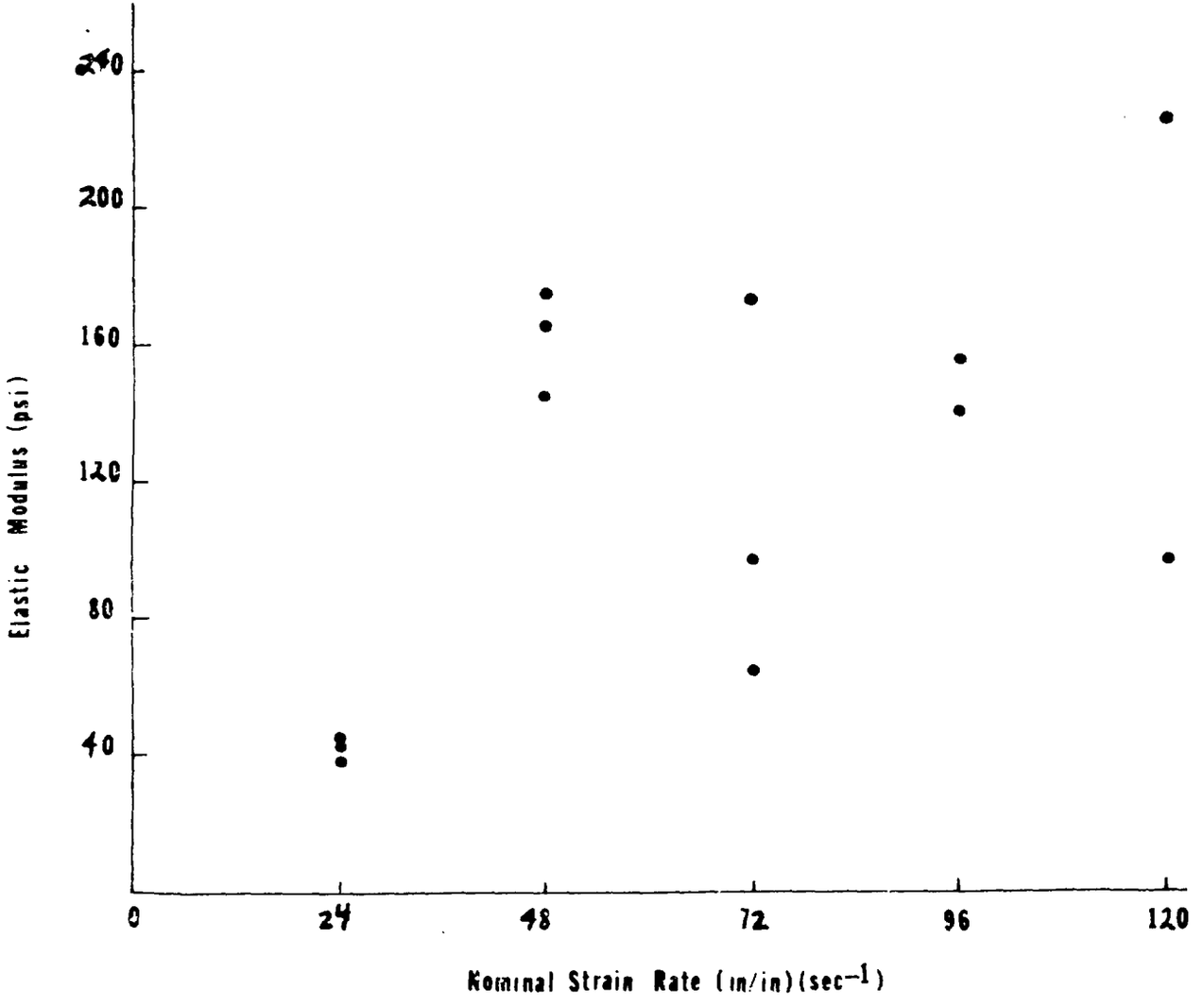

Figure 64: Elastic Modulus vs. Nominal Strain Rate - Drop Weight Tests

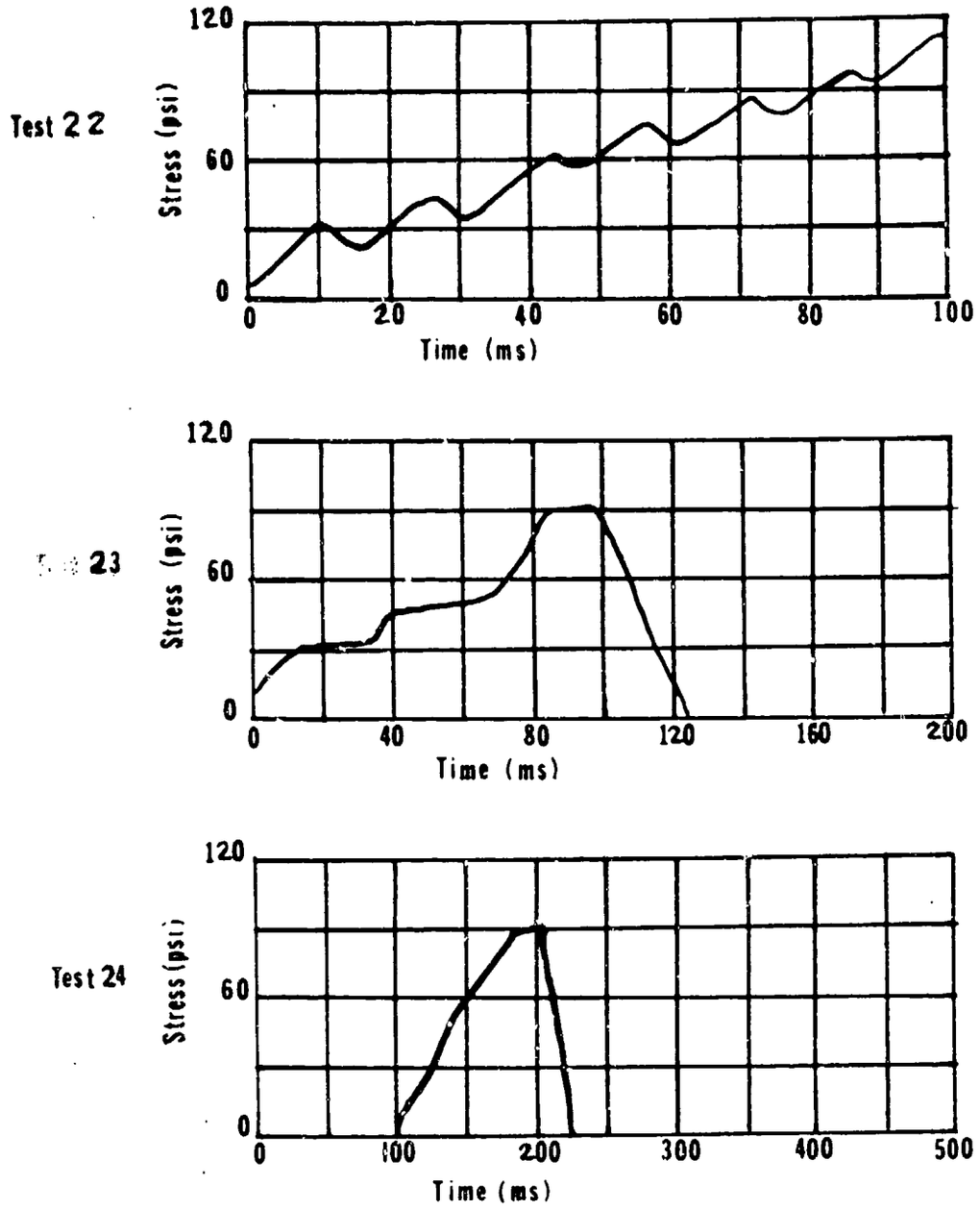

Figure 65: Stress vs. Time - Drop Weight Tests 22,23, and 24 - 24/sec

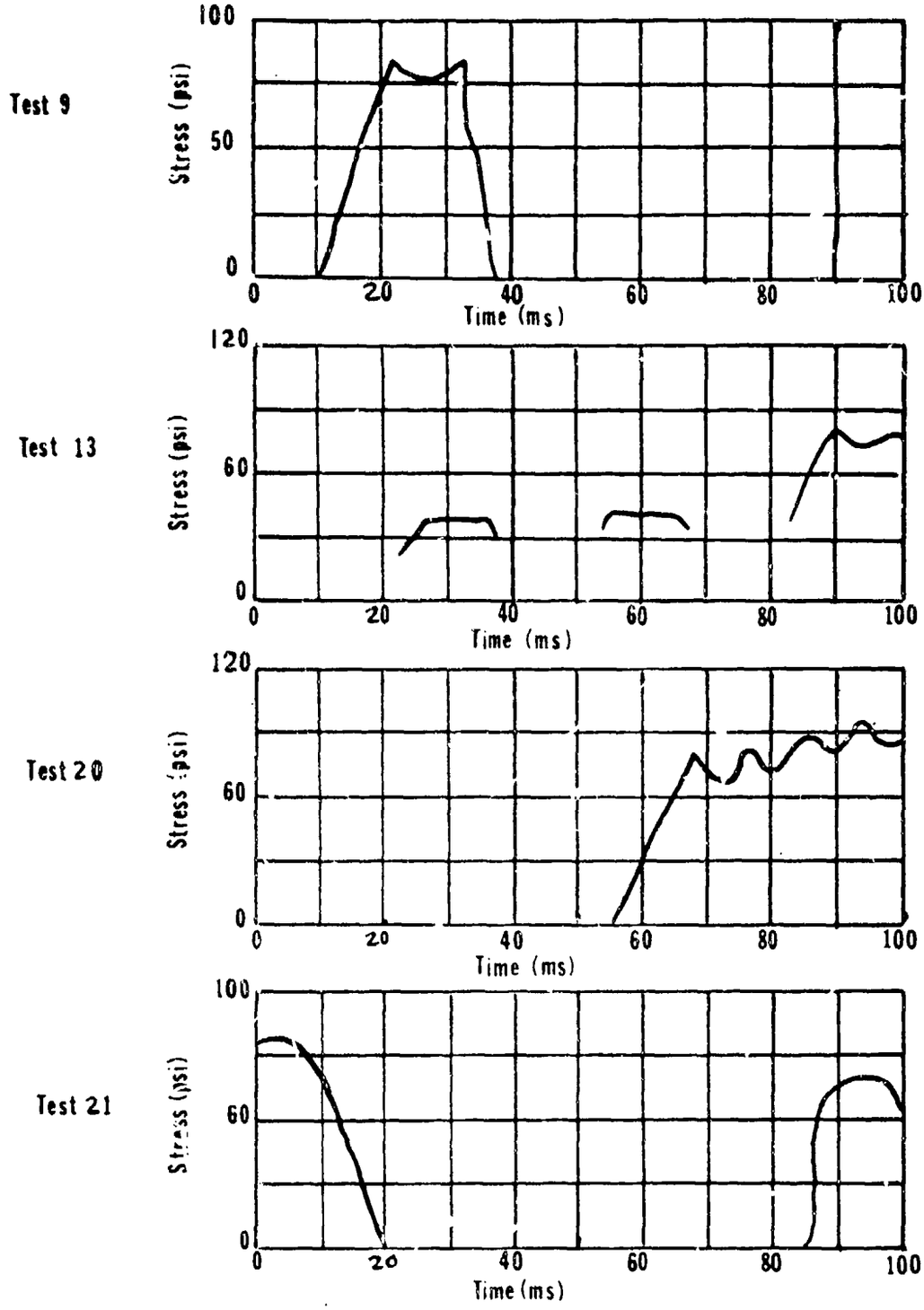

Figure 66: Stress vs. Time - Drop Weight Tests 9,13,20 and 21 - 48/sec

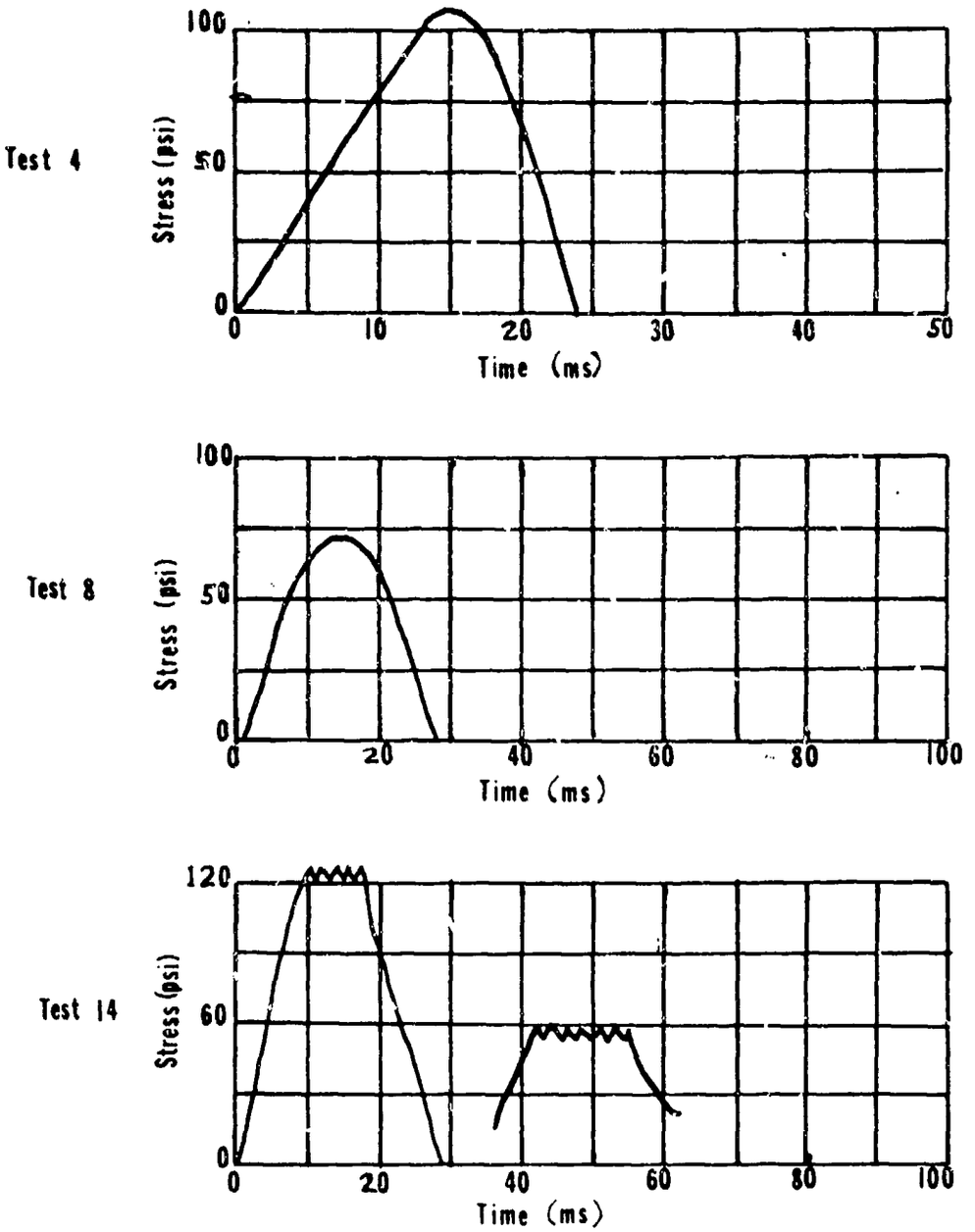

Figure 67: Stress vs. Time - Drop Weight Tests 4,8, and 14 - 72/sec

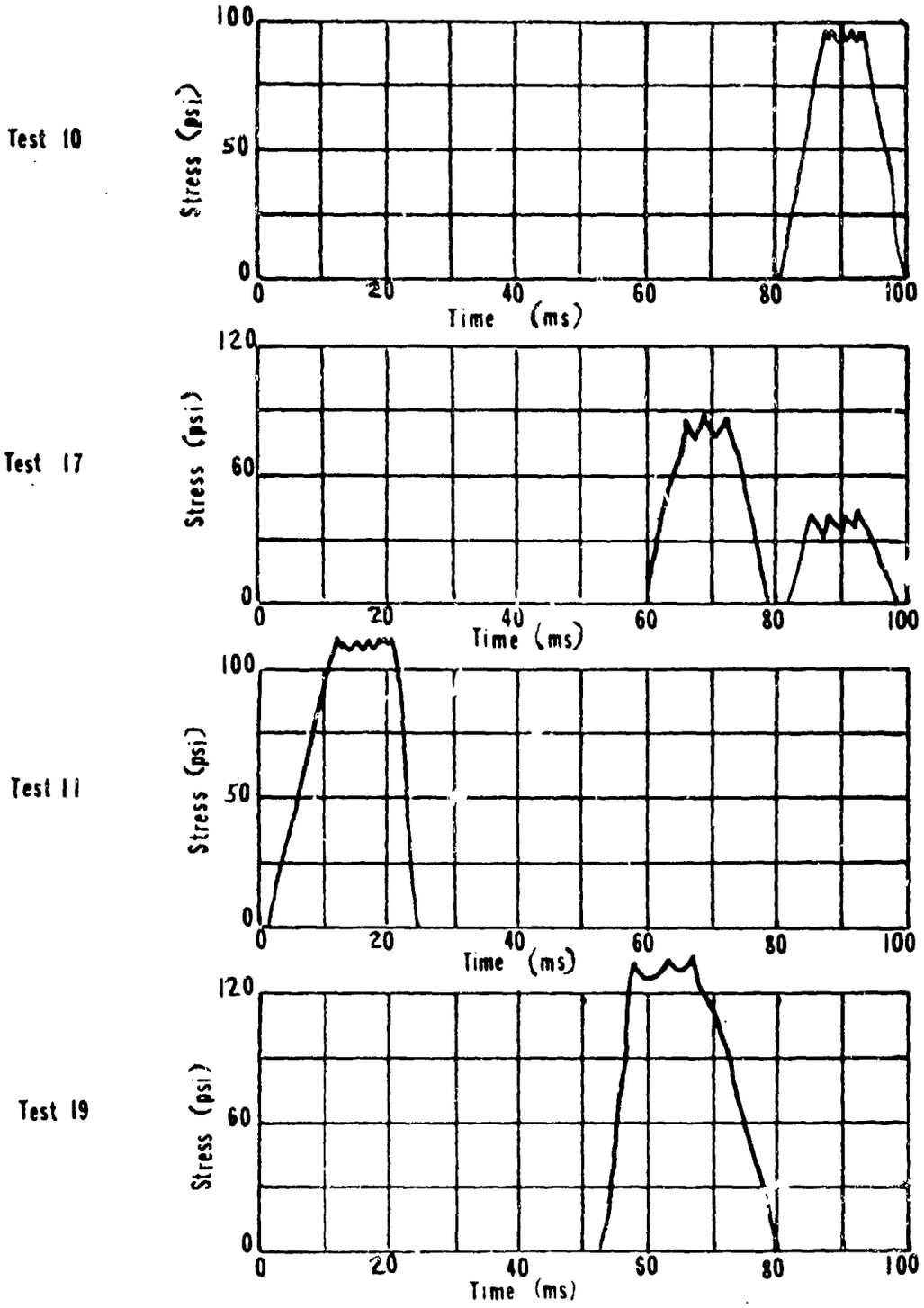

Figure 68: Stress vs. Time - Drop Weight Tests 10,17,11, and 19

Table X Summary of Drop Weight Tests

Test No.	Height (ft)	Rise tf Time (ms)	Peak Stress (psi)	ϵ at fracture	Strain Rate (sec^{-1})	E (psi)
22	1	100	105	2.4	24	44
23	1	90	90	2.2	24	42
24	1	100	90	2.4	24	38
9	4	12	85	1.0	48	145
13	4	10	85	0.48	48	175
20	4	10	80	0.48	48	165
21	4	--	100	---	48	---
4	9	15	105	1.1	72	97
8	9	15	70	1.1	72	65
14	9	10	125	0.73	72	175
10	16	7	95	0.67	96	140
17	16	6	90	0.58	96	155
11	25	10	115	1.2	120	96
19	25	5	125	0.6	120	225

10.2.5 Gas Gun Tests

10.2.5.1 Apparatus

The gelatin specimens were stretched to fracture by hitting a set of movable grips with a steel projectile fired from a compressed gas gun. Like the drop weight tests, two gelatin specimens were broken during each test run, but the stress-time curve was only observed on one sample. The projectile was a 2" long, 1" diameter cylinder moving at velocities from 250-650 ft/sec. The load cell was connected to the oscilloscope as in the drop weight tests. The load cell was calibrated each time before a test run. The gelatin specimens were taken out of the refrigerator, placed in the grip and the test was run immediately. The peak stress and the rise time, t_r, were obtained for each run.

The mass of the projectile was 1 lb. and the mass of the movable grips was 3 lb. If one assumes an elastic collision between the two, then conservation of energy and conservation of momentum require that the grips move with one half the projectile velocity (see Appendix I). This result was used to compute crosshead velocities for known (measured) projectile velocities.

10.2.5.2 Results

The results of the gun test are shown in Table XI. The peak stress continued to increase as the strain rate was increased. See Figure 69. The gas gun test is classified as a "hard test machine" test (instead of soft) because the energy required to fracture the specimen is so much less than the kinetic energy available. The elastic modulus appeared to increase linearly as the strain rate increased, but the modulus was much lower than the preceding drop weight moduli, (between 15-46 psi over the test range). See Figure 70. The modulus was calculated by dividing the product of the gauge length and the peak stress by the product of the crosshead velocity and the rise time. The rise time, t_r, is the time of fracture determined from the stress-time curve. Individual stress-time curves are shown in Figures 71 through 73.

10.2.6 Comparison of Results

Peak stress increased when the strain rate became larger. A stress of 9.5 psi fractured a specimen at 8×10^{-4}/sec whereas 160 psi was required for fracture at a strain rate of 575/sec. See Figure 74.

Strain at fracture increased from 0.50 to 2.4 as the strain rate went from 5×10^{-4}/sec to 24/sec. See Figures 31 and 63. A sharp decline in fracture strain occurred from 2.4 to 0.5 when the strain rate went from 24/sec to 48/sec.

The elastic modulus did not show a clear and simple trend as the strain rate increased. See Figure 75. The elastic modulus decreased as the strain rate increased from 4×10^{-3}/sec to 8×10^{-1}/sec. The modulus remained at about 30-50 psi from strain rates of 1.0/sec to 24/sec. A sharp increase in the elastic modulus occurred between 24/sec to 48/sec in the drop weight tests, and continued to increase to an apparent peak of 225 psi

Table XI Summary of Gun Tests

Test No.	Pressure (psi)	t, μs	Peak Stress (psi)	Vo (ft/sec)	V (ft/sec)	Strain Rate (ft/ft)(sec^{-1})	E (psi)
1	200	14	80	250	125	375	15
2	300	11	110	300	150	450	22
3	400	8	120	350	175	525	29
5	500	8	140	400	200	600	29
6	600	8	100	500	250	750	17
7	700	7	135	550	275	825	23
8	1000	10	145	600	300	900	16
9	1500	3	135	650	325	975	46
10	1500	9	160	650	325	975	18

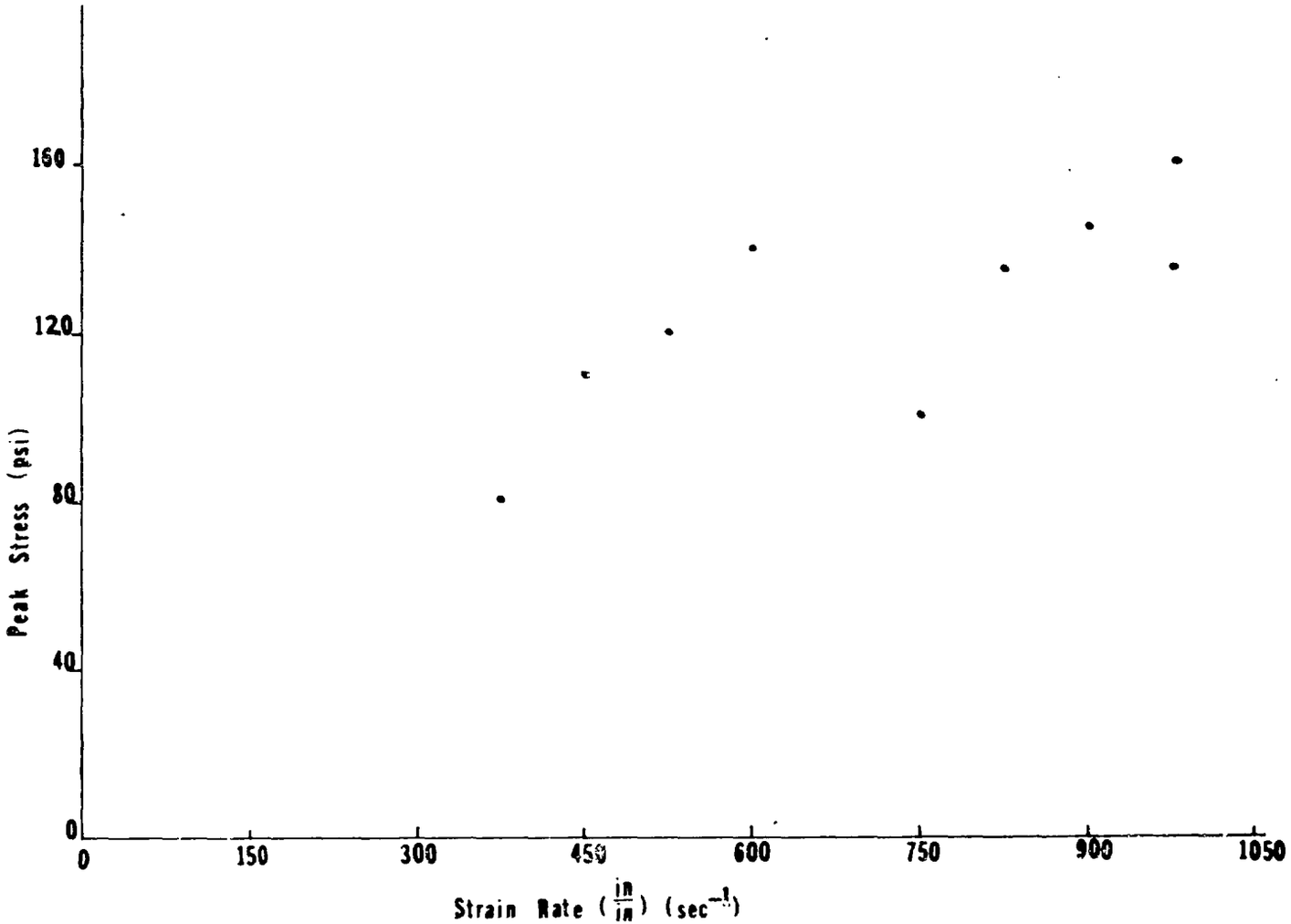

Figure 69: Peak Stress vs. Strain Rate - Gun Tests

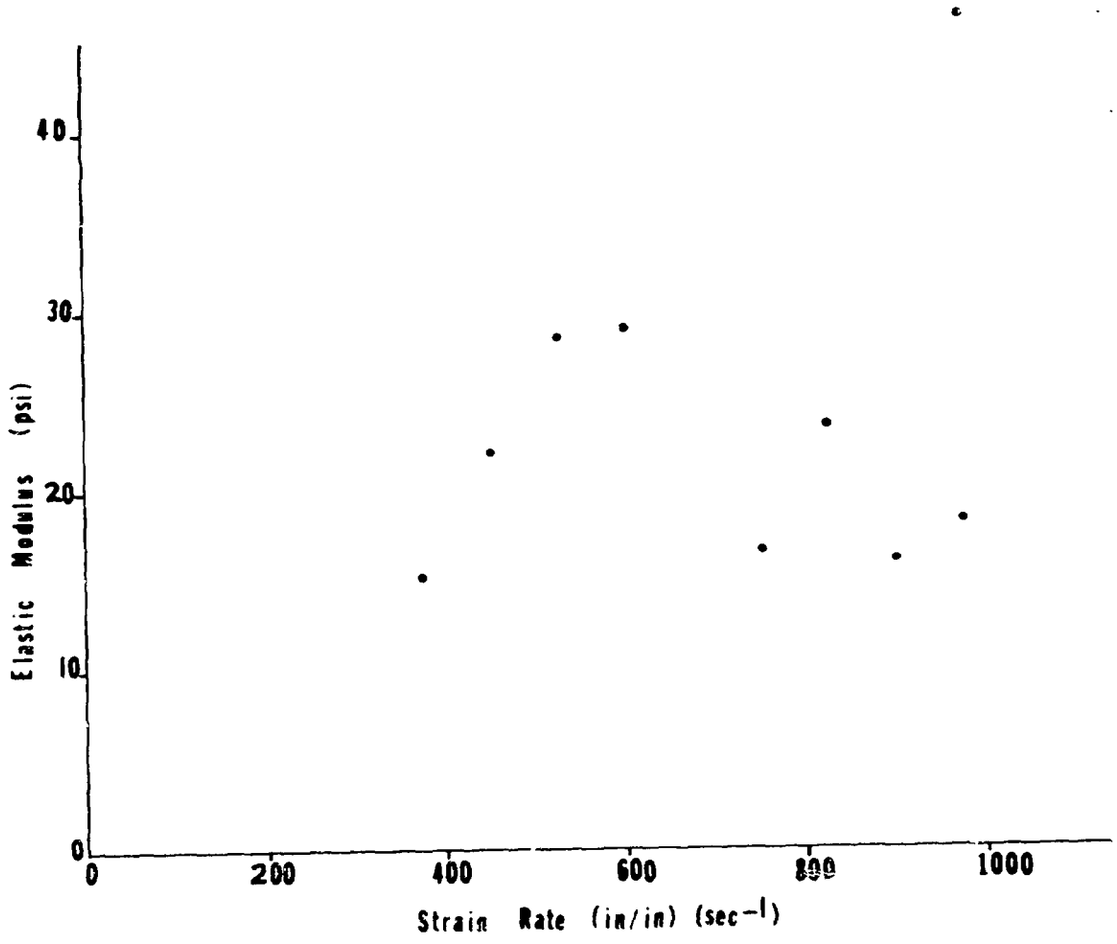

Figure 70: Elastic Modulus vs. Strain Rate - Gun Tests

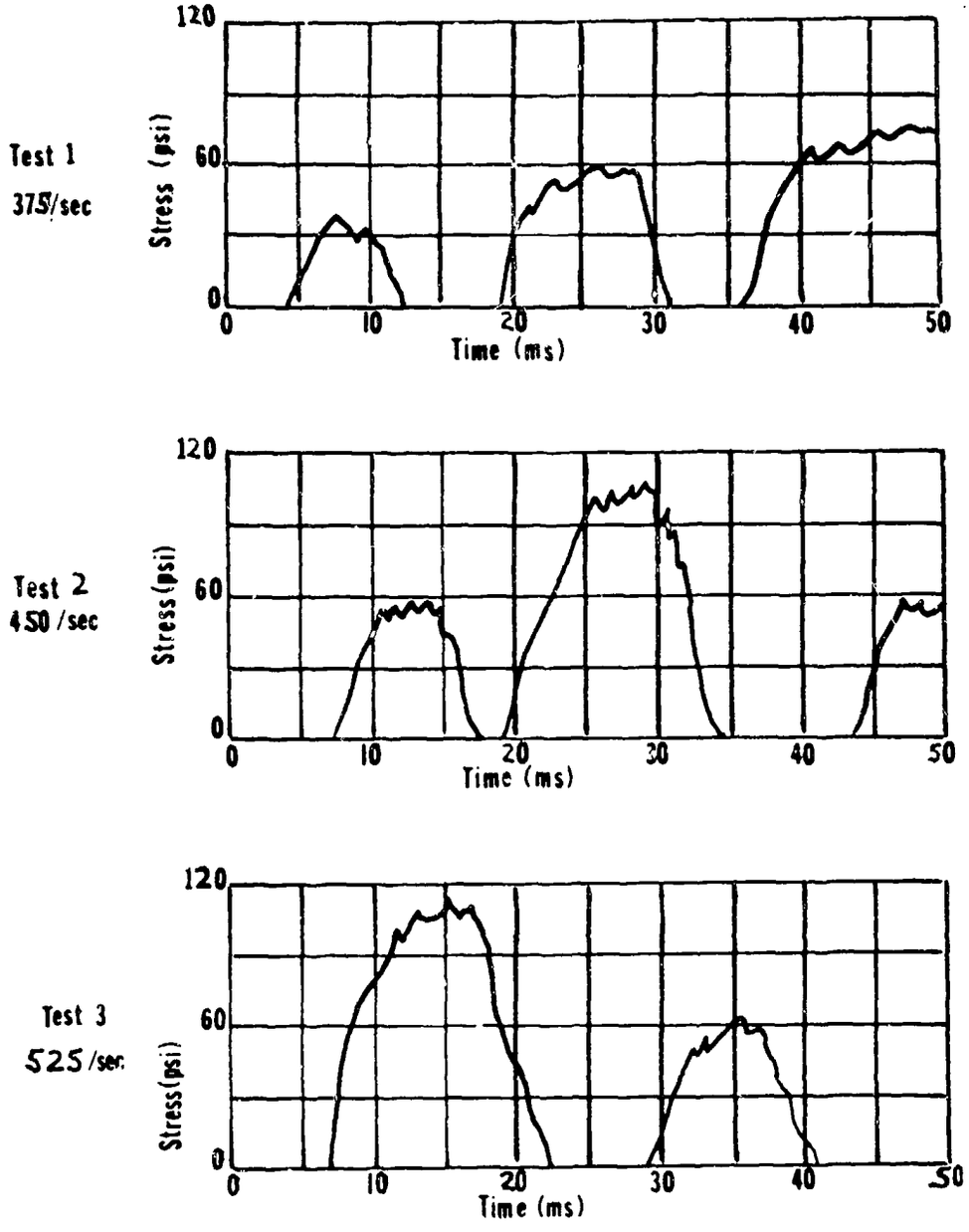

Figure 71: Stress vs. Time - Gun Tests 1,2 and 3

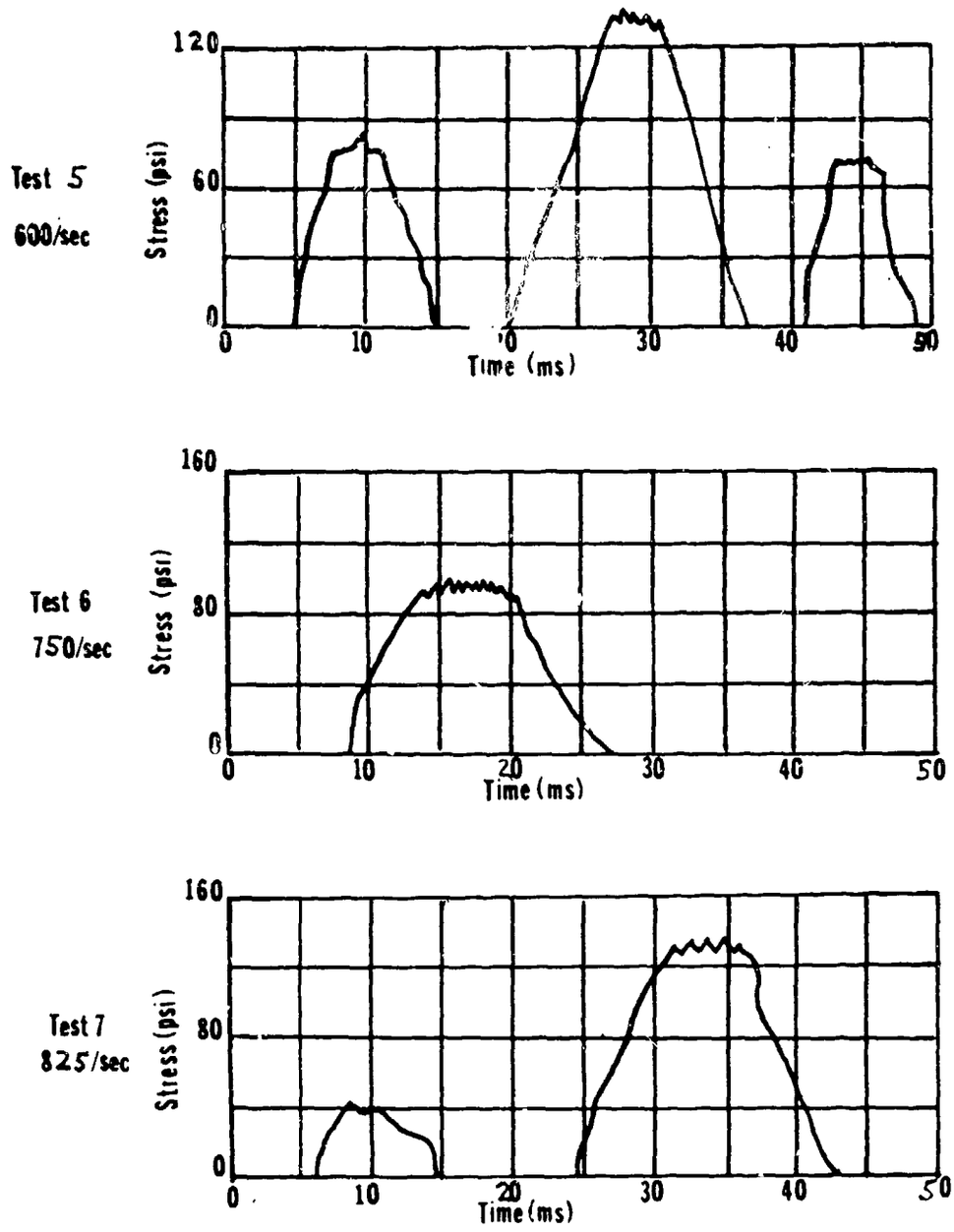

Figure 72: Stress vs. Time - Gun Tests 5,6 and 7

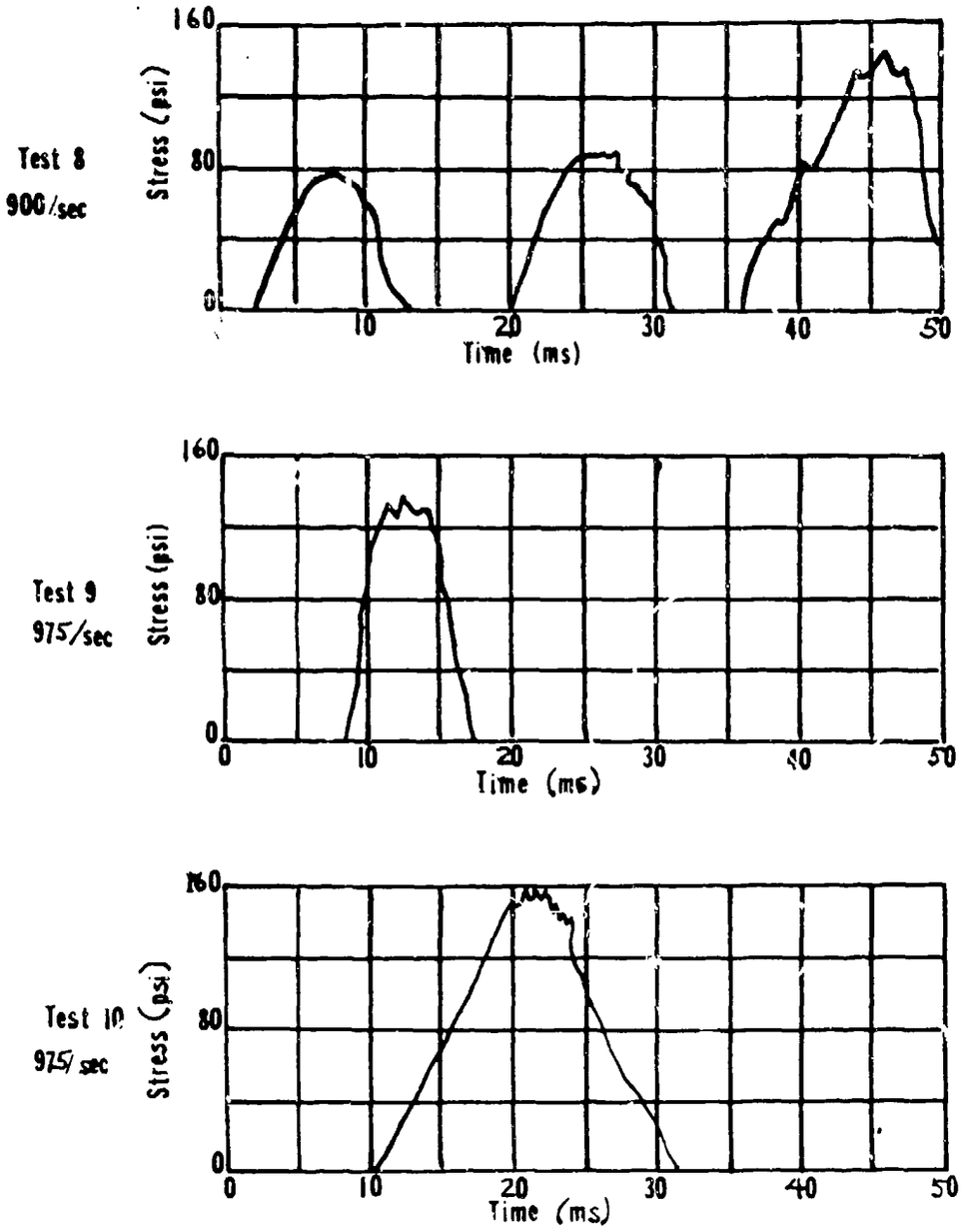

Figure 73: Stress vs. Time - Gun Test 8, 9 and 10

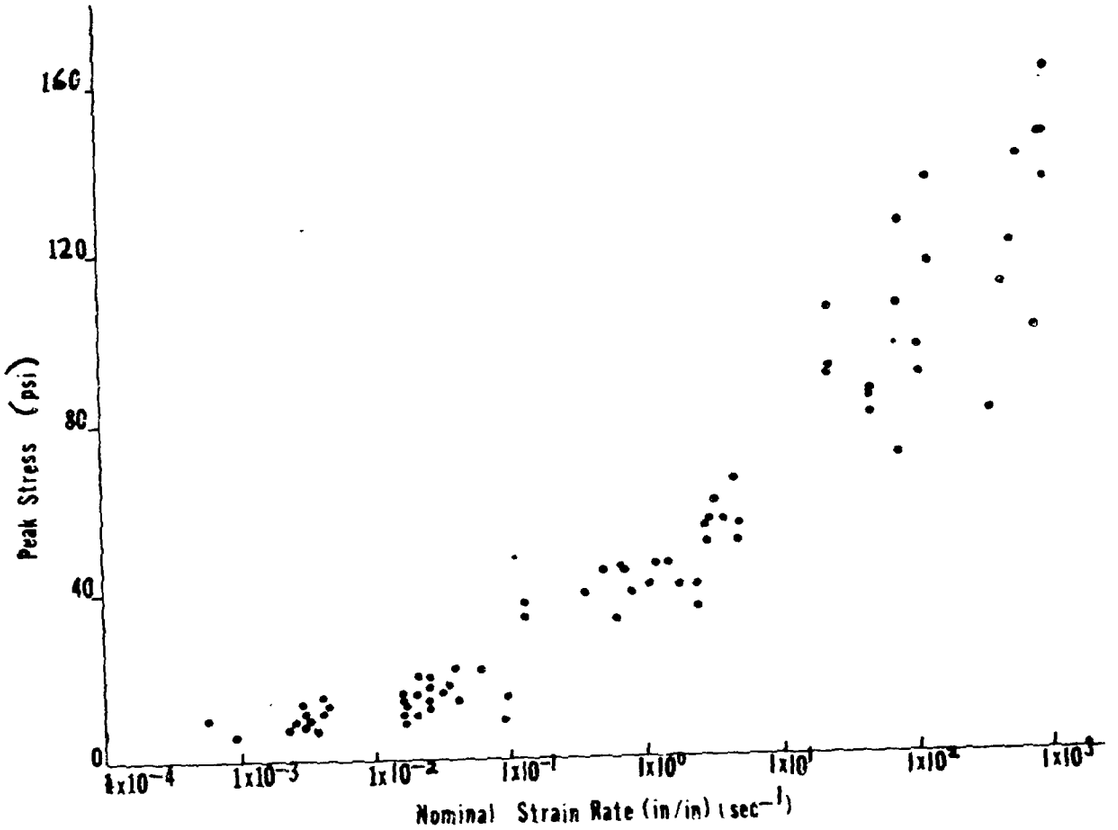

Figure 74: Peak Stress vs. Strain Rate - Composite of all Tests

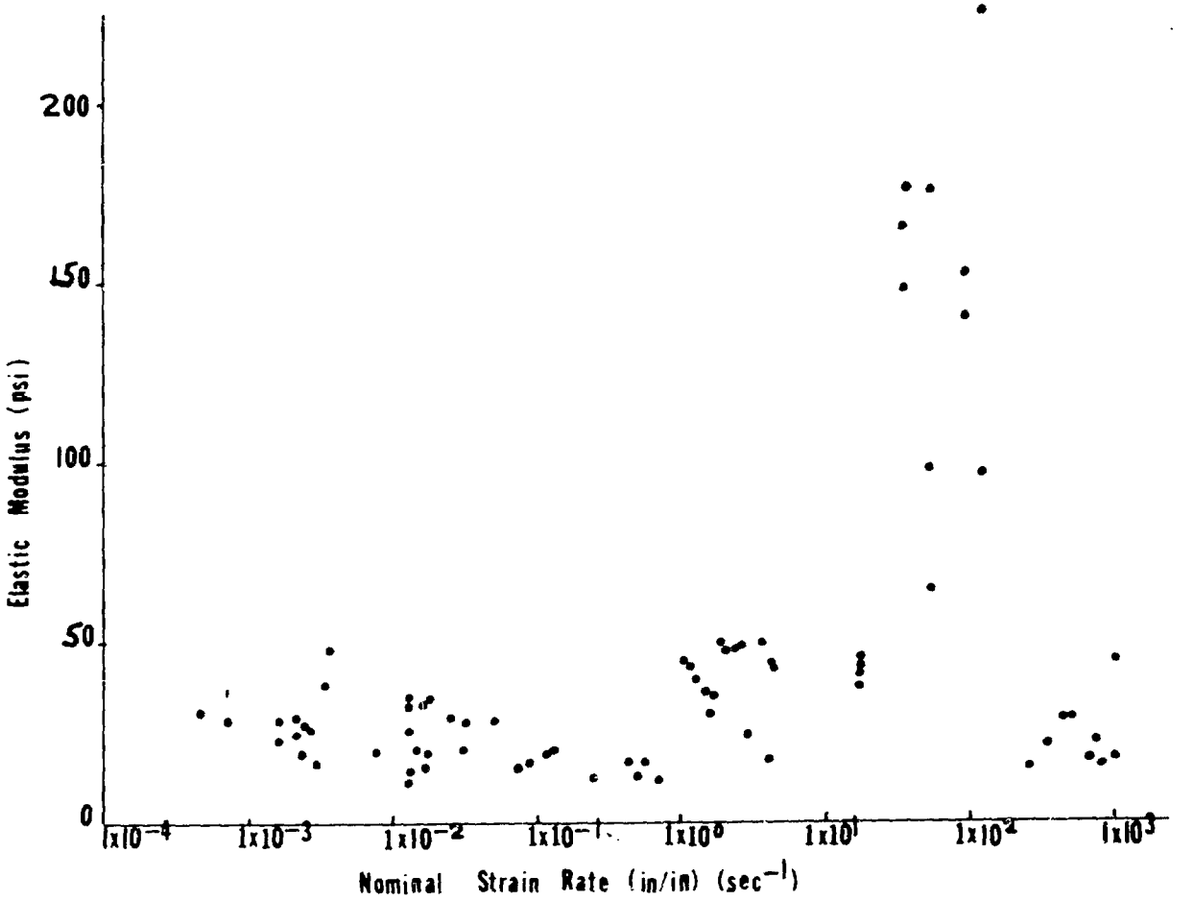

Figure 75: Elastic Modulus vs. Strain Rate - Composite of all Tests

at a strain rate of 120/sec. The elastic moduli (15-46 psi) of the gun tests were much less than the elastic moduli of the drop weight tests.

10.2.7 Fracture Surfaces

When tensile specimens fractured at strain rates below 2×10^{-2}/sec, the fracture surface exhibited very fine striations radiating from the point of crack initiation. The presence of the fine striations caused a diffusely reflecting surface. At strain rates above 2×10^{-2}/sec, a smooth glassy surface appeared in the portion of the fracture surface which fractured last. This glassy surface was free of striations and was a specular reflecting surface. As the strain rate increased further, the portion occupied by the glassy surface became larger until it covered the entire fracture surface. It is fair to assume the glassy surface characterized the higher velocities of crack propogation.

10.2.8 Ultrasonic Wave Velocity

The ultrasonic propogation velocity in gelatin, V, was measured. By the general relation $V = \sqrt{E/\rho}$, Young's modulus could be calculated from the velocity using the gelatin density.

The tests were performed with a Model 6600 Matec Pulse Modulator and Receiver with a Matec Model 950B RF Plug-in Unit. A 1.0"x0.5" Aerotech Gamma 2.25 MHz transducer was used. Table XII shows the results.

Table XII Ultrasonic Test Results

Run No.	n (intervals)	d (cm)	t (μ sec)	V (cm/μ sec)
1	2	2.555	32.5	0.157
2	2	2.675	35.0	0.153
3	4	8.892	230	0.155
4	6	8.892	337.5	0.158

$$\langle V \rangle = 0.156 \text{ cm}/\mu \text{ sec} = 1.56 \times 10^5 \text{ cm/sec}$$

$$V = \sqrt{E/\rho}$$

$$\rho = 1.060 \text{ g/cm}^3$$

$$E = \rho v^2 = (1.060 \text{ g/cm}^3)(1.56 \times 10^5 \text{ cm/sec})^2$$

$$= 2.56 \times 10^{10} \frac{\text{dyne}}{\text{cm}^2} = 3.7 \times 10^5 \text{ psi}$$

Although the meaning of strain rate is not clear for this type of excitation, the fact that the excitation occurred at 2.25 MHz implies that the modulus calculated in this fashion in some way represents the limit of high strain rate.

10.2.9 Shear Tests

10.2.9.1 Apparatus

The shear specimen consisted of a thin gelatin sheet bonded between two overlapping metal plates. The gelatin specimen was about 1/8" thick and 1" square. See Figure 76. The metal plates were sanded to leave a fresh metal surface and then thoroughly washed in detergent and water to degrease the metal surface. Unfinished leather was first bonded to the metal plates with contact cement, Duco cement, or epoxy cement and allowed to dry completely. The leathered plates were properly overlapped and spaced in pairs before gelatin was cast between them and refrigerated. The contact cement and the Duco cement prematurely failed between the plates and the leather when a sufficient force (10 lb.) was applied. The epoxy cement produced a suitable shear specimen. The leather, however, was not a rigid material; it deformed under the application of a shear stress. The strain measured in a shear test using leather was a combination of leather strain and gelatin strain.

When 1/8" gelatin layers were bonded to freshly cleaned metal plates with Eastman 910 adhesive (methyl-2-cyanoacrylate), the gelatin sheared without the failure of the gelatin-metal bond. The only strain measured in this case was the strain in the gelatin. The drying time for the Eastman 910 was only a few minutes. The shear specimens used for data were then made using Eastman 910.

The shear specimen was placed in slotted grips on the oil cylinder test apparatus. The specimens were pulled longitudinally. A clip gauge was fastened to each plate, bridging the gelatin. The stress was measured by the simple beam load cell described previously. Stress and strain were recorded on Foxboro Dynalog recorders. The specimens were taken out of the refrigerator and pulled within 2 minutes so that the gelatin temperature was between 5-10°C.

10.2.9.2 Results

Figures 77 through 87 and Table XIII show the results of the shear tests. Shear strain is equal to the displacement, l, divided by the thickness of the gelatin shear specimen. The shear stress is the shear load divided by the specimen area. The shear modulus for each test was calculated from the initial slope of the stress-strain curve. The strain rate was calculated by dividing the strain at some point along the initial slope of the stress-strain curve by the corresponding time found on the strain-time curve.

All shear tests were conducted with specimens made by using Eastman 910. The shear modulus varied from 4.2 to 23 psi. Figures 88 and 89 show shear modulus versus shear strain rate and shear modulus versus peak shear stress respectively.

10.2.10 Coefficient of Friction

The coefficient of rolling friction was measured experimentally using two smooth gelatin wheels rotated in contact with one another. Two seven foot strips of gelatin were placed around the rims of two

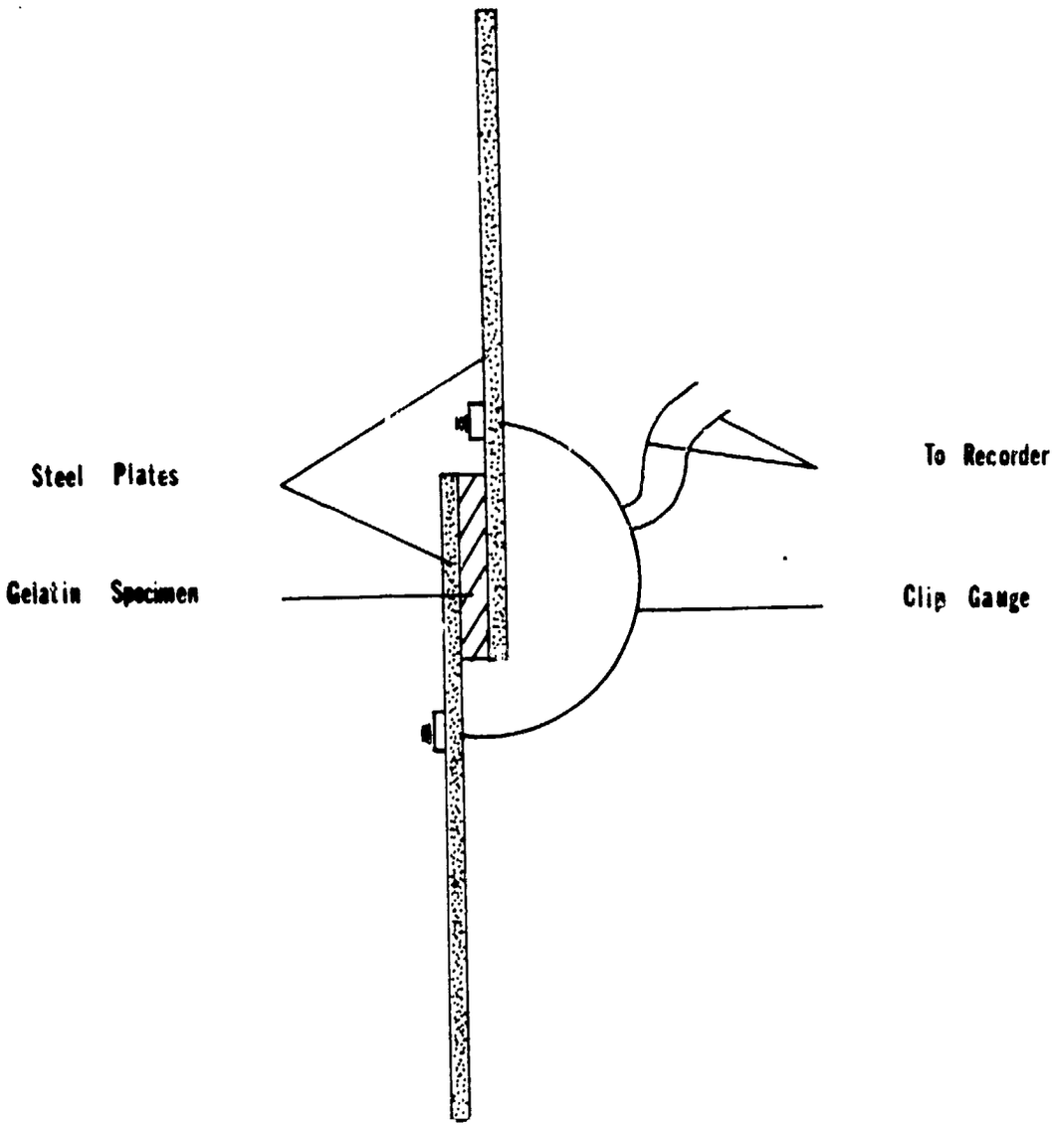

Figure 76: Shear Test Geometry

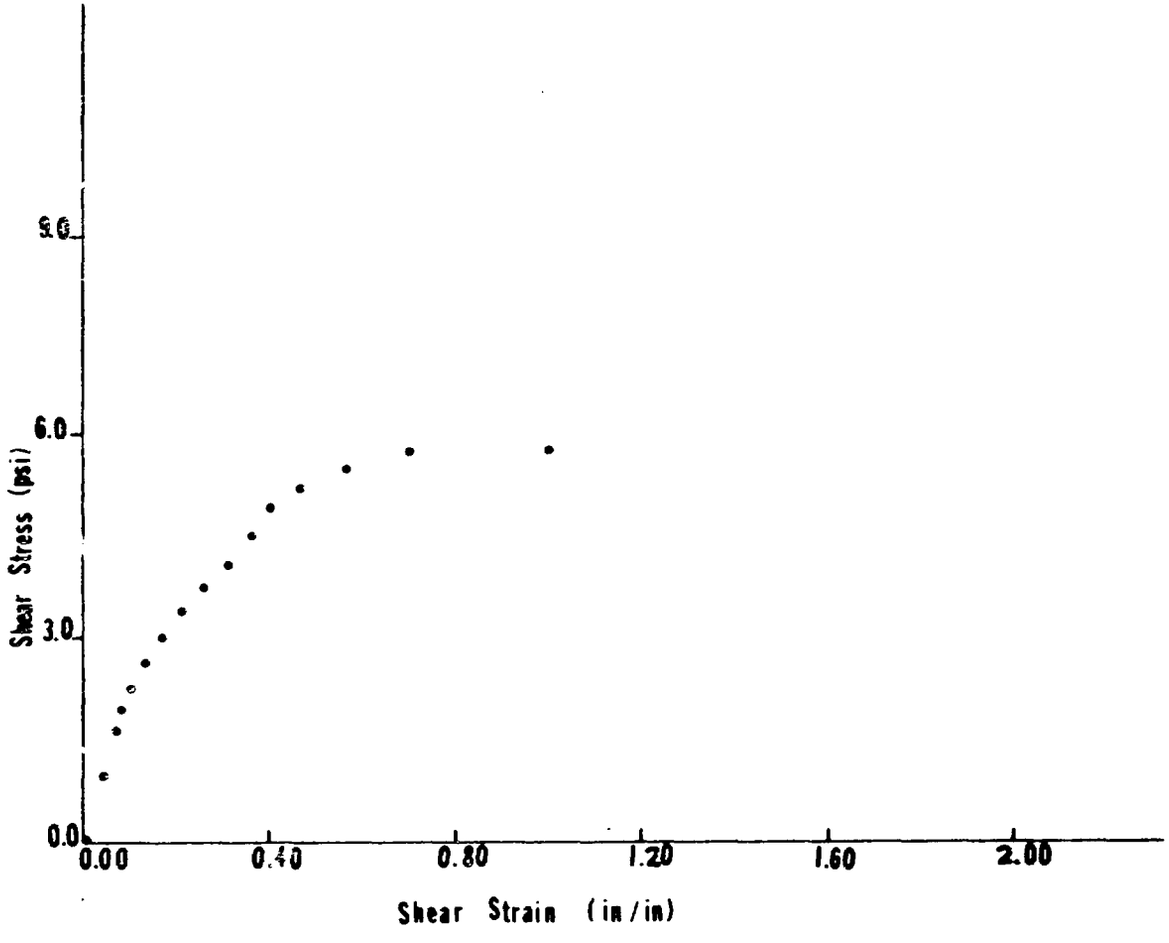

Figure 77: Shear Stress vs. Shear Strain - Sample 24 - 0.0075/sec

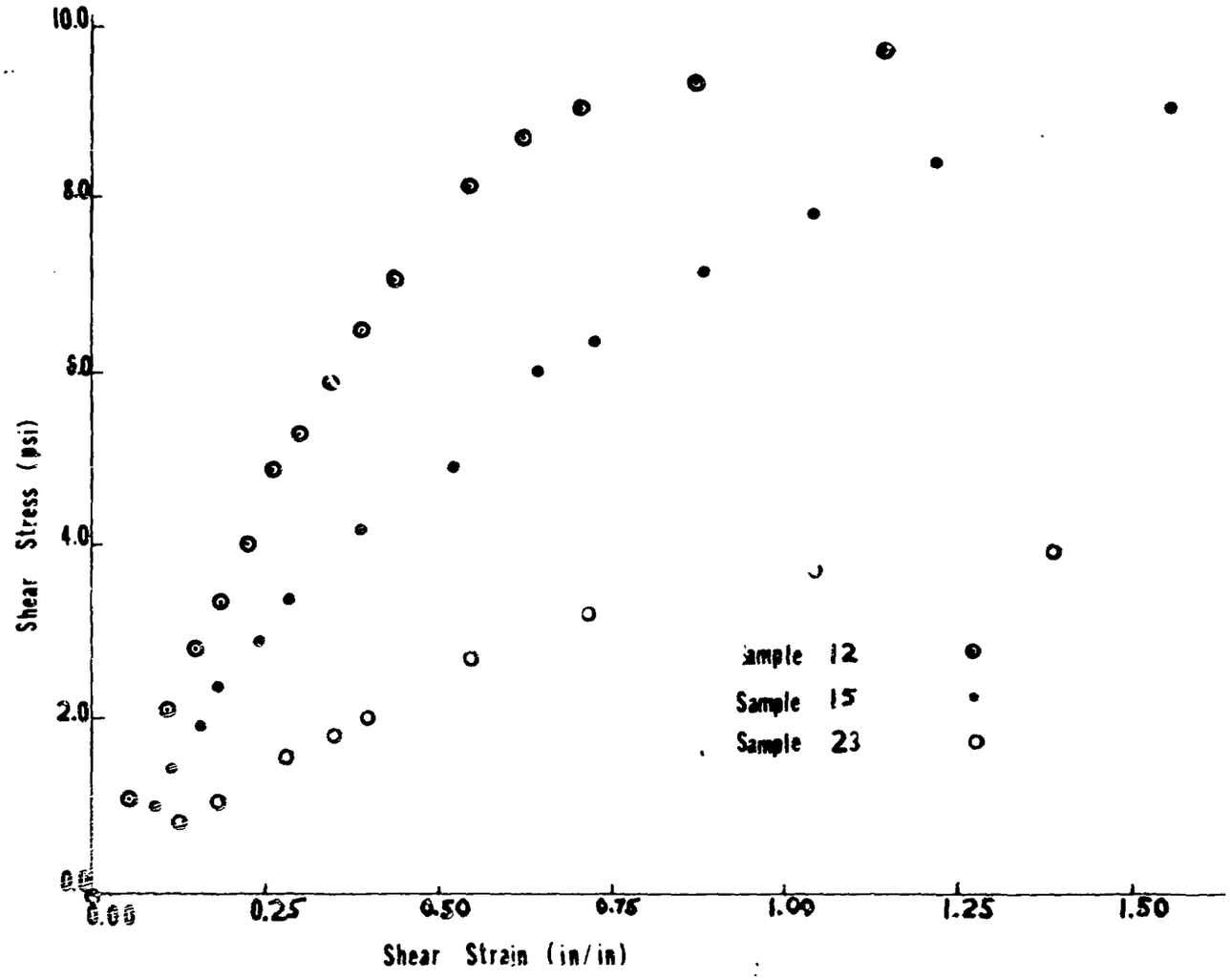

Figure 78: Shear Stress vs. Shear Strain - Sample 12, 15 and 23 - 0.016/sec

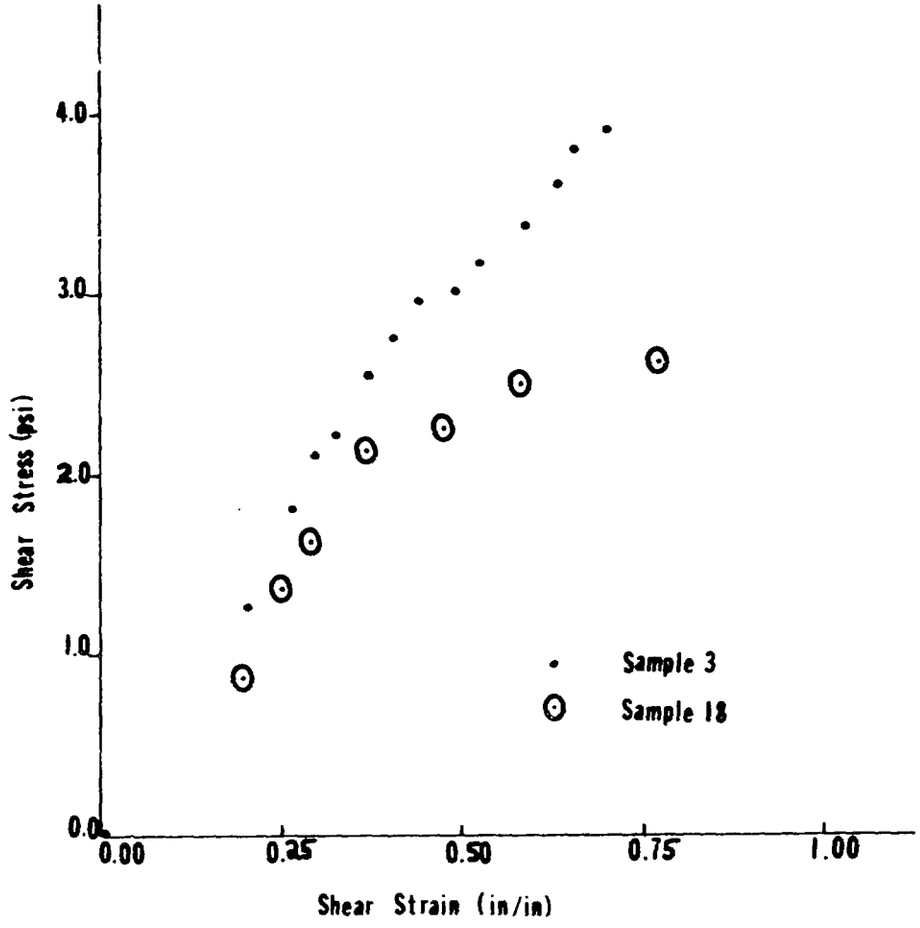

Figure 70: Shear Stress vs. Shear Strain - Samples 3 and 18 - 0.04/sec

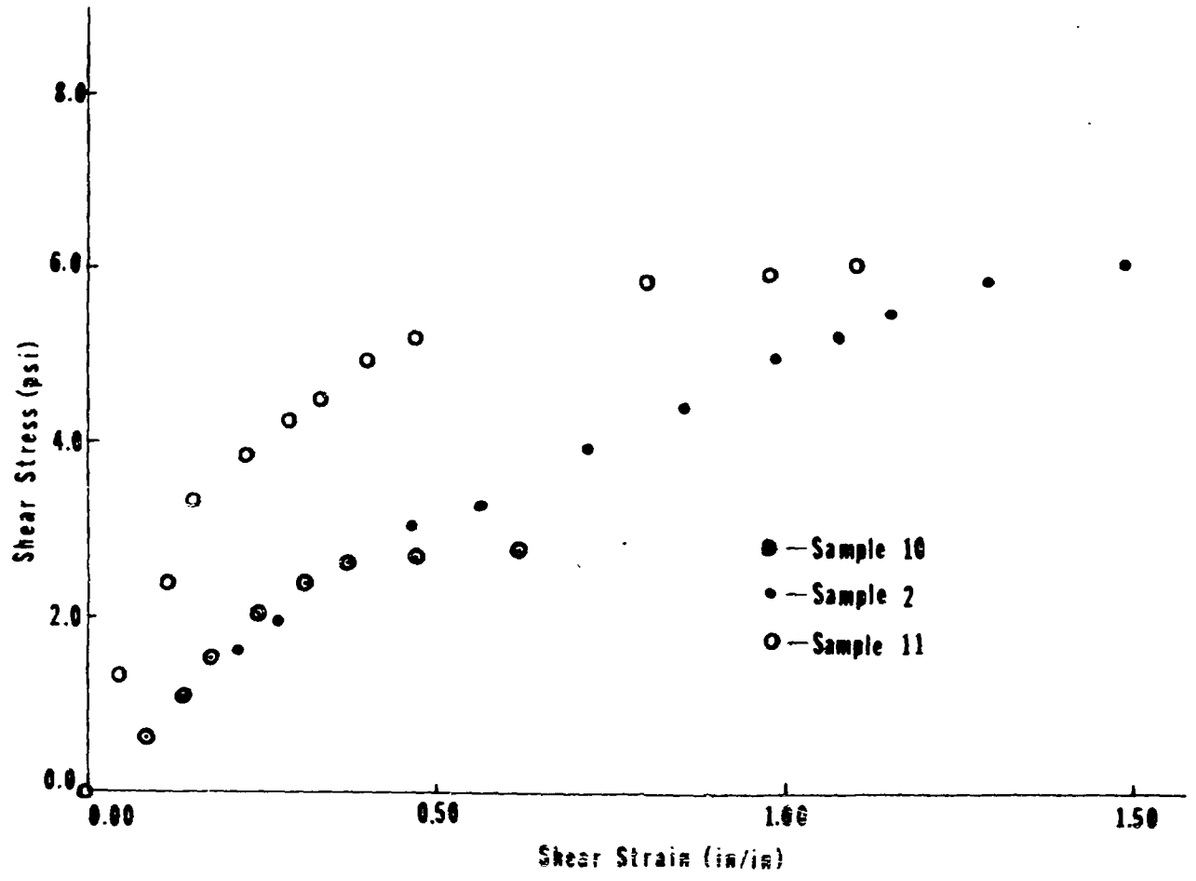

Figure 80: Shear Stress vs. Shear Strain - Samples 2, 10, and 11 - 0.062/sec

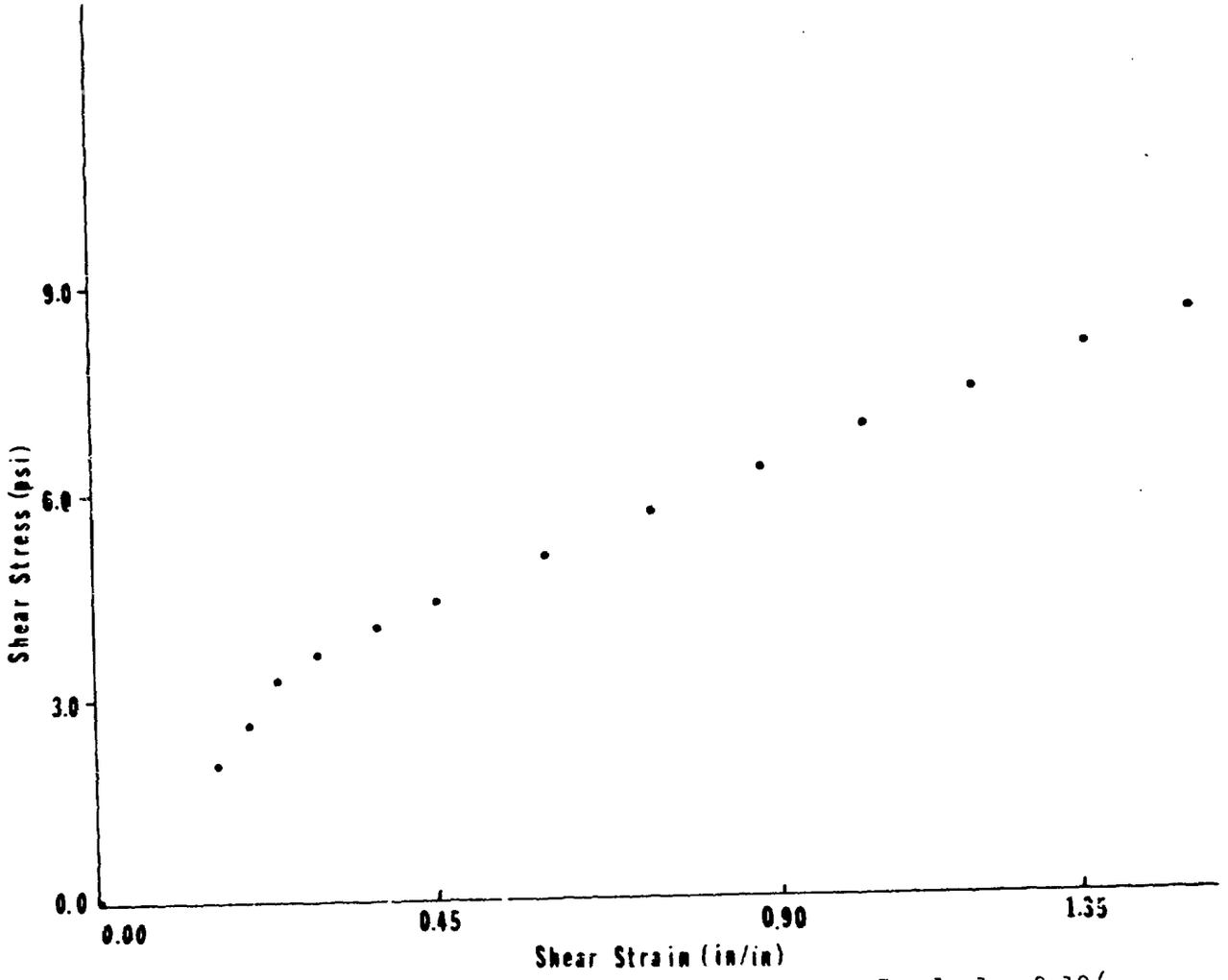

Figure 81: Shear Stress vs. Shear Strain - Sample 1 - 0.10/sec

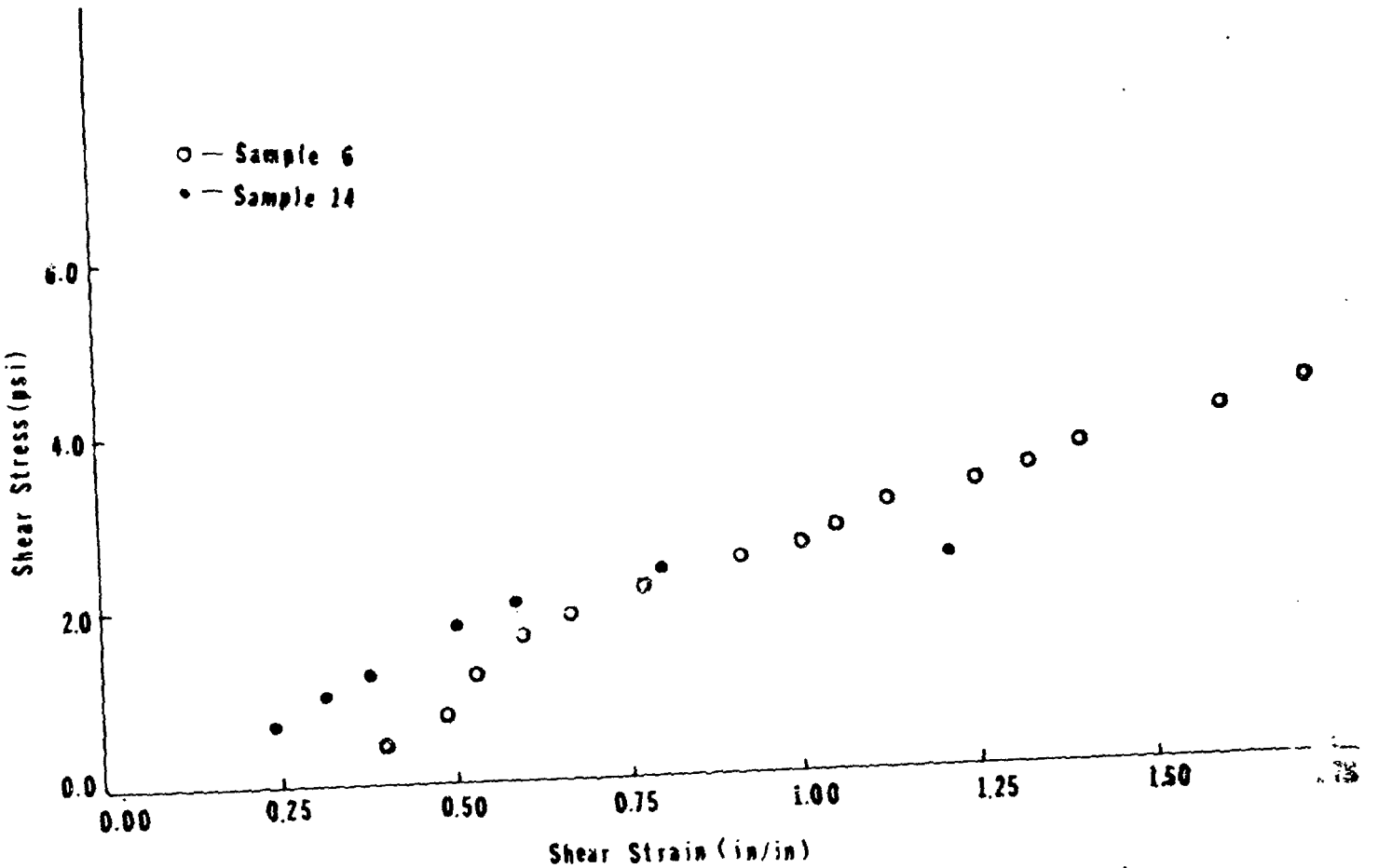

Figure 82: Shear Stress vs. Shear Strain - Samples 6 and 14 - 0.123/sec

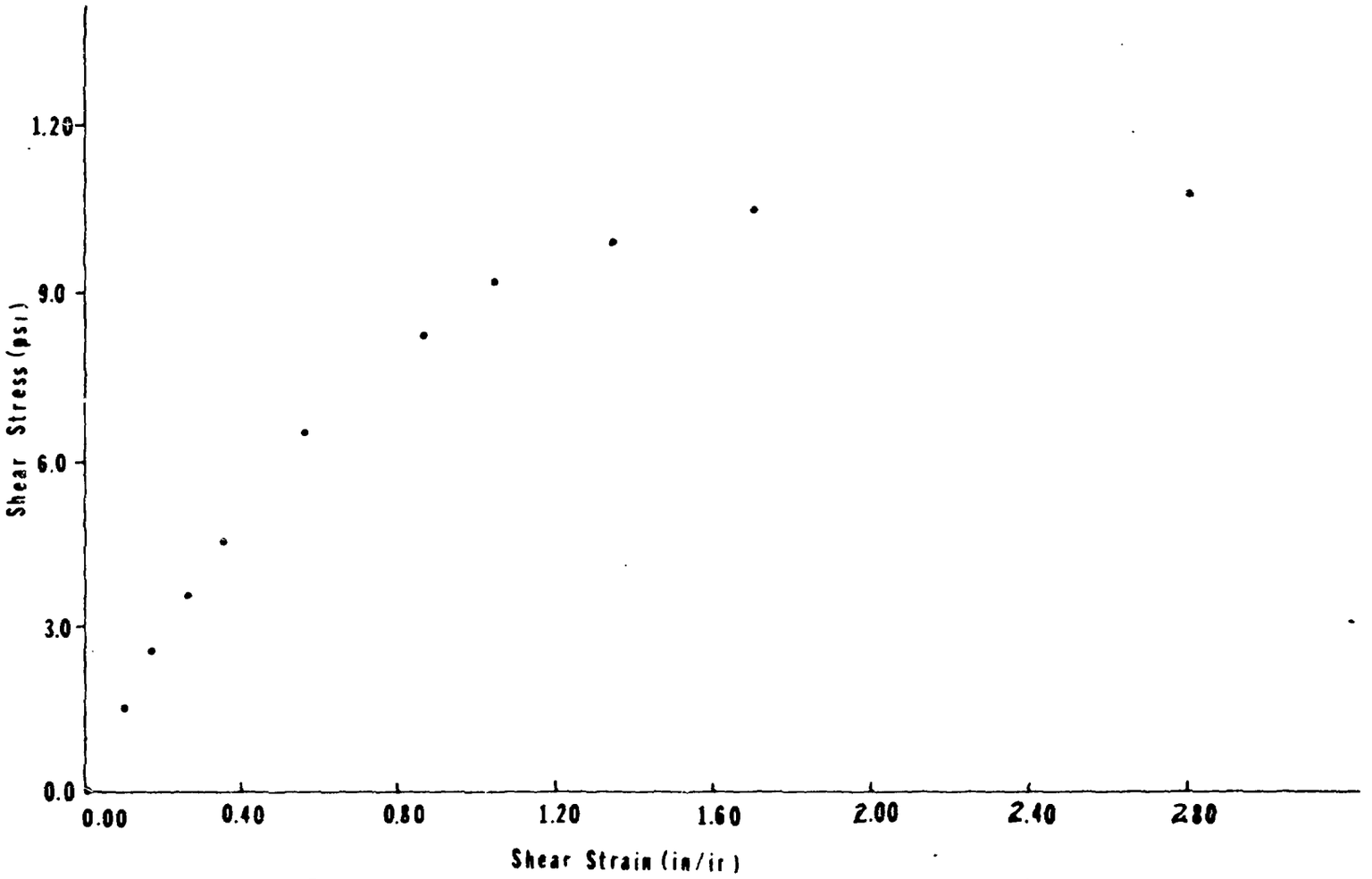

Figure 83: Shear Stress vs. Shear Strain - Sample 22 - 0.123/sec

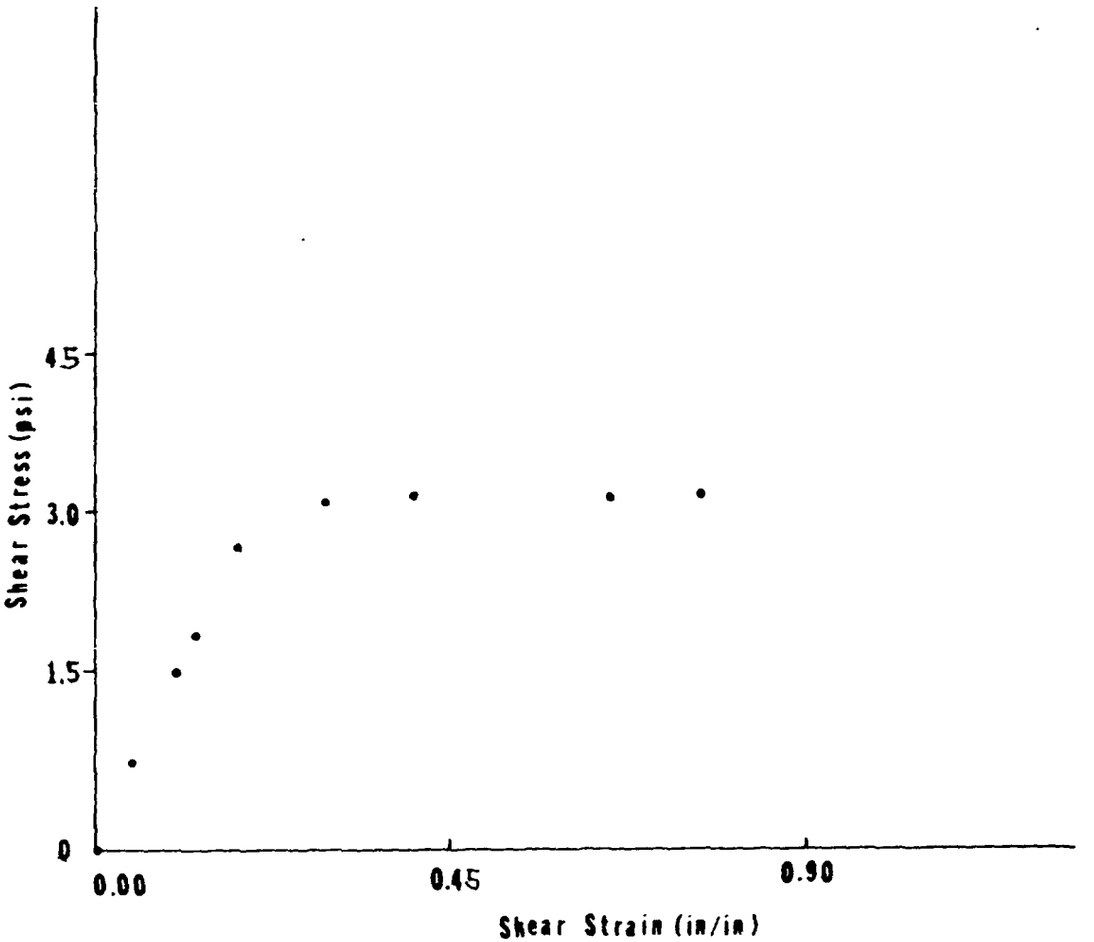

Figure 84: Shear Stress vs. Shear Strain - Sample 16 - 0.126/sec

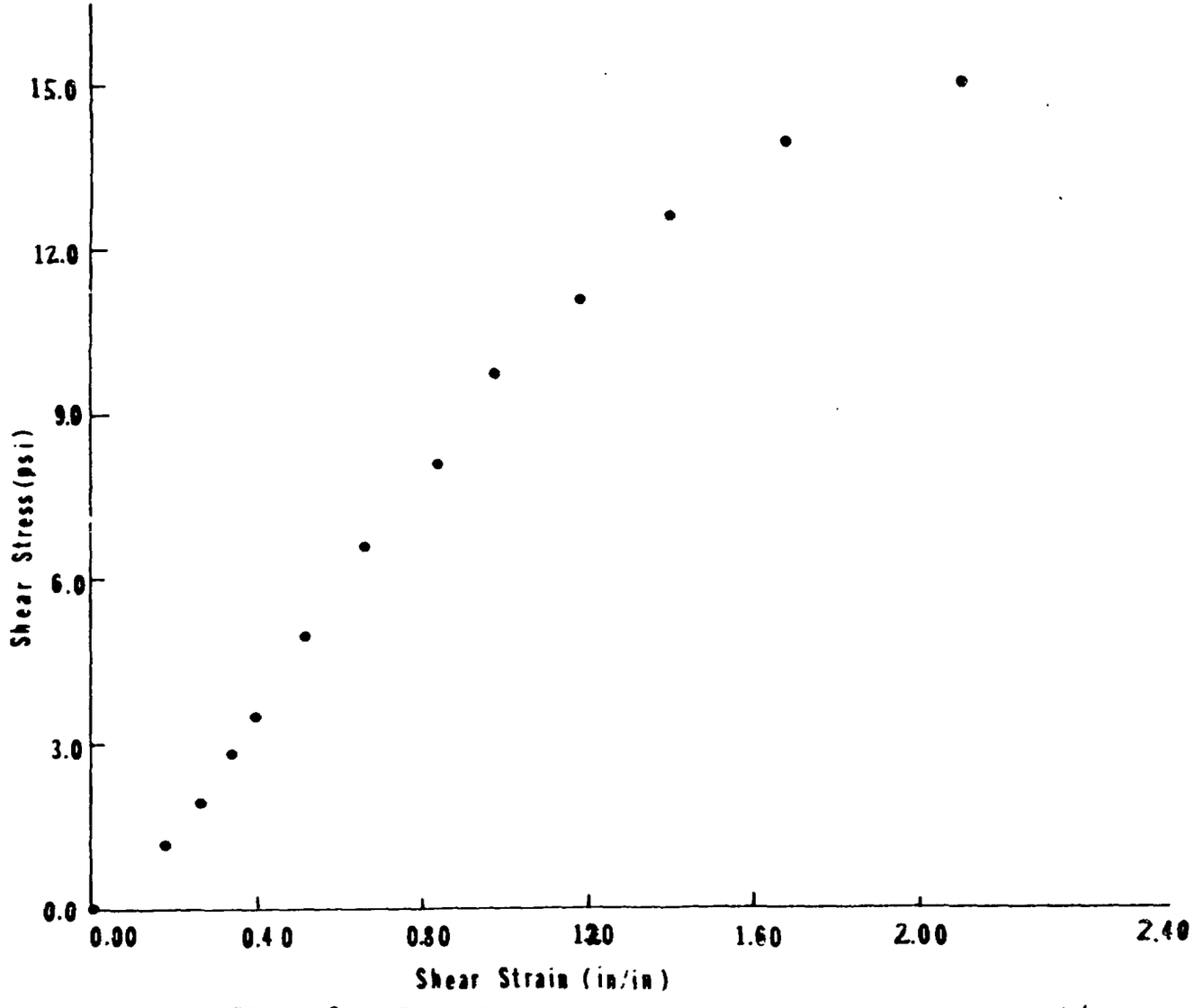

Figure 85: Shear Stress vs. Shear Strain - Sample 20 - 0.154/sec

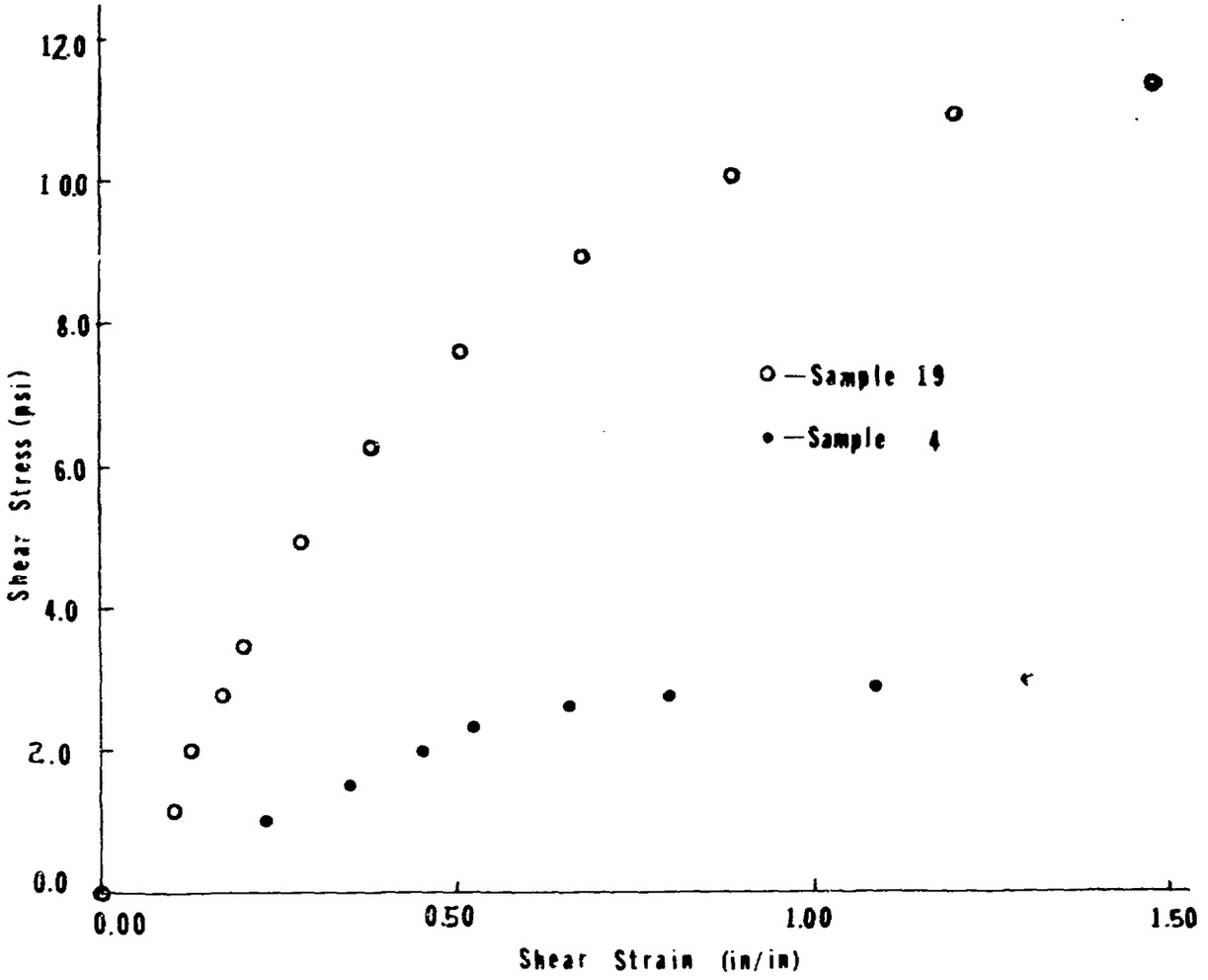

Figure 86: Shear Stress vs. Shear Strain - Samples 4 and 19 - 0.18/sec

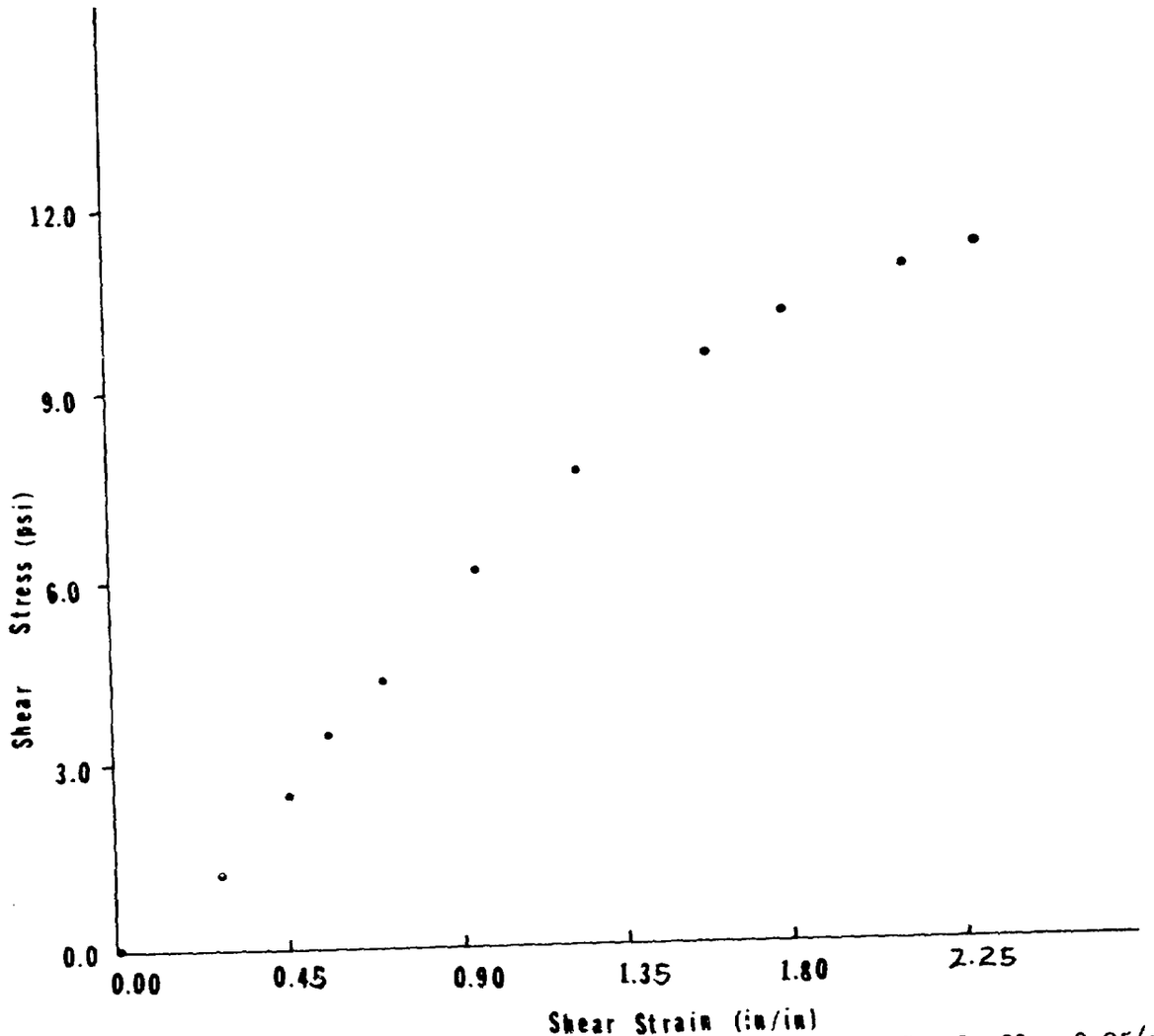

Figure 87: Shear Stress vs. Shear Strain - Sample 21 - 0.35/sec

Table XIII Shear Test Results

Test No.	Gelatin Area (in^2)	Gelatin Thickness (in)	Age (days)	Peak Shear Stress (psi)	Shear Strain (in/in)	Shear Stress (psi)	Shear Strain Rate (/sec)	G (psi)
24	0.85	0.126	4	5.8	0.40	8.0	0.0075	20.0
12	0.92	0.119	2	9.6	0.42	7.6	0.012	18.1
23	0.90	0.130	4	3.9	0.38	2.3	0.016	6.2
15	0.84	0.100	4	9.0	0.50	6.2	0.021	12.4
3	0.95	0.119	2	3.9	0.42	2.8	0.033	6.7
18	0.80	0.120	4	2.6	0.42	3.0	0.048	7.1
10	0.83	0.105	3	2.8	0.48	3.8	0.058	8.0
11	0.76	0.114	3	5.9	0.44	10.0	0.060	22.7
2	0.89	0.120	2	6.1	0.42	2.8	0.067	6.1
1	0.94	0.115	2	7.3	0.44	4.7	0.102	7.3
6	0.93	0.117	3	4.3	0.43	2.8	0.117	6.7
22	0.82	0.132	4	10.8	0.38	5.5	0.123	14.5
16	0.74	0.115	4	3.1	0.44	6.2	0.126	14.1
14	0.90	0.124	4	2.4	0.42	1.8	0.130	4.5
20	0.77	0.130	4	15.2	0.38	4.4	0.154	11.5
4	0.92	0.114	2	2.8	0.44	1.8	0.175	4.2
19	0.90	0.123	4	11.1	0.41	6.8	0.185	16.5
21	0.84	0.113	4	11.2	0.44	3.2	0.35	7.3

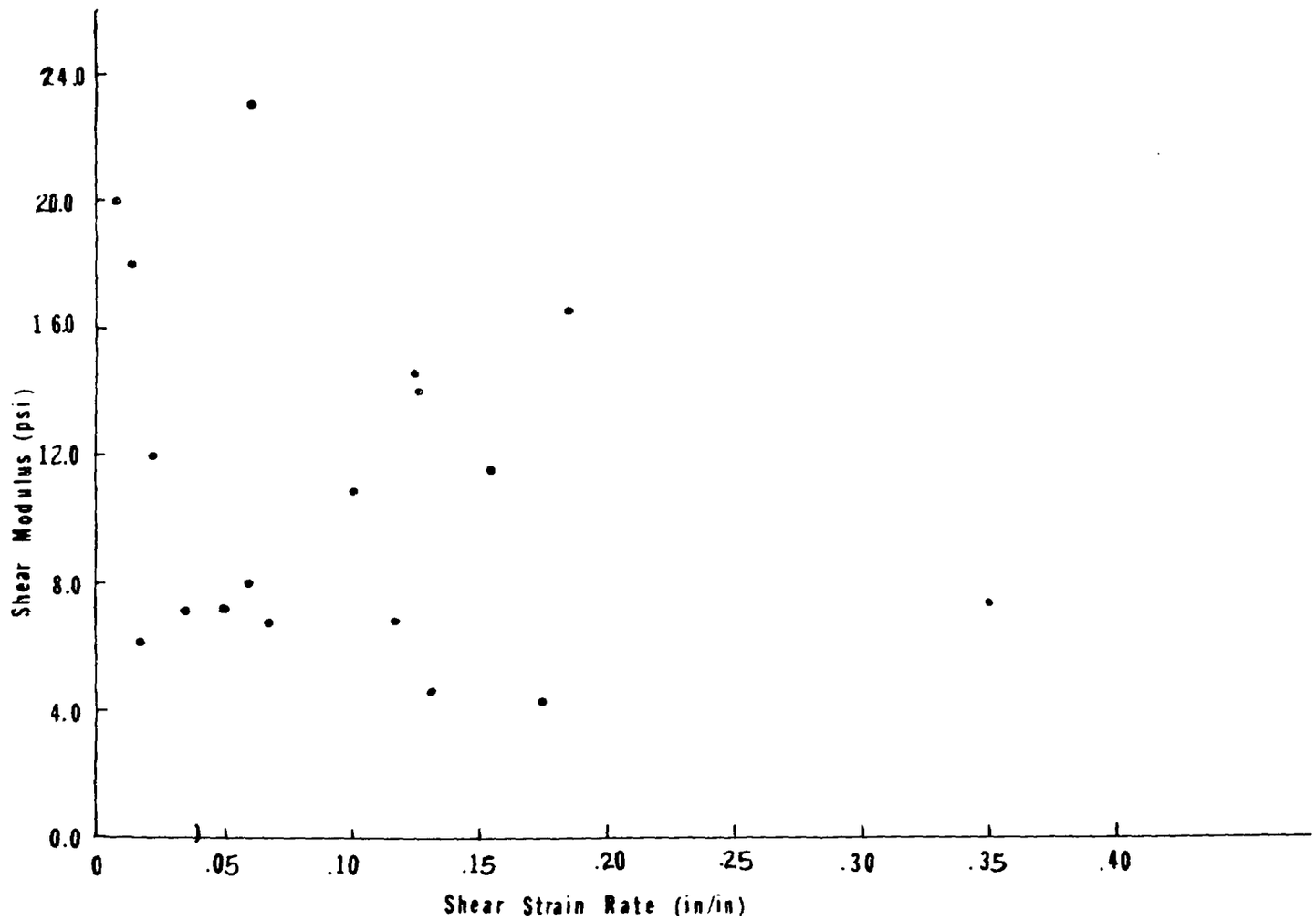

Figure 88: Shear Modulus vs. Shear Strain Rate

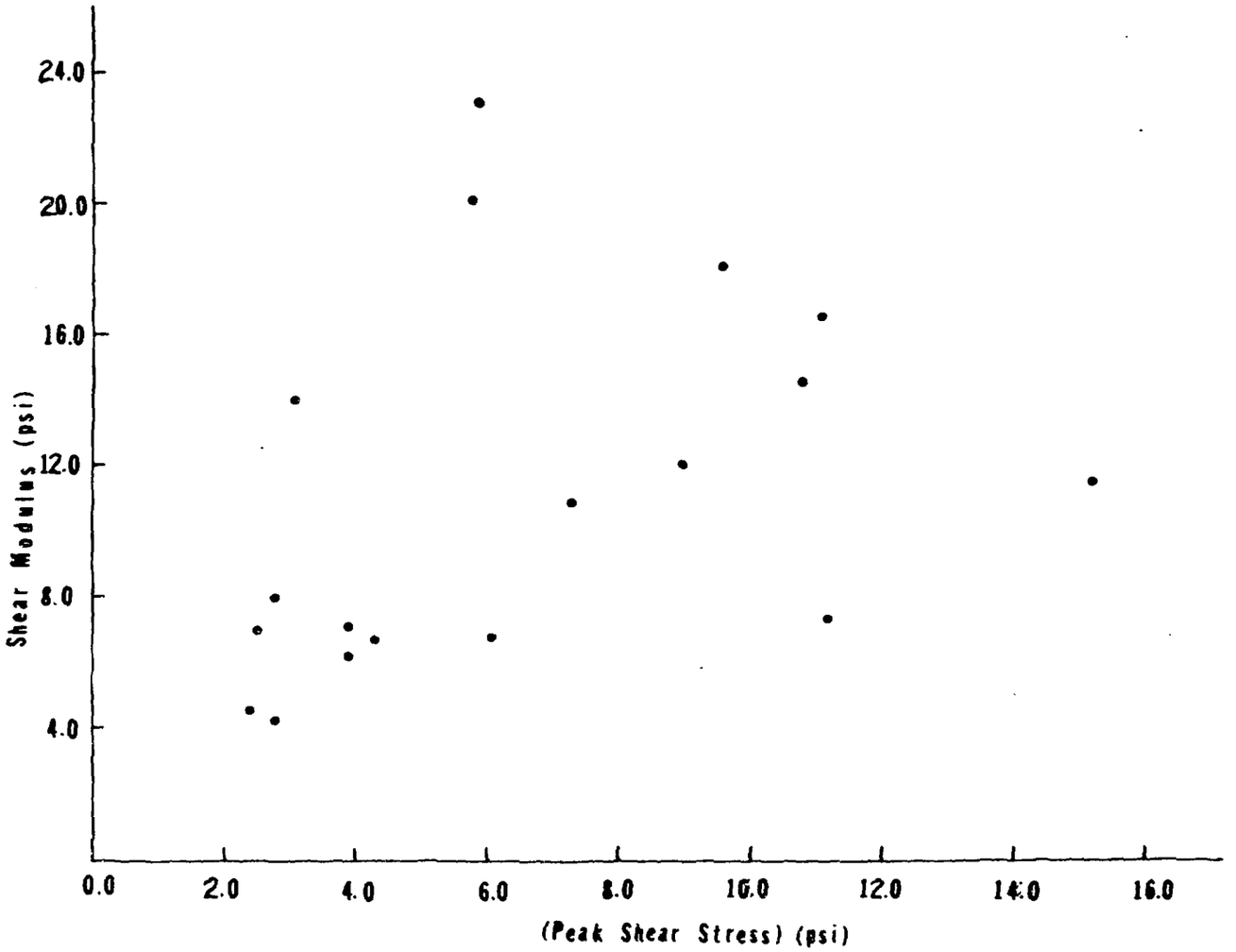

Figure 89: Shear Modulus vs. Peak Shear Stress

bicycle wheels. Both wheels were free to rotate about their own axles. The axle of one wheel was held rigidly in place while the other wheel was allowed to move in its plane of rotation using a hinged mounting arrangement. Placing weights on the movable wheel mounting framework would create a known normal force at the point of contact with the fixed wheel.

By accounting for the energy losses when a known energy was placed into the system, the rolling coefficient of friction could be calculated. A known energy input was created by letting known weights drop through known distances while doing work causing the wheel to rotate. On each wheel, a fishing cord was tied to a weight and fitted in a slot around a pulley mounted on the wheel. The total work, W, done on each wheel by dropping the weight is the energy input on that wheel.

The analysis in Appendix J shows that merely knowing the total number of revolutions the wheels make before stopping is enough to determine the coefficient of rolling friction (if the same is known for the wheels when they are not in contact). Table XIV summarizes the results. The rolling coefficient of friction ranged from 0.0142 to 0.0351.

Table XIV Coefficient of Rolling Friction

Test No.	m (lb)	N (lb)	n (rev)	w (ft-lb)	q (ft-lb)	Gelatin contact area (in)	μ_{roll}
1	1.3	3.3	14	2.84	96	2.62	0.0152
2	1.3	3.3	14.5	2.84	96	2.62	0.0142
3	1.3	6.8	6.25	2.84	96	3.06	0.0185
4	1.3	6.8	6.67	2.84	96	3.06	0.0173
5	1.3	10.0	3.67	2.84	96	3.12	0.0222
13	3.3	4.4	22.33	7.2	161	2.62	0.0184
14	3.3	4.4	22.25	7.2	161	2.62	0.0184
11	3.3	6.8	8.5	7.2	161	3.06	0.0351
12	3.3	6.8	8.75	7.2	161	3.06	0.0341
6	3.3	10.0	9.5	7.2	161	3.12	0.0212
7	3.3	10.0	9.25	7.2	161	3.12	0.0218
8	3.3	14.8	4.67	7.2	161	3.32	0.0301
9	3.3	14.8	4.5	7.2	161	3.32	0.0313
10	5.3	14.8	6.67	7.2	198	3.32	0.0339

11.0 Conclusions

A nominal value for density of the 20% gelatin is 1.060 gm/ml. When stored at 7°C in 37-38% humidity, the density increases slowly for 7 to 20 days, rising to 1.090 g/ml. After that, it increases 0.008 to 0.010 g/ml per day. There seems to be a limiting maximum density of 1.310 to 1.320 g/ml after 40 days. This range corresponds to roughly 80-90% gelatin by weight.

A nominal value for thermal conductivity is 8.5×10^{-4} cal $sec^{-1} {}^{o}C^{-1} cm^{-1}$. The average specific heat is 0.72 cal $g^{-1} {}^{o}C^{-1}$. The gelatin can be

characterised by an equivalent passive circuit in which there is a specific capacitance of 0.01 farad-cm/cm^2 if the applied field is less than 0.6 volts/cm. Above this, the field apparently breaks bonds, causing electrical properties to change radically. Below the critical field, the specific capacitance appears independent of applied field.

Fracture stress ranged from 6 psi to 160 psi over a range of strain rates from 6×10^{-4}sec^{-1} to 975 sec^{-1}. Elastic modulii varied from 12 psi to 225 psi over the same range of strain rates.

Shear stress at fracture varied from 2.6 psi to 15.2 psi over strain rates from 8×10^{-3}sec^{-1} to 0.4sec^{-1}. The shear modulii varied from 4.2 psi to 23 psi over the same range of strain rates. Fracture strains in tensile tests ranged from 0.32 to 2.4 over the range of strain rates investigated.

A viscoelastic transition is found between strain rates of 8×10^{-4} sec^{-1} and 2×10^{-3}sec^{-1}. An ultrasonic wave velocity of 1.56×10^5 cm/sec was measured at 2.25MH , with a corresponding elastic modulus of 3.7×10^5 psi. The coefficient of rolling friction is between 1.4×10^{-2} and 3.5×10^{-2}.

No piezoelectric behavior was observed. Application of fields both above and below the critical field strength did not alter the stress birefringence of the gelatin. A surface polarisation exists on the gelatin, but the effect is small (a few mv). Fracture surfaces change from diffuse reflectors to specular reflectors as the crack propagation rate increases.

12.0 References

1. Veis, A., The Macromolecular Chemistry of Gelatin, p 23. Academic Press, N. Y., 1964.
2. Ames, W. M., Journ. Am. Chem. Soc., 78, 6239-6244, Dec. 1956.
3. Marks, E. M. "Gelatin," Encyclopedia of Chemical Technology, 2nd ed. Vol. 10, 1966, (499-509,) p 499.
4. See discussion of isoelectric and isoionic points (which are usually taken to be equivalent) and differences in definition of each in The Macromolecular Chemistry of Gelatin, Veis, Academic Press, N. Y. 1964, pp 107-112.
5. Ward A. G. and P. R. Saunders, "Rheology of Gelatin," Rheology, Vol. 2, Academic Press, N. Y. 1956, p 314.
6. Marks, op. cit. p. 501
7. Kind & Knox Gelatin Co., 1000 N. 5th St., Camden, N. J. 08102
8. Standard Methods for the Sampling and Testing of Gelatins, Gelatin Manufacturers Institute of America, Inc., 501 Fifth Ave., New York., p 14.
9. Ibid, p 14.
10. "Heat Conductivity," CRC Handbook of Chemistry and Physics, 36th ed. p 2252.
11. Castillo, A. "Photoelastic Study of Gelatin Models," p 20, Army Material Command FSTC-HT-23-1316-73.
12. "Constant Humidity," CRC Handbook of Chemistry and Physics, 36th ed. p 2310.
13. "Hexane Soluability" CRC Handbook of Chemistry and Physics, 36th ed. p 963.
14. Castallan G. W., "Vapor Pressure of Salt Hydrates", Physical Chemistry, 2nd. ed., Addison - Wesley, 1971, pp 346-7
15. "Hydrated Salt Preparation" CRC Handbook of Chemistry and Physics, 36th ed., p 1597
16. "Viscoelasticity", W. Flugge, Blaisdell Publishing Co., Waltham, Mass., 1967, chap. 2.

APPENDIX A

DENSITY OF 20% GELATIN

Type of Preparation	Density (g/ml) Measurements	Avg.	Avg. Deviation
Large - 8750g	1.059, 1.060 1.059, 1.058 1.094, 1.058 1.058, 1.058 1.061, 1.058	1.063	± 0.005
Small - 500g	1.056, 1.058 1.059, 1.060 1.060, 1.060 1.057, 1.057 1.058, 1.058	1.058	± 0.001
Small - 500g	1.058, 1.058 1.057, 1.057 1.058	1.058	± 0.001
Small - 500g	1.060, 1.061 1.060, 1.061 1.060, 1.060 1.059, 1.060	1.060	± 0.001

APPENDIX B

THERMAL CONDUCTIVITY

Run 1 8/6/73

V = 12 V
R = 300 ohms
radius of gelatin specimen 1.94 cm
thickness of gelatin specimen 0.814 cm
temp. of specimen against source 10.8°C
temp. of specimen against sink 2.0°
temp. diff. across sample 8.8°C

Power = $I^2R = V^2/R = 144\ V^2/300$ ohms = 0.480 watts

$$\text{thermal conductivity} = \frac{0.480 \text{ watts}}{4.184 \frac{\text{watts sec}}{\text{calorie}}} \cdot \frac{0.814 \text{ cm}}{(1.94 \text{ cm})^2\ (8.8^\circ\text{C})}$$

T.C. = 0.000895 cal/(sec cm^2) (°C/cm)

Run 2 8/27/73

V = 12V
R = 200 ohms
radius of gelatin specimen 2.03 cm
thickness of gelatin specimen 1.32 cm

temp. of specimen against source 20.6°C
temp. of specimen against sink 0.0°
temp. diff. across sample 20.6°C

Power = $I^2R = V^2/R = 144V^2/200$ ohms 0.720 watts

$$\text{thermal conductivity} = \frac{0.720 \text{ watts}}{4.184 \frac{\text{watts sec}}{\text{calorie}}} \cdot \frac{(1.32 \text{ cm})}{(2.03 \text{ cm})^2\ (20.6^\circ\text{C})}$$

T.C. = 0.000851 cal/(sec cm^2) (°C/cm)

Run 3 8/28/73

V = 12 V
R = 200 ohms
radius of gelatin specimen 2.08 cm
thickness of gelatin specimen 1.26 cm
temp. of specimen against source 19.8°C
temp. of specimen against sink 0.0°
temp. diff. across sample 19.8°C

Power = $V^2/R = 144\ V^2/200$ ohms = 0.720 watts

$$\text{thermal conductivity} = \frac{0.720 \text{ watts}}{4.184 \frac{\text{watts sec}}{\text{calorie}}} \cdot \frac{(1.26 \text{ cm})}{(2.08 \text{ cm})^2\ (19.8^\circ\text{C})}$$

T.C. = 0.000806 cal/(sec cm^2) (°C/cm)

APPENDIX C

SPECIFIC HEAT CALCULATION

Specific heat of hexane in CRC Handbook of Chemistry of Physics, 36th edition, p 2100, is 0.600 cal/g °C.

Quantity of heat lost by hexane:

(0.600 cal/g°C) (mass of bath) (temp. change of bath) = calories lost by bath

Calories lost by bath = calories gained by sample

Specific heat of sample

$$\frac{\text{Calories gained by sample}}{(\text{mass of sample})\ (\text{temp. change of sample})} = \text{Specific heat of gelatin}$$

Classes 1-4

The bath lost 300-400 calories; the temperature change of the bath was 2-4°C; the mass of bath was 300-500 g.

Temperature change of sample was around 15°C.

Class 5, multi-sample runs, 3 blocks immersed

The bath lost around 600 calories; the temperature change of bath was 6-10°C; the mass of bath was 100-200 g.

Temperature change of sample was around 6-10°C.

See pages 7 through 9 for explanation of classes 1 through 5.

APPENDIX D

THE DENSITY OF GELATIN VERSUS COMPOSITION

Wt. % Gelatin	Sample Densities g/ml	Avg. Density	Avg. Deviation
5.0 %	1.010, 1.008, 1.010, 1.010	1.010 g/ml	±0.0005 g/ml
10.0 %	1.028, 1.032, 1.026, 1.028, 1.028, 1.030, 1.031, 1.027, 1.037, 1.030	1.029 g/ml	±0.002 g/ml
12.5 %	1.036, 1.036, 1.034, 1.038, 1.039, 1.039, 1.034, 1.033, 1.036, 1.034	1.036 g/ml	±0.002 g/ml
15.0 %	1.041, 1.040, 1.042, 1.042, 1.042, 1.040, 1.040, 1.040, 1.040, 1.040	1.041 g/ml	±0.001 g/ml
17.5 %	1.053, 1.054, 1.054, 1.051, 1.052, 1.051, 1,052, 1.052 1.052	1.052 g/ml	±0.001 g/ml
20.0 %	1.056, 1.058, 1.059, 1.060, 1.060, 1.060, 1.057, 1.057, 1.058, 1.058	1.058 g/ml	±0.001 g/ml

APPENDIX D (Cont'd)

Wt. % Gelatin	Sample Densities g/ml	Avg. Density	Avg. Deviation
22.5 %	1.063, 1.064, 1.063, 1.062 1.064, 1.062, 1.062, 1.065, 1.062, 1.064	1.063 g/ml	±0.001 g/ml
25.0 %	1.076, 1.076, 1.075, 1.076 1.077, 1.077, 1.076, 1.076, 1.077, 1.075	1.076 g/ml	±0.001 g/ml
27.5 %	1.084, 1.081, 1.082, 1.084, 1.082, 1.083, 1.081, 1.082, 1.082, 1.081	1.081 g/ml	±0.001 g/ml
30.0%	1.092, 1.092, 1.092, 1.093, 1.092, 1.092, 1.092, 1.092, 1.093	1.092 g/ml	±0.0002 g/ml

APPENDIX E

SUMMARY OF DENSITY STORAGE TIME MEASUREMENTS

Days Sample in Container	Lower Level Gelatin Density	Upper Level Gelatin Density	Average	Average Deviation
0	1.061, 1.059, 1.060, 1.059, 1.058, 1.058, 1.058, 1.058, 1.058, 1.094		1.063	±0.005
3	1.076, 1.057, 1.057		U=1.063 L=1.066	±0.006 ±0.001
4	1.067, 1.066	1.062, 1.058	U=1.060 L=1.069	±0.002 ±0.002
5	1.067, 1.071	1.060	U=1.060 L=1.067	±0.001
7	1.068, 1.066	1.058, 1.058	U=1.058 L=1.077	±0.001
11	1.076, 1.073	1.064, 1.062	U=1.063 L=1.076	±0.001 ±0.004
14	1.072, 1.080	1.063, 1.060	U=1.061	±0.002
18	1.073	1.061, 1.061, 1.058	U=1.060	±0.001
28		1.062, 1.060, 1.058	U=1.060	±0.001
35	1.084, 1.138, 1.155, 1.124		L=1.125	±0.033
46		1.065, 1.078, 1.068, 1.067	U=1.070	±0.004
50		1.079, 1.070, 1.093, 1.089	U=1.083	±0.008
60	1.231, 1.211, 1.257	1.080, 1.071, 1.069, 1.066	U=1.072	±0.004
67	1.233, 1.208, 1.233, 1.214	1.070, 1.085, 1.091, 1.087	L=1.233	±0.016
		1.132, 1.076, 1.070, 1.072	I=1.222 U=1.087	±0.010 ±0.022

APPENDIX F

SUMMARY OF DENSITY - STORE TIME MEASUREMENTS: SERIES A

Sample Number	Weight in Air (g)	Weight in Hexane (g)	Density g/ml	Storage Container	Void Enclosed
1-0	27.78	10.53	1.063		
2-0	29.40	10.71	1.061		
3-0	28.58	10.45	1.062	Avg. density of	
4-0	26.66	9.76	1.062	samples 1-10=	
5-0	30.95	11.14	1.060	1.062±0.001g	
6-0	29.43	10.71	1.062		
7-0	28.87	10.54	1.062	$s=8.8 \times 10^{-4}$	
8-0	29.93	10.87	1.061		
9-0	26.87	9.84	1.063		
10-0	30.37	11.00	1.061		
11-1	30.52	11.10	1.064	1	-
12-2	29.89	10.82	1.065	1	-
13-3	23.91	8.76	1.070	1	-
14-6	23.96	8.93	1.083	1	-
15-7	24.81	9.22	1.082	1	-
16-8	23.85	8.83	1.076	1	-
17-9	25.23	9.37	1.078	1	-
18-10	24.44	9.034	1.078	1	-
19-13	24.75	9.20	1.079	1	-
20-14	23.75	8.88	1.084	1	-
21-15	23.17	8.58	1.079	1	-
22-16	22.02	8.36	1.094	1	-
23-17	24.30	9.06	1.084	1	-
24-17	21.30	8.11	1.090	2	-
25-17	10.54	4.53	1.181	2	-
26-20	21.95	8.26	1.089	1	-
27-21	21.28	8.09	1.089	1	-
28-22	20.48	7.76	1.090	1	-
29-22	12.86	5.27	1.146	2	-
30-22	19.89	7.63	1.094	2	-
31-23	22.11	8.01	1.060	1	-
32-23	13.34	5.50	1.151	2	-
33-24	23.34	8.73	1.081	1	-
34-24	14.54	5.88	1.134	2	-
35-27	18.27	7.05	1.101	1	-
36-27	15.31	6.05	1.117	2	-
37-28	18.12	7.02	1.107	1	-
38-28	13.63	5.39	1.120	2	-
39-29	9.08	4.08	1.230	4	-
40-29	9.16	4.97	1.477	2	-
41-30	5.72	2.71	1.284	4	-
42-30	13.40	5.46	1.139	2	-
43-31	7.41	3.52	1.289	4	-
44-31	8.91	4.00	1.226	2	-
45-35	7.19	3.49	1.314	4	-
46-35	10.73	4.14	1.103	2	-
47-36	5.89	2.84	1.306	4	-

APPENDIX F (Cont'd)

Sample Number	Weight in Air (g)	Weight in Hexane (g)	Density g/ml	Storage Container	Void Enclosed
48-36	8.34	3.81	1.243	2	-
49-37	7.19	3.45	1.302	4	-
50-37	8.95	4.06	1.237	2	-
51-38	6.23	3.03	1.305	4	-
52-38	8.12	3.78	1.284	2	-
12-38	8.24	3.88	1.266	1	-
21-38	9.78	4.33	1.202	1	-
53-41	6.33	3.22	1.316	4	-
54-41	8.04	3.71	1.255	2	-
55-42	6.75	3.27	1.314	4	-
56-42	7.34	3.47	1.281	2	-
57-43	6.44	3.11	1.314	4	-
58-43	7.61	3.60	1.286	2	-
59-44	6.14	3.00	1.330	5	-
60-44	8.42	3.79	1.234	2	B
61-48	7.13	3.34	1.274	5	B
62-48	7.87	3.60	1.254	2	B
13-48	6.16	2.99	1.313	1	-
27-48	7.68	3.47	1.234	1	B
63-50	6.44	3.12	1.316	5	-
64-50	6.61	3.18	1.310	2	-
16-50	6.81	3.26	1.308	1	-
38-51	5.97	2.88	1.314	2	-
39-51	6.47	3.13	1.319	4	-
16-51	6.77	3.27	1.314	1	-
40-52	6.79	3.28	1.312	2	-
41-52	5.02	2.44	1.326	4	-
15-52	7.34	3.58	1.319	1	-
42-55	6.56	3.18	1.324	2	-
43-55	6.53	3.20	1.324	4	-
16-55	6.68	3.26	1.315	1	-
44-57	6.53	3.19	1.318	2	-
45-57	6.50	3.20	1.328	4	-
16-57	6.64	3.24	1.314	1	-
11-58	7.25	3.54	1.321	1	-
46-58	6.99	3.41	1.318	2	-
47-58	5.48	2.69	1.323	4	-

B : Void enclosed in gelatin sample
- : No void enclosed

APPENDIX G

SUMMARY OF DENSITY - STORE TIME MEASUREMENTS: SERIES B

Sample Number	Weight in Air (g)	Weight in Hexane (g)	Density g/ml	Enclosed Void
1-0B	29.23	10.56	1.060	-
2-0B	28.32	10.26	1.060	-
3-0B	31.93	11.47	1.054	-
4-3B	28.81	10.55	1.071	-
5-4B	26.81	9.86	1.069	-
6-5B	23.21	8.64	1.075	-
7-6B	26.41	9.75	1.072	-
8-7B	23.07	8.57	1.073	-
9-10B	22.51	8.43	1.084	-
10-11B	23.23	8.76	1.085	-
11-12B	21.06	7.95	1.089	-
12-13B	18.65	7.15	1.099	-
13-14B	20.28	7.84	1.106	-
14-18B	16.02	6.31	1.115	-
15-19B	14.92	6.01	1.134	-
1-20B	10.33	5.14	1.345	-
2-21B	12.93	5.34	1.143	-
3-24B	11.77	5.03	1.184	-
4-25B	11.37	4.92	1.192	-
1-25B	9.74	5.46	1.207	-
5-26B	12.86	5.24	1.150	-
6-27B	9.26	4.05	1.211	B
7-27B	7.78	3.34	1.254	B
6-31B	7.78	3.57	1.254	B
6-33B	7.37	3.45	1.267	B
8-33B	7.74	3.55	1.250	-
11-34B	8.38	3.86	1.254	-
14-35B	7.44	3.46	1.262	B
1-40B	6.84	3.28	1.293	B
2-41B	6.74	3.21	1.287	B

B : Enclosed void in gelatin sample
- : No enclosed void

APPENDIX H

SURFACE POLARITY OF GELATIN SOLIDS

Surface	Sample 1	Sample 1-A	Sample 2	Sample 3	Sample 4	Sample 5
top when cast	-5mv	-9mv	-2mv	+2mv	+4mv	+4mv
bottom when cast	-2	-8	-2	+1	-1	+7
side 1	-3		-4	+1	+1	+4
side 2	-8		-4	+7	+3	+4
side 3	-4		-2	+6	+7	+3
side 4	+3		-2	+5	+3	+2
top when cast (interchanged electrodes)	-1			+3	+3	
bottom when cast (interchanged electrodes)	+3			-4	-1	

Sample 1 was cast in lucite molds, 9 days old
Sample 1-A old surfaces melted away, new surfaces exposed
Sample 2 was cast in lucite mold, 9 days old
Sample 3 " " " glass " , 19 hours old
Sample 4 " " " cardboard mold largely in darkness, also was prepared in darkness
Sample 5 was prepared and cast largely in darkness in glass mold immersed in hexane during measurements

The potentials listed are with respect to a ground electrode, which in each case is on the face opposite the listed "surface". Cases listed as "interchanged electrodes" follow the same convention, except the electrodes are physically interchanged. All electrodes are chromium plated steel.

APPENDIX I

CROSSHEAD VELOCITY FOR GAS GUN TESTS

Let m = projectile mass
M = moveable crosshead mass
v_o = initial projectile velocity
v = final projectile velocity
V = final crosshead velocity

The crosshead is initially at rest, so conservation of momentum requires:

$$mv_o = mv + MV \tag{1}$$

and conservation of energy requires:

$$\frac{mv_o^2}{2} = \frac{mv^2}{2} + \frac{MV^2}{2} \tag{2}$$

rewriting (2):

$$\frac{m}{M} = \frac{m}{M}\left(\frac{v}{v_o}\right)^2 + \left(\frac{V}{v_o}\right)^2 \tag{3}$$

but rewriting (1):

$$\frac{V}{v_o} = \frac{m}{M}\left(1 - \frac{v}{v_o}\right)$$

so (3) can be rewritten as:

$$\frac{m}{M} = \frac{m}{M}\left(\frac{v}{v_o}\right)^2 + \left(\frac{m}{M}\right)^2\left(1 - \frac{v}{v_o}\right)^2$$

collecting terms, this becomes:

$$-\left(\frac{v}{v_o}\right)^2\left(\frac{m}{M}\right)\left[1 + \frac{m}{M}\right] + \left(\frac{v}{v_o}\right)\left(2\,\frac{m^2}{M^2}\right) + \frac{m}{M}\left(1 - \frac{m}{M}\right) = 0$$

using the general solution to a quadratic equation, and then simplifying, we get:

$$\left(\frac{v}{v_o}\right) = \left(\frac{m}{m+M}\right) \pm \left(\frac{M}{m+M}\right)$$

In this case:

$$m = 1$$
$$M = 3$$
$$\frac{v}{v_o} = \left(\frac{1}{4}\right) \pm \left(\frac{3}{4}\right)$$
$$\frac{v}{v_o} = 1,\ -\frac{1}{2}$$
$$\frac{v}{v_o} = 1 \Rightarrow \text{no impact}$$
$$\frac{v}{v_o} = -\frac{1}{2} \Rightarrow v = -\frac{v_o}{2} \quad \text{physically meaningful}$$

Therefore: $$V = \frac{m}{M}\left(v_o - v\right) = \frac{1}{3}\left(v_o + \frac{v_o}{2}\right) = \frac{v_o}{2}$$

APPENDIX J

COEFFICIENT OF ROLLING FRICTION

Let W = work done on one wheel by the dropping weight

$W = W_{\perp} + W_{var}$

$W_{\perp}$ = work done with string $\perp$ to radius of pulley

W_{var} = work done with string at a variable angle to pulley just before string pulls off pulley

$W_{\perp} = MgH = Mg\ (23")$
where H = distance weight falls with string $\perp$ to radius

$W_{var} = Mgr \int_0^{\theta_{max}} \cos\theta\ d\theta = Mgr \sin \theta_{max}$
where θ is the angle the wheel rotates through after the string is no longer $\perp$ radius, and θ_{max} is the angle at which string pulls off pulley

$$\theta_{max} = \frac{3\frac{1}{2}"}{r_{pulley}} = \frac{3\frac{1}{2}"}{5\ 3/4"} = 0.61 \text{ radians}$$

$W_{var} = Mg\ (5\ 3/4")\ \sin\ (0.61) = Mg\ (3.2")$

$\therefore\ W = W_{\perp} + W_{var} = Mg\ (23" + 3.2")$

$\therefore\ W = \frac{26.2"}{12"}$ Mg foot-lbs, where Mg is in lbs.

* * * * * * * *

Let U represent the total energy loss of the system

let u_1 = energy loss of 1st wheel due to gelatin in "n" revolutions

let u_2 = energy loss of 2nd wheel due to gelatin in "n" revolutions

let u_1° = energy loss of 1st wheel due to other dissipation mechanisms in "n" revolutions

let u_2° = energy loss of 2nd wheel due to other dissipation mechanisms in "n" revolutions

Then $U = u_1 + u_2 + u_1^{\circ} + u_o^{\circ}$

let N = normal force (load) on gelatin

then $\mu_{roll}\ N$ = frictional force in direction of rotation

so $\mu_{roll}\ N(\pi Dn) = u_1 + u_2$
where D = wheel diameter (including gelatin)

* * * * * * * *

If wheel #1 turns q_1 times with energy input w_1 when there is no contact between the two wheels,

And if wheel #2 turns q_2 times with energy input w_1 when there is no contact between the two wheels,

Then the total energy loss (when there is no contact between wheels) per revolution is given by

$$\frac{w_1}{q_1} + \frac{w_1}{q_2}$$

Then the total energy loss (with no contact) for "n" revolutions is

$$u_1^o + u_2^o = nw_1\left(\frac{1}{q_1} + \frac{1}{q_2}\right)$$

Calibration runs at the highest initial velocity (the 5.3 lb weight) showed wheel #2 turns 3/4 the number of turns wheel #1 makes before it stops when there is no contact between wheels.

$$q_2 = 3/4\ q_1$$

$$u_1^o + u_2^o = nw_1\left[\frac{1}{q_1} + \frac{4}{3q_1}\right] = \frac{7}{3}\frac{nw_1}{q_1}$$

* * * * * * * *

So $U = 2W = u_1 + u_2 + u_1^o + u_2^o$ in "n" revolutions when the wheels are in contact

$$2W = \mu_{roll}\, N\pi Dn + \frac{7}{3}\frac{nw_1}{q_1}$$

$$\therefore\ \mu_{roll} = \frac{2W}{\pi NDn} - \frac{7w}{3q_1 N\pi D}$$

where N = normal force between wheels in lbs.

D = wheel diameter including gelatin in feet = 2.13 ft

W = (2.18) x (drop weight in lbs) ft-lbs used when wheels are in contact (same W is used for each wheel)

n = number of revolutions before stopping when wheels are in contact

w_1 = (2.18) x (drop weight in lbs) ft-lbs used when wheels are not in contact (same weight used on each wheel)

q_1 = number of revolutions of wheel #1 before stopping when wheels are not in contact